Neural Plasticity

Neurorehabilitation: Neural Plasticity and Functional Recovery 2018

Lead Guest Editor: Toshiyuki Fujiwara
Guest Editors: Junichi Ushiba and Surjo R. Soekadar

Neurorehabilitation: Neural Plasticity and Functional Recovery 2018

Neural Plasticity

Neurorehabilitation: Neural Plasticity and Functional Recovery 2018

Lead Guest Editor: Toshiyuki Fujiwara
Guest Editors: Junichi Ushiba and Surjo R. Soekadar

Editorial Board

Contents

Hindawi
Neural Plasticity
Volume 2019, Article ID 7812148, 3 pages
https://doi.org/10.1155/2019/7812148

Editorial

Neurorehabilitation: Neural Plasticity and Functional Recovery 2018

Toshiyuki Fujiwara[1], **Junichi Ushiba**[2,3,4] **and Surjo R. Soekadar**[5,6]

[1]*Department of Rehabilitation Medicine, Juntendo University Graduate School of Medicine, 2-1-1 Hongo, Bunkyo, Tokyo 113-8421, Japan*
[2]*Faculty of Science and Technology, Keio University, 3-14-1 Hiyoshi, Kohoku-ku, Yokohama, Kanagawa 223-8522, Japan*
[3]*Keio Institute of Pure and Applied Sciences (KiPAS), Keio University, 3-14-1 Hiyoshi, Kohoku-ku, Yokohama, Kanagawa 223-8522, Japan*
[4]*Department of Biosciences and Informatics, Faculty of Science and Technology, Keio University, 3-14-1 Hiyoshi, Kohoku-ku, Yokohama, Kanagawa 223-8522, Japan*
[5]*Clinical Neurotechnology Laboratory, Department of Psychiatry and Psychotherapy, Neuroscience Research Center (NWFZ), Charité-University Medicine Berlin, Germany*
[6]*Department of Psychiatry and Psychotherapy, Eberhard-Karls-University Tübingen, Germany*

Correspondence should be addressed to Surjo R. Soekadar; surjo.soekadar@charite.de

Received 15 November 2018; Accepted 6 December 2018; Published 21 January 2019

Over the last decades, many axiomatic and dominating views on the functional architecture and workings of the mammalian central nervous system (CNS) had to be fundamentally reconsidered. Although the dominating view that the mature mammalian CNS is structurally immutable was repeatedly challenged, e.g., by studies showing collateral axonal sprouting and intracortical synaptic plasticity after a spinal cord injury (SCI) in cats [1, 2], the capacity of the lesioned CNS to reorganize was only fully appreciated after Merzenich and colleagues introduced their famous deafferentation studies in the 1980s [3, 4]. Besides showing that topographic cortical representations are maintained dynamically throughout life, they also provided compelling evidence that this self-organizing capacity of the CNS can relate to neurological recovery [5–7].

Based on this new understanding of CNS plasticity and the factors driving it, Taub et al. introduced a novel rehabilitation procedure that now belongs to the established repertoire of physiotherapists worldwide (Constraint-Induced Movement Therapy, CIMT) [7–9]. Being a good example for the successful translation of insights from basic research findings collected over several decades in animal studies into a new treatment strategy used in hospitals all over the world, the development of CIMT also exemplifies the long, strenuous and often very difficult path from bench to bedside.

This special issue acknowledges this challenging path and provides a forum for presenting the latest views and findings in the field of neurorehabilitation. Besides featuring a comprehensive review on the state-of-the-art in experimental stroke research by A.-S. Wahl ("State-of-the-Art Techniques to Causally Link Neural Plasticity to Functional Recovery in Experimental Stroke Research") and cognitive rehabilitation in Parkinson's disease by M. Díez-Cirarda et al. ("Neurorehabilitation in Parkinson's Disease: A Critical Review of Cognitive Rehabilitation Effects on Cognition and Brain"), this special issue includes a study by S.-L. Liew et al. that evaluated brain activity during action observation of 24 stroke survivors and 12 age-matched healthy controls using functional magnetic resonance imaging (fMRI) ("Laterality of Poststroke Cortical Motor Activity during Action Observation Is Related to Hemispheric Dominance"). They found that action observation is lateralized to the dominant, rather than ipsilesional, hemisphere. As this may reflect an interaction between the lesioned hemisphere and the dominant

hemisphere in driving lateralization of brain activity after stroke, they conclude that this finding should be carefully considered when characterizing poststroke neural activity.

M. R. Pereira-Jorge et al. ("Anatomical and Functional MRI Changes after One Year of Auditory Rehabilitation with Hearing Aids") describe the anatomical and functional MRI changes related to one year of auditory rehabilitation with hearing aids (HA) across 14 individuals diagnosed with bilateral hearing loss. While they found a reduction in activity in the auditory and language systems and an increase in visual and frontal cortical areas, the use of HA over one year increase the activity in the auditory and language cortices as well as multimodal integration areas. Moreover, they found an increased cortical thickness in multimodal integration areas, particularly the very caudal end of the superior temporal sulcus, the angular gyrus, and the insula. P. Álvarez Merino et al. ("Evidence Linking Brain Activity Modulation to Age and to Deductive Training") investigated the effect of deductive reasoning training on modulation of electric brain activity and compared this modulation between younger (mean age 21 ± 3.39 years) and older (mean age 68.92 ± 5.72 years) healthy adults. While younger adults showed symmetric bilateral activity in anterior brain areas in their study, older adults showed asymmetrical activity in anterior and posterior brain areas. They conclude that bilateral brain activity modulation may be an age-dependent mechanisms to maintain cognitive function under high demand.

To better understand the role of serotonergic receptors for functional recovery after SCI, K. Miazga et al. analyzed the mRNA of serotonergic 5-HT2A and 5-HT7 receptors (encoded by Htr2a and Htr7 genes) in motoneurons of rats with and without SCI ("Intraspinal Grafting of Serotonergic Neurons Modifies Expression of Genes Important for Functional Recovery in Paraplegic Rats"). They found that intraspinal grafting of serotonergic neurons can modify the expression of Htr2a and Htr7 genes suggesting that upregulation of these genes might account for the improved locomotion found after intraspinal grafting.

Based on a number of studies suggesting a neuroprotective effect of green tea (*Camellia sinensis*), P. M. Sosa et al. investigated whether green tea and red tea have a comparable effect on motor deficits and striatum oxidative damage in rats with hemorrhagic stroke ("Green Tea and Red Tea from *Camellia sinensis* Partially Prevented the Motor Deficits and Striatal Oxidative Damage Induced by Hemorrhagic Stroke in Rats"). They found that the two teas seemed equally effective.

M S. Sherwood et al. evaluated resting cerebral perfusion before and after transcranial direct current stimulation (tDCS), a form of transcranial electric stimulation (tES), applied to the left prefrontal cortex to investigate the underlying neural mechanisms of tDCS on cognitive brain functions ("Repetitive Transcranial Electrical Stimulation Induces Quantified Changes in Resting Cerebral Perfusion Measured from Arterial Spin Labeling"). They found that tDCS increased cerebral perfusion across many areas of the brain as compared to sham stimulation. As this effect originated in the locus coeruleus linked to the noradrenergic system, the authors suggest that the broad behavioral effects of frontal lobe tDCS might relate to a modulation of the locus coeruleus that excites the noradrenergic system.

S. Betti et al. ("Testing rTMS-Induced Neuroplasticity: A Single Case Study of Focal Hand Dystonia") used 1 Hz repetitive transcranial magnetic stimulation (rTMS) targeting the left primary motor cortex (M1) of an individual diagnosed with focal hand dystonia. rTMS was applied over five daily thirty-minute sessions. Using a fine-grained kinematic analysis, they found that rTMS resulted in improved motor coordination, a finding that underlines the importance of adopting measures that are sufficiently sensitive to detect behavioral improvements.

Only recently, novel neurotechnological tools, such as brain/neural-machine interfaces (B/NMI) [10–14] or closed-loop brain and spinal cord stimulation [15], were developed that provide promising means to modulate CNS plasticity triggering neural recovery. A remarkable demonstration of these new targeted neurotechnologies was recently provided by Wagner et al. [16] demonstrating restoration of walking in individuals who sustained a spinal cord injury several years ago with permanent motor deficits despite extensive rehabilitation efforts. A few months of individualized spatiotemporal electrical stimulation of the lumbosacral spinal cord resulted in regained voluntary control over previously paralyzed muscles, even in the absence of stimulation.

As our understanding of the underlying mechanisms of neural recovery improves and neurotechnologies advance, more of such demonstrations will be ahead of us. We hope that this special issue will contribute towards such improved understanding of the relationship between neural plasticity and functional recovery and will give new impulses on how neurorehabilitation can be advanced through neurotechnological tools.

Conflicts of Interest

The guest editors declare that there is no conflict of interest.

Toshiyuki Fujiwara
Junichi Ushiba
Surjo R. Soekadar

References

[1] C.-N. Liu and W. W. Chambers, "Intraspinal sprouting of dorsal root axons; development of new collaterals and preterminals following partial denervation of the spinal cord in the cat," *A.M.A. Archives of Neurology and Psychiatry*, vol. 79, no. 1, pp. 46–61, 1958.

[2] F. H. Gage, A. Bjorklund, and U. Stenevi, "Local regulation of compensatory noradrenergic hyperactivity in the partially denervated hippocampus," *Nature*, vol. 303, no. 5920, pp. 819–821, 1983.

[3] M. M. Merzenich, J. H. Kaas, J. Wall, R. J. Nelson, M. Sur, and D. Felleman, "Topographic reorganization of somatosensory cortical areas 3b and 1 in adult monkeys following restricted deafferentation," *Neuroscience*, vol. 8, no. 1, pp. 33–55, 1983.

[4] J. H. Kaas, M. M. Merzenich, and H. P. Killackey, "The reorganization of somatosensory cortex following peripheral nerve

damage in adult and developing mammals," *Annual Review of Neuroscience*, vol. 6, no. 1, pp. 325–356, 1983.

[5] W. M. Jenkins, M. M. Merzenich, M. T. Ochs, T. Allard, and E. Guic-Robles, "Functional reorganization of primary somatosensory cortex in adult owl monkeys after behaviorally controlled tactile stimulation," *Journal of Neurophysiology*, vol. 63, no. 1, pp. 82–104, 1990.

[6] C. Xerri, M. M. Merzenich, B. E. Peterson, and W. Jenkins, "Plasticity of primary somatosensory cortex paralleling sensorimotor skill recovery from stroke in adult monkeys," *Journal of Neurophysiology*, vol. 79, no. 4, pp. 2119–2148, 1998.

[7] E. Taub, "Movement in nonhuman primates deprived of somatosensory feedback," *Exercise and Sport Sciences Reviews*, vol. 4, pp. 335–374, 1976.

[8] E. Taub, G. Uswatte, and R. Pidikiti, "Constraint-induced movement therapy: a new family of techniques with broad application to physical rehabilitation–a clinical review," *Journal of Rehabilitation Research and Development*, vol. 36, no. 3, pp. 237–251, 1999.

[9] E. Taub, N. E. Miller, T. A. Novack et al., "Technique to improve chronic motor deficit after stroke," *Archives of Physical Medicine and Rehabilitation*, vol. 74, no. 4, pp. 347–354, 1993.

[10] J. Ushiba and S. R. Soekadar, "Brain-machine interfaces for rehabilitation of poststroke hemiplegia," *Progress in Brain Research*, vol. 228, pp. 163–183, 2016.

[11] S. R. Soekadar, N. Birbaumer, M. W. Slutzky, and L. G. Cohen, "Brain-machine interfaces in neurorehabilitation of stroke," *Neurobiology of Disease*, vol. 83, pp. 172–179, 2015.

[12] S. R. Soekadar, M. Witkowski, C. Gómez et al., "Hybrid EEG/EOG-based brain/neural hand exoskeleton restores fully independent daily living activities after quadriplegia," *Science Robotics*, vol. 1, no. 1, 2016.

[13] J. Clausen, E. Fetz, J. Donoghue et al., "Help, hope, and hype: ethical dimensions of neuroprosthetics," *Science*, vol. 356, no. 6345, pp. 1338-1339, 2017.

[14] S. Crea, M. Nann, E. Trigili et al., "Feasibility and safety of shared EEG/EOG and vision-guided autonomous whole-arm exoskeleton control to perform activities of daily living," *Scientific Reports*, vol. 8, no. 1, article 10823, 2018.

[15] A. Jackson and J. B. Zimmermann, "Neural interfaces for the brain and spinal cord–restoring motor function," *Nature Reviews. Neurology*, vol. 8, no. 12, pp. 690–699, 2012.

[16] F. B. Wagner, J. B. Mignardot, C. G. le Goff-Mignardot et al., "Targeted neurotechnology restores walking in humans with spinal cord injury," *Nature*, vol. 563, no. 7729, pp. 65–71, 2018.

Hindawi
Neural Plasticity
Volume 2018, Article ID 1401579, 10 pages
https://doi.org/10.1155/2018/1401579

Research Article

Evidence Linking Brain Activity Modulation to Age and to Deductive Training

P. Álvarez Merino, C. Requena, and F. Salto

Department of Psychology, Sociology and Philosophy, University of León, Campus de Vegazana, s/n, 24071 León, Spain

Correspondence should be addressed to P. Álvarez Merino; paulaalvarezmerino@gmail.com

Received 22 February 2018; Revised 29 August 2018; Accepted 14 October 2018; Published 25 November 2018

Guest Editor: Junichi Ushiba

Electrical brain activity modulation in terms of changes in its intensity and spatial distribution is a function of age and task demand. However, the dynamics of brain modulation is unknown when it depends on external factors such as training. The aim of this research is to verify the effect of deductive reasoning training on the modulation in the brain activity of healthy younger and older adults ($N = 47$ (mean age of 21 ± 3.39) and $N = 38$ (mean age of 68.92 ± 5.72)). The analysis reveals the benefits of training, showing that it lowers cerebral activation while increasing the number of correct responses in the trained reasoning task ($p < 0.001$). The brain source generators were identified by time-averaging low-resolution brain electromagnetic tomography (sLORETA) current density images. In both groups, a bilateral overactivation associated with the task and not with age was identified. However, while the profile of bilateral activation in younger adults was symmetrical in anterior areas, in the older ones, the profile was located asymmetrically in anterior and posterior areas. Consequently, bilaterality may be a marker of how the brain adapts to maintain cognitive function in demanding tasks in both age groups. However, the differential bilateral locations across age groups indicate that the tendency to brain modulation is determined by age.

1. Introduction

Brain activity adapts in time to the cognitive needs of an organism, altering its intensity and its distribution which can be measured through modulations in electrical brain activity [1]. Scientific literature offers two different approaches to the complex phenomenon of the electrical brain signal's modulation. One explicative strategy focuses on overactivation of brain activity as a function of the demand of tasks [2], while a second perspective explains modulation in terms of age and focuses on the idiosyncrasy of brain aging [3]. Many studies have verified how brain overactivation correlates with better performance in cognitive tasks. For example, the performance of older people who participated in a digit span task was better if they exhibited a bilateral pattern of brain activity compared to those who did not show such bilaterality [4]. Another memory study involving older adults with high and low memory capacities and younger adults reported that both the older adults with low memory capacity and the younger adults showed prefrontal asymmetry with greater activity in the right hemisphere [3]. While the performance of the younger adults was the most successful, that of the older adults with low memory capacity was the least. In the older adults with better memory, a pattern of bilateral activity was evidenced with similar results to those of the younger adults. When the task is more demanding for these older adults, the left prefrontal cortex is also activated. That is, a supplementary activation reflects the additional effort that these older adults make in order to access information [5]. On the other hand, the approach based on the difficulty gradient of the task describes the increment in brain activation and the involvement of wider brain areas as an adaptive strategy for functional performance both in older and in younger adults [6]. In this regard, an investigation in which younger and older adults had to resolve memory tasks of different complexity levels found that the dorsolateral prefrontal cortex was overactivated in older adults in order to achieve a performance similar to that of younger adults. In addition,

as the difficulty increased, the dorsolateral prefrontal cortex in younger adults activated as well [7].

The second perspective attributes brain activity modulation to age [8]. Namely, the cerebral plastic behavior in older adults makes it possible for them to relearn a new activation mode which is manifested in a deactivation of posterior regions along with a higher activation in previous regions [9]. For example, in tasks requiring the intervention of basic cognitive operations such as visual perception, the highest activation is not located in the posterior cognitive regions of older adults. This brain behavior is associated with age, but it does not necessarily involve cognitive decline [10]. In this regard, an extensive research study tested age-related cerebral changes using an episodic memory task (high complexity) as well as a visual perception one (low complexity) [11]. The results showed that regardless of the complexity of the task, a higher activation was localized in the prefrontal cortex. In addition, this activation correlates with better cognitive function, as opposed to an inverse correlation between performance and activity in the occipital region. Other studies have also shown age-related changes in the brain and cognitive strategies to solve executive control tasks [12]. In particular, the experiment was carried out with younger and older adults who faced a task with consecutive pairs whereby the first one constituted a cue and the second one a target. Subjects were instructed to respond to the target whenever it was preceded by the same cue. Otherwise, they should omit or refrain from responding. The results showed that, with age, the executive control strategies shifted in temporal distribution. That is, they were proactive in younger adults during the presentation of the cue and reactive in older adults in response to the target presentation. In addition, the neuroimaging analysis showed that only younger adults displayed higher activation of the dorsolateral prefrontal cortex and left hippocampus when the cue appeared rather than when the target was presented. On the other hand, it reveals an idiosyncratic behavior of cerebral aging in the amount of cognitive resources that are activated by the demand of a cognitive task. There seems to be a ceiling effect linked to how high the difficulty of the demand is in older adults, since brain activity lessens if the task is too hard [13]. An investigation in which younger and older adults had to resolve memory tasks of different complexity levels found that the prefrontal cortex was overactivated in both younger and older adults to achieve performance success [7]. However, beyond a certain level of demand, in older adults as opposed to younger adults, brain activity decreased, and so did their performance [14].

All in all, there is evidence of both task-dependent and age-dependent factors in brain activity modulation. Demanding tasks modulate brain activity both in younger and in older adults. However, simultaneously beyond the task demand, there is also idiosyncratic aged brain behavior. The state of the art includes two basic results: (1) when older adults face a demanding task, they require more brain activation than younger adults to obtain a similar performance level [6] and (2) when the task is demanding for all age groups, younger adult brains manifest an increased activation while older adult brains tend to diminish their brain activity [15, 16]. However, there are no known experimental studies that analyze the effect of training on the modulation of brain activity which in turn would help to clarify the relationship between the two explanatory approaches to brain modulation.

The current study is aimed at examining the modulation of EEG brain activity in a highly demanding cognitive task in younger and older adults before and after a reasoning training. In particular, the following hypotheses were tested experimentally: (a) baseline EEG activity will show a bilateral overactivation in younger adults rather than in older ones, (b) the posttraining evaluation will show bilateral overactivation in the older adults while it will disappear in the younger ones, and (c) the effect of training improves deductive reasoning performance by increasing the number of valid responses and decreasing the reaction time in both age groups.

2. Materials and Methods

2.1. Participants. Eighty-five subjects, divided into two age groups, voluntarily participated in this study. The group of younger adults consisted of 47 subjects with an average age of 24.21 ± 3.39 years. These subjects were students from the University of León whose participation was rewarded with 1 academic credit. On the other hand, the group of older adults consisted of another 38 subjects with an average age of 68.92 ± 5.72 years. These subjects were contacted through the senior center of León Council.

All participants were screened to be right-handed with normal or corrected vision and not currently under any stress (i.e., exams, job interviews, and grief). Additionally, older adults were screened to be cognitively intact (Mini-Mental Status Exam ≥ 28) [17]. This study was approved by the Ethics Committee of the University of León in 2017, and it was carried out following the deontological standards recognized by the Helsinki Declaration of 1975 (as revised in the 52nd Annual General Assembly in Edinburgh, Scotland, in October 2000), the standards of Good Clinical Practice, and the Spanish Legal Code regulating clinical research involving human subjects (Royal Decree 223/2004 about regulation of clinical trials).

2.2. Procedure. The experimental design consists of 99 deductive reasoning tasks that are presented in a time window of 3.5 seconds which includes the presentation of the task and the response time. There was an interval of 200 ms between tasks. Tasks were presented through the Mind Tracer (Neuronic S.A., Havana) on a 23-inch NEC screen. Subjects were requested to minimize their blinking as well as their postural movements. The program also provides conductual information about the number of correct and incorrect answers and reaction times.

For the basal evaluation and for posttraining evaluation, 99 deductive tasks were designed corresponding to the three types presented above. 33 items for each type of tasks were randomly distributed. In the basal evaluation, subjects were instructed to mandatorily respond to this instruction: "If the item follows a rule based on properties regarding figures, colors, number, shape, or shading, press the 'Ctrl' key;

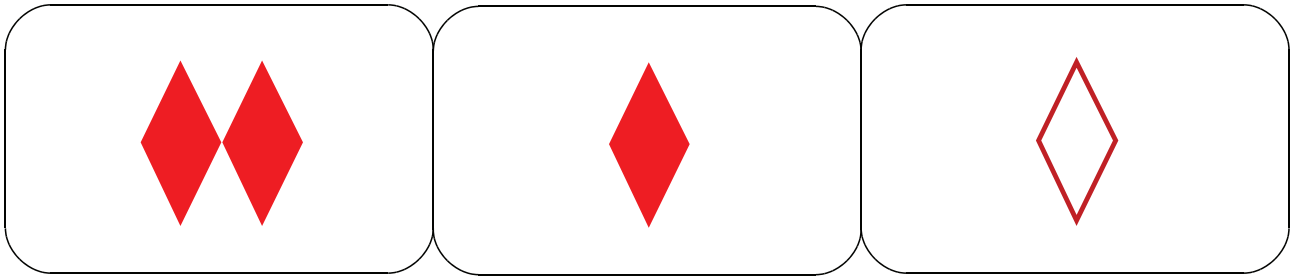

Figure 1: Case 1 type.

otherwise, press the 'spacebar' key." Notice that in the basal evaluation, the subject had no information or hints about the contents of the rules. The task was new and highly demanding, since the subject lacked any hints and did not know the rules of the task. For the posttraining, the subjects followed this instruction: "If the three cards have two or more properties in common, then (and only then) they form a set." In this case, subjects would respond by pressing the "Ctrl" key and otherwise by pressing the spacebar.

The initial registration lasted about 40 minutes: 20 minutes to prepare the EEG system (cleaning, placement of the electrodes, etc.) using MEDICID (Neuronic S.A., Havana) and another 20 minutes to run the test. After the initial recording, subjects undertook behavioural training of reasoning in a single session followed by a posttraining recording, with an approximate duration of 70 minutes: 30 minutes for the training itself and the remaining time for EEG data recording.

2.3. Stimuli. The paradigm used during the EEG acquisition was based on a subset of the cards that compose the deck of the card game set. The game was unknown to all participants, and it was instrumental in the training and evaluation of elemental logical deductions. This kind of task was chosen because human deductive abilities are known to be, under certain specific conditions, rather invariant with respect to age, culture, and education. In particular, the reduction of cognitive resources accompanying aging does not impede the preservation of elementary deductive abilities [18], specifically if inferential conclusions are relevant to their premises [17, 19]. Even if the cultural context partially determines reasoning, elementary deductive inference remains invariant across cultures [20] and education levels [21]. Additionally, deductive inferences occur both in linguistic and in visual support [22]. That is, there are deductions which are not sentential sequences of premises and conclusions but logically valid visual inferences such as those present in diagrams or geometrical proofs. Finally, an interesting peculiarity of deductive reasoning is its easiness to produce new tasks with simple instructions where it is easy to measure and control both the logical complexity (number of instances of employed rules) and the relational complexity (number of variables). In this research, these measures offer an objective demand gradient.

The deductive tasks presented and evaluated in this study are elementary logical (first order) inferences realized over a subset of the card game set. The cards presented items with certain characteristics: shape, color, number, and shading. There are three shapes, two colors, two numbers, and two shadings. Each item presents a trio of cards which shares zero, one, two, or three of these characteristics. By definition, any trio is a set if and only if the three cards share at least two properties. Determining whether an item (trio) is or is not a set is a purely deductive task, namely, a finite sequence of inferences which can be developed in a logically valid way and follows a recursive procedure which computes the truth values of the premises. Given that the subject perceives the properties of each card, the exercise of computing or deducing if the trio is a set is an elementary logical task. In the simplest scenario, it is enough to apply the definition of a set to verify that in fact, the cards in the trio share two properties. This situation automatically applies the rule of modus ponens (deduce B from {A, if A then B}). In the more complex scenario, instead of directly applying the definition after positive cases, we have counterexamples. In this case, the rule of modus tollens (deduce notA from {notB, if A then B}) can be used.

To elucidate the experimental design, we show an example of each of the three kinds of items presented to the subjects in the evaluation tests. Only in the first kind of case (see Figure 1) do the three cards share at least two properties, and consequently the trio satisfies the definition of a set.

The three cards in Figure 1 share the same shape and color; therefore, they are a set. From the only presentation of the trio and the application of negationless deductive rules, the reasoner may deduce that the item is a set. Observe how the reasoner may deduce the conclusion without going through all the properties of all objects in the cards: once form and color are shared, there is no need for further verifications.

The second type of case is a trio which shares only one property (see Figure 2).

The three cards share shape, but no other property. Therefore, this item is not a set. The inference behind this conclusion contains an application of the modus tollens rule, since by this rule the subject can refute each of the other properties (color, number, and shading) one by one.

Finally, Figure 3 shows the example of the third type of case in which no properties are shared by any card of the trio.

The subject may easily verify property by property that a characteristic is not shared in the trio, deducing by modus tollens that the trio is not a set. Note that in the three types of cases, the whole inference is elementary and deductively valid. Moreover, it is remarkable that the second and third

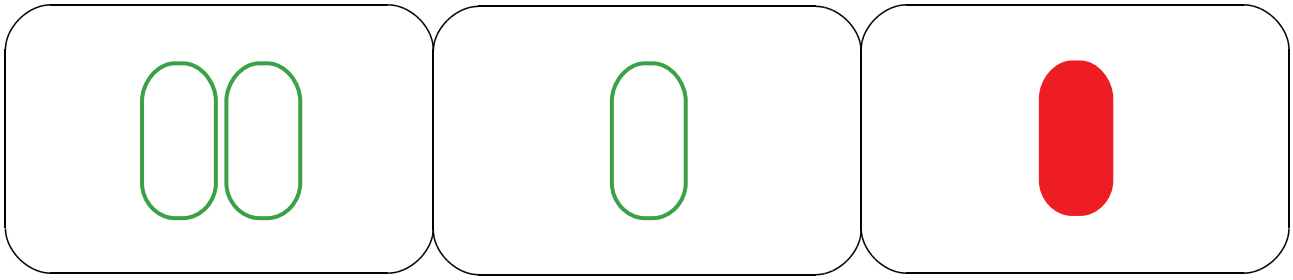

Figure 2: Case 2 type.

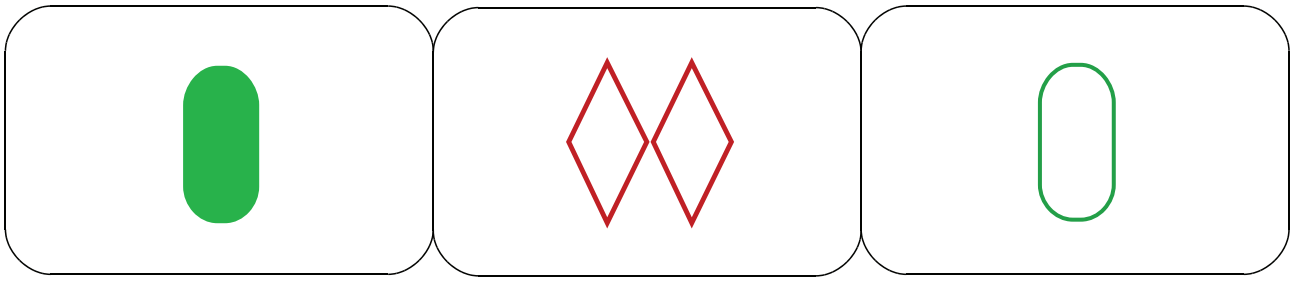

Figure 3: Case type 3.

types of cases have a slightly greater logical complexity than case 1, but their relational complexity is identical.

2.4. Training. All subjects received a personalized one-on-one training, which took place in the same session as the postevaluation. The point of the training was to produce valid deductive inferences by means of recursive or computable logical procedures which would prove whether a given item was (or was not) part of a set. In its first stage, the training focused on identifying sets and practicing at least 15 exercises of type 1 tasks with items that were not present in the basal evaluation. In its second stage, the training made the subject explain her deductive process out loud to the researcher who then corrected her as necessary. Since several logically equivalent procedures are equally acceptable, the personalized training adapts to the heuristical strategies proposed by the subject in case they are logically valid. Remarkably, the deductive training does not purport to teach the subject to reason logically but to bring into explicit conscience the logical properties of the inferences she already makes. For example, the conjunction operator (logical operator for "and") allows the subject to go over several cards to accumulate available conclusions. This initial training phase ends when the subject says she understands the task of identifying positive cases of a set and does not commit two consecutive errors in type 1 trials.

In the third training phase, the subject herself proposed examples of items that would be a set and described her reasoning out loud. Once her proposals were adequate, the training for types 2 and 3 began, which consisted of making the subject aware of the use of modus tollens to infer counterexamples to sets. For example, if one card did not share a property with another one in a given item, it was deduced to be a counterexample to a set. The training finished when the subject expressed her cognizance of the task and did not commit any errors. The standard duration of the personalized training process was between 20 and 30 minutes for each subject.

3. EEG Recording and Analysis

The EEG was recorded with a 64-channel amplifier (Neuronic System, Havana) and specific acquisition software (Neuronic EEG/Edition EEG Software). Reference electrodes were placed on the earlobes. In addition, electrooculography (EOG) was registered using three pairs of external electrodes in order to record the horizontal and vertical movement of the eyes. Electrode impedance was set for each subject before data collection but always kept below 5 kΩ. The recording was carried out using an Electrocap with Ag/AgCl electrodes, which made it possible to analyze the active scalp areas of the subjects. ERP signals and stimulus markers were continuously recorded at a sampling frequency of 200 Hz during the 20-minute presentation of the task. The signals were filtered using a band-pass finite impulse response filter with a Hamming window between 1 and 70 Hz. In addition, a 50 Hz notch filter was used in order to remove the power line artifact. Finally, a three-step artifact rejection algorithm was applied to minimize oculographic and myographic artifacts [23]: (1) components related to eye blinks, according to a visual inspection of the scalp maps and their temporal activations from independent component analysis (ICA), were discarded [24], (2) segmentation of each 3.5-second trial into one 1.5 s length trial ranging from 200 ms before stimulus onset to 1300 ms after stimulus onset, and (3) the thresholding of amplitude in each trial was established in five standard deviations of the signal. That is, trials in which at least five channels contained two samples that exceeded the threshold were taken out. Only correct answers were considered for further analysis. Next, a sliding window approach was used

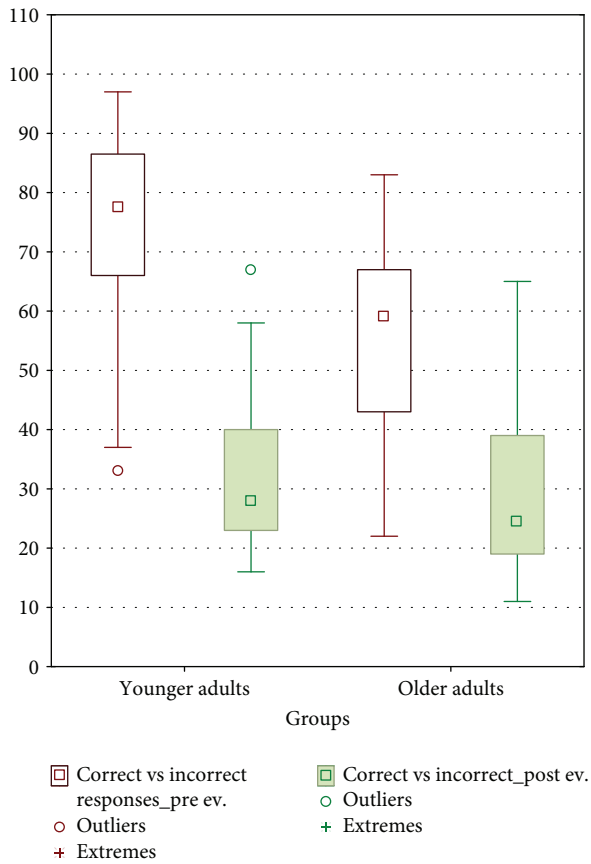

Figure 4: Mean and SD of correct and incorrect responses in younger and older adults.

for the localization of the major activation of each trial. Windows of 150 ms with an overlap of 90% were selected for measures of brain activity before and after training. Peak amplitude measurement took into account the most negative peak value within the temporal window of 400 to 550 ms after the stimulus.

3.1. Source Localization. This technique has been widely used to study the neural correlations of cognition, because it combines a high temporal resolution of the EEG technique with a reasonable spatial identification of the electrical signal of the cortical sources [25] (see http://www.uzh.ch/keyinst/NewLORETA/sLORETA/sLORETA.htm). The sLORETA software divides the brain into a total of 6239 cubic voxels with a resolution of 5 mm and estimates the density of the current sources [26].

In the current investigation, the source localization was estimated with the analysis of 64 electrodes located in the frontal, medial, temporal, and bilateral parietal regions. The subjects were registered using the International 10-20 system. The sources were calculated for every subject and each age group at the temporal window of 400 to 550 ms with the Brain Cracker (Neuronic S.A., Havana) which used the low-resolution electromagnetic tomography (LORETA implemented in sLORETA [26]). sLORETA source current density is calculated from the scalp-recorded ERP using a realistic head model from the Montreal Neurological Institute (MNI) [27], in which the 3-D solution space was restricted to only the cortical gray matter [28]. The ERP voltage topographic maps were made by plotting color-coded isopotentials obtained by interpolating the voltage values between the scalp electrodes in specific latencies. Voxelwise nonparametrical statistics as implemented in sLORETA were used.

4. Results

EEG records were processed using the "EEG edition" software (Neuronic S.A., Havana). Descriptive analyses for each group were calculated using a toolbox from MATLAB R2015a, which was developed in the laboratory of the researchers. Statistical analyses were performed using Statistica (Statistica 10). Brain Cracker and sLORETA software were used to determine source localization [26].

4.1. Correct versus Incorrect Responses. In relation to the number of correct responses in the basal evaluation, the younger adults obtained an average of 32.08 ± 12.29 whereas the group of older adults obtained an average of 31.05 ± 15.86. Regarding the number of correct response evaluations posttraining, the younger adults obtained an average of 74.79 ± 14.45 whereas the older adults obtained an average of 55.13 ± 16.94 (Figure 4).

To evaluate the effects of this training, a repeated measures model was used. The difference in the number of correct/incorrect responses between both age groups was significant ($F_{1,84} = 24.186$, $p = 0.001$), just like in postevaluation ($F_{1,84} = 188.596$, $p = 0.001$). It shows that the interaction between groups and postevaluation is significant ($F_{1,84} = 14.674$, $p = 0.001$) and the level of confidence was 0.95.

Post hoc analysis using the Tukey test revealed significant differences in the pre-postevaluation, both in the group of younger adults ($p < 0.001$) and in the group of older adults ($p < 0.001$). The training had a greater effect on the group of younger adults (Table 1 and Figure 5).

4.2. Reaction Times. The average reaction time in the basal evaluation was 1869.33 ± 608.79 ms for younger adults and 2097.89 ± 1046.77 ms for the older ones. The same parameter posttraining was 2898.50 ± 917.93 ms for younger adults and 2275.42 ± 635.92 ms for older adults (Figure 6).

To evaluate the effects of this training, a repeated measures model was used. The difference in reaction times between both age groups was not significant ($F_{1,84} = 1.700$, $p = 0.195$). However, the posttraining shows significant differences ($F_{1,84} = 40.920$, $p = 0.001$), especially in the group of younger adults. This is verified in the effect of the interaction, which is also significant ($F_{1,84} = 20.410$, $p = 0.001$), because the level of confidence is 0.95.

Post hoc analysis using the Tukey test reveals significant differences in the pre-postevaluation in the group of younger adults ($p < 0.001$) but not in the older adults ($p < 0.780$) (Table 2 and Figure 7).

4.3. Analysis of Source Localization with sLORETA. The descriptive analyses show that, in the basal evaluation of younger adults, there is activity in the right hemisphere

Table 1: Repeated measures analysis of variance for the number of correct and incorrect responses preevaluation and postevaluation in younger and older adults.

Effect	Repeated measures analysis of variance with effect sizes and powers (data_saveMeanxTask_repeated measures) Sigma-restricted parameterization Effective hypothesis decomposition				
	SS	Dgr. of freedom	MS	F	p
Intercept	395255.1	1	395255.1	2105.690	0.001
Groups	4539.9	1	4539.9	24.186	0.001
Error	15767.5	84	187.7		
Correct vs. incorrect	47302.5	1	47302.5	188.596	0.001
Correct vs. incorrect ∗ groups	3680.4	1	3680.4	14.674	0.001
Error	21068.3	84	250.8		

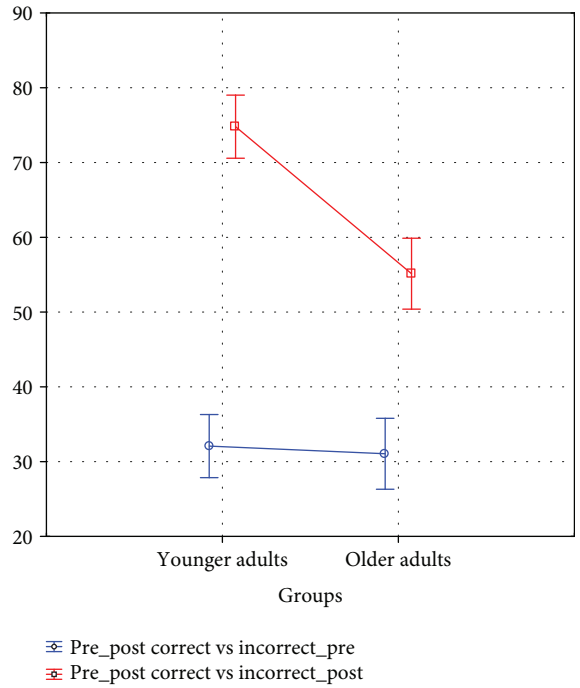

Figure 5: Significant differences between correct/incorrect responses preevaluation and postevaluation, within age groups.

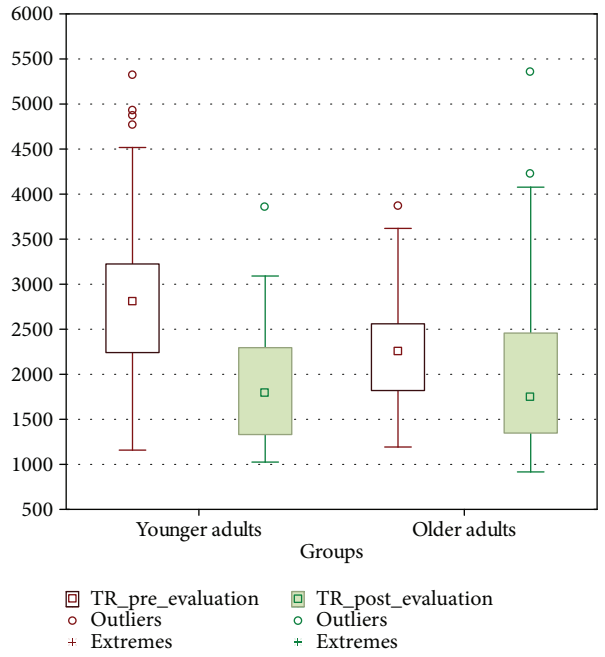

Figure 6: Mean and SD of reaction times in younger and older adults.

gyrus: orbitofrontal, superior temporal, and postcentral, as well as in the insula; there is also activity in the left superior, middle, and inferior temporal gyri. After training, that is, in the postevaluation of the group of younger adults, the activity was observed in the left hemisphere gyrus: angular, middle temporal, superior, and middle frontal (Figure 8).

In older adults, the activity in the basal evaluation was observed in the left superior and middle frontal gyrus, right parietal superior lobe, and right postcentral gyrus. In the group of older adults, the activity in the postevaluation was observed in the left postcentral gyrus and in the right lateral orbitofrontal gyrus (Figure 9).

5. Discussion

To the best of our knowledge, this is the first cerebral study assessing a reasoning training task in younger and older adults. The results confirm the effects of cognitive training on the brain and behavior, since the posttraining evaluation showed less brain activity and a better performance in the proposed cognitive task in both younger and older adults. On the other hand, the results confirmed hypothesis (a) of greater activation in younger adults during the basal evaluation compared to older adults. However, the results do not confirm hypothesis (b) since there were no increases in brain activity in older adults after training. In addition, hypothesis (c) on the effects of training on psychological variables is partially verified. The number of correct answers increased in the posttraining tasks; at the same time, reaction times grew unexpectedly. Globally considered cerebral results show that older adults may have less efficient cerebral resources for cognitive processing. Posttraining performance among older subjects is comparatively poor with respect to younger subjects, evidencing older adults' reduced cognitive capacity to buffer high demands. In addition, the trend of lower brain

Table 2: Repeated measures analysis of variance for the reaction time preevaluation and postevaluation in younger and older adults.

Effect	Repeated measures analysis of variance with effect sizes and powers (data_saveMeanxTask_repeated measures) Sigma-restricted parameterization Effective hypothesis decomposition				
	SS	Dgr. of freedom	MS	F	p
Intercept	885743564	1	885743564	921.6854	0.001
Groups	1633924	1	1633924	1.7002	0.019
Error	80724353	84	961004		
TR	15492871	1	15492871	40.9207	0.327
TR ∗ groups	7727593	1	7727593	20.4106	0.195
Error	31802969	84	378607		

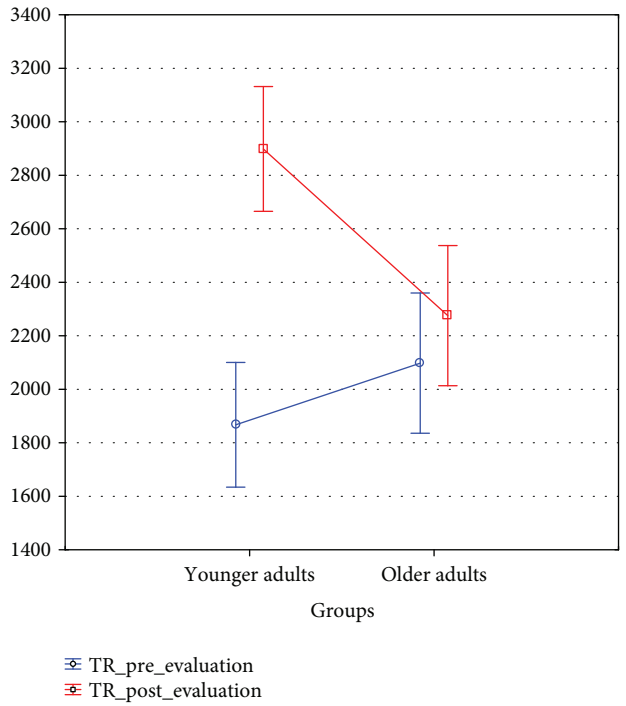

Figure 7: Significant differences between reaction times preevaluation and postevaluation, within age groups.

activation and worse performance in older adults, in both the baseline task and posttraining, may be interpreted as an age-dependent phenomenon rather than as a result of the demand of the task.

Through the psychological behavior of the participants, it is observed that both the number of successes and the reaction times increased after training in the two age groups. However, after training, the number of correct answers in younger adults reached almost 75% compared to the number of correct answers of the older ones that reached a little more than 50%. These results are consistent with an extensive body of information that supports a greater neurobiological decline that accompanies aging and explains why older adults obtain worse results than younger adults in cognitive performance tests [13, 29]. However, aging studies reveal large interindividual differences in cognitive performance where older adults' cognitive performance may equal that of younger adults with training and practice [30]. In this sense, the ACTIVE longitudinal study shows that older subjects who receive cognitive training maintain an improved capacity to reason above the baseline for ten years [31].

The increased reaction times after training, specifically in the younger group, contradict the hypothesis stated in the present study, which was based on the usual assumption that training an ability implies the diminution of the time required for its processing. However, when the peculiarities of the type of trained reasoning are taken into account, the increase in processing time is an index of robust cerebral consequences of training. The reasoning process applied by subjects after training is a computational step-by-step procedure which is fully explicit and compositional. That is, subjects must first process the cards composing the items, then combine them and apply the definition of a set. This is a well-known recursive or computational task [32] which consumes time as a linear function of its logical and relational complexity. In neuroscientific literature, there are only some initiatory studies on neural realizations of compositional processes in the brain [33, 34].

Therefore, while, in the untrained (basal) evaluation, the subject induced which rules could be applied without clues, in the trained version, the subject computed or applied deductive rules in a recursive and compositional way. Trained subjects did not need to grope for heuristic shortcuts as they had to in the basal evaluation. In this case, increased time is consequently an evidence of the effect of training.

The results in the source localization show a greater cerebral activation in the basal evaluation (which is more demanding) in both age groups. Bilateral cooperation is present in the realization of the basal evaluation, but the activation in the group of younger adults is located in the frontal areas, while in the group of older adults, the activation affects posterior as well as anterior areas (see Figures 8 and 9). In this case, the reviewed literature [35] attributes this kind of overrecruitment to a compensatory activation that allows a task to be successfully carried out. It is important to note that in the basal evaluation, the subject must discover the rules that fit the elements of each item. Therefore, the basal evaluation involves a greater use of cerebral and cognitive resources than if the instructions of the task are already known. In the case of older adults, both perceptive resources and more complex abstract resources are used in the basal evaluation, which contradicts the results of the reviewed literature [36]. In particular, some investigations found that due to the loss of sensory acuity, there was a decrease in the activation of anterior areas in favor of the activation of posterior areas [10, 37]. This loss means that basic cognitive operations and familiar tasks become more complex for older adults, and they have to relearn new modulations of brain activity and cognitive resources. However, the fact that the task of the study is visual explains in part why there is brain activity in the anterior areas.

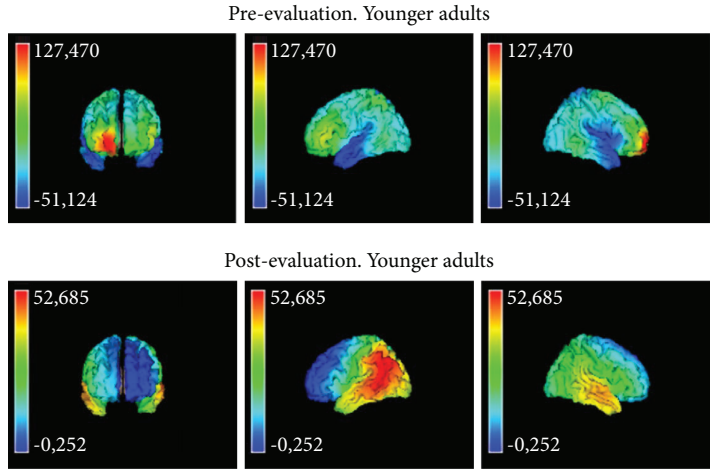

Figure 8: Analysis of source localization pre-postevaluation in younger adults.

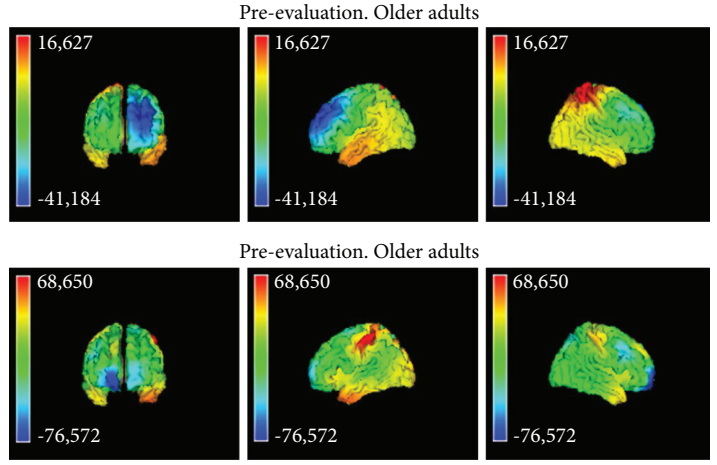

Figure 9: Analysis of source localization in basal and posttraining evaluation, within age groups.

The localization of sources of brain activity after training in younger adults goes from being bilateral to focal. In particular, activation is now focused on the left medial angular gyrus, the temporal and frontal areas, and the left superior frontal area. Other investigations also related these cerebral areas to deductive reasoning [38]. Therefore, the results show that the estimate of the demand of the task posttraining in this group has decreased with respect to the baseline task. In the case of older adults, the training does not cause such remarkable brain activity changes, and the strategy of bilateral activation of anterior and posterior areas is maintained. In particular, the parietal and fronto-orbital areas are activated, which again produces a wide overlap between the perceptual and abstract resources also used in the basal evaluation. The surprising lower brain activation posttraining with respect to the basal evaluation contradicts hypothesis (b) about older adults. One explanation could be a ceiling effect linked to high levels of demand in older adults [1]. That is, when older adults face a demanding task that is beyond their capacity, their performance level and brain activity both decrease [13]. However, the better cognitive results and the fact that the activation in the two groups is lower after training are proofs of the effect of training on cognitive and cerebral activity.

In summary, bilaterality may be a marker of how the brain adapts to maintain cognitive function in demanding tasks in both age groups. However, the differential bilateral locations across age groups indicate that the tendency of the brain to modulate is determined by age. One limitation of the study concerns the fact that all tasks are visual, thus restricting the possibility of verifying if posterior activation in older adults is due to the visual tasks. The high demand of the tasks and the short training period of the study may explain why older subjects improved 20% less than younger adults. Future research should replicate these results with nonvisual tasks and longer training periods to profoundly understand the benefits obtained from practice and training at a neurological level.

Data Availability

The data used to support the findings of this study are available from the corresponding author upon request.

Conflicts of Interest

The authors declare that they have no conflicts of interest.

References

[1] J. R. Rieck, K. M. Rodrigue, M. A. Boylan, and K. M. Kennedy, "Age-related reduction of BOLD modulation to cognitive difficulty predicts poorer task accuracy and poorer fluid reasoning ability," *NeuroImage*, vol. 147, no. 1, pp. 262–271, 2017.

[2] F. Grandi and J. Tirapu Ustárroz, "Neurociencia cognitiva del envejecimiento: modelos explicativos," *Revista Española de Geriatría y Gerontología*, vol. 52, no. 6, pp. 326–331, 2017.

[3] R. Cabeza, "Hemispheric asymmetry reduction in older adults: the HAROLD model," *Psychology and Aging*, vol. 17, no. 1, pp. 85–100, 2002.

[4] P. A. Reuter-Lorenz, J. Jonides, E. E. Smith et al., "Age differences in the frontal lateralization of verbal and spatial working memory revealed by PET," *Journal of Cognitive Neuroscience*, vol. 12, no. 1, pp. 174–187, 2000.

[5] D. Barulli and Y. Stern, "Efficiency, capacity, compensation, maintenance, plasticity: emerging concepts in cognitive reserve," *Trends in Cognitive Sciences*, vol. 17, no. 10, pp. 502–509, 2013.

[6] G. T. Stebbins, M. C. Carrillo, J. Dorfman et al., "Aging effects on memory encoding in the frontal lobes," *Psychology and Aging*, vol. 17, no. 1, pp. 44–55, 2002.

[7] K. A. Cappell, L. Gmeindl, and P. A. Reuter-Lorenz, "Age differences in prefontal recruitment during verbal working memory maintenance depend on memory load," *Cortex*, vol. 46, no. 4, pp. 462–473, 2010.

[8] A. Osorio, S. Fay, V. Pouthas, and S. Ballesteros, "Ageing affects brain activity in highly educated older adults: an ERP study using a word-stem priming task," *Cortex*, vol. 46, no. 4, pp. 522–534, 2010.

[9] D. Payer, C. Marshuetz, B. Sutton, A. Hebrank, R. C. Welsh, and D. C. Park, "Decreased neural specialization in old adults on a working memory task," *Neuroreport*, vol. 17, no. 5, pp. 487–491, 2006.

[10] J. Ansado, O. Monchi, N. Ennabil, S. Faure, and Y. Joanette, "Load-dependent posterior–anterior shift in aging in complex visual selective attention situations," *Brain Research*, vol. 1454, pp. 14–22, 2012.

[11] A. H. Gutchess, R. C. Welsh, T. Hedden et al., "Aging and the neural correlates of successful picture encoding: frontal activations compensate for decreased medial-temporal activity," *Journal of Cognitive Neuroscience*, vol. 17, no. 1, pp. 84–96, 2005.

[12] I. T. Z. Dew, N. Buchler, I. G. Dobbins, and R. Cabeza, "Where is ELSA? The early to late shift in aging," *Cerebral Cortex*, vol. 22, no. 11, pp. 2542–2553, 2012.

[13] J. R. Rieck, K. M. Rodrigue, M. A. Boylan, and K. M. Kennedy, "Age-related reduction of BOLD modulation to cognitive difficulty predicts poorer task accuracy and poorer fluid reasoning ability," *NeuroImage*, vol. 147, pp. 262–271, 2017.

[14] N. J. Schneider-Garces, B. A. Gordon, C. R. Brumback-Peltz et al., "Span, CRUNCH, and beyond: working memory capacity and the aging brain," *Journal of Cognitive Neuroscience*, vol. 22, no. 4, pp. 655–669, 2010.

[15] C. Opdebeeck, A. Martyr, and L. Clare, "Cognitive reserve and cognitive function in healthy older people: a meta-analysis," *Aging, Neuropsychology, and Cognition*, vol. 23, no. 1, pp. 40–60, 2016.

[16] M. F. Folstein, S. E. Folstein, and P. R. McHugh, ""Mini-mental state": a practical method for grading the cognitive state of patients for the clinician," *Journal of Psychiatric Research*, vol. 12, no. 3, pp. 189–198, 1975.

[17] E. L. Beatty and O. Vartanian, "The prospects of working memory training for improving deductive reasoning," *Frontiers in Human Neuroscience*, vol. 9, p. 56, 2015.

[18] J. M. Tommerdahl, W. McKee, M. Nesbitt et al., "Do deductive and probabilistic reasoning abilities decline in older adults?," *Journal of Applied Biobehavioral Research*, vol. 21, no. 4, pp. 225–236, 2016.

[19] P. Álvarez Merino, C. Requena Hernández, and F. Salto Alemany, "La integración más que la edad influye en el rendimiento del razonamiento deductivo," *International Journal of Developmental and Educational Psychology*, vol. 1, no. 2, p. 221, 2016.

[20] H. Mercier, "The argumentative theory: predictions and empirical evidence," *Trends in Cognitive Sciences*, vol. 20, no. 9, pp. 689–700, 2016.

[21] H. Markovits, J. Brisson, P. L. de Chantal, and C. M. St-Onge, "Elementary schoolchildren know a logical argument when they see one," *Journal of Cognitive Psychology*, vol. 28, no. 7, pp. 877–883, 2016.

[22] G. Allwein and J. Barwise, *Logical Reasoning with Diagrams*, Oxford University Press, 1996.

[23] J. Gomez-Pilar, J. Poza, A. Bachiller, C. Gómez, V. Molina, and R. Hornero, "Neural network reorganization analysis during an auditory oddball task in schizophrenia using wavelet entropy," *Entropy*, vol. 17, no. 12, pp. 5241–5256, 2015.

[24] S. Makeig, S. Debener, J. Onton, and A. Delorme, "Mining event-related brain dynamics," *Trends in Cognitive Sciences*, vol. 8, no. 5, pp. 204–210, 2004.

[25] R. Thatcher, D. North, and C. Biver, "LORETA EEG phase reset of the default mode network," *Frontiers in Human Neuroscience*, vol. 8, no. 1, p. 529, 2014.

[26] R. D. Pascual-Marqui, R. J. Biscay, J. Bosch-Bayard et al., "Assessing direct paths of intracortical causal information flow of oscillatory activity with the isolated effective coherence (iCoh)," *Frontiers in Human Neuroscience*, vol. 8, p. 448, 2014.

[27] J. Mazziotta, A. Toga, A. Evans et al., "A probabilistic atlas and reference system for the human brain: International Consortium for Brain Mapping (ICBM)," *Philosophical Transactions of the Royal Society of London B: Biological Sciences*, vol. 356, no. 1412, pp. 1293–1322, 2001.

[28] J. L. Lancaster, M. G. Woldorff, L. M. Parsons et al., "Automated Talairach atlas labels for functional brain mapping," *Human Brain Mapping*, vol. 10, no. 3, pp. 120–131, 2000.

[29] N. Raz and K. M. Rodrígue, "Differential aging of the brain: patterns, cognitive correlates and modifiers," *Neuroscience & Biobehavioral Reviews*, vol. 30, no. 6, pp. 730–748, 2006.

[30] C. Requena, A. Turrero, and T. Ortiz, "Six-year training improves everyday memory in healthy older people. Randomized controlled trial," *Frontiers in Aging Neuroscience*, vol. 8, no. 1, p. 135, 2016.

[31] G. W. Rebok, K. Ball, L. T. Guey et al., "Ten-year effects of the advanced cognitive training for independent and vital elderly cognitive training trial on cognition and everyday functioning in older adults," *Journal of the American Geriatrics Society*, vol. 62, no. 1, pp. 16–24, 2014.

[32] G. S. Boolos, J. P. Burgess, and R. C. Jeffrey, *Computability and Logic*, Cambridge University Press, 2002.

[33] N. T. Franklin and M. J. Frank, "Compositional clustering in task structure learning," *PLOS Computational Biology*, vol. 14, no. 4, article e1006116, 2018.

[34] C. Reverberi, K. Görgen, and J. D. Haynes, "Compositionality of rule representations in human prefrontal cortex," *Cerebral Cortex*, vol. 22, no. 6, pp. 1237–1246, 2012.

[35] N. R. Lighthall, S. A. Huettel, and R. Cabeza, "Functional compensation in the ventromedial prefrontal cortex improves memory-dependent decisions in older adults," *The Journal of Neuroscience*, vol. 34, no. 47, pp. 15648–15657, 2014.

[36] C. L. Grady, J. M. Maisog, B. Horwitz et al., "Age-related changes in cortical blood flow activation during visual processing of faces and location," *The Journal of Neuroscience*, vol. 14, no. 3, pp. 1450–1462, 1994.

[37] S. W. Davis, N. A. Dennis, S. M. Daselaar, M. S. Fleck, and R. Cabeza, "Que PASA? The posterior-anterior shift in aging," *Cerebral Cortex*, vol. 18, no. 5, pp. 1201–1209, 2008.

[38] G. Baggio, P. Cherubini, D. Pischedda, A. Blumenthal, J. D. Haynes, and C. Reverberi, "Multiple neural representations of elementary logical connectives," *NeuroImage*, vol. 135, pp. 300–310, 2016.

Hindawi
Neural Plasticity
Volume 2018, Article ID 9303674, 13 pages
https://doi.org/10.1155/2018/9303674

Research Article

Anatomical and Functional MRI Changes after One Year of Auditory Rehabilitation with Hearing Aids

M. R. Pereira-Jorge,[1] K. C. Andrade,[2] F. X. Palhano-Fontes,[2] P. R. B. Diniz,[3] M. Sturzbecher,[1] A. C. Santos,[1,4] and D. B. Araujo[2]

[1]*Department of Neuroscience and Behavior, University of São Paulo, Ribeirao Preto, SP, Brazil*
[2]*Brain Institute/Onofre Lopes University Hospital, Federal University of Rio Grande do Norte (UFRN), Natal, RN, Brazil*
[3]*Department of Internal Medicine, Federal University of Pernambuco, Recife, PE, Brazil*
[4]*Department of Internal Medicine, University of São Paulo, Ribeirao Preto, SP, Brazil*

Correspondence should be addressed to D. B. Araujo; draulio@neuro.ufrn.br

Received 23 February 2018; Revised 8 July 2018; Accepted 8 August 2018; Published 10 September 2018

Academic Editor: Surjo R. Soekadar

Hearing aids (HAs) are an effective strategy for auditory rehabilitation in patients with peripheral hearing deficits. Yet, the neurophysiological mechanisms behind HA use are still unclear. Thus far, most studies have focused on changes in the auditory system, although it is expected that hearing deficits affect a number of cognitive systems, notably speech. In the present study, we used audiometric evaluations in 14 patients with bilateral hearing loss before and after one year of continuous HA use and functional magnetic resonance imaging (fMRI) and cortical thickness analysis in 12 and 10 of them compared with a normal hearing control group. Prior to HA fitting, fMRI activity was found reduced in the auditory and language systems and increased in visual and frontal areas, expanding to multimodal integration cortices, such as the superior temporal gyrus, intraparietal sulcus, and insula. One year after rehabilitation with HA, significant audiometric improvement was observed, especially in free-field Speech Reception Threshold (SRT) test and functional gain, a measure of HA efficiency. HA use increased fMRI activity in the auditory and language cortices and multimodal integration areas. Individual fMRI signal changes from all these areas were positively correlated with individual SRT changes. Before rehabilitation, cortical thickness was increased in parts of the prefrontal cortex, precuneus, fusiform gyrus, and middle temporal gyrus. It was reduced in the insula, supramarginal gyrus, medial temporal gyrus, occipital cortex, posterior cingulate cortex, and claustrum. After HA use, increased cortical thickness was observed in multimodal integration regions, particularly the very caudal end of the superior temporal sulcus, the angular gyrus, and the inferior parietal gyrus/superior temporal gyrus/insula. Our data provide the first evidence that one year of HA use is related to functional and anatomical brain changes, notably in auditory and language systems, extending to multimodal cortices.

1. Introduction

Peripheral hearing deficits have a profound impact on the central auditory system, hampering individual communication and social interaction [1]. Individuals with hearing impairment can benefit from rehabilitation with cochlear implant (CI) and acoustic hearing aid (HA) devices. In both cases, patients experience significant improvement in their general condition, including cognitive abilities such as memory and language comprehension [2, 3].

Little is known, however, about neurophysiological mechanisms underlying these beneficial changes, and most knowledge on the topic is still based on animal models. Lesions to different segments of the auditory system are associated with specific changes in the neuronal representation of sound stimuli in cats [4], monkeys [5], mice [6], birds [7], and rabbits [8]. Furthermore, molecular and electrophysiological evidences show that rehabilitation with CI, for instance, leads to changes in the auditory system [8, 9].

In humans, advances in neuroimaging have expanded considerably the exploration of the auditory system, both in normal hearing subjects [10] and in patients with hearing impairment [11, 12]. Positron emission tomography (PET) and functional MRI (fMRI) have already found consistent

reduced activity of the auditory cortex in patients with hearing deficits [13, 14], which is at least partially recovered with CI and HA [12, 14, 15].

Only very few studies used neuroimaging to probe the impact of auditory rehabilitation over higher cognitive functions, and most of them have focused on language cortices, particularly Wernicke's area (Brodmann area—BA22) [12, 16]. In general, auditory deprivation leads to decreased activation of this area, which is recovered at least partially by rehabilitation, for instance, with CI [17]. It has been regarded as a fact that the use of hearing devices allows access to the auditory information to language centers, therefore leading to increased activity of this area. However, to our knowledge, these are still no solid evidence suggesting that this is the case or if there are other mechanisms involved. Thus, the first aim of this longitudinal study is to investigate the impact of HA use over audiometric scales, anatomical and functional MRI, and their correlations.

Furthermore, it is well known that the integration of auditory and visual information greatly improves the ability of language comprehension [18]. In fact, patients with hearing deficits often exhibit increased activity in areas related to visual functions, during auditory stimulation [19, 20]. Therefore, we also aimed to deeply explore brain areas involved in multimodal integration, such as the superior temporal sulcus (STS), the middle intraparietal sulcus (IT, BA40), the inferior frontal gyrus (IFG, BA44, BA45, and BA47), and the insula (BA13). The second objective of this study was to explore effects of auditory deprivation and recovery in sensory integration systems, for aurally delivered stimuli.

2. Material and Methods

This work was approved by the Ethics and Research Committee of the University of São Paulo, Ribeirao Preto School of Medicine (no. 2413/2007). Written informed consent was obtained from all participants. The data that support the findings of this study are available from the corresponding author upon request.

2.1. Subjects. Two groups participated in the current study: 14 postlingual deaf patients (P) with sensorineural hearing loss (5 women, age = 51.29 ± 18.8 years) and 11 normal hearing control group (CG) (5 women, age = 46.54 ± 19.88 years). At the time of recruitment, all patients had mild to severe bilateral sensorineural hearing loss and were referred to us by an otorhinolaryngologist for HA use (see Suppl. Table 1 for clinical details).

2.2. Audiometric Evaluation and Hearing Aid. The HAs used were manufactured by Widex (Lynge, Denmark). Four patients were fitted with completely in the canal (CIC) HA, and ten patients were fitted with intracanal (ITC) HA, with digital processing and compression (Suppl. Table 1). During the first two months of HA fitting, patients were evaluated weekly. After acclimatization, all patients were asked to use the HA for at least 10 hours a day.

Audiological evaluation followed the Brazilian protocol and occurred twice: right before HA fitting and right after one year of continuous HA use. All patients underwent pure tone audiometry tests by air and bone in an acoustic cabin, with headphones, for the following frequencies: 250 Hz, 500 Hz, 1000 Hz, 2000 Hz, 3000 Hz, 4000 Hz, 6000 Hz, and 8000 Hz. The pure tone auditory threshold was defined as the minimum level of sound intensity necessary for the pure tone, at each frequency, to be perceived. Patients were instructed to press a button every time they heard a sound (whistle) in the ear being tested. The tones began at higher sound levels that were gradually lowered from 120 dB to 15 dB. In patients with asymmetric loss, we started with the better ear. The test was performed for all frequencies on one ear first and then the other ear. Pure tone averages (PTA) were computed as the average of the thresholds obtained for the frequencies of 500, 1000, and 2000, according to Davis and Silverman [21].

Also, in an acoustic cabin, we evaluated the patient's ability to recognize speech sounds and measured the Speech Reception Threshold (SRT) for disyllables [22]. SRT is defined as the lowest sound level in which the patient is able to perceive and to repeat out loud correctly 50% of the words presented.

Subjects were also submitted to bone pure tone audiometry in which a pure tone signal is delivered by a bone vibrator (coupled to the arc) placed onto the individuals' mastoid. Hearing thresholds were obtained for the same frequencies used in the air pure tone audiometry. Only patients with sensorineural hearing loss were included, defined as those with equal thresholds measured by air and bone audiometry.

Pure tone audiometry and SRT were also performed in free field. Patients were positioned in an acoustic cabin, this time without headphones [22]. They were instructed to press a button whenever they perceived a sound stimulus. Free-field evaluation allows the calculation of functional gain (FG), a procedure defined by Pascoe [23], and is used to evaluate the efficiency of HA interventions. It consists of computing the percentage change in free field by comparing aided and unaided thresholds, i.e., with and without HA in place.

We first performed the evaluation without HA in place and then with HA positioned in one ear only, while the other ear remained without HA. Functional gain (FG) = aided threshold minus the unaided threshold. Thresholds were obtained for each ear separately. Patients remained seated with one ear pointing to a speaker positioned in the horizontal plane of the ear. First, the tested ear had the HA in place, while the other ear was unaided. Then, HA was removed, and a new threshold was obtained, this time with both ears unaided. The same procedure was repeated with the other ear pointing to the speaker.

Between-group comparison (patients vs. control group) was assessed by the Mann–Whitney U test, while within-group differences (patients before HA use × patients after HA use) were inspected by the Wilcoxon test for two dependent samples.

2.3. fMRI Acquisition. There were two MRI sessions: right before HA fitting and after one year of HA use. Subjects were scanned in a 1.5 T scanner (Siemens, Magneton Vision, Erlangen, Germany) with a commercially available TX/RX

head coil. fMRI acquisition used an echo-planar imaging (EPI) sequence, with the following parameters: 66 volumes, each one composed of 16 axial slices covering both hemispheres, TR = 4600 ms, TE = 60 ms, *flip angle* = 90°, FOV = 220 mm, matrix = 128 × 128, and slice thickness = 5 mm.

Whole brain anatomical T1-weighted images were also acquired using a 3D gradient-recalled echo (GRE) sequence, with the following parameters: TR = 9.7 ms, TE = 4.0 ms, matrix size = 256 × 256, *flip angle* = 12°, FOV = 256 mm, slice number = 154, and slice thickness = 1 mm.

2.4. Experimental Paradigm. fMRI auditory stimuli were delivered by MRI compatible headphones (Siemens, Erlangen, Germany) maintaining the same sound level in both ears and for both sessions: before and after HA fitting. The task consisted of listening to a story, presented in a block design, with five blocks of the story (27.5 seconds each) interrupted with five blocks of rest (27.5 seconds each) [24]. The same story was used in both sessions, recorded by a male voice, and delivered to both ears, using the same sound level in both sessions and for all patients (30 dB). Subjects were asked to report the story's content after each session, and story comprehension was rated using a 0–5 Likert scale (0—did not understand at all, 1—understood isolated words, 2—understood 25% of the story, 3—understood 50% of the story, 4—understood 75% of the story, and 5—understood the entire story). Prior to fMRI acquisition, subjects were carefully instructed not to move while in the scanner and to pay as much attention as possible to the story being told.

2.5. fMRI Analysis. fMRI data were processed using BrainVoyager QX 1.86 (Brain Innovation, Maastricht, Netherlands) according to the same procedures described elsewhere [24, 25]. Preprocessing steps consisted of motion correction, high pass temporal filter at 0.01 Hz, spatial filtering (FWHM = 4 mm), and transformation into Talairach space. fMRI group differences were analyzed using a fixed-effect general linear model (GLM) with separate subject predictors. Clusters were selected using a threshold corrected for multiple comparisons ($q[\mathrm{FDR}] < 0.05$) and with an extension of at least 50 mm^3. Group analysis included 2 orthogonal contrasts: (i) controls (CG) vs. patients before intervention (PB) and (ii) patients before intervention (PB) vs. patients after intervention (PA).

2.6. Correlation Analysis. A *Pearson* correlation analysis was used to assess whether individual fMRI β-values were correlated with individual changes in SRT with headphones, computed as a global difference between thresholds observed before and after intervention, according to [SRT (right ear before) + SRT (left ear before)] – [SRT (right ear after) + SRT (left ear after)]. Correlation was computed in specific regions of interest (ROI), involved in the auditory and Wernicke's area (BA22, BA41, and BA42), as well as in brain areas related to multimodal integration, such as the superior temporal sulcus (STS), the middle intraparietal sulcus (IT), and the insula.

2.7. Cortical Thickness (CT). In order to evaluate whether the use of the HA would also be associated with neuroanatomical changes, we used FreeSurfer image analysis suite for cortical reconstruction and volumetric segmentation, which is documented and freely available for download online (http://surfer.nmr.mgh.harvard.edu/). Processing was performed on a Mac-Pro OS X 10.8.2, 2 × 2.26 GHz Quad-Core Intel Xeon. Preprocessing steps included grey/white segmentation, segmentation of the pial surface, for final computation of cortical thickness (CT) maps [26]. Statistical significance was set at $p < 0.01$.

3. Results

3.1. Audiometric Evaluation. Figure 1(a) shows the pure tone averages (PTA) obtained with headphones for all groups. PTA with headphones in the control group (CG) revealed a threshold of 15.68 ± 8.34 dBHL for the right and 14.66 ± 8.47 dBHL for the left ear, which are within the range of normality for adults (0–25 dBHL). Supplementary Figure 1 shows the CG thresholds with headphones for all tested frequencies. Supplementary Table 2 shows individual CG PTA.

Before intervention, PTA with headphones in the patient group was 53.58 ± 12.94 dBHL for the right ear and 54.33 ± 12.10 dBHL for the left ear (Figure 1(a)). After one year of HA use, PTA changed to 53.03 ± 13.61 dBHL and 52.00 ± 11.77 dBHL, respectively, for the right and left ears, which were not significantly different from baseline (Figure 1(a)). We found statistically significant differences between controls and patients before intervention ($p < 0.001$, Figure 1(a)). All patients showed a tonal threshold superior to 25 dBHL for all frequencies tested, both before and after interventions (see Suppl. Figure 2 and Suppl. Table 3 for individual results).

Figure 1(b) shows Speech Reception Threshold (SRT) with headphones for all groups studied. The SRT measured with headphones in the CG is considered normal: 10.91 ± 7.01 dBHL and 11.36 ± 7.10 dBHL for the right ear and the left ear, respectively (Figure 1(b)). At baseline, patients showed SRT of 45.71 ± 14.92 and 46.43 ± 11.67 for the right and left ears, respectively (Figure 1(b)). These values reduced significantly after HA use and averaged 36.79 ± 15.14 for the right ear ($p < 0.001$) and 38.21 ± 11.03 ($p < 0.002$) for the left ear (Figure 1(b)). Although a significant improvement was observed, SRT with headphones was still significantly different between controls and patients after HA use, for both ears ($p < 0.0001$, Figure 1(b)). Supplementary Tables 2 and 4 show individual SRT with headphones for all groups studied.

Free-field PTA and SRT were evaluated in patients only (Figure 2). Before HA use, free-field PTA thresholds averaged 33.15 ± 8.48 dBHL (right ear) and 32.68 ± 10.29 dBHL (left ear). After HA use, free-field PTA improved significantly in both ears ($p < 0.001$), reaching 27.68 ± 5.64 dBHL (right ear) and 28.27 ± 7.40 dBHL (left ear). Supplementary Table 5 shows individual free-field PTA, and Supplementary Figure 3 shows free-field tonal audiometry for all frequencies.

Likewise, free-field SRT improved significantly after HA use for both ears ($p < 0.001$, Figure 2(b)). It changed from 24.93 ± 8.36 dBHL (right ear) and 25.71 ± 5.50 dBHL (left ear) to 17.86 ± 8.48 dBHL (right ear) and 18.21 ± 4.64 dBHL

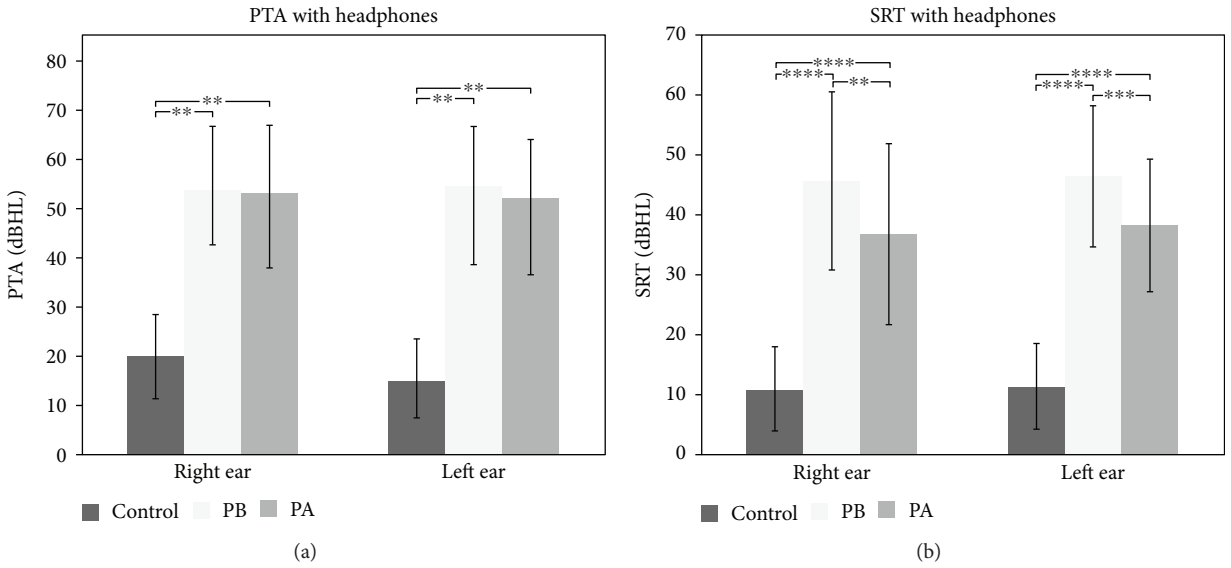

Figure 1: (a) PTA and (b) SRT with headphones of the control group, the patients before HA use (PB), and patients after HA use (PA). (a) Mean and standard deviations are shown for right and left ears. Results of PTA with headphones revealed statistical differences ($^{**}p < 0.001$) in both ears between the CG and PB and PA. When comparing the PB with the PA, statistically significant difference was observed only for the left ear ($^{*}p < 0.04$). (b) SRT results with headphones demonstrated statistically significant results between PB and PA for the right ear ($^{**}p < 0.001$) and for the left ear ($^{***}p < 0.002$). Moreover, statistical analysis indicated significant differences between the GC and PB and PA ($^{*}p < 0.0001$, for both ears).

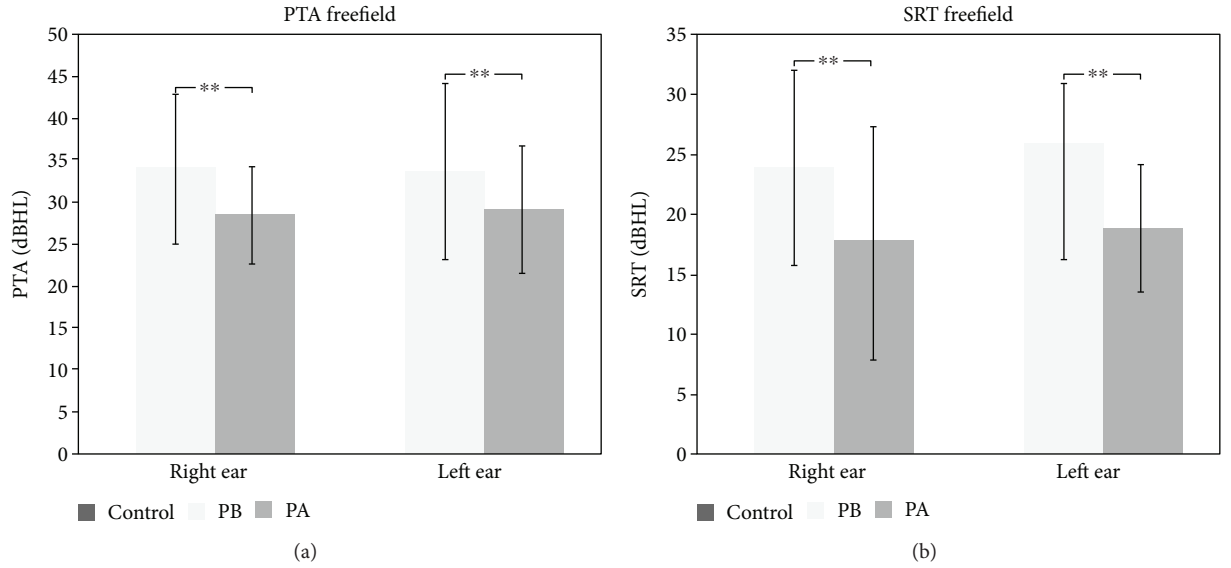

Figure 2: (a) PTA and (b) SRT in free field for the patients before (PB) and after (PA) HA use. Mean and standard deviation are shown for right and left ears before and after HA use. (a) PTA results in free field demonstrated statistically significant changes induced by HA use in both ears ($^{**}p < 0.001$). (b) SRT evaluation in free field also showed a significant improvement in both ears ($^{**}p < 0.001$).

(left ear) after HA use (Figure 2(b)). Supplementary Table 6 shows the individual free-field SRT results.

Both PTA and SRT functional gain (FG) improved significantly after HA use. PTA-FG improved significantly for both ears, from 33.15 ± 8.48 dB to 27.68 ± 5.64 dB (right ear, $p = 0.001$) and from 32.68 ± 10.29 dB to 28.27 ± 7.40 dB for the left ear. SRT-FG also showed significant improvement from 23.93 ± 8.36 dB to 17.50 ± 9.15 dB ($p = 0.001$, right ear) and from 25.71 ± 5.49 dB to 18.21 ± 4.64 dB ($p = 0.001$, left ear).

3.2. fMRI. Two patients (#5 and #14) had to be excluded from further fMRI analysis due to excessive motion artifact

(translation > 2 mm) in at least one of the two sessions, leaving 12 subjects in the final fMRI dataset.

The fMRI task was designed to engage auditory and language receptive fields [25, 27]. Indeed, in control subjects, it produced a robust activation in the auditory cortex for the contrast task (story) vs. baseline in the transverse temporal gyrus (BA41 and BA42) and language centers including Wernicke's area (BA22) (see Suppl. Figure 4 and Suppl. Table 7).

Figure 3 shows the fMRI results for the comparison between controls and patients before (PB) HA use. Statistical maps were much more diffuse in patients than in controls (Figure 3, Tables 1 and 2). Our results suggest that auditory deprivation is represented by decreased activity in the bilateral auditory cortex (BA41 and BA42) and Wernicke's area (Figure 3, Table 1). We also found increased activity in large portions of the frontal and occipital lobes, including bilateral visual areas (BA17, BA18, and BA19) and areas involved in multimodal integration, such as bilateral superior temporal sulcus (STS), middle intraparietal sulcus (IT, BA40), bilateral inferior frontal gyrus (IFG, BA44, BA45, and BA47), and the insula (BA13) (Figure 3, Table 2).

Figure 4 shows the fMRI results from the direct comparison between patients before (PB) vs. after (PA) HA use. Rehabilitation with HA leaded to increased activity of the left transverse temporal gyrus (BA40, BA41), Wernicke's area (left BA22), the left insula (BA13), and left superior frontal gyrus (BA8) (Figure 4, Table 3). We also found that intervention leads to reduced activity in left visual association areas (BA18, BA19), middle and superior frontal gyri (BA9, BA10, and BA46), and the thalamus (Figure 4, Table 4).

Figure 5 shows the correlation between individual changes in fMRI β-values and changes in SRT. We observed significant positive correlations in bilateral BA22 ($p < 0.006$, left; $p < 0.04$, right), left BA41 ($p < 0.04$), left BA42 ($p < 0.01$), left insula ($p < 0.05$), and left superior temporal gyrus ($p < 0.05$).

3.3. Cortical Thickness Analysis. Cortical thickness (CT) could not be estimated in two patients (#5 and #14) due excessive motion artifact in at least one of the sessions.

Figure 6 shows CT significant differences between controls and patients at baseline (PB). Before intervention, patients presented significant increased CT in bilateral prefrontal cortex (BA9 and BA10), precuneus/superior parietal gyrus (BA7), fusiform gyrus (BA37), and right posterior (BA39) and central portions (BA21) of the middle temporal gyrus (Figure 6, Table 5). We observed reduced CT bilaterally in portions of the visual cortex (BA17 and BA18), insula (BA13), supramarginal gyrus (BA40), left superior (BA41) and middle (BA21) temporal gyri, right parahippocampus (BA35), right posterior cingulate cortex (BA31), and the claustrum (Figure 6, Table 6).

When directly comparing patients before (PB) and after (PA) HA use, cortical thickness was increased in the left angular gyrus (BA39), located at the very caudal end of the superior temporal sulcus and in the right inferior parietal gyrus/superior temporal gyrus/posterior insula (BA13) (Figure 7, Table 7). We did not find areas of significant reduced CT after interventions when compared to baseline values of the patients.

4. Discussion

In this study, we explored audiometric, anatomical, and functional brain changes following a one year of continuous HA use in postlingual deaf patients. We observed improved audiometric scores after intervention, particularly of speech recognition, together with fMRI signal increase in the primary auditory cortex, Wernicke's area, and visual areas. HA use also led to decreased fMRI activity in multimodal integration regions, such as the superior temporal sulcus (STS), the middle intraparietal sulcus (IT), and the insula. We observed significant positive correlations between changes in the speech recognition test and increased activity in the primary auditory cortex, Wernicke's area, left insula, and left STS. We also found increased cortical thickness after HA use in the left angular gyrus (BA39) and in the right posterior parietal/temporal junction, including the posterior insula.

Our measured pure tone averages (PTA) suggest that binaural HA fitting in individuals with postlingual sensorineural hearing loss steadies the deterioration of peripheral hearing, as already observed in previous reports [28]. In our study, patients also improved their SRT, both with headphones and in free field. It is well demonstrated that the rehabilitation with HA improves speech recognition, already at six to twelve weeks of HA use [29–31]. We also observed increased functional gain (FG), both for PTA and SRT measurements. Overall, our audiometric results suggest a significant benefit of HA use in speech recognition tasks, while the peripheral auditory system (cochlea, auditory nerve) may not evolve after HA use.

Compared to the control group, patients engaged much broader portions of the brain, including regions in the frontal, parietal, and occipital lobes (Tables 1 and 2). After HA use, activity was reduced in frontal and occipital regions and increased in the auditory cortex, Wernicke's area, and regions involved multimodal integration (Table 4).

Our observations are consistent with previous neuroimaging studies that reported increased activity in auditory-related cortices after CI [13–15]. Besides the auditory system, our results suggest increased activity in the primary and visual association occipital regions (Tables 3 and 4). Increased activity in visual areas has been reported in both fMRI and MEG, in patients with hearing loss [20]. Previous fMRI studies suggest that rehabilitation with CI increases the activity in the left middle occipitotemporal junction (BA37 and BA19) and in the posterior inferior temporal region (BA21 and BA37) [15]. Furthermore, the activity of visual cortex shortly after implantation seems to be related to the level of auditory recovery after cochlear implantation [19], and changes in functional connectivity across visual, temporal, and inferior frontal cortices have important consequences for subsequent CI outcome [32].

Such observations highlight the importance of multimodality as a fundamental aspect of human brain organization. Indeed, the old notion that sensory inputs are

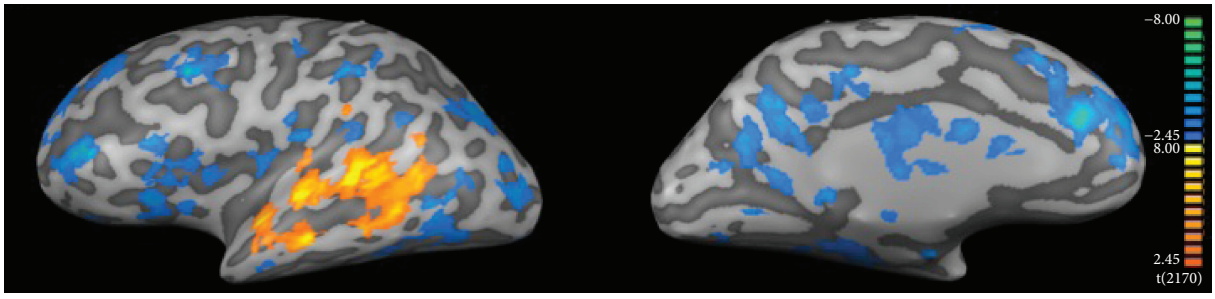

(a)

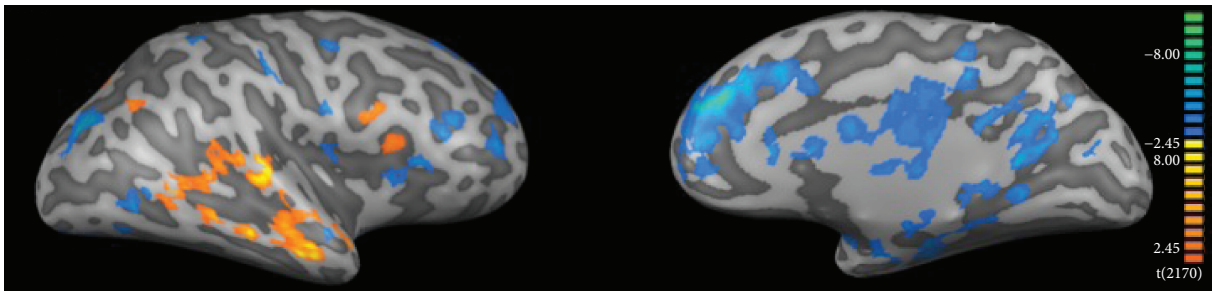

(b)

Figure 3: fMRI group analysis: controls versus patients before HA use. (a) Left and (b) right hemispheres, respectively. Color code indicates statistical significance. Warm colors (red-yellowish) show regions where activity was greater in controls than in PB, and cool colors (blue-greenish) show the opposite contrast (PB > CG). Clusters were selected with a $q[\text{FDR}] < 0.05$ and size of at least 50 mm^3.

Table 1: Brain regions with increased fMRI activity in controls (CG) when compared to patients before HA use (PB). The center of the cluster for each brain region is represented in Talairach coordinates (x, y, and z), followed by its respective standard deviations (in parentheses). Clusters were selected using a $q[\text{FDR}] < 0.05$ and a cluster size of at least 50 mm^3.

Brain region	Hem	Cluster size	Talairach coordinates			BA
			x	y	z	
Middle temporal gyrus	L	2403	−60 (5)	−33 (14)	0 (7)	21, 22, 37, 39
Middle temporal gyrus	R	855	59 (4)	−26 (15)	−3 (6)	21, 22, 37, 39
Transverse temporal gyrus	L	226	−53 (8)	−20 (4)	11 (1)	41, 42
Superior temporal gyrus	L	2893	−56 (6)	−18 (21)	3 (9)	22, 39, 41, 42
Superior temporal gyrus	R	1255	54 (6)	−12 (19)	0 (8)	22, 39, 41, 42
Inferior frontal gyrus	R	278	47 (2)	16 (4)	0 (14)	47
Inferior frontal gyrus	L	107	−51 (3)	15 (5)	0 (12)	47
Middle frontal gyrus	L	223	−2 (1)	−2 (4)	50 (2)	6

Hem = hemisphere; L = left; R = right; and BA = Brodmann area.

processed in specific and unimodal cortices is outdated [33]. For instance, studies in congenitally blind subjects have consistently found increased activity in the primary visual cortex during auditory stimulus processing [34, 35]. Moreover, several lines of evidence indicate that under certain circumstances and for specific visual tasks, hearing impairment leads to increased visual ability following congenital deafness [36]. In our study, we observed augmented fMRI activation of striate cortex (BA17) and extrastriate visual areas (BA18 and BA19), before rehabilitation. Increased recruitment of the visual system of hearing-impaired individuals in response to auditory stimuli has been reported in previous PET studies [37, 38]. Such findings have been interpreted as a result of the increased demand for visual cues during speech processing in individuals with hearing deficits [38]. Possibly as a result of reduced demand, HA use was associated with reduced activity in the secondary and associative visual areas (BA18 and BA19).

Increased activity in frontal areas may reflect increased effort, inner speech with speech production, and/or increased audiovisual (AV) cooperation. In fact, after one year of HA use, we observed significant increased activity in bilateral auditory cortices. Besides, we have found increased activity in Wernicke's area (BA22) (Table 4) and reduced activity in visual areas, such as BA18 and BA19 (Table 3). Together, these results may show a different balance in AV interaction, with a reactivation of auditory speech areas and a more leftward lateralized network, i.e., a more physiological speech processing, less demanding after HA use. The recent study suggests that hearing loss impacts audiovisual speech

Table 2: Brain regions with increased fMRI activity in patients before HA use (PB) when compared to controls (CG). The center of the cluster for each brain region is represented in Talairach coordinates (x, y, and z), followed by its respective standard deviations (in parentheses). Clusters were selected using a $q[\text{FDR}] < 0.05$ and a cluster size of at least 50 mm^3.

Brain region	Hem	Cluster size	Talairach coordinates			BA
			x	y	z	
Cuneus	R	601	14 (5)	−78 (6)	11 (4)	17, 18
Lingual gyrus	R	872	20 (7)	−73 (11)	−2 (5)	17, 18, 19
Lingual gyrus	L	930	−19 (6)	−66 (11)	−3 (5)	17, 18, 19
Precuneus	R	355	12 (7)	−61 (8)	25 (5)	19
Precuneus	L	392	−13 (11)	−59 (8)	29 (7)	19
Fusiform gyrus	R	489	33 (7)	−60 (12)	−12 (3)	19, 37
Fusiform gyrus	L	770	−32 (9)	−62 (19)	−13 (3)	18, 19, 37
Middle occipital gyrus	L	565	−33 (8)	−80 (8)	3 (8)	18, 19
Superior temporal gyrus	L	178	−45 (5)	−43 (13)	19 (8)	13, 22, 41, 39
Superior temporal gyrus	R	152	43 (7)	−52 (5)	20 (3)	13, 22, 39
Inferior temporal gyrus	L	318	−53 (5)	−38 (27)	−10 (9)	19, 20
Middle temporal gyrus	L	374	−49 (10)	−45 (25)	2 (11)	19, 21
Parahippocampal gyrus	R	1131	24 (6)	−22 (14)	−14 (7)	28, 34, 35, 36, hippocampus, amygdala
Parahippocampal gyrus	L	1237	−25 (8)	−26 (12)	−12 (7)	27, 28, 34, 35, 36, hippocampus, amygdala
Cingulate gyrus	L	1206	−7 (5)	−2 (28)	34 (5)	23, 24, 31, 32
Cingulate gyrus	R	2492	7 (4)	−2 (22)	34 (5)	23, 24, 30, 31, 32
Anterior cingulate	L	482	−10 (5)	37 (3)	18 (5)	32
Anterior cingulate	R	935	8 (5)	35 (9)	15 (7)	24, 32, 33
Posterior cingulate	L	873	−6 (6)	−54 (6)	17 (5)	23, 29, 30, 31
Posterior cingulate	R	974	8 (7)	−54 (9)	15 (5)	23, 29, 30, 31
Insula	R	616	37 (4)	4 (18)	12 (6)	13
Insula	L	1213	−38 (5)	−5 (19)	12 (8)	13
Inferior frontal gyrus	L	796	−45 (8)	16 (6)	10 (13)	6, 9, 10, 44, 45, 46, 47
Middle frontal gyrus	L	2596	−6 (5)	39 (11)	28 (10)	6, 8, 9, 10
Middle frontal gyrus	R	2607	7 (4)	41 (10)	26 (11)	6, 8, 9, 10
Middle frontal gyrus	R	242	38 (7)	23 (20)	27 (12)	6, 9, 10, 46
Middle frontal gyrus	L	1416	−37 (8)	26 (20)	29 (14)	6, 8, 9, 10, 46
Superior frontal gyrus	R	882	11 (6)	53 (5)	29 (5)	8, 9, 10
Superior frontal gyrus	L	1932	−15 (10)	48 (13)	32 (10)	6, 8, 9, 10
Precentral gyrus	L	465	−44 (5)	2 (6)	32 (11)	4, 6, 9, 43
Precentral gyrus	R	497	45 (6)	−7 (7)	34 (9)	4, 6
Inferior parietal lobe	L	467	−44 (6)	−37 (7)	38 (7)	39, 40
Caudate	L	876	−14 (7)	−6 (16)	16 (6)	
Caudate	R	938	18 (6)	−11 (17)	17 (6)	
Thalamus	L	489	−7 (5)	−16 (8)	9 (5)	
Thalamus	R	1144	16 (6)	−17 (7)	10 (4)	

Hem = hemisphere; L = left; R = right; and BA = Brodmann area.

processing accompanied by changed activity in frontal brain areas, which are modulated by the level of hearing loss [39].

Clinical observations have demonstrated the impact of hearing impairment on higher cognitive processes [2], which can be at least partially recovered by auditory rehabilitation. For instance, it has been observed significant improvements of learning and speech in children after CI [15]. Interestingly, we observed significant correlations between individual fMRI signal changes in auditory (BA41 and BA41) and Wernicke's areas (BA22) and individual change in SRT. This finding links, to our knowledge for the first time, clinical evidence of improved language abilities in patients with hearing loss after auditory rehabilitation with acoustic amplification.

Our results also suggest increased recruitment of brain areas involved in multimodal integration, after HA use, observed as increased fMRI activity in the superior temporal sulcus (STS), the middle intraparietal sulcus (IT, BA40), the inferior frontal gyrus (IFG, BA44, BA45, and BA47), and the insula (BA13). It is possible that HA use improved the quality of information provided by the auditory system to

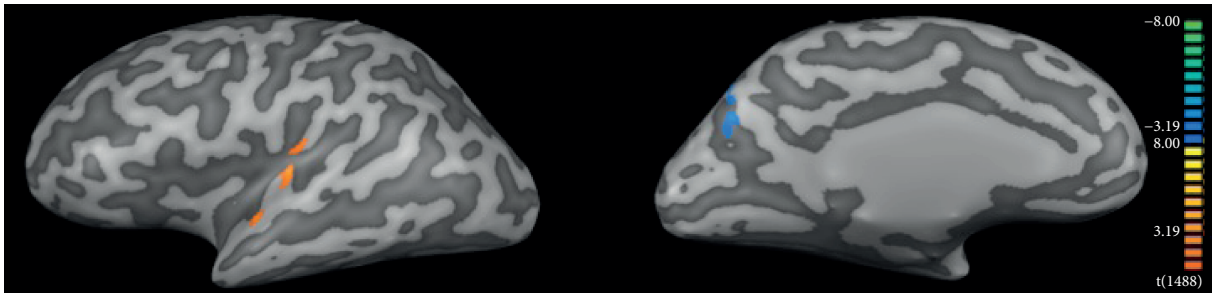

(a)

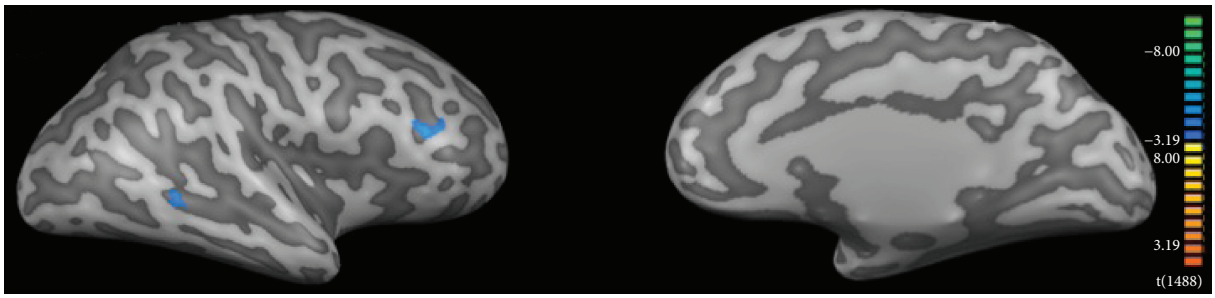

(b)

Figure 4: fMRI group analysis: patients before HA use (PB) versus patients after HA use (PA). (a) Left and (b) right hemispheres, respectively. Color code indicates statistical significance. Warm colors (red-yellowish) show regions where activity was greater in PA than in PB, and cool colors (blue-greenish) show the opposite contrast (PB > PA). Clusters were selected with a $q[\text{FDR}] < 0.05$ and size of at least 50 mm^3.

Table 3: Brain regions with increased fMRI activity in patients before HA use (PB) when compared to patients after HA use (PA). The center of the cluster for each brain region is represented in Talairach coordinates (x, y, and z), followed by its respective standard deviations (in parentheses). Clusters were selected using a $q[\text{FDR}] < 0.05$ and a cluster size of at least 50 mm^3.

Brain region	Hem	Cluster size	Talairach coordinates			BA
			x	y	z	
Cuneus	L	118	−12 (2)	−76 (2)	32 (1)	18, 19
Precuneus	L	156	−15 (2)	−73 (5)	33 (6)	19
Middle frontal gyrus	R	260	43 (3)	37 (5)	17 (2)	10, 46
Middle frontal gyrus	R	89	6 (2)	47 (1)	28 (2)	9
Superior frontal gyrus	R	70	6 (2)	49 (1)	30 (2)	9
Superior frontal gyrus	L	102	−4 (1)	55 (2)	25 (2)	9
Thalamus	R	325	12 (3)	−22 (3)	14 (2)	

Hem = hemisphere; L = left; R = right; and BA = Brodmann area.

Table 4: Brain regions with increased fMRI activity in patients after HA use (PA) when compared to patients before HA use (PB). The center of the cluster for each brain region is represented in Talairach coordinates (x, y, and z), followed by its respective standard deviations (in parentheses). Clusters were selected using a $q[\text{FDR}] < 0.05$ and a cluster size of at least 50 mm^3.

Brain region	Hem	Cluster size	Talairach coordinates			BA
			x	y	z	
Superior temporal gyrus	L	476	−51 (5)	−1 (10)	1 (4)	21, 22, 41
Transverse temporal gyrus	L	178	−42 (4)	−23 (2)	12 (1)	40, 41
Superior frontal gyrus	L	295	−6 (2)	40 (4)	46 (3)	8
Insula	L	109	−39 (4)	−23 (7)	12 (4)	13

Hem = hemisphere; L = left; R = right; and BA = Brodmann area.

speech integration centers, changing the balance between visual and auditory inputs. In fact, the process of multisensory integration is apparently based upon a weighed estimation of each sensorial input, which in turn depends on the reliability of the information contained in each modality [40]. In further supporting of this hypothesis is

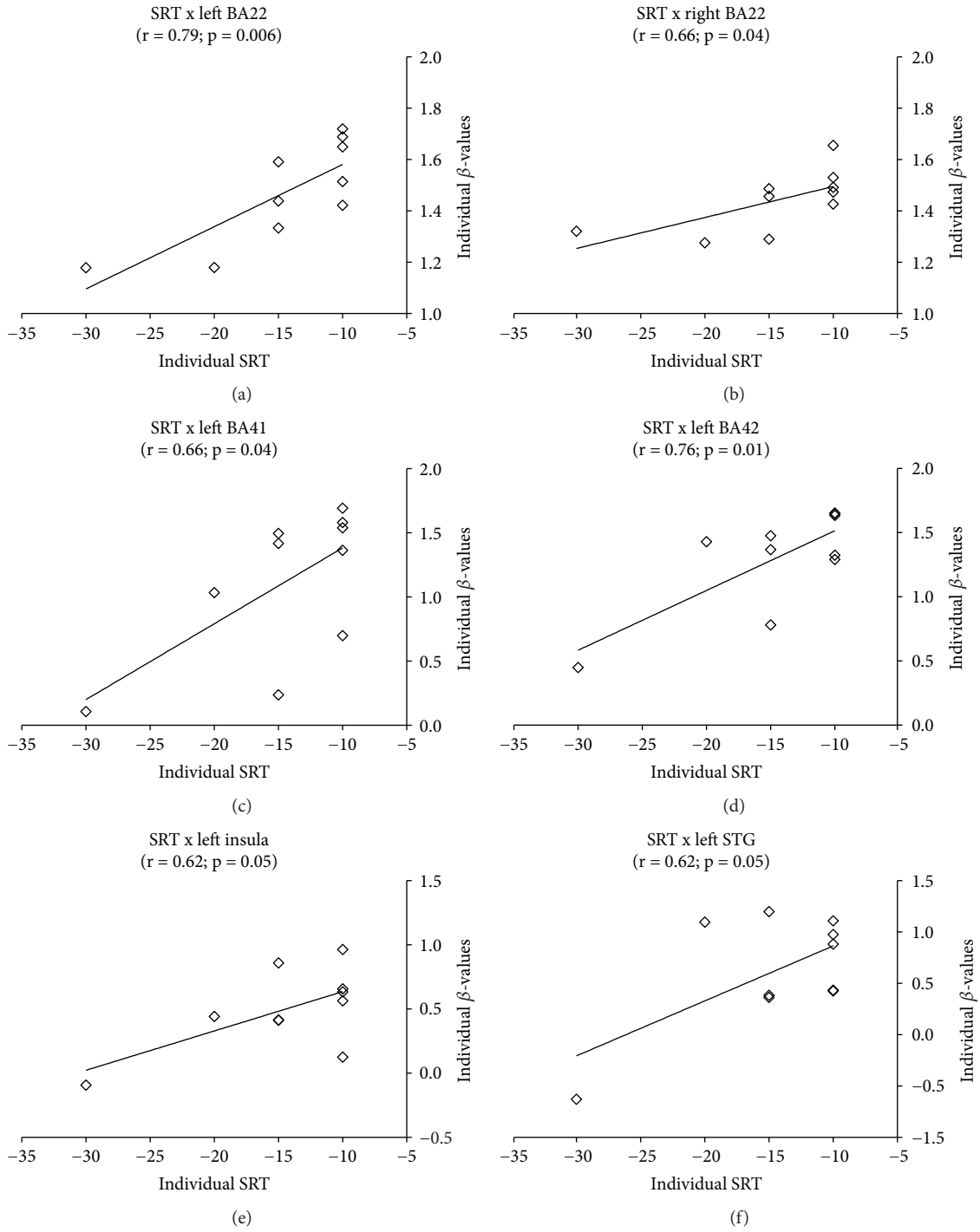

Figure 5: Pearson correlations between individual SRT changes and individual fMRI β-values changes. SRT with headphones changes were computed as a global difference between thresholds observed before and after intervention, according to [SRT (right ear before) + SRT (left ear before)] − [SRT (right ear after) + SRT (left ear after)]. Only regions that presented statistically significant correlation are shown. Significant correlations were found only after HA use in (a) left BA22, (b) right BA22, (c) left BA41, (d) left BA42, (e) left insula, and (f) left STG.

the significant positive correlation found between individual fMRI signal changes in the left insula and left STG with individual changes in SRT, such that the greater the SRT improvement, the greater was the fMRI signal change.

The aim of our study was not limited to investigate functional reorganization due to HA use, but it also explored neuroanatomical changes. Before HA use, cortical thickness (CT) was reduced in the visual cortex (BA17 and BA18), primary auditory cortex (BA41), and multimodal cortex (BA13 and BA40) and increased CT was found in the associative somatosensory cortex (BA7), prefrontal cortex (BA9 and BA10), and middle temporal/fusiform gyrus (BA37). Only a

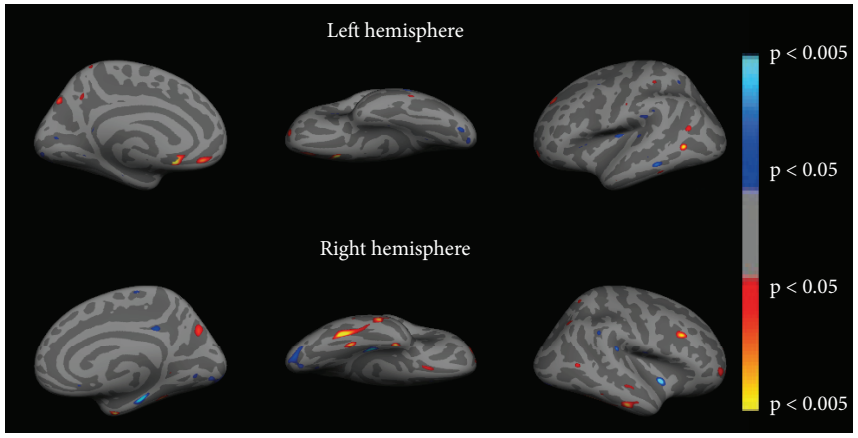

Figure 6: Cortical thickness changes of the patients before HA use (PB) when compared to the control group (CG). Color code indicates p values. Warm colors (red-yellowish) show regions where cortical thickness was greater in PB than in the controls, and cool colors (blue-greenish) show the opposite contrast (CG > PB).

Table 5: Regions of increased cortical thickness in patients at baseline (PB) when compared to controls (CG). Mean cortical thickness is expressed in mm. The numbers in parentheses correspond to standard deviations. Statistical significance was based at $p < 0.01$.

Brain region	Hem	Nvox	Talairach coordinates			BA	PB	CG	p value
			x	y	z		Mean (SD)	Mean (SD)	
Medial orbitofrontal gyrus	L	176	−9.0	37.8	−13.5	10	3.12 (0.36)	2.54 (0.35)	0.001
Middle frontal gyrus	L	111	−21.2	52.3	−9.7	10	2.83 (0.41)	2.45 (0.20)	0.010
Middle frontal gyrus	R	226	38.9	20.0	25.7	9	2.89 (0.22)	2.59 (0.21)	0.005
Superior parietal gyrus	L	209	−16.6	−70.1	37.3	7	2.35 (0.29)	2.00 (0.30)	0.010
Superior parietal gyrus	R	55	22.6	−53.5	57.5	7	2.28 (0.16)	2.01 (0.28)	0.010
Precuneus	L	58	−7.8	−52.7	37.5	7	2.96 (0.37)	2.50 (0.40)	0.010
Precuneus	R	279	18.8	−66.1	34.2	7	2.49 (0.29)	2.21 (0.16)	0.010
Fusiform gyrus	R	626	40.7	−48.7	−11.0	37	3.28 (0.16)	2.84 (0.25)	0.0002
Fusiform gyrus	L	127	−50.9	−58.3	3.3	37	3.08 (0.21)	2.59 (0.29)	0.0003
Middle temporal gyrus	R	281	54.5	−20.4	−18.6	21	3.34 (0.26)	2.95 (0.30)	0.005
Middle temporal gyrus	R	56	49.4	−59.1	7.4	39	3.11 (0.21)	2.73 (0.38)	0.010
Entorhinal gyrus	R	161	30.2	−3.5	−29.0	36	3.94 (0.50)	3.33 (0.31)	0.003

Hem = hemisphere; L = left; R = right; BA = Brodmann area; Nvox = number of voxels in the cluster; SD = standard deviation; PB = patients before HA use; CG = control group.

few studies have used MRI to investigate neuroanatomical changes due to auditory deprivation, and the results are not consistent. A seminal study used voxel-based morphometry (VBM) in prelingually deaf subjects and identified significant reduced volume only in the left posterior STG [41]. In a more recent study, VBM and CT analysis were applied to evaluate individuals with profound sensorineural hearing loss [42]. No brain structure in the patient group presented increased volume or CT, but the cortical thickness of the primary visual area (BA17) was significantly smaller in patients than in the control group [42]. In another study, CT was investigated in adolescents with prelingual deafness and significant CT differences were found in the right middle occipital gyrus, right precuneus, left gyrus rectus, and left posterior cingulate gyrus [43, 44].

After HA use, our results indicate increased CT at the very caudal end of the STS, including the left angular gyrus (BA39) and the inferior parietal gyrus/superior temporal gyrus/posterior insula (BA13). All of these regions are related to multimodality, and it is tempting to associate these anatomical changes to the functional ones detected by fMRI. Although there are evidence giving support to a possible link between functional and anatomical changes observed by MRI, this is still a matter of debate [45]. Indeed, in some brain areas, the observed increased fMRI activity was related to a reduced CT, as for instance BA17 before HA use. On the other hand, sensory integration areas, such as the left insula, showed increased CT and increased fMRI activity after HA use.

This study has a number of caveats and limitations worth mentioning. First, our sample size was limited to 12 patients in the final functional and anatomical datasets. Second, the absence of a control group (patients without intervention), where patients would be placed on a waiting list for follow-up intervention. However, the nature of this 1-year longitudinal study hinders such design. During audiologic assessments,

Table 6: Regions of reduced cortical thickness in patients at baseline (PB) when compared to controls (CG). Mean cortical thickness is expressed in mm. The numbers in parentheses correspond to standard deviations. Statistical significance was set at $p < 0.01$.

Brain region	Hem.	Nvox	Talairach coordinates			BA	PB	CG	p value
			x	y	z		Mean (SD)	Mean (SD)	
Insula	R	144	44.5	−35.3	19.9	13	2.54 (0.22)	2.87 (0.21)	0.003
Insula	L	166	−34.5	−14.9	13.5	13	2.93 (0.24)	3.35 (0.35)	0.005
Supramarginal gyrus	R	64	52.6	−39.3	30.6	40	2.66 (0.27)	3.09 (0.37)	0.007
Supramarginal gyrus	L	100	−55.8	−29.1	21.9	40	2.76 (0.34)	3.13 (0.29)	0.010
Superior temporal gyrus	L	55	−42.6	−28.7	5.0	41	2.71 (0.40)	3.34 (0.61)	0.010
Middle temporal gyrus	L	116	−58.4	−38.2	−9.3	21	2.92 (0.47)	3.61 (0.33)	0.001
Parahippocampal gyrus	R	336	23.8	−24.1	−19.0	35	3.06 (0.20)	3.43 (0.30)	0.004
Lateral occipital gyrus	R	462	21.5	−89.6	−2.2	17	2.13 (0.29)	2.55 (0.30)	0.004
Lingual gyrus	R	45	8.7	−69.9	3.9	18	2.15 (0.29)	2.55 (0.39)	0.010
Middle occipital gyrus	L	71	−23.1	−82.8	−6.5	18	2.19 (0.32)	2.69 (0.37)	0.004
Posterior cingulate	R	99	8.4	−34.9	33.0	31	3.00 (0.42)	3.67 (0.55)	0.006
Claustrum	R	187	35.5	−4.0	−4.6	—	3.40 (0.53)	4.16 (0.40)	0.001

Hem = hemisphere; L = left; R = right; BA = Brodmann area; Nvox = number of voxels in the cluster; SD = standard deviation; PB = patients before HA use; CG = control group.

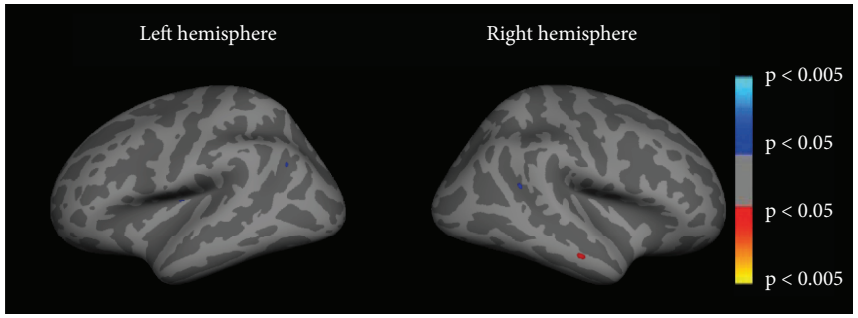

Figure 7: Cortical thickness changes of the patients before HA use (PB) when compared to patients after HA use (PA). Color code indicates p values. Warm colors (red-yellowish) show regions where cortical thickness was greater in PB than PA, and cool colors (blue-greenish) show the opposite contrast (PA > PB).

Table 7: Regions of increased cortical thickness in the patients after HA use (PA) when compared to patients before HA use (PB). Mean cortical thickness is expressed in mm. The numbers in parentheses correspond to standard deviations. Statistical significance was based at $p < 0.01$.

Brain region	Hem	Nvox	Talairach coordinates			BA	PB	PA	p value
			x	y	z		Mean (SD)	Mean (SD)	
Inferior parietal gyrus/superior temporal gyrus/posterior insula	R	36	44.7	−44.5	18.8	13	2.57 (0.28)	2.97 (0.29)	0.010
Angular gyrus	L	31	−38.6	−58.9	29.9	39	2.73 (0.37)	3.06 (0.29)	0.003

Hem = hemisphere; L = left; R = right; BA = Brodmann area; Nvox = number of voxels in the cluster; SD = standard deviation; PB = patients before HA use; PA = patients after HA use.

the nontested ear was not masked or plugged. Therefore, especially in case of mild HL, we might have observed an additive effect between the HA ear and the non-HA ear, and the observed audiometric changes may have been biased by the protocol we used. The same story was presented in both fMRI sessions (before and after HA use), and therefore, our fMRI results are susceptible to habituation. We used a fixed-effects model in the fMRI analysis, which limits our conclusions to the population studied. We did not retest the control group after one year.

To our knowledge, this is the first study which is aimed at investigating audiometric and neuroimaging changes induced by HA use in patients with long-lasting auditory deprivation. Audiometric observations were complemented by neuroimaging investigation, both functional and anatomical cortical thicknesses, to assist in understanding the

neurophysiological mechanisms behind hearing rehabilitation. Furthermore, the correlation found between individual fMRI and SRT further paves the perspective for the use of functional neuroimaging as a clinical tool in audiology.

Data Availability

The data used to support the findings of this study are available from the corresponding author upon request.

Conflicts of Interest

The authors declare that there is no conflict of interest regarding the publication of this paper.

Acknowledgments

This work was supported by the São Paulo Research Foundation (FAPESP), Brazilian National Council for Scientific and Technological Development (CNPq), and CAPES, a foundation from the Ministry of Education, Brazil. Thanks are due to Sandra Moroti for MRI scanning, to Dr. Elson Rodrigues for helping with patient screening and for the diagnosis hearing loss type, and to the patients.

Supplementary Materials

Supplementary Figure 1: pure tone audiometry for each frequency tested with headphones in the control group. Supplementary Figure 2: pure tone audiometry for each frequency tested with headphones for the group of patients before (PB) and after (PA) HA use. Supplementary Figure 3: pure tone audiometry for each frequency tested in free field, for patients before (PB) and after (PA) HA use. Supplementary Figure 4: fMRI statistical maps of the control group. Supplementary Table 1: clinical and audiometric information of the patients. Supplementary Table 2: individual PTA and SRT with headphones for the control group (CG). Supplementary Table 3: individual PTA with headphones for patients before (PB) and after (PA) HA use. Supplementary Table 4: individual SRT with headphones of the group of patients before (PB) and after (PA) HA use. Supplementary Table 5: individual PTA in free field of the group of patients before (PB) and after (PA) HA use. Supplementary Table 6: individual SRT in free field for patients before (PB) and after (PA) HA use. Supplementary Table 7: statistically significant fMRI response in the control group. *(Supplementary Materials)*

References

[1] C. D. Mulrow, M. R. Tuley, and C. Aguilar, "Sustained benefits of hearing-aids," *Clinical Research*, vol. 39, pp. A593–A593, 1991.

[2] M. K. Pichora-Fuller and G. Singh, "Effects of age on auditory and cognitive processing: implications for hearing aid fitting and audiologic rehabilitation," *Trends in Amplification*, vol. 10, no. 1, pp. 29–59, 2006.

[3] A. Y. Choi, H. J. Shim, S. H. Lee, S. W. Yoon, and E. J. Joo, "Is cognitive function in adults with hearing impairment improved by the use of hearing aids?," *Clinical and Experimental Otorhinolaryngology*, vol. 4, no. 2, pp. 72–76, 2011.

[4] R. Rajan, D. R. F. Irvine, L. Z. Wise, and P. Heil, "Effect of unilateral partial cochlear lesions in adult cats on the representation of lesioned and unlesioned cochleas in primary auditory cortex," *The Journal of Comparative Neurology*, vol. 338, no. 1, pp. 17–49, 1993.

[5] M. K. Schwaber, P. E. Garraghty, and J. H. Kaas, "Neuroplasticity of the adult primate auditory cortex following cochlear hearing loss," *The American Journal of Otology*, vol. 14, no. 3, pp. 252–258, 1993.

[6] J. F. Willott, L. M. Aitkin, and S. L. McFadden, "Plasticity of auditory cortex associated with sensorineural hearing loss in adult C57BL/6J mice," *The Journal of Comparative Neurology*, vol. 329, no. 3, pp. 402–411, 1993.

[7] B. Ryals and E. Rubel, "Hair cell regeneration after acoustic trauma in adult *Coturnix* quail," *Science*, vol. 240, no. 4860, pp. 1774–1776, 1988.

[8] Y. Chung, K. E. Hancock, S. I. Nam, and B. Delgutte, "Coding of electric pulse trains presented through cochlear implants in the auditory midbrain of awake rabbit: comparison with anesthetized preparations," *The Journal of Neuroscience*, vol. 34, no. 1, pp. 218–231, 2014.

[9] J. B. Fallon, D. R. F. Irvine, and R. K. Shepherd, "Cochlear implant use following neonatal deafness influences the cochleotopic organization of the primary auditory cortex in cats," *Journal of Comparative Neurology*, vol. 512, no. 1, pp. 101–114, 2009.

[10] E. Amaro, S. C. R. Williams, S. S. Shergill et al., "Acoustic noise and functional magnetic resonance imaging: current strategies and future prospects," *Journal of Magnetic Resonance Imaging*, vol. 16, no. 5, pp. 497–510, 2002.

[11] D. Bilecen, E. Seifritz, E. W. Radu et al., "Cortical reorganization after acute unilateral hearing loss traced by fMRI," *Neurology*, vol. 54, no. 3, pp. 765–767, 2000.

[12] D. S. Lazard, H. J. Lee, E. Truy, and A. L. Giraud, "Bilateral reorganization of posterior temporal cortices in post-lingual deafness and its relation to cochlear implant outcome," *Human Brain Mapping*, vol. 34, no. 5, pp. 1208–1219, 2013.

[13] J. S. Lee, D. S. Lee, S. H. Oh et al., "PET evidence of neuroplasticity in adult auditory cortex of postlingual deafness," *The Journal of Nuclear Medicine*, vol. 44, no. 9, pp. 1435–1439, 2003.

[14] J. H. Hwang, C. W. Wu, J. H. Chen, and T. C. Liu, "Changes in activation of the auditory cortex following long-term amplification: an fMRI study," *Acta Oto-Laryngologica*, vol. 126, no. 12, pp. 1275–1280, 2006.

[15] E. Kang, D. S. Lee, H. Kang et al., "Neural changes associated with speech learning in deaf children following cochlear implantation," *NeuroImage*, vol. 22, no. 3, pp. 1173–1181, 2004.

[16] A. L. Giraud, C. J. Price, J. M. Graham, and R. S. J. Frackowiak, "Functional plasticity of language-related brain areas after cochlear implantation," *Brain*, vol. 124, no. 7, pp. 1307–1316, 2001.

[17] J. Rouger, S. Lagleyre, J. F. Démonet, B. Fraysse, O. Deguine, and P. Barone, "Evolution of crossmodal reorganization of the voice area in cochlear-implanted deaf patients," *Human Brain Mapping*, vol. 33, no. 8, pp. 1929–1940, 2012.

[18] G. A. Calvert, R. Campbell, and M. J. Brammer, "Evidence from functional magnetic resonance imaging of crossmodal

binding in the human heteromodal cortex," *Current Biology*, vol. 10, no. 11, pp. 649–657, 2000.

[19] K. Strelnikov, J. Rouger, J. F. Demonet et al., "Visual activity predicts auditory recovery from deafness after adult cochlear implantation," *Brain*, vol. 136, no. 12, pp. 3682–3695, 2013.

[20] Y. T. Zhang, Z. J. Geng, Q. Zhang, W. Li, and J. Zhang, "Auditory cortical responses evoked by pure tones in healthy and sensorineural hearing loss subjects: functional MRI and magnetoencephalography," *Chinese Medical Journal*, vol. 119, no. 18, pp. 1548–1554, 2006.

[21] H. Davis and S. R. Silverman, *Hearing and Deafness*, Holt, Rinehart & Winston of Canada Ltd, 1970.

[22] A. W. Bronkhorst and R. Plomp, "Binaural speech-intelligibility in noise for hearing-impaired listeners," *The Journal of the Acoustical Society of America*, vol. 86, no. 4, pp. 1374–1383, 1989.

[23] D. P. Pascoe, "Frequency responses of hearing aids and their effects on the speech perception of hearing-impaired subjects," *Annals of Otology, Rhinology & Laryngology*, vol. 84, no. 5, Supplement, pp. 5–40, 1975.

[24] D. Araujo, D. B. De Araujo, O. M. Pontes-Neto et al., "Language and motor *f*MRI activation in polymicrogyric cortex," *Epilepsia*, vol. 47, no. 3, pp. 589–592, 2006.

[25] C. A. Estombelo-Montesco, M. Sturzbecher Jr., A. K. D. Barros, and D. B. de Araujo, "Detection of auditory cortex activity by fMRI using a dependent component analysis," in *Advances in Experimental Medicine and Biology*, vol. 657, pp. 135–145, Springer, 2010.

[26] B. Fischl, M. I. Sereno, and A. M. Dale, "Cortical surface-based analysis: II: inflation, flattening, and a surface-based coordinate system," *NeuroImage*, vol. 9, no. 2, pp. 195–207, 1999.

[27] M. J. Sturzbecher, W. Tedeschi, B. C. T. Cabella, O. Baffa, U. P. C. Neves, and D. B. de Araujo, "Non-extensive entropy and the extraction of BOLD spatial information in event-related functional MRI," *Physics in Medicine & Biology*, vol. 54, no. 1, pp. 161–174, 2009.

[28] R. M. Hurley, "Onset of auditory deprivation," *Journal of the American Academy of Audiology*, vol. 10, no. 10, pp. 529–534, 1999.

[29] B. C. J. Moore, J. I. Alcántara, and J. Marriage, "Comparison of three procedures for initial fitting of compression hearing aids. I. Experienced users, fitted bilaterally," *British Journal of Audiology*, vol. 35, no. 6, pp. 339–353, 2001.

[30] G. H. Saunders and J. M. Kates, "Speech intelligibility enhancement using hearing-aid array processing," *The Journal of the Acoustical Society of America*, vol. 102, no. 3, pp. 1827–1837, 1997.

[31] T. Wittkop and V. Hohmann, "Strategy-selective noise reduction for binaural digital hearing aids," *Speech Communication*, vol. 39, no. 1-2, pp. 111–138, 2003.

[32] D. S. Lazard and A. L. Giraud, "Faster phonological processing and right occipito-temporal coupling in deaf adults signal poor cochlear implant outcome," *Nature Communications*, vol. 8, article 14872, 2017.

[33] A. Ghazanfar and C. Schroeder, "Is neocortex essentially multisensory?," *Trends in Cognitive Sciences*, vol. 10, no. 6, pp. 278–285, 2006.

[34] L. B. Merabet and A. Pascual-Leone, "Neural reorganization following sensory loss: the opportunity of change," *Nature Reviews Neuroscience*, vol. 11, no. 1, pp. 44–52, 2010.

[35] O. Collignon, G. Vandewalle, P. Voss et al., "Functional specialization for auditory–spatial processing in the occipital cortex of congenitally blind humans," *Proceedings of the National Academy of Sciences of the United States of America*, vol. 108, no. 11, pp. 4435–4440, 2011.

[36] D. Bavelier, M. W. G. Dye, and P. C. Hauser, "Do deaf individuals see better?," *Trends in Cognitive Sciences*, vol. 10, no. 11, pp. 512–518, 2006.

[37] A. L. Giraud, C. J. Price, J. M. Graham, E. Truy, and R. S. J. Frackowiak, "Cross-modal plasticity underpins language recovery after cochlear implantation," *Neuron*, vol. 30, no. 3, pp. 657–664, 2001.

[38] A. L. Giraud and E. Truy, "The contribution of visual areas to speech comprehension: a PET study in cochlear implants patients and normal-hearing subjects," *Neuropsychologia*, vol. 40, no. 9, pp. 1562–1569, 2002.

[39] S. Rosemann and C. M. Thiel, "Audio-visual speech processing in age-related hearing loss: stronger integration and increased frontal lobe recruitment," *NeuroImage*, vol. 175, pp. 425–437, 2018.

[40] N. W. Roach, J. Heron, and P. V. McGraw, "Resolving multisensory conflict: a strategy for balancing the costs and benefits of audio-visual integration," *Proceedings of the Royal Society B: Biological Sciences*, vol. 273, no. 1598, pp. 2159–2168, 2006.

[41] D. K. Shibata, "Differences in brain structure in deaf persons on MR imaging studied with voxel-based morphometry," *American Journal of Neuroradiology*, vol. 28, no. 2, pp. 243–249, 2007.

[42] J. Li, W. Li, J. Xian et al., "Cortical thickness analysis and optimized voxel-based morphometry in children and adolescents with prelingually profound sensorineural hearing loss," *Brain Research*, vol. 1430, pp. 35–42, 2012.

[43] W. Li, J. Li, J. Xian et al., "Alterations of grey matter asymmetries in adolescents with prelingual deafness: a combined VBM and cortical thickness analysis," *Restorative Neurology and Neuroscience*, vol. 31, no. 1, pp. 1–17, 2013.

[44] M. Yang, H. J. Chen, B. Liu et al., "Brain structural and functional alterations in patients with unilateral hearing loss," *Hearing Research*, vol. 316, pp. 37–43, 2014.

[45] M. P. Harms, L. Wang, J. G. Csernansky, and D. M. Barch, "Structure–function relationship of working memory activity with hippocampal and prefrontal cortex volumes," *Brain Structure and Function*, vol. 218, no. 1, pp. 173–186, 2013.

Hindawi
Neural Plasticity
Volume 2018, Article ID 5769861, 12 pages
https://doi.org/10.1155/2018/5769861

Research Article

Repetitive Transcranial Electrical Stimulation Induces Quantified Changes in Resting Cerebral Perfusion Measured from Arterial Spin Labeling

Matthew S. Sherwood,[1,2] **Aaron T. Madaris**,[1,2] **Casserly R. Mullenger**,[1] **and R. Andy McKinley**[3]

[1]*Infoscitex, a DCS company, 4027 Colonel Glenn Hwy, Beavercreek, OH 45431, USA*
[2]*Department of Biomedical, Industrial & Human Factors Engineering, Wright State University, 3640 Colonel Glenn Hwy, Dayton, OH 45435, USA*
[3]*Air Force Research Laboratory, U.S. Air Force, 2510 Fifth Street, Bldg 840, Wright-Patterson AFB, OH 45433-7951, USA*

Correspondence should be addressed to Matthew S. Sherwood; matt.sherwood@wright.edu

Received 23 March 2018; Revised 23 July 2018; Accepted 8 August 2018; Published 5 September 2018

Academic Editor: Junichi Ushiba

The use of transcranial electrical stimulation (TES) as a method to augment neural activity has increased in popularity in the last decade and a half. The specific application of TES to the left prefrontal cortex has been shown to produce broad cognitive effects; however, the neural mechanisms underlying these effects remain unknown. In this work, we evaluated the effect of repetitive TES on cerebral perfusion. Stimulation was applied to the left prefrontal cortex on three consecutive days, and resting cerebral perfusion was quantified before and after stimulation using arterial spin labeling. Perfusion was found to decrease significantly more in a matched sham stimulation group than in a group receiving active stimulation across many areas of the brain. These changes were found to originate in the locus coeruleus and were broadly distributed in the neocortex. The changes in the neocortex may be a direct result of the stimulation or an indirect result via the changes in the noradrenergic system produced from the altered activity of the locus coeruleus. These findings indicate that anodal left prefrontal stimulation alters the activity of the locus coeruleus, and this altered activity may excite the noradrenergic system producing the broad behavioral effects that have been reported.

1. Introduction (AM)

Transcranial electrical stimulation (TES) has experienced increased interest over the last 15 years [1]. The application of TES using a weak, constant current delivered to the scalp is referred to as transcranial direct current stimulation (tDCS) [2]. This method has been presented by many groups as a feasible process for stimulation of the brain to augment neural activity [3–7]. The specific application of tDCS with the anode placed over the left prefrontal cortex has been routinely applied in the literature with demonstrable behavioral effects in combating performance decrements associated with vigilance [8], decreasing the effect of fatigue on cognitive performance [9, 10], accelerating learning processes [2, 3, 11, 12], enhancing multitasking performance [13], and improving procedural memory [14].

Clark et al. [11] implemented 2 mA anodal left prefrontal tDCS while performing a task involving the identification of threat-related objects in a naturalistic environment. Using dynamic Bayesian network analysis, they indicated that the right frontal and parietal cortices were involved in the learning processes of their identification task. Furthermore, they reported that the group receiving full-current (2 mA) tDCS performed significantly better than the one that received low-current (0.1 mA) stimulation. McKinley et al. [12] provided support for the findings of Clark and colleagues using a realistic visual search task implanted with synthetic aperture radar images. They stated that participants

who received anodal left prefrontal tDCS attained enhanced visual search accuracies compared to those supplied with sham or no stimulation. Effects of anodal left prefrontal tDCS have also been observed in decreasing the effects of fatigue on cognitive performance. Using a cohort of 30 participants (10 placebo gum, 10 caffeine gum with sham tDCS, and 10 2 mA anodal left prefrontal tDCS with placebo gum), McIntire et al. [9] performed psychomotor vigilance tasks, delayed matching-to-sample working memory tasks, and the Mackworth clock test throughout 30 hours of continuous wakefulness. They reported improved latencies in working memory tasks and faster reaction times in psychomotor tasks in the groups receiving active tDCS and caffeine gum compared to placebo throughout the sleep deprivation period. Altogether, these findings provide evidence for the central role of the prefrontal cortex in vigilance, accelerated learning, fatigue, and multitasking performance but indicate that tDCS may be utilized to maintain performance levels in environments requiring little to no rest or settings required sustained attentional focus.

Despite the broad applications of tDCS and those specific to anodal left prefrontal stimulation, the neural mechanisms underlying tDCS are not well understood. It has been suggested that anodal tDCS increases excitability in the neocortex [6] by altering neuronal membrane potentials [15]. This theory is supported by findings of enhanced glutamatergic activity following the application of anodal tDCS [2]. Neuroplasticity, the ability of the brain to form and restructure synaptic connections [16], is thought to coincide with increased glutamatergic activity [2] as evidenced in the lasting behavioral effects from tDCS (e.g., [9, 10]) and the acceleration of learning processes [3, 11, 12]. However, recent evidence suggests that the neuroplastic effects of tDCS have some dependence on synaptic activity during stimulation [7].

A growing method for studying neural processes is through the measurement of cerebral perfusion. The *in vivo* quantification of cerebral perfusion (referred to as cerebral blood flow (CBF) mL/100 mg/min) can be performed noninvasively using magnetic resonance imaging (MRI) through an arterial spin labeling (ASL) pulse sequence [17, 18]. ASL is a clinical method that has been used to identify early pathophysiological changes in Alzheimer's disease and other disorders such as dementia [18, 19]. In comparison to signals based on blood oxygen, CBF has better reliability and intersubject variability [20]. Furthermore, CBF is directly responsible for the delivery of glucose and oxygen. Both oxygen and glucose are necessary to maintain adenosine triphosphate (ATP) production and need to be replenished to support continued neural activity. Although CBF is not a direct measure of neural activity, it is a tightly coupled correlate: CBF changes with neural activity such as that which occurs during task activation or with changing metabolism [21]. Evidence published just this year indicates that this coupling is electrical: extracellular K^+ activates capillary endothelial cells which then signal upstream arteriolar dilation [22]. The extracellular concentration of K^+ increases during neural activity, thereby signaling enhanced vasodilation and increased blood flow to the supporting capillary bed.

The study of resting CBF in anodal left prefrontal tDCS may provide critical insights as increased glutamatergic activity associated with anodal tDCS would manifest as enhanced cerebral perfusion. Few previous studies have utilized ASL to assess the neural effects of tDCS. In some studies, anodal tDCS led increased regional CBF in the brain tissue underneath the stimulation site, with reliable and reproducible results within and between subjects. Furthermore, transfer effects were observed in brain regions functionally connected to the stimulation site [7]. Importantly, immediate and lasting changes in CBF have been associated with anodal left prefrontal tDCS [23]. The goal of this study is to enhance our understanding of the underlying neural mechanisms associated with repetitive anodal tDCS to the left prefrontal cortex through the study of resting cerebral perfusion. The study consisted of anodal left prefrontal tDCS applied on three consecutive days with the same procedures performed on each day to assess the additive effects of tDCS. In this work, we present preliminary findings of a larger, ongoing study.

2. Materials and Methods

2.1. Participants. A total of 28 healthy, active duty, Air Force military members recruited from Wright-Patterson Air Force Base volunteered to participate in this study. Participants were excluded from participation if they had any neurological or psychological diagnoses; vision, hearing, or motor control impairments; or recent trauma or hospitalization. Participants were also excluded if they currently took any medication which may affect cognitive function or if they were dependent on alcohol, caffeine, or nicotine. Written informed consent was obtained from each participant prior to any experimental procedures which were approved by the Air Force Research Laboratory Institutional Review Board at Wright-Patterson Air Force Base under Protocol number FWR20130126H. Participants eligible for compensation (i.e., if participation occurred in an off-duty status) received equal remuneration. Of the 28 participants recruited, eight were excluded due to medical disqualification ($n = 2$), incomplete data or corrupted data ($n = 2$), or failure to complete all three sessions in three consecutive days ($n = 4$).

Participants were randomly assigned to one of two groups. Both groups received the same instructions and performed the same tasks with the exception of the stimulation that was received. In the experimental group (ACT, $n = 11$, mean age $= 24.5 \pm 2.6$), 2 mA stimulation was provided for 30 minutes while in the control group (CON, $n = 9$, mean age $= 25.9 \pm 3.2$) sham stimulation consisting of 2 mA stimulation for 30 s. Participants in each group were blinded to the validity of the simulation (i.e., not aware of the stimulation condition) and naïve to TES (i.e., first time receiving TES).

All participants completed three experimental sessions on three consecutive days. Each session was separated by 24 hours. The sessions were conducted in the evening so as to not conflict with the working day but also due to the MRI availability. Participants completed the experimental sessions in groups of two with staggered start times (see Table 1). Start

Table 1: Starting times for the experimental procedures. Participants completed the three sessions in groups of two with staggered start times.

Procedure	Participant 1			Participant 2		
	Local start time	ASL scan time	Local end time	Local start time	ASL scan time	Local end time
Prestimulation MRI	5:00 pm	6:10 pm	6:15 pm	6:15 pm	7:25 pm	7:30 pm
Transcranial DC stimulation	6:30 pm	n/a	7:00 pm	7:55 pm	n/a	8:25 pm
Poststimulation MRI	7:30 pm	8:40 pm	8:45 pm	8:45 pm	9:55 pm	10:00 pm

times were held consistent across the three sessions and were counterbalanced across groups.

2.2. Transcranial DC Stimulation. On each of the three sessions, anodal stimulation was applied to the left prefrontal cortex (approximately F3) with the cathode placed on the contralateral bicep. During stimulation, participants completed a 30 min laboratory vigilance task [24]. The electric stimulation (MagStim DC Stimulator, Magstim Company Limited, Whitland, UK) delivered a constant 2 mA through a ring of five custom Na/NaCl electrodes. The electrodes were arranged in a 1.6 cm radius circle and separated by 0.1 cm (outer edge to outer edge). The same ring configuration was used at the cathode location. The 2 mA stimulation was distributed evenly among the five electrodes. The stimulator is battery-powered and utilizes multistage current monitoring to ensure constant current levels are delivered to the anode. Each electrode was placed in a small "cup" and secured to the participant using medical bandages. The electrode cups were filled with highly conductive gel (SignaGel, Parker Laboratories, Fairfield, NJ) to ensure current transfer to the scalp.

2.3. MRI Acquisition. At each session, MRI data was acquired prior to and approximately 0.5 hours following the application of tDCS. The MRI acquisition consisted of the following sequences: a 12 min resting-state functional MRI (fMRI), three 10 min task fMRIs, T1-weighted MRI, diffusion tensor imaging (DTI), magnetic resonance spectroscopy (MRS), and resting ASL. As this work is part of a larger, ongoing study, we will only be presenting the resting ASL data in this work. However, it is important to discuss the three task fMRIs where participants completed a dual (verbal and spatial) *n*-back task. This task was conducted in a boxcar design with 48 s control and task blocks, each with 16–3 s trials. During each trial, a letter was displayed on a 3×3 grid for 500 ms. Participants were asked to provide one response if the current letter was the same as the *n*th previous letter that was presented and another response if the current letter was in the same position on a 3×3 grid as the *n*th previous letter. For control blocks, the letter was replaced with a dot and participants were instructed to provide one response if the dot was on the right side of the grid and another for the left. For the first run, *n* was set to 2. *n* for the second run was determined from the performance of the first run (if performance was 90 or above, *n* incremented; if less than 70, *n* decremented; otherwise, *n* remained the same) and the third run from the second.

Structural (T1-weighted) images were acquired using a 3D brain volume imaging (BRAVO) pulse sequence which uses an inversion recovery prepared fast spoiled gradient echo (FSPGR). The structural images were acquired using a 256×256 element matrix, 172 slices oriented to the anterior commissure- (AC-) posterior commissure (PC) plane, $1\,mm^3$ isotropic voxels, 0.8 phase field of view factor, inversion time (TI) = 450 ms, TE = 3.224 ms, a flip angle of 13°, and an autocalibrated reconstruction for Cartesian sampling with a phase acceleration factor of 1.0 for the first session and 2.0 for all remaining sessions. All MRI procedures were conducted on a 3 Tesla (T) MRI (Discovery 750w, GE Healthcare, Madison, WI) using a 24-channel head coil.

Images of cerebral perfusion were acquired approximately 20 minutes prior to the application of tDCS and approximately 1.5 hours after the conclusion of stimulation using a pseudocontinuous arterial spin labeling (pcASL) technique [25] with inversion (tagging) pulses administered immediately inferior to the imaging volume. All images were acquired true axial (oriented perpendicular to the scanner bore) using a postlabel delay time (PLD) of 2025 ms. Five background suppression pulses were applied to reduce the signal of stationary tissues [26–28] and improve signal-to-noise ratio (SNR) of arterial blood. A 3D fast spin echo (3D FSE) sequence was used for acquisition of the imaging volume. To reduce motion sensitivity, improve acquisition time, and minimize susceptibility artifacts, a stack-of-spirals readout gradient starting at the center of the k-space was used [29]. A total of 8 spiral arms were used for k-space sampling. Echoes were rebinned to Cartesian space in a 128×128 matrix, with TR = 4640 ms, TE = 10.7 ms, voxel size = 1.875×1.875 mm, slice thickness = 4 mm, and flip angle = 111°. The sequence acquired a total of 3 tag/control pairs. The total acquisition time was 4 min 46 s. During the scan, participants were instructed to remain awake and focus on a fixation dot presented on the display. This condition has demonstrated significantly greater reliability in resting-state functional MRI across all within-network connections, as well as within default-mode, attention, and auditory networks when compared to eyes open (no specified fixation) and closed methods [30].

2.4. Data Processing and Analysis. Cerebral perfusion was quantified from ASL. CBF maps were computed from the automated functions in the GE reconstruction software. First, the 3 tagged and 3 control volumes were averaged in place (without motion correction). Then, difference images were calculated for all participants by subtracting the average tagged volume from the average control volume. Finally, quantitative CBF maps were generated from the difference images, the associated proton

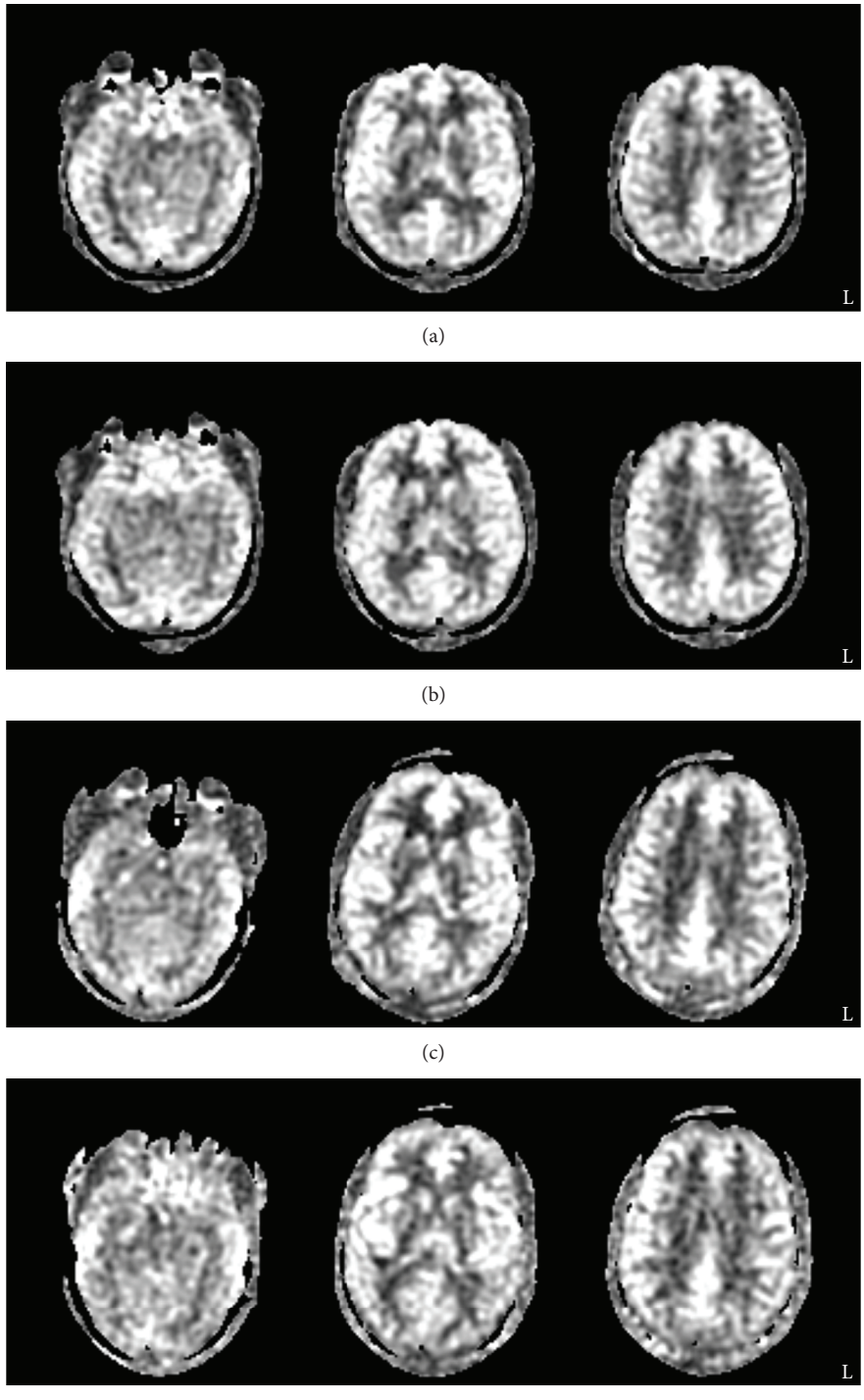

Figure 1: Raw CBF maps for (a) day 1 prestimulation and (b) day 3 poststimulation from a single CON participant and (c) day 1 prestimulation and (d) day 3 poststimulation from a single ACT participant.

density- (PD-) weighted volumes, and a standard single compartment model [31–33].

The CBF maps from each day and session were exported from the MRI scanner and processed using the FMRIB Software Library (FSL) [34, 35] on a 74-core Rocks Cluster Distribution (http://www.rocksclusters.org) high-performance computing system capable of running 120 threads in parallel (see Figure 1, e.g., CBF maps). First, the PD-weighted images acquired were registered to the individual's high-resolution structural image by estimating motion from a boundary-based registration method which includes a fieldmap-based distortion correction [36]. Then, the individual's high-

resolution structural image was registered to the MNI-152 T1-weighted 2 mm template provided in FSL [37, 38] using a 12-parameter model [39, 40]. In order to coregister all volumes, the CBF maps were converted to standard space using the transforms responsible for morphing the PD-weighted image of each data set to the structural image and the structural image to the template.

Next, group nonparametric statistical analyses were performed on the session 1 prestimulation and session 3 poststimulation coregistered CBF maps in a voxelwise fashion. Due to our mixed-model design and how the data would need to be permuted, an analysis of variance (ANOVA) was not possible using this approach. Instead, two separate analyses were performed. In the first, analyses were conducted separately for each group to evaluate the effect of the session. This analysis determined the statistical significance of differences in CBF (evaluated as increased perfusion from session 1 prestimulation to session 3 poststimulation) using permutation testing implemented in FSL's randomise [41, 42]. Null t distributions for contrasts representative of the main effect of the session were derived by performing 500,000 random permutations of the data [43]. A final t statistic was computed for each voxel by determining the probability of exceeding the t statistic from the known arrangement. Following this analysis, we implemented a clustering method to account for false positives due to the multiple comparisons [44]. This method considered adjacent voxels with a t statistic of 1.96 or greater to be a cluster. The significance of each cluster was estimated and compared to a threshold of $p < 0.05$ using Gaussian random field theory. The significance of voxels that either did not pass the significance level threshold or do not belong to a cluster was set to zero.

The second analysis assessed the interaction of the group and session using a single unpaired approach. Prior to this analysis, changes in CBF between the session 1 prestimulation and session 3 poststimulation coregistered CBF maps were calculated at the individual level. Then, the statistical significance of the variation in CBF between sessions and groups was determined using permutation testing implemented in FSL's randomise. Null t distributions for contrasts representative of the interaction of the session and group were derived by performing 500,000 random permutations. The clustering method outlined above was implemented to account for false positives due to multiple comparisons.

3. Results and Discussion

Paired permutation testing revealed a few small clusters with significant increases in resting CBF resulting from repetitive 2 mA stimulation of the left prefrontal cortex (Table 2, Figure 2). Localized increases in CBF were observed in several regions of the brainstem and cerebellum including the substantia nigra (SN). Cortically, bilateral changes in CBF were observed in the middle frontal, superior frontal, and inferior frontal gyri. Lateralized cortical changes were observed in the right rectal gyrus and precuneus and in the left supramarginal gyrus, paracentral lobule, parahippocampal gyrus, thalamus, caudate, and posterior cingulate cortex (PCC). However, the majority of the cortical effects appeared in white matter.

Table 2: The largest 15 clusters identified with an average increase in perfusion between prestimulation at session 1 and poststimulation at session 3 (ΔCBF) for the ACT group.

Volume (mm^3)	Max t-statistic	Max ΔCBF (mL/100 mg/min)	Max ΔCBF location (mm)		
			X	Y	Z
8000	7.23	13.45	−4	16	64
3824	5.28	15.00	16	−52	34
3320	3.76	10.27	−36	−60	52
3136	4.61	15.73	50	14	28
2832	4.66	8.64	−8	−12	10
2632	5.39	9.09	6	−12	12
2312	4.21	9.45	29	−40	38
2280	3.68	17.82	0	−28	44
1984	4.87	11.73	42	12	34
1800	5.00	13.09	−34	−26	−22
1528	6.58	10.09	40	32	4
1048	3.57	12.00	40	−72	−52
1032	3.79	9.18	−22	−36	10
864	6.59	13.73	0	−44	28
768	3.07	14.00	−6	−48	−52

In contrast to the ACT group, paired permutation testing performed on the group receiving repetitive sham stimulation identified significant decreases in resting CBF (Table 3, Figure 3). This included a large cluster encompassing multiple subcortical brain regions. This also comprised of a bilateral decrease in the superior frontal gyrus. Furthermore, lateralized cortical decreases were observed in the right middle frontal gyrus, inferior frontal gyrus, precentral gyrus, superior temporal gyrus, thalamus, and putamen and in the left cuneus, precuneus, cingulate gyrus, fusiform gyrus, middle temporal gyrus, and medial frontal gyrus.

The unpaired permutation testing analyzed the difference in resting CBF from session 1 prestimulation to session 3 poststimulation between the ACT and CON groups. This analysis revealed an overall significantly larger decrease in resting CBF for the CON group (Tables 4 and 5). This included a large cluster encompassing multiple subcortical and cortical brain regions. This cluster is identified as the fusiform gyrus in Table 4 but also included projections beginning in the locus coeruleus (LC) and projecting through the SN and PCC. This also comprised of localized clusters across several cortical regions. CBF in the bilateral superior frontal gyrus was found to increase in the ACT group but decrease in the CON group. This effect also appeared in right-lateralized regions: inferior frontal and middle frontal gyri. Left-lateralized clusters in the medial frontal gyrus and fusiform and right-lateralized clusters in the precentral gyrus, thalamus, and putamen showed a significant decrease in perfusion in the CON group, but no significant changes were observed in the ACT group. The opposite was observed for the left inferior parietal lobule.

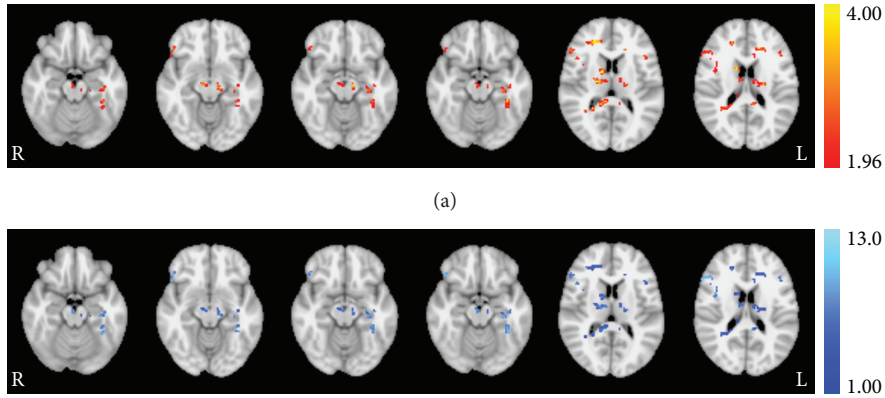

Figure 2: Session effect revealed from permutation testing for the ACT group. (a) Statistically significant (t-statistic) regions with altered CBF from baseline to session 3 poststimulation and (b) corresponding increases in quantified perfusion (mL/100 mg/min). Axial images taken at MNI coordinates $x = -18$, -12, -14, -16, 12, and 18 mm.

Table 3: The largest 15 clusters identified with an average decrease in perfusion between prestimulation at session 1 and poststimulation at session 3 (ΔCBF) for the CON group.

Volume (mm^3)	Max t-statistic	Max ΔCBF (mL/100 mg/min)	Max ΔCBF location (mm)		
			X	Y	Z
204,208	11.3	−23.00	−4	76	64
4016	7.41	−12.78	16	−20	34
3528	4.83	−24.56	−36	−60	52
2912	5.37	−12.67	50	14	28
2560	3.91	−13.11	−8	−12	10
1976	8.95	−13.89	6	−12	12
1344	4.34	−12.22	32	−40	38
1336	5.01	−9.44	0	−28	44
1296	5.84	−9.56	42	12	34
1112	4.75	−15.33	−34	−26	−22
944	5.48	−13.00	40	32	4
840	5.35	−20.44	40	−72	−52
832	4.62	−9.89	−22	−36	10
824	7.72	−22.11	0	−44	28
816	4.38	−9.89	−16	−42	30

Systematic group variations in thickness or atrophy in gray matter and/or different gyrification patterns are plausible and may have resulted in some or all of the effects observed. To evaluate the possibility of anatomical variations between groups, we performed voxel-based morphometry (VBM) to investigate voxelwise differences in local gray matter volume and/or topography. This analysis utilized brain-extracted structural images to first produce a template. In order to not bias the template towards one group, 2 random subjects from the ACT group were not included in this step to ensure an equal number of samples represent each group. The brain-extracted images were segmented automatically into gray matter, affine-registered to the gray matter International Consortium for Brain Mapping (ICBM) 152 template [38], concatenated, and averaged. The average image was flipped along the x-axis, and the mirror images were reaveraged. The gray matter images were reregistered to the average template using nonlinear registration, concatenated, averaged, and flipped along the x-axis. A final symmetric gray matter template was created by averaging the mirror images from the nonlinear registration. Next, gray matter templates for all subjects were created and nonlinearly registered to the custom gray matter template. A compensation for gray matter variations due to the nonlinear transformation was introduced using the Jacobian of the warp field [45]. All the registered gray matter volumes were spatially smoothed using a Gaussian kernel (sigma = 4 mm). Finally, an unpaired t-test was performed to compare the gray matter volumes across groups using a permutation (number of permutations = 500,000) approach performed in FSL randomise. A threshold-free cluster enhancement method was utilized to correct for multiple comparisons. No significant findings were observed in this analysis indicating neither the thickness or atrophy in gray matter nor different gyrification patterns existed between groups. Furthermore, this suggests that these anatomical variations could not have caused the observed variations in perfusion.

The unpaired permutation analysis represents the interaction between the session and group and, thus, reveals the effects on cerebral perfusion attributable to the application of anodal left prefrontal tDCS. Cerebral perfusion measured from ASL is a correlate of metabolic processes [21]. In general, small, focal increases in perfusion were found in the group receiving 2 mA anodal left prefrontal tDCS across 3 consecutive days while a widespread decrease was observed in the group receiving sham stimulation. This implies metabolism was consistent in recurrent tDCS, and decreased metabolism is associated with sham stimulation.

Our study population was limited to active duty military members, and the study was executed in the evening after typical work days, although we did not measure or control

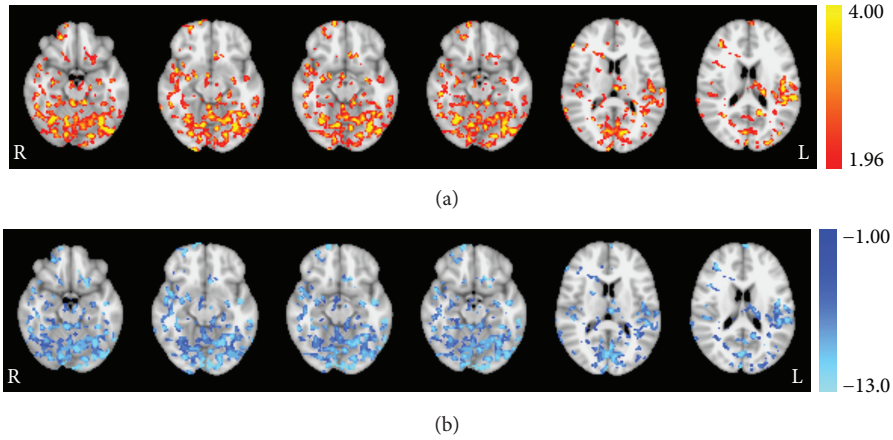

Figure 3: Session effect revealed from permutation testing for the CON group. (a) Statistically significant (t-statistic) regions with altered CBF from baseline to session 3 poststimulation and (b) corresponding decreases in quantified perfusion (mL/100 mg/min). Axial images taken at MNI coordinates $x = -18, -12, -14, -16, 12$, and 18 mm.

Table 4: Clusters identified with a significantly larger increase in perfusion from prestimulation at session 1 to session 3 poststimulation for the ACT group than for the CON group.

Hemisphere	Lobe	Gyrus	Volume (mm^3)	Max t-statistic	Max t-statistic location (mm)		
					X	Y	Z
Left	Temporal	Fusiform gyrus	15,784	5.14	−44	−56	−12
Right	Frontal	Inferior frontal gyrus	1445	5.66	60	20	4
Left	Parietal	Inferior parietal lobule	981	4.09	−32	−28	38
Left	Frontal	Superior frontal gyrus	715	4.09	−16	50	−20
Right	Parietal	Inferior parietal lobule	454	4.13	38	12	26
Left	Parietal	Superior parietal lobule	412	3.96	−44	−58	58
Left	Frontal	Precentral gyrus	293	4.43	−36	2	24
Right	Temporal	Fusiform gyrus	252	3.87	50	−32	−28
Right	Temporal	Middle temporal gyrus	210	3.93	42	0	−26
Right	Temporal	Inferior temporal gyrus	208	5.34	68	−30	−18
Right	Limbic	Cingulate	206	4.82	20	−4	42
Right	Parietal	Postcentral gyrus	177	3.24	62	−12	24
Right	Frontal	Precentral gyrus	176	3.08	50	2	48
Right	Limbic	Anterior cingulate cortex	166	3.67	12	22	−12
Left	Frontal	Medial frontal gyrus	148	3.42	−12	2	60
Left	Frontal	Superior frontal gyrus	131	3.93	−6	32	62
Right	Frontal	Superior frontal gyrus	101	3.78	18	70	−6
Right		Thalamus	95	3.64	8	−10	18
Right	Frontal	Middle frontal gyrus	87	3.37	22	20	64
Right	Parietal	Postcentral gyrus	86	3.54	44	−20	46
Left	Limbic	Anterior cingulate cortex	82	3.35	−14	30	22
Right	Limbic	Cingulate	80	3.53	24	−18	44
Left	Frontal	Medial frontal	80	3.28	−8	30	40
Left	Frontal	Superior frontal gyrus	77	2.91	−2	68	18
Left	Temporal	Fusiform gyrus	73	4.27	−46	−12	−28
Left	Frontal	Precentral gyrus	73	3.35	−38	−6	46
Right	Occipital	Lingual gyrus	71	3.45	26	−102	−6
Right		Putamen	71	3.09	−32	−8	−2

Table 5: Average CBF (±SEM) for each session/group from the clusters identified with a significantly larger increase in perfusion from prestimulation at session 1 to session 3 poststimulation for the ACT group than for the CON group.

Cluster	ACT		CON	
	Day 1 prestimulation CBF (mg/100 mL/min)	Day 3 poststimulation CBF (mg/100 mL/min)	Day 1 prestimulation CBF (mg/100 mL/min)	Day 3 poststimulation CBF (mg/100 mL/min)
L. fusiform gyr.	46.05 ± 1.67	49.12 ± 2.72	54.32 ± 2.95	44.92 ± 3.11
R. inf. front. gyr.	45.66 ± 1.74	51.35 ± 2.66	55.39 ± 2.14	48.77 ± 1.80
L. inf. par. lob.	41.91 ± 2.33	46.66 ± 2.85	53.84 ± 2.97	48.20 ± 2.31
L. sup. front. gyr.	43.85 ± 1.66	49.38 ± 2.28	54.18 ± 3.77	45.59 ± 2.08
R. inf. par. lob.	54.02 ± 2.71	60.72 ± 3.61	62.01 ± 2.61	56.53 ± 2.17
L. sup. par. lob.	46.36 ± 2.06	51.62 ± 2.46	57.50 ± 3.72	51.70 ± 2.37
L. precentral gyr.	47.67 ± 2.56	54.85 ± 3.32	60.10 ± 3.59	53.57 ± 2.24
R. fusiform gyr.	45.13 ± 1.75	49.94 ± 2.78	54.71 ± 2.83	47.77 ± 2.10
R. mid. temp. gyr.	35.97 ± 1.72	38.91 ± 2.66	44.12 ± 3.19	36.85 ± 2.29
R. inf. temp. gyr.	54.20 ± 2.66	60.18 ± 3.50	67.23 ± 3.00	59.48 ± 3.20
R. cingulate	26.44 ± 1.62	29.40 ± 1.67	31.46 ± 1.57	26.75 ± 1.24
R. postcentral gyr.	55.16 ± 2.92	58.52 ± 3.74	66.35 ± 2.57	58.83 ± 3.34
R. precentral gyr.	50.97 ± 2.50	55.60 ± 3.57	59.40 ± 2.75	52.78 ± 2.22
R. ant. cing. cort.	43.86 ± 2.98	47.93 ± 3.31	50.55 ± 1.89	43.44 ± 2.40
L. med. front. gyr.	38.35 ± 2.21	44.37 ± 2.64	50.01 ± 2.87	44.60 ± 1.31
L. sup. front. gyr.	45.39 ± 2.39	51.99 ± 1.73	58.87 ± 3.47	52.62 ± 2.46
R. sup. front. gyr.	55.52 ± 1.68	61.90 ± 3.42	70.82 ± 5.29	59.93 ± 2.77
R. thalamus	37.73 ± 2.26	43.27 ± 2.47	42.38 ± 1.91	39.36 ± 2.03
R. mid. front. gyr.	47.86 ± 3.26	54.08 ± 3.30	60.84 ± 2.89	52.83 ± 2.26
R. postcentral gyr.	44.32 ± 1.83	49.13 ± 2.65	51.83 ± 3.68	45.45 ± 3.21
L. ant. cing. cort.	26.56 ± 1.71	31.58 ± 1.28	38.40 ± 4.57	31.94 ± 1.78
R. cingulate	45.18 ± 3.25	49.41 ± 3.54	54.01 ± 2.76	46.79 ± 1.87
L. med. front. gyr.	21.89 ± 1.24	26.22 ± 1.71	27.54 ± 1.55	24.80 ± 1.47
L. sup. front. gyr.	48.97 ± 1.86	54.11 ± 4.37	60.99 ± 5.80	51.25 ± 3.37
L. fusiform gyr.	43.57 ± 2.65	49.91 ± 3.64	58.01 ± 2.42	52.00 ± 2.71
L. precentral gyr.	37.09 ± 1.91	40.43 ± 2.50	47.73 ± 3.50	39.29 ± 2.63
R. lingual gyr.	39.00 ± 1.94	41.87 ± 1.60	46.74 ± 3.45	40.15 ± 2.49
R. putamen	47.96 ± 3.36	48.57 ± 2.53	56.82 ± 4.07	46.27 ± 3.81

sleep/wake times. After three consecutive days of study participation as outlined in Table 1, it is only reasonable that the participants would be experiencing symptoms of fatigue. Hypoperfusion measured from ASL has been observed and detailed in patients with chronic fatigue syndrome [46–48] and associated with cognitive fatigue in healthy individuals [49]. Furthermore, hypometabolism has been observed in patients with chronic fatigue syndrome [50] and multiple sclerosis with fatigue [51]. The results from our CON group are consistent with this postulation and these previous findings; however, the findings from our ACT group are not. We theorize that left prefrontal tDCS provides some neural mechanism that counteracts this neural effect of fatigue. Behaviorally, left prefrontal tDCS has been shown to reduce the cognitive decline associated with fatigue in a similar group of active duty military members in an extended wakefulness study [9]. Anodal tDCS applied to the motor cortex has also been shown to have behavioral effects from fatigue in patients with multiple sclerosis [52]. However, there are no studies to date that have evaluated the neural effects of tDCS on fatigue.

The altered perfusion observed in this work can be traced to the LC. The LC is well known as the largest noradrenergic nucleus in the brain. The noradrenergic system is responsible for the synthesis, storage, and release of norepinephrine. Although the LC is relatively small, it is the primary source of norepinephrine for the neocortex. Projections from the LC are diverse, innervating most of the central nervous system [53]. Norepinephrine is a neurotransmitter associated with increased arousal and alertness [46–48], enhances long-term and working memory processes [54], and promotes vigilance and sensory processing [55]. The evidence presented in this work suggests that repetitive 2 mA tDCS applied to the left prefrontal cortex sustains the metabolic activity of the LC (Figure 4) which may result in an increased production of norepinephrine and a decreased effect of fatigue. In this work, measurements of resting perfusion were collected approximately

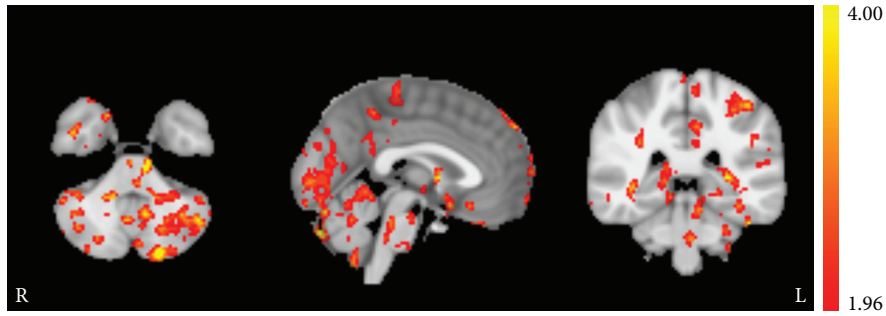

Figure 4: Session/group interaction effects (t-statistic) in the locus coeruleus revealed from permutation testing. The ACT group had significantly larger perfusion increases in the locus coeruleus from baseline to session 3 poststimulation compared to the CON group. The axial (left), sagittal (middle), and coronal (right) images were taken from MNI coordinates $z = -40$ mm, $y = -36$ mm, and $x = 0$ mm, respectively.

1.5 hrs following the conclusion of stimulation. Therefore, this effect remains following stimulation; however, it is not known how long this effect persists. Previous sleep deprivation studies utilizing anodal left prefrontal tDCS observed single-session behavioral effects that persisted for many hours [9, 10]. Effects such as this and the current findings could be derived from activation of the noradrenergic system.

Attention involves both top-down and bottom-up modulation. In bottom-up modulation, salient stimuli capture attention involuntarily while top-down modulation can direct attention as well as inhibit bottom-up processes. The ability to voluntarily direct attention (i.e., attentional control) varies significantly and substantially across individuals [56]. Top-down modulation of attention involves a variety of brain regions including the middle frontal gyrus, ACC, and superior parietal lobule. Each of these regions were found to have enhanced perfusion following repetitive 2 mA anodal tDCS to the left prefrontal cortex (Figure 5), suggestive of increased attentional control.

Objects can be classified based upon the observation of physical properties such as shape, color, and texture. Semantic memory, general knowledge that has accumulated through life, can aid the classification process. The fusiform gyrus is theorized to largely contribute to processes involving semantic memory [57]. The large increase in perfusion in the occipital cortex, including the fusiform gyrus (Figure 6), is suggestive of enhanced utilization of semantic processes, increased semantic memory, and/or a heightened ability to recognize objects.

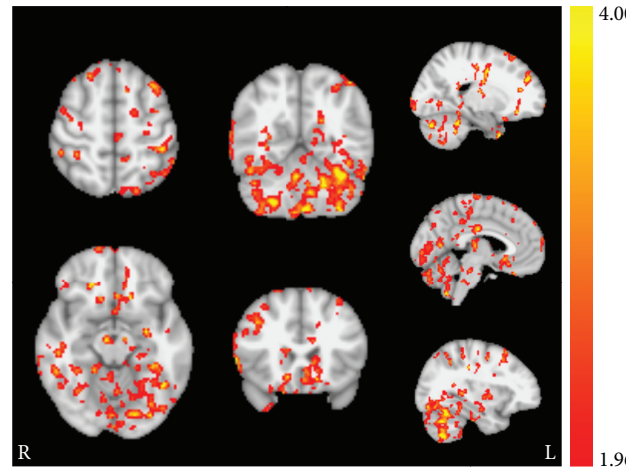

Figure 5: Session/group interaction effects (t-statistic) in the top-down attentional control network revealed from permutation testing. The ACT group had significantly larger perfusion increases in the right middle frontal gyrus, bilateral ACC, and left superior lobule from baseline to session 3 poststimulation compared to the CON group. The axial (left) images were taken from MNI coordinates $z = -14$ (top) and 56 (bottom) mm, sagittal (middle) images were taken from $y = -58$ (top) and 22 (bottom) mm, and coronal (right) images were taken from $x = 35$ (top), 47 (center), and 61 (bottom) mm.

4. Conclusions

This study examined the effect of repetitive tDCS on cerebral perfusion. Anodal left prefrontal tDCS was used to apply 2 mA to the scalp for 30 minutes on three consecutive days. Measures of resting cerebral perfusion were acquired before and after stimulation on each day using ASL. Widespread increases in perfusion, indicative of increased metabolism, were observed; however, general decreases were observed in a matched group receiving sham tDCS. Furthermore, perfusion increased significantly more in the active stimulation group across many areas of the brain. These increases originated in the LC and spread extensively to regions in the neocortex supporting functions such as object recognition and top-down attentional modulation. The changes in the neocortex may be a direct result of the stimulation or an indirect result via the changes in the noradrenergic system produced from the altered LC activity. These findings help understand the broad behavioral effects that have been demonstrated using anodal left prefrontal tDCS. Future work is necessary to identify if the observed changes in perfusion correlate with altered metabolism but should also address the transiency of these effects.

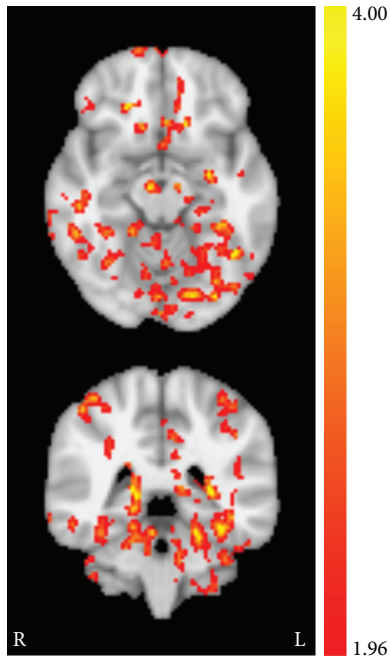

Figure 6: Session/group interaction effects (t-statistic) in the fusiform gyrus revealed from permutation testing. The ACT group had significantly larger perfusion increases in the right middle frontal gyrus, bilateral ACC, and left superior lobule from baseline to session 3 poststimulation compared to the CON group. The axial (top) and coronal (bottom) images were taken from MNI coordinates $z = -14$ mm and $y = -40$ mm, respectively.

Data Availability

This project is funded by a DoD contract, and the data is not available for public release at this time.

Disclosure

The opinions expressed herein belong solely to the authors. They do not represent and should not be interpreted as being those of or endorsed by the Department of Defense or any other branch of the federal government. The U.S. Government is authorized to reproduce and distribute reprints for governmental purposes notwithstanding any copyright notation thereon. The voluntary, fully informed consent of the subjects used in this research was obtained as required by 32 CFR 210 and DODI 3216.02_AFI 40-402.

Conflicts of Interest

Matthew Sherwood received compensation for this work as a consultant through DCS Corporation and is also employed by Wright State University. Dr. Sherwood serves an unpaid role as a member of Aaron Madaris' Dissertation Committee at Wright State University. Aaron Madaris received compensation for this work as an intern through DCS Corporation and is also a student at Wright State University. All other authors declare no conflicts of interest.

Acknowledgments

This work was supported by the Air Force Research Laboratory (AFRL) under the Human Interface and Research Technology program (Contract FA8650-14-D-6500).

References

[1] F. Fregni, M. A. Nitsche, C. K. Loo et al., "Regulatory considerations for the clinical and research use of transcranial direct current stimulation (tDCS): review and recommendations from an expert panel," *Clinical Research and Regulatory Affairs*, vol. 32, no. 1, pp. 22–35, 2015.

[2] B. A. Coffman, M. C. Trumbo, R. A. Flores et al., "Impact of tDCS on performance and learning of target detection: interaction with stimulus characteristics and experimental design," *Neuropsychologia*, vol. 50, no. 7, pp. 1594–1602, 2012.

[3] L. M. Bullard, E. S. Browning, V. P. Clark et al., "Transcranial direct current stimulation's effect on novice versus experienced learning," *Experimental Brain Research*, vol. 213, no. 1, pp. 9–14, 2011.

[4] V. P. Clark, B. A. Coffman, M. C. Trumbo, and C. Gasparovic, "Transcranial direct current stimulation (tDCS) produces localized and specific alterations in neurochemistry: a 1H magnetic resonance spectroscopy study," *Neuroscience Letters*, vol. 500, no. 1, pp. 67–71, 2011.

[5] N. Lang, H. R. Siebner, N. S. Ward et al., "How does transcranial DC stimulation of the primary motor cortex alter regional neuronal activity in the human brain?," *The European Journal of Neuroscience*, vol. 22, no. 2, pp. 495–504, 2005.

[6] D. Liebetanz, "Pharmacological approach to the mechanisms of transcranial DC-stimulation-induced after-effects of human motor cortex excitability," *Brain*, vol. 125, no. 10, pp. 2238–2247, 2002.

[7] X. Zheng, D. C. Alsop, and G. Schlaug, "Effects of transcranial direct current stimulation (tDCS) on human regional cerebral blood flow," *NeuroImage*, vol. 58, no. 1, pp. 26–33, 2011.

[8] J. T. Nelson, R. A. McKinley, E. J. Golob, J. S. Warm, and R. Parasuraman, "Enhancing vigilance in operators with prefrontal cortex transcranial direct current stimulation (tDCS)," *NeuroImage*, vol. 85, pp. 909–917, 2014.

[9] L. K. McIntire, R. A. McKinley, C. Goodyear, and J. Nelson, "A comparison of the effects of transcranial direct current stimulation and caffeine on vigilance and cognitive performance during extended wakefulness," *Brain Stimulation*, vol. 7, no. 4, pp. 499–507, 2014.

[10] L. McIntire, R. Andy McKinley, J. Nelson, and C. Goodyear, "Transcranial direct current stimulation (tDCS) versus caffeine to sustain wakefulness at night when dosing at start-of-shift," in *Advances in Neuroergonomics and Cognitive Engineering*, K. Hale and K. Stanney, Eds., vol. 488 of Advances in Intelligent Systems and Computing, pp. 157–172, Springer International Publishing, Cham, 2017.

[11] V. P. Clark, B. A. Coffman, A. R. Mayer et al., "TDCS guided using fMRI significantly accelerates learning to identify concealed objects," *NeuroImage*, vol. 59, no. 1, pp. 117–128, 2012.

[12] R. A. McKinley, L. McIntire, N. Bridges, C. Goodyear, and M. P. Weisend, "Acceleration of image analyst training with transcranial direct current stimulation," *Behavioral Neuroscience*, vol. 127, no. 6, pp. 936–946, 2013.

[13] J. Nelson, R. A. McKinley, C. Phillips et al., "The effects of transcranial direct current stimulation (tDCS) on multitasking

throughput capacity," *Frontiers in Human Neuroscience*, vol. 10, p. 589, 2016.

[14] R. Andy McKinley, L. McIntire, J. Nelson, J. Nelson, and C. Goodyear, "The effects of transcranial direct current stimulation (tDCS) on training during a complex procedural task," in *Advances in Neuroergonomics and Cognitive Engineering*, K. Hale and K. Stanney, Eds., vol. 488 of Advances in Intelligent Systems and Computing, Springer, Cham, 2017.

[15] L. J. Bindman, O. C. J. Lippold, and J. W. T. Redfearn, "Long-lasting changes in the level of the electrical activity of the cerebral cortex produced by polarizing currents," *Nature*, vol. 196, no. 4854, pp. 584-585, 1962.

[16] C. Pittenger and R. S. Duman, "Stress, depression, and neuroplasticity: a convergence of mechanisms," *Neuropsychopharmacology*, vol. 33, no. 1, pp. 88–109, 2008.

[17] D. S. Williams, D. J. Grandis, W. Zhang, and A. P. Koretsky, "Magnetic resonance imaging of perfusion in the isolated rat heart using spin inversion of arterial water," *Magnetic Resonance in Medicine*, vol. 30, no. 3, pp. 361–365, 1993.

[18] G. Xu, H. A. Rowley, G. Wu et al., "Reliability and precision of pseudo-continuous arterial spin labeling perfusion MRI on 3.0 T and comparison with ^{15}O-water PET in elderly subjects at risk for Alzheimer's disease," *NMR in Biomedicine*, vol. 23, no. 3, pp. n/a–293, 2010.

[19] M. Grade, J. A. Hernandez Tamames, F. B. Pizzini, E. Achten, X. Golay, and M. Smits, "A neuroradiologist's guide to arterial spin labeling MRI in clinical practice," *Neuroradiology*, vol. 57, no. 12, pp. 1181–1202, 2015.

[20] M. J. Weber, J. A. Detre, S. L. Thompson-Schill, and B. B. Avants, "Reproducibility of functional network metrics and network structure: a comparison of task-related BOLD, resting ASL with BOLD contrast, and resting cerebral blood flow," *Cognitive, Affective, & Behavioral Neuroscience*, vol. 13, no. 3, pp. 627–640, 2013.

[21] A. Borogovac and I. Asllani, "Arterial spin labeling (ASL) fMRI: advantages, theoretical constrains and experimental challenges in neurosciences," *International Journal of Biomedical Imaging*, vol. 2012, Article ID 818456, 13 pages, 2012.

[22] T. A. Longden, F. Dabertrand, M. Koide et al., "Capillary K +-sensing initiates retrograde hyperpolarization to increase local cerebral blood flow," *Nature Neuroscience*, vol. 20, no. 5, pp. 717–726, 2017.

[23] C. J. Stagg, R. L. Lin, M. Mezue et al., "Widespread modulation of cerebral perfusion induced during and after transcranial direct current stimulation applied to the left dorsolateral prefrontal cortex," *The Journal of Neuroscience*, vol. 33, no. 28, pp. 11425–11431, 2013.

[24] N. H. Mackworth, "The breakdown of vigilance during prolonged visual search," *Quarterly Journal of Experimental Psychology*, vol. 1, no. 1, pp. 6–21, 1948.

[25] A. C. Silva and S.-G. Kim, "Pseudo-continuous arterial spin labeling technique for measuring CBF dynamics with high temporal resolution," *Magnetic Resonance in Medicine*, vol. 42, no. 3, pp. 425–429, 1999.

[26] W. T. Dixon, M. Sardashti, M. Castillo, and G. P. Stomp, "Multiple inversion recovery reduces static tissue signal in angiograms," *Magnetic Resonance in Medicine*, vol. 18, no. 2, pp. 257–268, 1991.

[27] S. Mani, J. Pauly, S. Conolly, C. Meyer, and D. Nishimura, "Background suppression with multiple inversion recovery nulling: applications to projective angiography," *Magnetic Resonance in Medicine*, vol. 37, no. 6, pp. 898–905, 1997.

[28] F. Q. Ye, J. A. Frank, D. R. Weinberger, and A. C. McLaughlin, "Noise reduction in 3D perfusion imaging by attenuating the static signal in arterial spin tagging (ASSIST)," *Magnetic Resonance in Medicine*, vol. 44, no. 1, pp. 92–100, 2000.

[29] G. H. Glover, "Spiral imaging in fMRI," *NeuroImage*, vol. 62, no. 2, pp. 706–712, 2012.

[30] R. Patriat, E. K. Molloy, T. B. Meier et al., "The effect of resting condition on resting-state fMRI reliability and consistency: a comparison between resting with eyes open, closed, and fixated," *NeuroImage*, vol. 78, pp. 463–473, 2013.

[31] D. C. Alsop, J. A. Detre, X. Golay et al., "Recommended implementation of arterial spin-labeled perfusion MRI for clinical applications: a consensus of the ISMRM perfusion study group and the European consortium for ASL in dementia," *Magnetic Resonance in Medicine*, vol. 73, no. 1, pp. 102–116, 2015.

[32] D. C. Alsop and J. A. Detre, "Reduced transit-time sensitivity in noninvasive magnetic resonance imaging of human cerebral blood flow," *Journal of Cerebral Blood Flow & Metabolism*, vol. 16, no. 6, pp. 1236–1249, 1996.

[33] H. J. M. M. Mutsaerts, R. M. E. Steketee, D. F. R. Heijtel et al., "Inter-vendor reproducibility of pseudo-continuous arterial spin labeling at 3 Tesla," *PLoS One*, vol. 9, no. 8, article e104108, 2014.

[34] S. M. Smith, M. Jenkinson, M. W. Woolrich et al., "Advances in functional and structural MR image analysis and implementation as FSL," *NeuroImage*, vol. 23, Supplement 1, pp. S208–S219, 2004.

[35] M. W. Woolrich, S. Jbabdi, B. Patenaude et al., "Bayesian analysis of neuroimaging data in FSL," *NeuroImage*, vol. 45, no. 1, Supplement 1, pp. S173–S186, 2009.

[36] D. N. Greve and B. Fischl, "Accurate and robust brain image alignment using boundary-based registration," *NeuroImage*, vol. 48, no. 1, pp. 63–72, 2009.

[37] D. L. Collins, C. J. Holmes, T. M. Peters, and A. C. Evans, "Automatic 3-D model-based neuroanatomical segmentation," *Human Brain Mapping*, vol. 3, no. 3, pp. 190–208, 1995.

[38] J. Mazziotta, A. Toga, A. Evans et al., "A probabilistic atlas and reference system for the human brain: international consortium for brain mapping (ICBM)," *Philosophical Transactions of the Royal Society B: Biological Sciences*, vol. 356, no. 1412, pp. 1293–1322, 2001.

[39] M. Jenkinson and S. Smith, "A global optimisation method for robust affine registration of brain images," *Medical Image Analysis*, vol. 5, no. 2, pp. 143–156, 2001.

[40] M. Jenkinson, P. Bannister, M. Brady, and S. Smith, "Improved optimization for the robust and accurate linear registration and motion correction of brain images," *NeuroImage*, vol. 17, no. 2, pp. 825–841, 2002.

[41] M. J. Anderson and J. Robinson, "Permutation tests for linear models," *Australian & New Zealand Journal of Statistics*, vol. 43, no. 1, pp. 75–88, 2001.

[42] A. M. Winkler, G. R. Ridgway, M. A. Webster, S. M. Smith, and T. E. Nichols, "Permutation inference for the general linear model," *NeuroImage*, vol. 92, pp. 381–397, 2014.

[43] T. Nichols and A. Holmes, "Nonparametric permutation tests for functional neuroimaging," in *Human Brain Function: Second Edition*, pp. 887–910, Academic Press, 2004.

[44] K. J. Worsley, "Statistical analysis of activation images," in *Functional MRI: An Introduction to Methods*, P. M. Matthews,

P. Jezzard, and S. M. Smith, Eds., pp. 251–270, Oxford UP, London, 2001.

[45] C. D. Good, I. S. Johnsrude, J. Ashburner, R. N. A. Henson, K. J. Friston, and R. S. J. Frackowiak, "A voxel-based morphometric study of ageing in 465 normal adult human brains," *Neuroimage*, vol. 14, no. 1, pp. 21–36, 2001.

[46] B. Biswal, P. Kunwar, and B. H. Natelson, "Cerebral blood flow is reduced in chronic fatigue syndrome as assessed by arterial spin labeling," *Journal of the Neurological Sciences*, vol. 301, no. 1-2, pp. 9–11, 2011.

[47] S. M. MacHale, S. M. Lawrie, J. T. O. Cavanagh et al., "Cerebral perfusion in chronic fatigue syndrome and depression," *The British Journal of Psychiatry*, vol. 176, no. 6, pp. 550–556, 2000.

[48] D. C. Costa, C. Tannock, and J. Brostoff, "Brainstem perfusion is impaired in chronic fatigue syndrome," *QJM*, vol. 88, no. 11, pp. 767–773, 1995.

[49] J. Lim, W.-C. Wu, J. Wang, J. A. Detre, D. F. Dinges, and H. Rao, "Imaging brain fatigue from sustained mental workload: an ASL perfusion study of the time-on-task effect," *NeuroImage*, vol. 49, no. 4, pp. 3426–3435, 2010.

[50] U. Tirelli, F. Chierichetti, M. Tavio et al., "Brain positron emission tomography (PET) in chronic fatigue syndrome: preliminary data," *The American Journal of Medicine*, vol. 105, no. 3, pp. 54S–58S, 1998.

[51] U. Roelcke, L. Kappos, J. Lechner-Scott et al., "Reduced glucose metabolism in the frontal cortex and basal ganglia of multiple sclerosis patients with fatigue: a 18F-fluorodeoxyglucose positron emission tomography study," *Neurology*, vol. 48, no. 6, pp. 1566–1571, 1997.

[52] R. Ferrucci, M. Vergari, F. Cogiamanian et al., "Transcranial direct current stimulation (tDCS) for fatigue in multiple sclerosis," *NeuroRehabilitation*, vol. 34, no. 1, pp. 121–127, 2014.

[53] D. J. Chandler, "Evidence for a specialized role of the locus coeruleus noradrenergic system in cortical circuitries and behavioral operations," *Brain Research*, vol. 1641, Part B, pp. 197–206, 2016.

[54] V. Sterpenich, A. D'Argembeau, M. Desseilles et al., "The locus ceruleus is involved in the successful retrieval of emotional memories in humans," *The Journal of Neuroscience*, vol. 26, no. 28, pp. 7416–7423, 2006.

[55] C. W. Berridge, B. E. Schmeichel, and R. A. España, "Noradrenergic modulation of wakefulness/arousal," *Sleep Medicine Reviews*, vol. 16, no. 2, pp. 187–197, 2012.

[56] K. Fukuda and E. K. Vogel, "Human variation in overriding attentional capture," *The Journal of Neuroscience*, vol. 29, no. 27, pp. 8726–8733, 2009.

[57] M. Mion, K. Patterson, J. Acosta-Cabronero et al., "What the left and right anterior fusiform gyri tell us about semantic memory," *Brain*, vol. 133, no. 11, pp. 3256–3268, 2010.

Hindawi
Neural Plasticity
Volume 2018, Article ID 5158724, 8 pages
https://doi.org/10.1155/2018/5158724

Research Article

Green Tea and Red Tea from *Camellia sinensis* Partially Prevented the Motor Deficits and Striatal Oxidative Damage Induced by Hemorrhagic Stroke in Rats

Priscila Marques Sosa,[1,2,3] Mauren Assis de Souza,[1,2] and Pâmela B. Mello-Carpes[1,2,3]

[1]*Physiology Research Group, Stress, Memory and Behavior Lab, Federal University of Pampa, Uruguaiana, RS, Brazil*
[2]*Multicentric Graduate Program in Physiological Sciences, Federal University of Pampa, Uruguaiana, RS, Brazil*
[3]*Biological Sciences: Physiology Graduate Program, Federal University of Rio Grande do Sul, Porto Alegre, RS, Brazil*

Correspondence should be addressed to Pâmela B. Mello-Carpes; panmello@hotmail.com

Received 27 January 2018; Revised 17 June 2018; Accepted 16 July 2018; Published 2 August 2018

Academic Editor: Junichi Ushiba

Green tea from *Camellia sinensis* plays a well-established neuroprotective role in several neurodegenerative diseases, including intracerebral hemorrhage (ICH). However, the other teas of the same plant do not have their properties well understood; but they can be as effective as green tea as an alternative therapy. In this study, we investigated the effects of supplementation with green tea and red tea from *Camellia sinensis* on motor deficits and striatum oxidative damage in rats submitted to hemorrhagic stroke (ICH). Male Wistar rats were supplemented with green tea, red tea, or vehicle for 10 days prior to ICH induction. After injury, the rats were submitted to motor tests (open field for locomotion, rotarod for balance, and neurological deficit scale (NDS)) 1, 3, and 7 days after ICH induction, while the tea supplementation was maintained. Subsequently, the rats were euthanized to striatal tissue dissection for biochemical analyzes (lipid peroxidation, reactive oxygen species, glutathione levels, and total antioxidant capacity). ICH caused locomotor and balance deficits, as well as increased the neurological deficit (NDS). Only red tea prevented locomotor deficits after injury. Green tea and red tea prevented balance deficits on the seventh day after ICH. On NDS evaluation, green tea presented a better neuroprotection than red tea (until day 3 after ICH injury). In addition, ICH increased reactive oxygen species and lipid peroxidation levels, without altering antioxidant markers. Green and red teas were effective in decreasing the lipid peroxidation levels. Therefore, green and red teas partially prevented the motor deficits and striatal oxidative damage induced by ICH. Based on our results, we can consider that the two teas seem to be equally effective to prevent motor deficits and striatal oxidative damage induced by hemorrhagic stroke in rats.

1. Introduction

Intracerebral hemorrhage (ICH) is a common type of stroke associated with a considerable socioeconomic impact, disability, and mortality [1] and represents 15 to 20% of all stroke cases [2].

Some regions of the brain are more susceptible to stroke damage, including striatum, which is one of the most important regions for voluntary motor control [3]. After ICH, the hematoma components initiate an inflammatory signaling through the activation of microglia, which culminates on secondary damage [4, 5]. Progressive deterioration of brain tissues is classified as ICH secondary damage and plays an important role in neurological impairment [4]. These molecular events that occur during ICH increase the production of hydroxyl radicals and oxidation of lipids [6], which expose the brain to higher levels of reactive oxygen species (ROS). There is increasing evidence that oxidative stress contributes to ICH-induced secondary brain injury through the generation of ROS [7]. The biochemical events involved in secondary damage are not well described but represent an important therapeutic target after ICH [7].

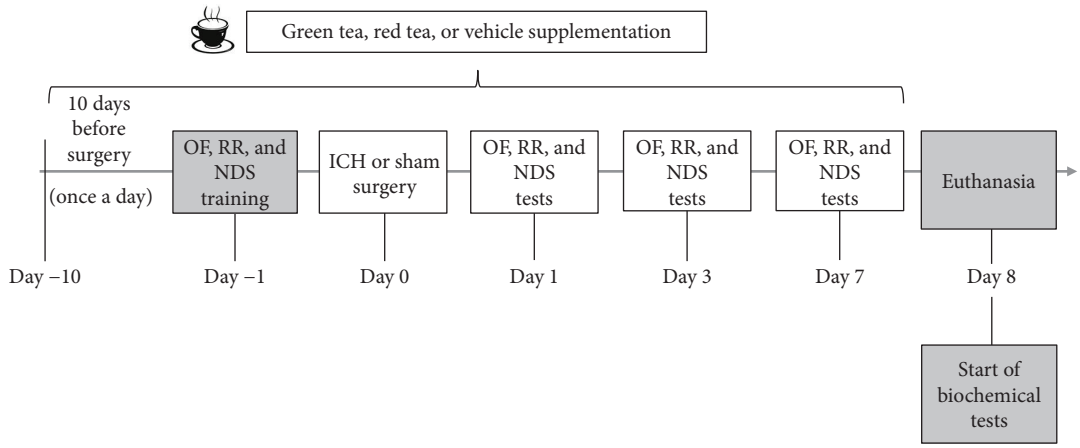

Figure 1: Experimental design. All rats were supplemented with green tea (GT), red tea (RT), or vehicle for 10 days prior to intracerebral hemorrhage (ICH). Twenty-four hours after, the rats were submitted to training in neuromotor tests (open field: OF; rotarod: RR; neurological deficit scale: NDS). In the following day (day 0), the rats were submitted to ICH or sham surgery following by 24 hours of recovery. On days 1, 3, and 7 after surgery, the rats were submitted to neuromotor tests. During all behavioral testing days, the rats continued to receive supplementation with tea or vehicle. On the eighth day, the rats were euthanized and the striatum were isolated to biochemical testing.

Despite the breakthrough in research, ICH treatments deserve great attention and further investigation. So, to seek adjuvant therapies that may prevent the progression of ICH secondary damage is important [8]. In this sense, interventions with potential antioxidants are being studied for treatment of damage caused by redox imbalance in brain tissues [9]. Antioxidants from natural products can slow or reverse the damage caused by excessive ROS production, as demonstrated in other models of neurodegenerative diseases related to oxidative damage [10, 11]. Several studies have shown the efficacy of the treatment with teas from *Camellia sinensis* as an antioxidant strategy [11, 12].

Green tea derived from *Camellia sinensis* contains a high content of flavonoids: epigallocatechin-3-gallate (EGCG), which accounts for approximately 59% of its total catechin content, epigallocatechin, epicatechin, and others [13]. Several studies have shown the antioxidant effects attributed to EGCG [14]. However, there are important variations in the herb's processing, and it can lead to changes in the content of flavonoids [15]. So, the different concentrations of catechins in the various types of tea derived from *Camellia sinensis* may be responsible for different neuroprotective effects of each one of them.

Recent studies comparing the therapeutic potential of the different teas of *Camellia sinensis* to protect from memory deficits in ischemia reperfusion (IR) [11] and in an Alzheimer disease model [16] have shown that, in addition to green tea, red tea also exerts an effective neuroprotection in these models. Other study performed by our team has already demonstrated the neuroprotective effect of green tea in ICH models [12]; however, comparative effects between the two teas were not analyzed in this model. Considering that both teas are very popular and accessible, studies comparing the neuroprotective effects of them are important. Here, we determine the neuroprotective potential of green tea and red tea from *Camellia sinensis* in the prevention of possible motor deficits and striatal oxidative damage in a model of intracerebral hemorrhage in adult rats.

2. Material and Methods

2.1. Animals and Experimental Design. Forty male Wistar rats (250–350 g) were obtained from the Central Vivarium of the Federal University of Santa Maria (UFSM-Santa Maria, RS, Brazil). The rats were housed 4 per cage and kept in a temperature-controlled room (24°C ± 1), with light/dark cycle of 12 h and food and water *ad libitum*. All the experiments were performed in accordance with the standards of the "Principles of laboratory animal care" (NIH publication No. 85-23, revised 1996) and were previously approved by the Institutional Animal Care and Use Committee (protocol #002/2017).

The rats were randomly divided into four groups: sham; intracerebral hemorrhage (ICH); intracerebral hemorrhage + green tea (ICH + GT); and intracerebral hemorrhage + red tea (ICH + RT). Rats received specific tea or vehicle for ten days prior to ICH surgery [12]. After, the animals were submitted to the training in neuromotor tests (open field, rotarod, and neuromotor deficit scale) and, in the following day, to the ICH or sham surgery. On days 1, 3, and 7 after surgery, the animals were tested in the neuromotor tests and after were euthanized to striatum dissection and preparation for biochemical essays. During the behavioral test period, the animals continued to receive tea or vehicle supplementation (Figure 1).

2.2. ICH Surgery. Surgical procedures were performed aseptically. The rats were anesthetized with ketamine and xylazine (i.p., 75 and 10 mg kg, resp.). Body temperature was maintained at 37°C during surgery using a surgical warming table. After placing the animals on the stereotactic table, a 3.5 mm hole was made to the right and 0.5 mm anterior to bregma. A 26-gauge needle (Hamilton, Hamilton, NV, USA syringe)

was inserted unilaterally into 6.5 mm in the right striatum to infuse 1 μl of sterile saline containing 0.2 U of bacterial collagenase (type IV). The needle was left in place for 5 min and then slowly withdrawn. The hole was sealed with a metal screw, suture threads were used to close the wound, and lidocaine was used at the suture site [17]. The same procedure was performed with the sham animals, except that the infusion did not contain collagenase, only saline.

2.3. Tea Supplementation. The two types of *Camellia sinensis* teas (green and red) were purchased directly from the same company (Madrugada Alimentos Ltda., Venâncio Aires, RS, Brazil), and prepared daily in the same way.

The teas were prepared with distilled water (95°C ± 5°C) and then the infusion was maintained rested and muffled for approximately 3 minutes, and after was filtered. Teas were administered via gavage (400 mg/ml/day), at room temperature [9].

Tea samples used in this study were analyzed by high-performance liquid chromatography (HPLC) to analyze the presence of epicatechin (EC), epigallocatechin (EGC), epigalocatechin gallate (EGCG), and epicatechin gallate (ECG) [18] (Table 1).

2.4. Behavioral Testing. To verify possible changes and/or deficits in motor function, the rats were trained in OF, RR, and NDS tasks 24 h prior to ICH or sham surgery. The tests were performed 24 h, 3 days and 7 days after the surgeries.

2.5. Open Field Test (OF). To evaluate the locomotor activity and the exploratory behavior of the rats, we used the open field apparatus. The open field consists in a box (60 cm in diameter × 45 cm in height) divided into 12 quadrants of the same surface area. The animals were gently placed in the open field arena (i.e., in the box), so that they could freely explore it for 5 min. The number of crossed lines (crossings) was counted [19]. After each rat testing, the arena was cleaned with 70% ethanol.

2.6. Rotarod Test (RR). In order to evaluate the influence of ICH in rats' motor coordination and balance, the RR test was used. The apparatus consists of a rotating cylinder (5 cm diameter × 8 cm wide × 20 cm high), with an automatic fall register. On the training day, the animals were placed in the static cylinder for 2 minutes for habituation. After the habituation time, the cylinder rotation was set at 16 rpm for 6 minutes, and the number of falls and latency for the first fall were recorded. In the test sessions, the animals were suspended for 6 minutes in the cylinder at a speed set in 20 rpm. The number of falls and latency for first fall were again recorded [20].

2.7. Neurological Deficit Scale (NDS). This test set is sensitive to striatal/motor damage [21]. The rats were trained in NDS before surgery, for reference. On test days after surgery, they were resubmitted to NDS. Briefly, the rats were evaluated for spontaneous movement, hind limb retraction, bilateral forefoot grip, contralateral forearm flexion, and beam trajectory. A maximum score of 14 indicates greater neurological impairment [22].

Table 1: Concentration of catechins (mg/ml) found in samples of the two teas from *Camellia sinensis*.

Catechins	Green tea	Red tea
(−)-Epigallocatechin	6412.14	ND
(−)-Epicatechin	5736.00	5442.34
(−)-Epigallocatechin gallate	9405.42	ND
(−)-Epicatechin gallate	2609.19	ND

ND: not detected.

2.8. Biochemical Analyses

2.8.1. Tissue Preparation. Rats were sacrificed 24 hours after the last test day. Their brains were removed, and the striatum ipsilateral to the lesion was quickly dissected and homogenized in 50 mM Tris HCl, pH 7.4 (1/10, *w*/*v*). The samples were centrifuged at 2400*g* for 10 min, and the supernatants (S1) were used for assay.

2.8.2. Lipid Peroxidation. Lipid peroxidation was assessed by the substances reactive to thiobarbituric acid (TBARS) test [23]. S1 aliquot was incubated with a solution of 0.8% thiobarbituric acid, acetic acid buffer (pH 3.2), and sodium dodecyl sulfate solution (8%) at 95°C for 2 h. The color reaction was measured at 532 nm. Results were expressed as nmol of malondialdehyde (MDA) per mg protein.

2.8.3. Reactive Oxygen Species (ROS) Levels. ROS levels were determined indirectly by fluorimetric method spectrum using 2′, 7′-dichlorofluorescein diacetate (DCFH-DA). The samples were incubated in the dark with 5 μl of DCFH-DA (1 mM). Oxidation monitoring was made of DCFH-DA to dichlorofluorescein (DCF) fluorescence by reactive oxygen species. The fluorescence emission intensity was performed at 520 nm (with excitation at 480 nm) for 60 minutes after the addition of DCFH-DA in spectrofluorimeter (Shimadzu RF-5301PC Model).

2.8.4. Glutathione (GSH) Levels. GSH levels were fluorometrically determined (Hissin and Hilf, 1976). An aliquot of homogenized sample was mixed (1 : 1) with perchloric acid ($HClO_4$) and centrifuged at 3000*g* for 10 min. This mixture was centrifuged, the protein pellet was discarded, and free thiols (SH) groups were determined in the clear supernatant. An aliquot of supernatant was incubated with orthophthaladehyde and fluorescence was measured at excitation of 350 nm and emission of 420 nm. Results were normalized by mg of protein and expressed as percent of control.

2.8.5. Total Antioxidant Capacity. Total antioxidant capacity was measure by ferric reducing/antioxidant power assay (FRAP). Working FRAP reagent was prepared by mixing 25 ml acetate buffer, 2.5 ml TPTZ solution, and 2.5 ml FeCl3.6H2O solution, and 10 μl of homogenate was added in the 300 μl working FRAP reagent in a microplate (Benzie and Strain, 1996). A standard curve with 10 μl trolox (concentrations of 15, 30, 60, 120, and 240 mM) and 300 μl working FRAP reagent was used. The microplate was incubated at 37°C for 15 min before reading in SpectraMax M5

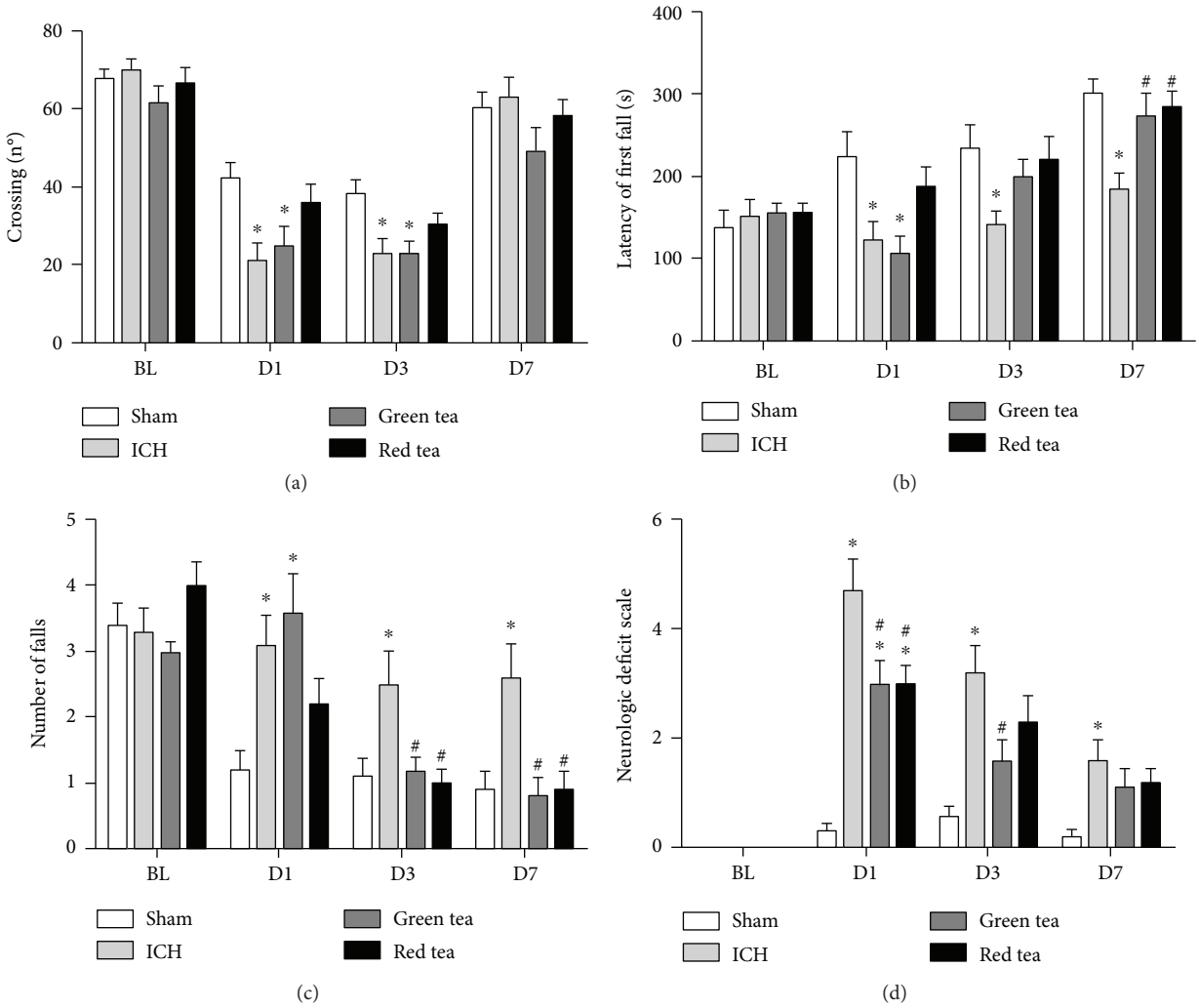

Figure 2: Effects of green and red tea administration on neuromotor function after ICH in rats. (a) Open field test: number of crossings; (b) rotarod test: latency to the first fall in seconds; (c) rotarod test: total number of falls; (d) neurological deficit scale: total score. Data are presented as the mean ± S.E.M. One-way ANOVA $^{*}P < 0.05$ in comparison to sham group, $^{\#}P < 0.05$ in comparison to the ICH group ($n = 10$/group).

Microplate Reader at 593 nm. Each sample was analyzed in triplicate.

2.8.6. Protein Determination. Protein content was measured colorimetrically by the method of Bradford [24] using bovine serum albumin (1 mg·ml^{-1}) as standard.

2.9. Statistical Analysis. Data were checked for normality of distribution using Shapiro-Wilk test. Results are presented as mean ± standard error of the mean (SEM). Results were analyzed by one-way ANOVA followed by Tukey's post hoc test, when appropriate. Significance level was set at 0.05 for all analyses.

3. Results

3.1. Behavioral Assessment. The locomotor activity was assessed using the OF test. The locomotor activity was different between the groups on days 1 ($F_{(3,\ 36)} = 4.621$, $P = 0.0078$, Figure 2(a)) and 3 ($F_{(3,\ 36)} = 4.771$, $P = 0.0067$, Figure 2(a)). However, on day 7 there was no difference between the groups ($F_{(3,\ 36)} = 1.563$, $P = 0.215$, Figure 2(a)). The post hoc test showed that the rats in the ICH group had decreased locomotor activity compared to sham rats on day 1 ($P < 0.05$, Figure 2(a)) and day 3 ($P < 0.05$, Figure 2(a)). On day 7, there was no difference in locomotor activity between the ICH and sham rats ($P > 0.05$). In addition, there are no differences on crossings between ICH and ICH + green tea groups on days 1 and 3 ($P > 0.05$, ICH versus ICH + teas Figure 2(a)). Importantly, ICH + red tea presented similar number of crossing to the control group on both days (D1: $P = 0.0078$; D3: $P = 0.0067$), while green tea did not present the same effect.

In rotarod test, there was a difference between the groups on days 1 ($F_{(3,\ 36)} = 5.264$, $P = 0.004$, Figure 2(b)), 3 ($F_{(3,\ 36)} = 2.925$, $P = 0.046$, Figure 2(b)), and 7 ($F_{(3,\ 36)} = 6.352$, $P = 0.001$, Figure 2(b)), considering the latency for the first fall. The rats in the ICH group presented a deficit in the

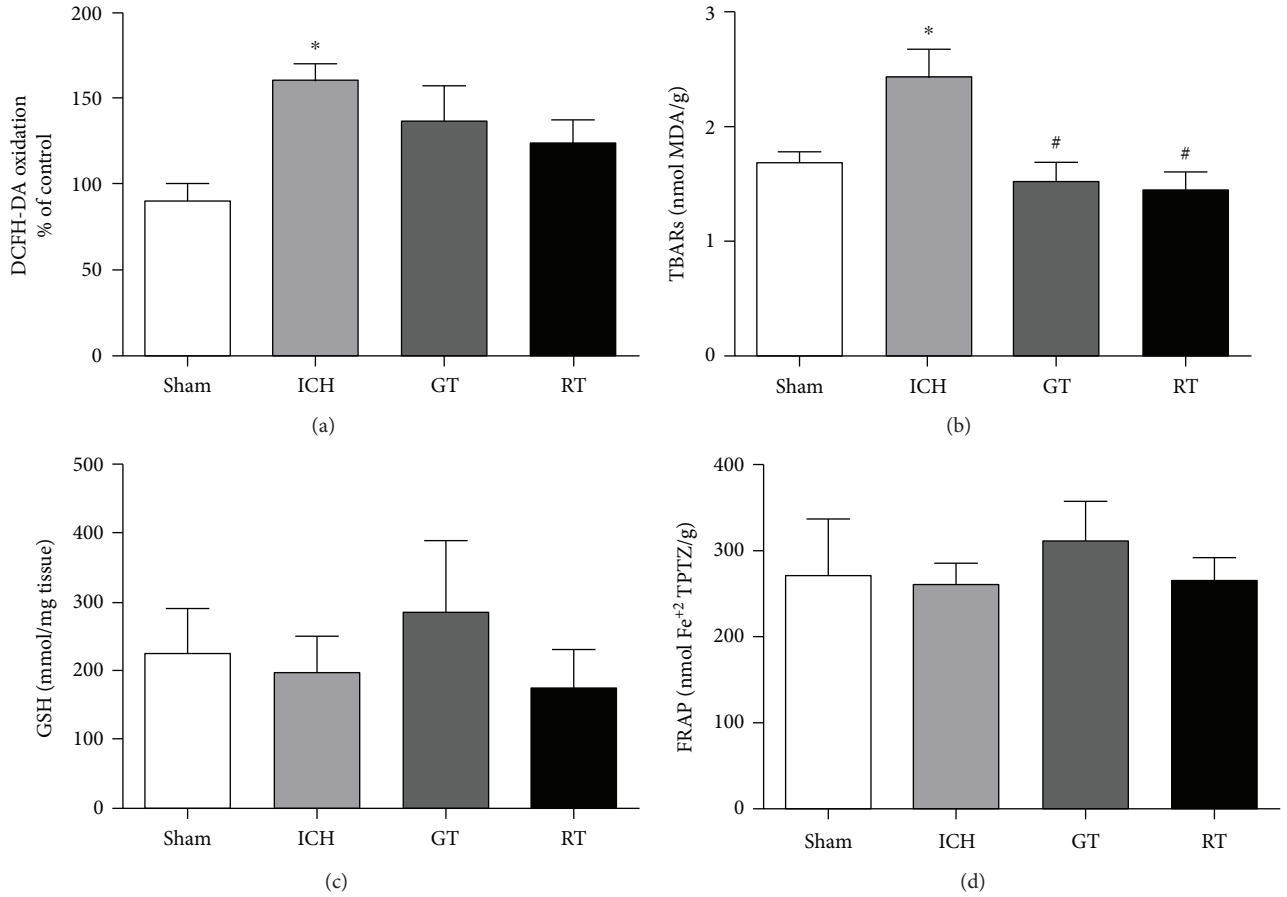

Figure 3: Effects of administration of green tea and red tea on oxidative stress, oxidative damage, and antioxidant markers on striatum after ICH in rats. (a) ROS levels by DCFH method; (b) lipid peroxidation by TBARS (thiobarbituric acid reactive substance); (c) glutathione levels (GSH); (d) total antioxidant capacity by FRAP method. Data are presented as the mean ± S.E.M. One-way ANOVA $^{*}P < 0.05$ in comparison to sham group; $^{\#}P < 0.05$ in comparison to ICH group ($n = 6$/group).

balance (shorter latency to the first fall than control animals) on days 1, 3, and 7 ($P < 0.05$, Figure 2(b)). GT and RT supplementation showed a neuroprotective effect on the seventh day ($P < 0.05$ for GT; $P < 0.01$ for RT; Figure 2(b)). In addition, there were no differences in the balance between ICH + ICH tea groups on days 1 and 3 ($P > 0.05$, ICH versus ICH + teas; Figure 2(b)), but ICH + RT presented a similar latency for the first fall than the control group on day 1 ($P = 0.04$, Figure 2(b)).

Considering the number of falls (rotarod test), we observed difference between the groups on days 1 ($F_{(3,\ 36)} = 5.698$, $P = 0.0027$, Figure 2(c)), 3 ($F_{(3,\ 36)} = 4.832$, $P = 0.0063$, Figure 2(c)), and 7 ($F_{(3,\ 36)} = 5.921$, $P = 0.002$, Figure 2(c)). The ICH rats showed a higher number of falls than sham rats on days 1, 3, and 7 ($P < 0.05$, Figure 2(c)). The GT reversed this deficit at days 3 ($P < 0.05$, Figure 2(c)) and 7 ($P < 0.01$, Figure 2(c)), as well as RT (D3: $P < 0.05$; D7: $P < 0.01$; Figure 2(c)), but only ICH + red tea presented similar number of falls to the control group on day 1 ($P > 0.05$, Figure 2(c)).

On neurological deficit (NDS) evaluation, we found differences between the groups on days 1 ($F_{(3.36)} = 20.47$, $P < 0.0001$, Figure 2(d)), 3 ($F_{(3.36)} = 7.704$, $P = 0.0004$, Figure 2(d)), and 7 ($F_{(3.36)} = 4.21$, $P = 0.013$, Figure 2(d)). ICH rats presented higher NDS score than sham rats on days 1 ($P < 0.0001$, Figure 2(d)), 3 ($P < 0.001$, Figure 2(d)), and 7 ($P < 0.05$, Figure 2(d)). The GT and RT were able to reverse these deficits on day 1 (GT: $P < 0.05$, RT: $P < 0.05$, Figure 2(d)), but, on day 3, only GT reversed the neurological deficit ($P < 0.05$, Figure 2(d)).

3.2. Biochemical Assays. Considering that the increase of oxidative stress is one of the secondary damage characteristics of ICH affected tissues, we evaluated the levels of oxidative species, the oxidative damage, the levels of GSH (an antioxidant marker), and the total antioxidant capacity in the striatum of rats.

A significant difference on the striatal level of oxidative species (DCFH) ($F_{(3,\ 20)} = 6.850$, $P = 0.0137$, Figure 3(a)) was observed. The post hoc showed that ICH rats presented increased ROS compared to the sham group ($P < 0.01$). Neither green tea ($P > 0.05$) nor red tea ($P > 0.05$) was able to reverse striatal oxidative stress.

There was difference between the groups on lipoperoxidation (TBARS) ($F_{(3,\ 20)} = 7.144$; $P = 0.0019$, Figure 3(b)). ICH rats showed an increase in lipoperoxidation compared

to sham rats ($P < 0.05$). Both green tea and red tea avoided this increase (GT: $P < 0.01$ versus ICH; RT: $P < 0.01$ *versus* ICH; Figure 3(b)).

Considering the antioxidant measures, we did not find differences between the groups in the GSH levels ($F_{(3,\ 20)} = 0.4608$, $P = 0.7127$, Figure 3(c)), as in the total antioxidant capacity (FRAP; $F_{(3,\ 20)} = 0.2767$, $P = 0.8415$, Figure 3(d)).

4. Discussion

In this study, we determined the neuroprotective potential of green tea and red tea on the motor deficits and striatal damage caused by hemorrhagic stroke in rats. Our major findings demonstrate that the two teas studied partially protect against neuromotor deficits and oxidative damage caused by ICH, and appear to be promoters of neuroprotection in this model. The different teas protect against neurological deficits mainly on the first and third day after the injury, avoiding locomotor (OF) and balance deficits (RR), general neuromotor function deficits (NDS), and contributing to avoid the increase of lipid peroxidation (TBARS).

ICH is associated with motor damage [25, 26] and cognitive impairments [27] that may be closely related to oxidative stress [28]. Our current results show that ICH generates locomotor and exploratory damage (OF), which is maintained for up to 3 days after injury. However, in this case, only the red tea was able to protect against such damage. A significant finding is that on the seventh day after the injury, a spontaneous recovery was observed in relation to the locomotor and exploratory activity, which is in agreement with Lu et al. [29], but prevents us from evaluating whether the teas have a protective effect in this case. Additionally, the results show that ICH rats presented a balance impairment (RR) until the seventh day after ICH, and that the green and red teas were able to protect against such damages on days 3 and 7 after the injury. The neuromotor deficit was also observed from the first to the seventh day after ICH in NDS test [22]. Green tea was effective to protect the damage on test day 1 and 3 after injury, while red tea was effective only on test day 1.

Strategies that propose the administration of antioxidant agents have been widely tested to prevent or treat hemorrhagic stroke [30, 31]. Previous studies have already demonstrated the neuroprotective effects of green tea on balance in ICH [12] and brain ischemia-reperfusion models [18, 32]. It is known that ICH injury mechanisms are related to increased free radical production and consequent oxidative stress [9, 28]. In this study, ICH induced an increase on striatum ROS and on lipid peroxidation. Green tea and red tea were able to protect the striatum tissue against lipid peroxidation. Any alteration on antioxidant markers was detected.

The administration of tea from *Camellia sinensis* and EGCG (the main component of green tea) has already been described as neuroprotective by its antioxidant effects in different models of brain injury [9, 28]. A recent study conducted in our laboratory that sought to evaluate the neuroprotective capacity of 4 teas from *Camellia sinensis* (green, red, white, and black) in an ischemic stroke model showed that the greatest protective effect on memory and oxidative stress is from green tea and red tea, since the best effects associated with green tea [11]. In another study using green, red, and black teas from *Camellia sinensis*, Schimidt and colleagues suggest that supplementation with green tea and red tea may avoid deficits in social and object recognition memories related to Alzheimer's disease, but only green tea avoids the hippocampal oxidative stress and damage induced in Alzheimer model [16]. These effects may be closely related to the greater amount of specific catechins present in green tea [33, 34], since some literature data suggest that the beneficial effects of teas are mainly related to catechins polyphenol and their derivatives [35]. However, this may not be the only explanation for their ability to neuroprotection. In addition to the antioxidant capacity, we cannot disregard the anti-inflammatory potential and inhibition of acetylcholinesterase action [36] of the *Camellia sinensis* teas, although these mechanisms are not completely clear.

The great amount of compounds in teas emphasizes the differences of mixture use or its isolated components. Here, considering that the neuroprotection effects could be related to the combined activity of the varios teas' compounds [37], we decided investigated the effects of the teas, and not of the isolated compounds, mainly because the teas mixture are available to population.

5. Conclusions

Green and red teas have been shown to be effective strategies, with similar effectiveness, to prevent some motor deficits and the striatal oxidative damage induced by ICH. The mechanisms involved in their protective role include the decrease of oxidative damage, that is, lipid peroxidation.

Data Availability

The data can be made available through request by e-mail pamelacarpes@unipampa.edu.br.

Additional Points

Highlights. Hemorrhagic stroke (ICH) causes motor deficits and oxidative damage in the striatum. Green tea and red tea partially avoided the motor deficits caused by ICH. Green tea and red tea avoided the striatal oxidative damage caused by ICH.

Conflicts of Interest

The authors declare that there is no conflict of interest regarding the publication of this paper.

Acknowledgments

This work was supported by research grants and fellowship from CAPES (Coordenação de Aperfeiçoamento de Pessoal de Nível Superior), Brazil; CNPq (Conselho Nacional de Pesquisa), Brazil; and Federal University of Pampa, Brazil. Priscila Marques Sosa was supported by FAPERGS/CAPES fellowship. Mauren Assis de Souza was supported by CAPES.

Pâmela B Mello-Carpes was supported by For Women in Science Program, L'Oreal Foundation & UNESCO, and CNPq.

References

[1] B. Bakhshayesh, M. Hosseininezhad, S. M. Seyed Saadat, M. Hajmanuchehri, E. Kazemnezhad, and A. R. Ghayeghran, "Predicting in-hospital mortality in Iranian patients with spontaneous intracerebral hemorrhage," *Iranian Journal of Neurology*, vol. 13, no. 4, pp. 231–236, 2014.

[2] R. L. Macdonald, R. T. Higashida, E. Keller et al., "Preventing vasospasm improves outcome after aneurysmal subarachnoid hemorrhage: rationale and design of CONSCIOUS-2 and CONSCIOUS-3 trials," *Neurocritical Care*, vol. 13, no. 3, pp. 416–424, 2010.

[3] R. Baez-Mendoza and W. Schultz, "The role of the striatum in social behavior," *Frontiers in Neuroscience*, vol. 7, p. 233, 2013.

[4] X. Lan, X. Han, Q. Li, Q. W. Yang, and J. Wang, "Modulators of microglial activation and polarization after intracerebral haemorrhage," *Nature Reviews Neurology*, vol. 13, no. 7, pp. 420–433, 2017.

[5] J. Shen, B. Chen, G. R. Zheng et al., "Detection of high serum concentration of CXC chemokine ligand-12 in acute intracerebral hemorrhage," *Clinica Chimica Acta*, vol. 471, pp. 55–61, 2017.

[6] S. M. Sadrzadeh and J. W. Eaton, "Hemoglobin-mediated oxidant damage to the central nervous system requires endogenous ascorbate," *The Journal of Clinical Investigation*, vol. 82, no. 5, pp. 1510–1515, 1988.

[7] X. Hu, C. Tao, Q. Gan, J. Zheng, H. Li, and C. You, "Oxidative stress in intracerebral hemorrhage: sources, mechanisms, and therapeutic targets," *Oxidative Medicine and Cellular Longevity*, vol. 2016, Article ID 3215391, 12 pages, 2016.

[8] J. S. Knutson, D. D. Gunzler, R. D. Wilson, and J. Chae, "Contralaterally controlled functional electrical stimulation improves hand dexterity in chronic hemiparesis: a randomized trial," *Stroke*, vol. 47, no. 10, pp. 2596–2602, 2016.

[9] K. J. Wu, M. T. Hsieh, C. R. Wu, W. G. Wood, and Y. F. Chen, "Green tea extract ameliorates learning and memory deficits in ischemic rats via its active component polyphenol epigallocatechin-3-gallate by modulation of oxidative stress and neuroinflammation," *Evidence-Based Complementary and Alternative Medicine*, vol. 2012, Article ID 163106, 11 pages, 2012.

[10] F. Shaki, Y. Shayeste, M. Karami, E. Akbari, M. Rezaei, and R. Ataee, "The effect of epicatechin on oxidative stress and mitochondrial damage induced by homocycteine using isolated rat hippocampus mitochondria," *Research in Pharmaceutical Sciences*, vol. 12, no. 2, pp. 119–127, 2017.

[11] A. Martins, H. L. Schimidt, A. Garcia et al., "Supplementation with different teas from Camellia sinensis prevents memory deficits and hippocampus oxidative stress in ischemia-reperfusion," *Neurochemistry international*, vol. 108, pp. 287–295, 2017.

[12] C. D. C. Altermann, M. A. Souza, H. L. Schimidt et al., "Short-term green tea supplementation prevents recognition memory deficits and ameliorates hippocampal oxidative stress induced by different stroke models in rats," *Brain Research Bulletin*, vol. 131, pp. 78–84, 2017.

[13] M. Assuncao, M. J. Santos-Marques, F. Carvalho, and J. P. Andrade, "Green tea averts age-dependent decline of hippocampal signaling systems related to antioxidant defenses and survival," *Free Radical Biology & Medicine*, vol. 48, no. 6, pp. 831–838, 2010.

[14] P. Bogdanski, J. Suliburska, M. Szulinska, M. Stepien, D. Pupek-Musialik, and A. Jablecka, "Green tea extract reduces blood pressure, inflammatory biomarkers, and oxidative stress and improves parameters associated with insulin resistance in obese, hypertensive patients," *Nutrition Research*, vol. 32, no. 6, pp. 421–427, 2012.

[15] M. B. Soares, A. P. Izaguirry, L. M. Vargas, A. S. L. Mendez, C. C. Spiazzi, and F. W. Santos, "Catechins are not major components responsible for the beneficial effect of Camellia sinensis on the ovarian δ-ALA-D activity inhibited by cadmium," *Food and Chemical Toxicology*, vol. 55, pp. 463–469, 2013.

[16] H. L. Schimidt, A. Garcia, A. Martins, P. B. Mello-Carpes, and F. P. Carpes, "Green tea supplementation produces better neuroprotective effects than red and black tea in Alzheimer-like rat model," *Food Research International*, vol. 100, Part 1, pp. 442–448, 2017.

[17] J. Caliaperumal, Y. Ma, and F. Colbourne, "Intra-parenchymal ferrous iron infusion causes neuronal atrophy, cell death and progressive tissue loss: implications for intracerebral hemorrhage," *Experimental Neurology*, vol. 237, no. 2, pp. 363–369, 2012.

[18] H. L. Schimidt, A. Vieira, C. Altermann et al., "Memory deficits and oxidative stress in cerebral ischemia-reperfusion: neuroprotective role of physical exercise and green tea supplementation," *Neurobiology of Learning and Memory*, vol. 114, pp. 242–250, 2014.

[19] J. S. Bonini, L. R. Bevilaqua, C. G. Zinn et al., "Angiotensin II disrupts inhibitory avoidance memory retrieval," *Hormones and Behavior*, vol. 50, no. 2, pp. 308–313, 2006.

[20] S. Stroobants, I. Gantois, T. Pooters, and R. D'Hooge, "Increased gait variability in mice with small cerebellar cortex lesions and normal rotarod performance," *Behavioural Brain Research*, vol. 241, pp. 32–37, 2013.

[21] M. R. D. Bigio, H. J. Yan, R. Buist, J. Peeling, and G. J. del Zoppo, "Experimental intracerebral hemorrhage in rats. Magnetic resonance imaging and histopathological correlates," *Stroke*, vol. 27, no. 12, pp. 2312–2320, 1996.

[22] L. M. Warkentin, A. M. Auriat, S. Wowk, and F. Colbourne, "Failure of deferoxamine, an iron chelator, to improve outcome after collagenase-induced intracerebral hemorrhage in rats," *Brain Research*, vol. 1309, pp. 95–103, 2010.

[23] H. Ohkawa, N. Ohishi, and K. Yagi, "Assay for lipid peroxides in animal tissues by thiobarbituric acid reaction," *Analytical Biochemistry*, vol. 95, no. 2, pp. 351–358, 1979.

[24] M. M. Bradford, "A rapid and sensitive method for the quantitation of microgram quantities of protein utilizing the principle of protein-dye binding," *Analytical Biochemistry*, vol. 72, no. 1-2, pp. 248–254, 1976.

[25] K. P. Wadden, T. S. Woodward, P. D. Metzak et al., "Compensatory motor network connectivity is associated with motor sequence learning after subcortical stroke," *Behavioural Brain Research*, vol. 286, pp. 136–145, 2015.

[26] A. M. Auriat, S. Wowk, and F. Colbourne, "Rehabilitation after intracerebral hemorrhage in rats improves recovery with enhanced dendritic complexity but no effect on cell proliferation," *Behavioural Brain Research*, vol. 214, no. 1, pp. 42–47, 2010.

[27] M. Huijben-Schoenmakers, A. Rademaker, and E. Scherder, "Cognition in relation to independency in older, comorbid stroke patients in a stroke unit," *International Journal of Geriatric Psychiatry*, vol. 32, no. 7, pp. 761–768, 2017.

[28] C. F. Chang, S. Cho, and J. Wang, "(−)-Epicatechin protects hemorrhagic brain via synergistic Nrf2 pathways," *Annals of Clinical and Translational Neurology*, vol. 1, no. 4, pp. 258–271, 2014.

[29] H. Lu, J. Shen, X. Song et al., "Protective effect of Pyrroloquinoline Quinone (PQQ) in rat model of intracerebral hemorrhage," *Cellular and Molecular Neurobiology*, vol. 35, no. 7, pp. 921–930, 2015.

[30] H. Rojas, T. Lekic, W. Chen et al., "The antioxidant effects of melatonin after intracerebral hemorrhage in rats," *Acta Neurochirurgica Supplementum*, vol. 105, pp. 19–21, 2008.

[31] E. Titova, R. P. Ostrowski, L. C. Sowers, J. H. Zhang, and J. Tang, "Effects of apocynin and ethanol on intracerebral haemorrhage-induced brain injury in rats," *Clinical and Experimental Pharmacology and Physiology*, vol. 34, no. 9, pp. 845–850, 2007.

[32] P. M. Sosa, H. L. Schimidt, C. Altermann et al., "Physical exercise prevents motor disorders and striatal oxidative imbalance after cerebral ischemia-reperfusion," *Brazilian Journal of Medical and Biological Research*, vol. 48, no. 9, pp. 798–804, 2015.

[33] H. F. Gu, Y. X. Nie, Q. Z. Tong et al., "Epigallocatechin-3-gallate attenuates impairment of learning and memory in chronic unpredictable mild stress-treated rats by restoring hippocampal autophagic flux," *PLoS One*, vol. 9, no. 11, article e112683, 2014.

[34] Y. J. Lee, D. Y. Choi, Y. P. Yun, S. B. Han, K. W. Oh, and J. T. Hong, "Epigallocatechin-3-gallate prevents systemic inflammation-induced memory deficiency and amyloidogenesis via Its anti-neuroinflammatory properties," *The Journal of Nutritional Biochemistry*, vol. 24, no. 1, pp. 298–310, 2013.

[35] S. Mandel, O. Weinreb, L. Reznichenko, L. Kalfon, and T. Amit, "Green tea catechins as brain-permeable, non toxic iron chelators to "iron out iron" from the brain," *Journal of Neural Transmission*, vol. 71, pp. 249–257, 2006.

[36] K. Ide, H. Yamada, N. Takuma et al., "Green tea consumption affects cognitive dysfunction in the elderly: a pilot study," *Nutrients*, vol. 6, no. 10, pp. 4032–4042, 2014.

[37] Y. Yang, M. Zhang, X. Kang et al., "Thrombin-induced microglial activation impairs hippocampal neurogenesis and spatial memory ability in mice," *Behavioral and Brain Functions*, vol. 11, no. 1, p. 30, 2015.

Hindawi
Neural Plasticity
Volume 2018, Article ID 4232706, 15 pages
https://doi.org/10.1155/2018/4232706

Research Article

Intraspinal Grafting of Serotonergic Neurons Modifies Expression of Genes Important for Functional Recovery in Paraplegic Rats

Krzysztof Miazga,[1] **Hanna Fabczak**,[1] **Ewa Joachimiak**,[1] **Małgorzata Zawadzka**,[1] **Łucja Krzemień-Ojak**,[1] **Marek Bekisz**,[1] **Anna Bejrowska**,[1] **Larry M. Jordan**,[2] **and Urszula Sławińska**[1]

[1]*Nencki Institute of Experimental Biology, Polish Academy of Sciences, Warsaw, Poland*
[2]*Department of Physiology and Phatophysiology, University of Manitoba, Winnipeg, MB, Canada*

Correspondence should be addressed to Urszula Sławińska; u.slawinska@nencki.gov.pl

Received 18 February 2018; Revised 23 May 2018; Accepted 4 June 2018; Published 25 July 2018

Academic Editor: Junichi Ushiba

Serotonin (5-hydroxytryptamine; 5-HT) plays an important role in control of locomotion, partly through direct effects on motoneurons. Spinal cord complete transection (SCI) results in changes in 5-HT receptors on motoneurons that influence functional recovery. Activation of 5-HT_{2A} and 5-HT_7 receptors improves locomotor hindlimb movements in paraplegic rats. Here, we analyzed the mRNA of 5-HT_{2A} and 5-HT_7 receptors (encoded by *Htr2a* and *Htr7* genes, resp.) in motoneurons innervating tibialis anterior (TA) and gastrocnemius lateralis (GM) hindlimb muscles and the tail extensor caudae medialis (ECM) muscle in intact as well as spinal rats. Moreover, the effect of intraspinal grafting of serotonergic neurons on *Htr2a* and *Htr7* gene expression was examined to test the possibility that the graft origin 5-HT innervation in the spinal cord of paraplegic rats could reverse changes in gene expression induced by SCI. Our results indicate that SCI at the thoracic level leads to changes in *Htr2a* and *Htr7* gene expression, whereas transplantation of embryonic serotonergic neurons modifies these changes in motoneurons innervating hindlimb muscles but not those innervating tail muscles. This suggests that the upregulation of genes critical for locomotor recovery, resulting in limb motoneuron plasticity, might account for the improved locomotion in grafted animals.

1. Introduction

Motoneurons (MNs) respond to 5-HT with an increase in excitability [1–3]. We and others have previously argued that 5-HT_{2A} and 5-HT_7 receptors are important in the initiation and control of locomotion [3–12], and that these receptors mediate hindlimb locomotor recovery produced in paraplegic animals after replacement of 5-HT neurons into the sublesional spinal cord by grafts of fetal brainstem [10, 13]. One of the effects of spinal cord transection, which interrupts the 5-HT pathway from the brainstem to the spinal cord, is plasticity in 5-HT receptors of spinal MNs [14, 15]. The 5-HT_7 receptors have been implicated in control of MNs or reflexes involved in respiration, jaw movement, micturition, and locomotion [16–21] as well as in the control of pain after spinal cord injury [22, 23], while the 5-HT_{2A} receptor has been implicated in the control of respiration, development of spasticity in tail and hindlimb digit MNs, and the recovery of locomotor capability after spinal cord injury [24–27]. Intraspinal grafting of serotonergic neurons leads to functional recovery and involves activation of 5-HT_{2A} and 5-HT_7 receptors [10]. We asked whether the facilitation of locomotion by our grafts might be mediated by plasticity in these key receptors that are necessary for locomotor recovery.

The 5-HT_7 receptor protein is found in MNs of the spinal cord [28], with some MN populations (e.g., Onuf's nucleus) more intensely labeled than others. MNs in the L4 spinal cord, where MNs to hindlimb muscles are located, displayed

a relatively low level of labeling. These receptors have been shown to have excitatory effects on some MNs, including phrenic MNs [29] and trigeminal MNs [19], but not hypoglossal respiratory MNs [30, 31].

The afterhyperpolarization (AHP) in many types of neurons is reduced by 5-HT, and this effect may be mediated by 5-HT_7 receptors [19, 32]. MNs of limb muscles have reduced AHPs during locomotion [33, 34], and lamprey MNs have reduced AHP due to 5-HT [35, 36]. This effect serves as a means of increasing MN spiking.

The 5-HT_{2A} receptor is abundant in ventral horn MNs [37, 38], with variable expression levels depending upon the functional role of the cell. For example, 5-HT_{2A} receptors are differentially distributed on MNs to the physiological extensor soleus muscle and extensor digitorum longus, a physiological flexor muscle [39]. Plasticity in the 5-HT_{2A} receptor protein has been examined after sacral spinal cord injury, where the changes have been suggested to underlie the development of tail spasticity (reviewed in [14, 15]). Contusive spinal cord injury at the thoracic level resulted in upregulation of 5-HT_{2A} receptor protein in MNs of the rostral dorsolateral nucleus innervating the plantar muscles of the foot, with an associated increase in the H-reflex recorded from the plantar muscles of the hindpaw [40]. Cervical spinal cord hemisections give rise to increased 5-HT_{2A} receptor protein in phrenic MNs and their subsequent increased excitability [27].

Chopek et al. [41] demonstrated that the extensor monosynaptic reflex in hindlimb MNs of passively cycled spinal rats responded to quipazine (a 5-HT_2 agonist). This plasticity could be related to changes in 5-HT receptors in MNs; 5-HT_{2A} receptor mRNA increased after injury and increased further after passive cycling [42]. An increase in 5-HT_{2A} mRNA after sacral SCI was observed in tail MNs [43]. Chopek et al. [42] found no change in 5-HT_7 receptor gene expression in lumbar MNs 3 months after spinal cord transection, but passive cycling increased 5-HT_7 receptor mRNA. Giroux et al. [44] found spinal 5-HT receptors increased at 15 and 30 days after spinal cord injury, but returned to baseline levels after 60 days or more. They used [3H]8-OH-DPAT to label 5-HT receptors, a ligand that can bind to 5-HT_7 receptors.

There is increasing evidence that activation of specific serotonin receptors in the spinal cord is effective for enhancing locomotor recovery in spinal rats [11, 45, 46]. Out of many serotonergic receptors present in the spinal cord, the 5-HT_{2A} and 5-HT_7 receptors are the major ones implicated in the control of locomotion [3, 6, 7, 12, 25, 47–49]. The most commonly used agonists that are effective in enhancing the locomotor hindlimb movements when applied systemically are quipazine, which has high affinity for both 5-HT_{2A} and 5-HT_{2C} receptors and 8-hydroxy-2-(di-n-propylamino)-tetralin (8-OH-DPAT), which binds selectively to 5-HT_7 and 5-HT_{1A} receptors [46, 47, 50]. We previously demonstrated that intraspinal grafting of embryonic brainstem tissue containing serotonergic neurons below a thoracic total transection enhances recovery of hindlimb locomotor movements [10, 13, 51]. We also demonstrated that graft-related recovery is mediated in part by 5-HT_{2A} and 5-HT_7 receptors because application of their antagonists diminished the restored hindlimb locomotor movements [10, 13]. Constitutive activity in 5-HT_2 receptors is implicated in the recovery of locomotion after SCI [25, 52], and intrathecal application of a selective 5-HT_7 receptor antagonist during unrestrained locomotion in intact adult rats [4] blocks voluntary locomotion. Similar effects were obtained with 5-HT_2 antagonists [53].

Here, we hypothesize that the plastic changes in these receptors that occur after spinal cord injury might be affected by the restoration of 5-HT innervation from grafted 5-HT neurons so as to reverse or normalize these changes. This hypothesis is consistent with the findings that the presence of 5-HT or other ligands for these receptors can downregulate, upregulate, or desensitize these 5-HT receptors [54, 55]. We tested this hypothesis on identified MNs of the lumbar enlargement that innervate muscles with known actions during locomotion (ankle flexor (TA), extensor (GM), and tail elevator (ECM)), and we attempted to induce plasticity in the receptors on these MNs using thoracic spinal cord transection. We monitored the changes in receptor mRNA expression produced in these identified lumbar MNs at 1 month and 4 months after spinal cord transection, and we determined whether intraspinal grafting of embryonic serotonergic neurons in spinal rats reverses the effects of spinal total transection on expression of these genes. We show, for the first time, that intraspinal grafting of embryonic serotonergic neurons reverses injury-evoked changes in 5-HT_{2A} and 5-HT_7 receptor gene expression in the MN populations supplying hindlimb but not tail muscles. We propose that these changes may account for the effects of the grafts on neural plasticity responsible for locomotor recovery achieved by intraspinal grafting of embryonic raphe nuclei in paraplegic rats. A preliminary report of these findings has been published [56].

2. Materials and Methods

Experiments were performed on WAG (Wistar Albino Glaxo) 3-month-old female rats ($n = 35$) at the time of spinal cord injury. All procedures were conducted with care to minimize pain and suffering of animals with the approval of the First Local Ethics Committee in Poland, according to the principles of experimental conditions and laboratory animal care of European Union and the Polish Law on Animal Protection.

2.1. Spinal Cord Transection. Complete spinal cord transection (SCI) was performed ($n = 23$) at the Th9/10 level under deep anesthesia (isoflurane: 5% to induce and then maintained with 2% in oxygen 0.2–0.3 l/min and Butomidor: 0.05 mg/kg b.w.) as previously described [10]. To prevent the possibility of axonal regrowth through the cavity of the lesion, 1-2 mm of spinal cord tissue was aspirated using a glass pipette. Then, the muscles and fascia overlying the paravertebral muscles were closed in layers using sterile sutures, and the skin was closed with stainless steel surgical clips. After surgery, the animals received a nonsteroidal anti-inflammatory and analgesic treatment (s.c., Tolfedine

4 mg/kg b.w.) and antibiotics (s.c., Baytril 5 mg/kg b.w.; gentamicin 2 mg/kg b.w.) for the following 5–7 days. The bladder was emptied manually twice a day until the voiding reflex was reestablished.

2.2. Grafting of Embryonic 5-HT Cells. One month after SCI, nine out of 23 spinal rats were selected randomly for intraspinal grafting of embryonic serotonergic cells (SCI_{TR}). Fourteen-day-old embryos (E14; E0—the day after mating) from time-pregnant female WAG rats were removed by Caesarean section and transferred to Hanks' buffered solution containing 0.5% glucose. A small piece of the embryonic caudal brainstem area containing the B1, B2, and B3 serotonergic regions was dissected under a microscope (for more details, see [10, 57]).

At the same time, the spinal cord of a recipient rat (isoflurane anesthesia, 5% to induce and then maintained with 2% in oxygen 0.2–0.3 l/min) was exposed by a small laminectomy at the Th11/12 vertebrae level (at least one segment below the total spinal cord transection), and a solid piece of embryonic tissue (approximately 2 μl) was injected by pressure into the spinal cord 1 mm below the pial surface through a sharpened micropipette attached to the Hamilton syringe. The micropipette was then slowly withdrawn to avoid graft movement. Control spinal rats ($n = 11$) were subjected to a sham grafting procedure where the operation was identical to that described above, but no tissue was injected into the spinal cord [10, 13, 51].

2.3. Behavioral Assessment of Locomotor Ability in Spinal Rats. Before starting the procedure of collecting data for qRT-PCR analysis, two months after grafting (3 months after complete spinal cord transection), all the rats were subjected to behavioral testing to confirm the quality of their hindlimb plantar stepping. This was established in rats suspended above a treadmill with their forelimbs and thorax placed on a platform and with their hindlimbs touching the treadmill belt. To elicit hindlimb movements, a tail pinch was used. Stimulation of tail has been used for eliciting locomotion in many cases of complete spinal cord transection [46, 58] and has been used in all prior attempts to reveal locomotor recovery after brainstem neuron grafting [10, 13, 57, 59, 60]. The tail stimulus was adjusted by the experimenter to maximize the quality of plantar stepping. All the spinal grafted rats considered for the further investigation of gene expression in defined MNs or for immunohistochemistry of the spinal cord presented good plantar walking performance and were not different from those described in our previous paper [10, 13, 51, 57].

2.4. Implantation of EMG Electrodes. To evaluate the quality of hindlimb movements, we routinely use electromyography (EMG). In rats from the SCI_{4m} group (three months after total transection) and in the rats from the SCI_{TR} group (two months after intraspinal grafting), bipolar electrodes for EMG recordings were implanted under isoflurane anesthesia (5% to induce and then maintained with 2% in oxygen 0.2–0.3 l/min) in Sol muscle (physiological extensor active during the stance phase of the step cycle) and TA muscle (physiological flexor active during the swing phase of the step cycle) of both hindlimbs. The electrodes were made of Teflon-coated stainless steel wire (0.24 mm in diameter; AS633, CoonerWire Co., Chatsworth, CA, USA). The tips of the electrodes with 1–1.5 mm of the insulation removed were pulled through a cutaneous incision on the back of the animal, and each of the hook electrodes was inserted into the appropriate muscle and secured by a suture [10, 51, 57]. The distance between the electrode tips in the muscle was 1-2 mm. The ground electrode was placed under the skin on the back of the animal in some distance from the hindlimb muscles. The connector with the other ends of the wires fixed to it, covered with dental cement (Spofa Dental, Prague, Czech Republic) and silicone (3140 RTV, Dow Corning), was secured to the back of the animal. After surgery, the animals received antibiotic treatment (Baytril, 5 mg/kg s.c.).

2.5. Tissue Preparation and Immunohistochemistry: Morphological Verification of Spinal Reactive Gliosis in Spinal Rats with and without the Graft. After testing the quality of locomotor hindlimb movements, three grafted rats and three spinal control rats without the graft were subjected to perfusion to prepare the spinal cord tissue for histological investigation of the graft condition and presence of inflammatory responses at the spinal level in which the MNs were collected.

For immunochemistry, the spinal cords were collected from the animals deeply anesthetized with pentobarbital and transcardially perfused with cold 0.1 M phosphate-buffered saline (PBS), pH 7.2, for 2-3 min and subsequently with cold 4% paraformaldehyde in PBS for 15 min. The spinal cords were postfixed and then cryoprotected gradually up to 30% sucrose in PBS, embedded in OCT, frozen on dry ice, and sectioned in a cryotome (12 μm). The collected cross sections were immobilized on poly-L-lysine-covered glass slides and stored at −20°C.

The primary antibodies that were used in the immunohistochemistry were mouse antiglial fibrillary acidic protein (GFAP, 1 : 1000, BD Pharmingen) for astrocytes and mouse neuronal nuclear protein antibody (NeuN, 1 : 100 Millipore) for neuronal labeling. Isolectin B4 (FITC-conjugated, 20 μg/ml, Sigma-Aldrich) was used for activated microglia detection. To identify 5-HT-positive fibers, rabbit anti-5-HT antibody (1 : 1000, ImmunoStar) was used. The Alexa Fluor secondary antibodies were used: 488-conjugated donkey antibody against mouse IgG, 647-conjugated goat antibody against mouse IgG, and 555-conjugated donkey antibody against rabbit IgG, (1 : 1000 Invitrogen). Nuclei were stained with DAPI dye (1 μg/ml in H_2O, Sigma-Aldrich).

For the immunostaining, frozen cross sections, after several rinses in PBS, were blocked in 10% normal donkey or donkey/goat serum with 0.5% Triton X-100 in PBS at RT for 2 h and then incubated overnight at 4°C with primary antibodies followed by incubation with fluorophore-conjugated secondary antibodies for 2 h at room temperature. The specimens were coverslipped in fluorescence mounting medium (Dako) after several washes in PBS and examined

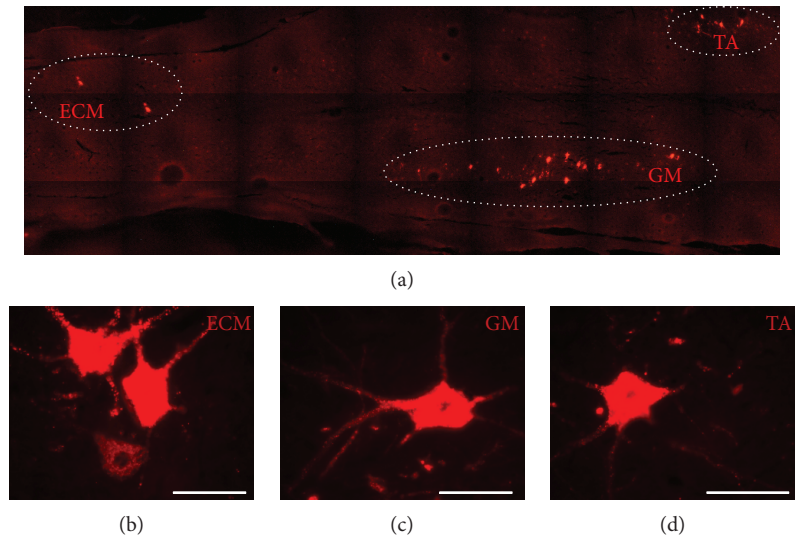

Figure 1: (a) Examples of labeled motoneurons (cholera toxin subunit B coupled with Alexa Fluor 555) innervating selected muscles: extensor caudae medialis (ECM) of the right side (b), gastrocnemius lateralis (GM) in the left hindlimb (c), and tibialis anterior (TA) in the right hindlimb (d). Scale bar: 50 μm.

on either a Zeiss Fluorescence Microscope Axio Imager.M2 or a Leica SP5 Laser Scanning Confocal Microscope.

2.6. Motoneuron Labeling. One week before the animal euthanasia, populations of MNs innervate the following muscles: TA of the right hindlimb, GM of the left hindlimb, and ECM of the right side of the tail were labeled by intramuscular injection by cholera toxin subunit B (CTB) coupled with Alexa Fluor 555 dye (see examples of CTB-labeled MNs innervating TA, GM, and ECM muscles in Figure 1). The TA and GM muscles were selected on the left and right sides to provide easy differentiation between the two MN pools innervating these two muscles when the same type of labeling was used in both of them. Also, the left ECM pool MN labeling (the most caudally localized) is a marker of the left side helping in identification of the GM MN pool. At the same time, the ECM and TA MN pools are separated with the most rostrocaudal distance. The ECM muscle was also selected because it plays a role in elevation of the tail, an indicator of functional recovery after spinal cord injury, according to the BBB score [61]. Animals were anesthetized using isoflurane (5% to induce and then maintained with 2% in oxygen 0.2–0.3 l/min), and proper muscles were exposed by small skin incisions enabling injection with 0.5% CTB using Hamilton syringe (TA and GM muscles 3×15 μl of CTB and ECM muscle 2×20 μl of CTB). The CTB injection was performed over a period of 2 minutes, the needle was slowly (2 min) withdrawn, and the skin incision was closed.

2.7. Htr2a and Htr7 Gene Expression Analysis

2.7.1. Experiment Scheme. In order to examine the *Htr2a* and *Htr7* gene expression in MNs innervating selected hindlimb and tail muscles, we performed experiments on 29 WAG female rats, in which specific motoneuron pools were labeled by injection of retrograde tracer molecules into a target muscle. Our investigations were performed on rats from four experimental groups: INT: intact ($n = 12$); SCI_{TR}: spinal cord injury followed by intraspinal transplantation of embryonic brainstem tissue containing serotonergic neurons ($n = 6$); SCI_{1m}: 1 month after spinal cord injury ($n = 5$); SCI_{4m}: 4 months after spinal cord injury ($n = 6$)-the time matched with the time of euthanasia of rats from the SCI_{TR} group.

Animals from the SCI_{1m} and SCI_{4m} groups were subjected to a spinal cord total transection procedure performed at the thoracic level. Animals from the INT group were the control animals that were not subjected to any procedure. Animals from the SCI_{TR} group received an intraspinal graft of 14-day-old rat embryonic brainstem one month after spinal cord total transection. Three months after intraspinal grafting in SCI_{TR} group and four months after complete transection in rats of both groups, SCI_{TR} and SCI_{4m} (seven days after motoneuron tracer injection with cholera toxin subunit B coupled with Alexa Fluor 555) rats were transcardially perfused with PBS solution to remove any blood-borne 5-HT receptors, and the spinal cord was dissected and prepared for further analysis (animals from the SCI_{4m} and SCI_{TR} groups were euthanized 4 months after spinal cord total transection).

2.7.2. Laser Capture Microdissection (LCM) of Selected Motoneurons. Spinal cord tissue was collected from animals that were deeply anesthetized and transcardially perfused with PBS solution. Then, the spinal cords were immediately dissected and frozen by fast immersion in isopentane (−80°C) and stored at −80°C until future processing. Horizontal sections (20 μm) of the lumbar-sacral spinal cord fragment were cut on the cryostat in −20°C and mounted on PEN Membrane Frame Slides (Applied Biosystems). Slides were stored at −80°C until future use.

Slides were dehydrated by immersion in increasing concentrations (70%, 90%, and 100%) of ethyl alcohol (ETOH) followed by immersion in xylene. Motoneuron collection was performed using an Arcturus Laser

Table 1: Description of assays used in real-time PCR.

Gene symbol	Reference number	Gene name	Assay ID	Amplicon length
Ppia	NM_017101.1	Cyclophilin A	Rn00690933_m1	149
Htr2a	NM_017254.1	Receptor 5-HT_{2A}	Rn00568473_m1	71
Htr7	NM_022938.2	Receptor 5-HT_7	Rn00576048_m1	85

Microdissection System (Applied Biosystems). Tissue sections were photographed using a filter set for Alexa Fluor 555 to identify CTB-labeled MNs. Individual MNs were dissected using UV laser and collected on *Cap Sure Macro LCM Caps* (Applied Biosystems). After incubation in lysis buffer (*Arcturus Pico Pure RNA Isolation Kit*, Applied Biosystems) for 30 minutes, the samples were stored at −80°C until future processing.

2.7.3. RNA Isolation. RNA was isolated using an *Arcturus Pico Pure RNA Isolation Kit* (Applied Biosystems) according to the manufacturer's instructions. Any residual genomic DNA was removed using supplementary DNAse I (*RQ1 RNase-Free DNase*, Promega) treatment. Three independent measurements of RNA concentration were obtained using NanoDrop (Thermo Scientific). RNA samples were pooled by mixing the same RNA amount isolated from one motoneuron population from all rats in a particular experimental group (i.e., equal amounts of RNA collected from the particular selected motoneuron populations in different rats in the same experimental group were pooled). RNA samples were stored at −80°C.

2.7.4. Reverse Transcription PCR and cDNA Preamplification. Reverse transcription PCR (RT-PCR) was performed in a *MJ Mini Personal Thermal Cycler* (Bio-Rad) using a *High Capacity cDNA Reverse Transcription Kit* (Applied Biosystems) according to the manufacturer's instructions (10 min, 25°C; 120 min, 37°C; 5 min, 85°C; storage 4°C) with use of 31 ng of purified RNA as a sample. Synthesized cDNA was stored at −20°C for future use.

Preamplification was performed to increase the number of cDNA copies to the level necessary for accurate detection in the real-time PCR reaction. cDNA was preamplified in *MJ Mini Personal Thermal Cycler* (Bio-Rad) using *TaqMan PreAmp Master Mix Kit* (Applied Biosystems). Reactions were conducted in standard conditions according to the preamplification kit manufacturer's instructions: 95°C for 10 min; then 14 cycles: 95°C for 15 s; 60°C for 4 min.

2.7.5. Real-Time PCR. Expression of the *Htr2a and Htr7* genes (encoding the 5-HT_{2A} and 5-HT_7 receptors, resp.) in the selected MN populations was measured by semiquantitative real-time PCR (qRT-PCR) using a *Step One Plus* (Applied Biosystems) thermocycler and TaqMan gene-specific FAM/MGB assays (Applied Biosystems). *Ppia* gene encoding cyclophilin A was used as the housekeeping gene. The description of TaqMan assays used in the qRT-PCR reaction is shown in Table 1.

Reactions were run in triplicate for each sample and for each assay in 20 μl reaction mix prepared in accordance with *TaqMan Gene Expression Master Mix* (Applied Biosystems) manufacturer recommendations. Reactions were run in standard, recommended by *TaqMan Gene Expression Master Mix* manufacturer conditions (2 min, 50°C; 10 min, 95°C; then 40 cycles: 15 s, 95°C; 1 min, 60°C). Relative expression levels of analyzed genes were then calculated using the comparative CT method.

2.8. Statistical Analysis. For comparison of results from two experimental groups, Student's *t*-test analysis was used after normal distribution was confirmed using Shapiro-Wilk test (Prism, GraphPad Software, La Jolla, CA). For statistical analysis of the results collected from qRT-PCR of more than two experimental groups that were expressed in relation to those established in INT rats, the nonparametric Kruskal-Wallis test for multiple independent sample comparison followed by Conover post hoc (further adjusted by the Holm family-wise error rate (FWER) method and in one case the method of Benjamini-Hochberg false discovery rate (FDR) when the FWER method just approached significance) was used (http://astatsa.com/KruskalWallisTest/).

3. Results

3.1. Locomotor Ability in Spinal Rats. As we published before, the SCI rats (SCI_{1m} and SCI_{4m}) presented very limited hindlimb movements [10, 11, 13, 46, 51]. Usually, their hindlimbs were outstretched passively behind the hindquarters without any spontaneous hindlimb movement present and there was hardly any EMG activity recorded in the hindlimb flexor (TA) and extensor (Sol) muscles (Figure 2(a)). In contrast, the hindlimbs of the SCI_{TR} rats moving in the home cage were abducted with partial flexion in the ankle joint or flexed at all joints with the foot plantar surface touching the ground, but without noticeable body weight support in spite presence of some EMG activity in hindlimb Sol and TA muscles (Figure 2(c)). Tail pinching in SCI rats suspended over a treadmill induced only irregular, limited hindlimb movements characterized by obvious lack of body weight support with no plantar stepping. EMG activity of hindlimb flexor and extensor muscles was irregular with lack of the long burst of Sol EMG activity related to the stance phase of the step cycle that is observed in normal locomotor activity of intact rats (Figure 2(b)). In SCI_{TR} rats suspended over the treadmill, tail pinch was effective to induce regular plantar hindlimb walking with nice regular EMG muscle activity with typical alternating pattern of EMG Sol versus TA bursts of activity and long burst of Sol related to the stance phase of step cycle in both hindlimbs (Figure 2(d)).

3.2. Morphological Verification of Reactive Gliosis in Spinal Rats with and without the Graft. As we published before

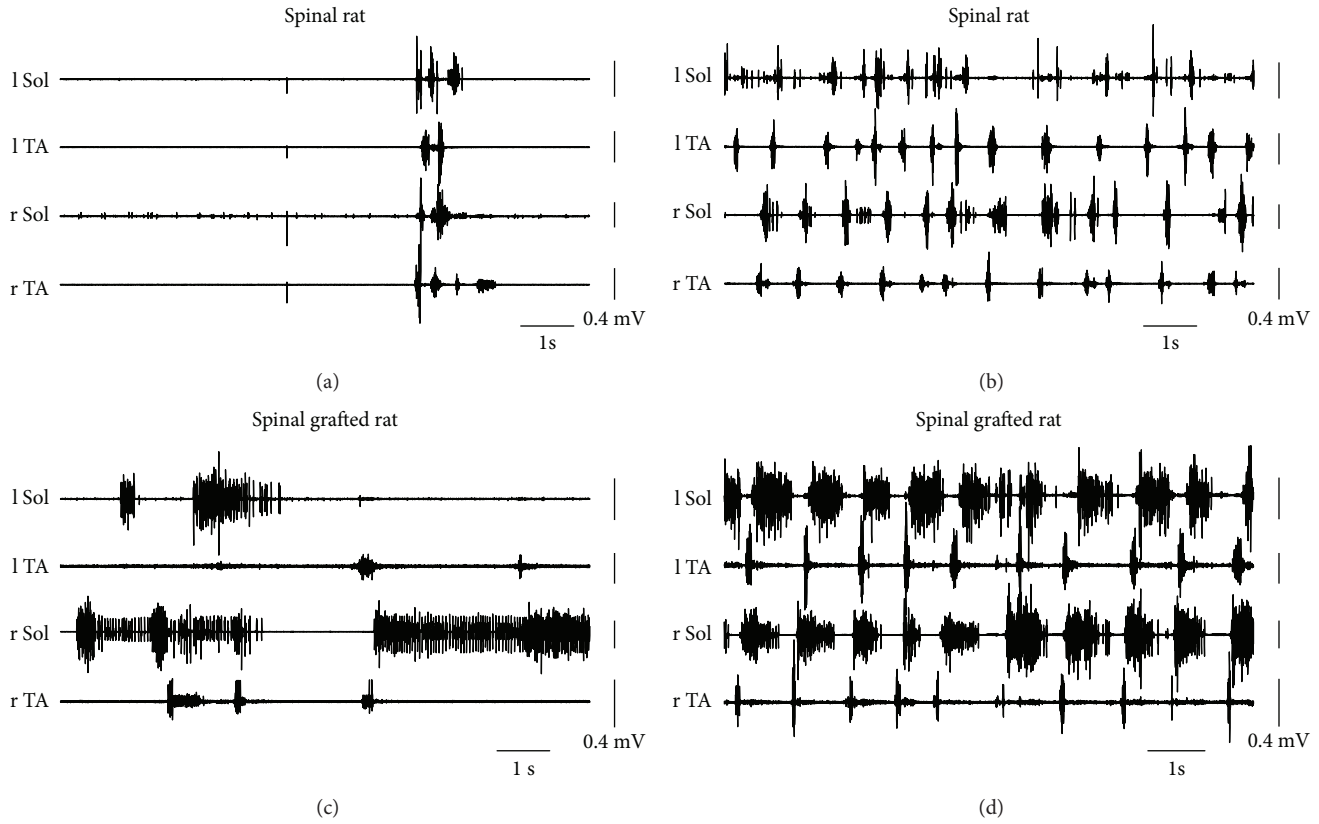

Figure 2: Examples of EMG recordings from hindlimb muscles of the spinal rats (a) and (b) and spinal grafted rat (c) and (d) during exploratory behavior in the home cage (a) and (c) and during locomotor-like hindlimb movements on a treadmill induced by tail pinching (b and d). Note that in spinal control rats during spontaneous movement in the home cage, the hindlimb muscles were usually silent but a brief episode of EMG activity could be induced by a sudden touch of the rat tail (a), while in the spinal grafted rats, the spontaneous EMG activity of Sol and TA muscles could be obtained without any external intervention (c) (for more details, see [10, 13, 51, 57]. Sol: soleus muscle; TA: tibialis anterior muscle; l/r: left/right.

[10, 51, 57], intraspinally grafted 5-HT neurons survive the grafting procedure and their axons grow into the distal part of the host spinal cord, spreading caudally for a considerable distance below the total transection. Figure 3(b) shows a representative example of fetal grafted tissue located in the spinal cord one/two segments below the total transection of the spinal grafted rat. The sham-operated spinal SCI_{4m} rats do not possess any 5-HT innervation in the spinal cord below the total transection (Figure 3(a)). Here, we also verified the presence of activated microglia and astrocytes in the spinal cord below transection in spinal rats with (SCI_{TR}) and without the graft (SCI_{4m}) long after the injury (4 months). While there was moderate microglia activation detectable within white matter and virtually no activation in grey matter at Th13/L1 (the level of a real or sham grafting), we were not able to detect any sign of inflammation at L4/L5 in any of the animals, regardless of whether they were sham or grafted ones (Figure 3 left and middle panels). Moreover, while we identified a slightly increased number of astrocytes in ventral horns at the grafting level compared to control, the same numbers of astrocytes were observed at L4/L5 in both SCI_{4m} and SCI_{TR} rats. However, none of the detected astrocytes showed the morphology of reactive cells (Figure 3, right panel). Thus, we assumed that 4 months after transplantation of embryonic tissue, there is no inflammatory reaction in the ventral horn at and below of L4/L5 spinal cord levels, where our samples were taken. This finding demonstrates that a role for inflammation in changes in 5-HT receptors such as previously suggested after sacral spinal cord injury [43] does not apply in our case.

3.3. Htr2a and Htr7 Gene Expression in MNs of Intact Adult Rats. The relative abundance of the distinct mRNAs was established by the minimal number of amplification cycles necessary to detect a given mRNA and was presented at graph as $1/\Delta Ct$ value. In all analyzed populations of MNs innervating the TA, GM, and ECM muscles, expression of *Htr2a* and *Htr7* genes (encoding 5-HT_{2A} and 5-HT_7 receptors, resp.) was detectable and expression of *Htr2a* gene in all analyzed motoneurons was significantly higher (Student's t-test $p < 0.0001$) than expression of gene encoding 5-HT_7 serotonin receptor (Figure 4).

3.4. Htr2a Gene Expression in MNs. In comparison to INT rats, in SCI_{1m} rats, the *Htr2a* gene expression was reduced by ~60% in TA MNs (nonparametric Kruskal-Wallis test (df: 3, $p = 0.015$) with Conover post hoc test $p < 0.001$) and by ~50% in the GM MNs (nonparametric Kruskal-Wallis test

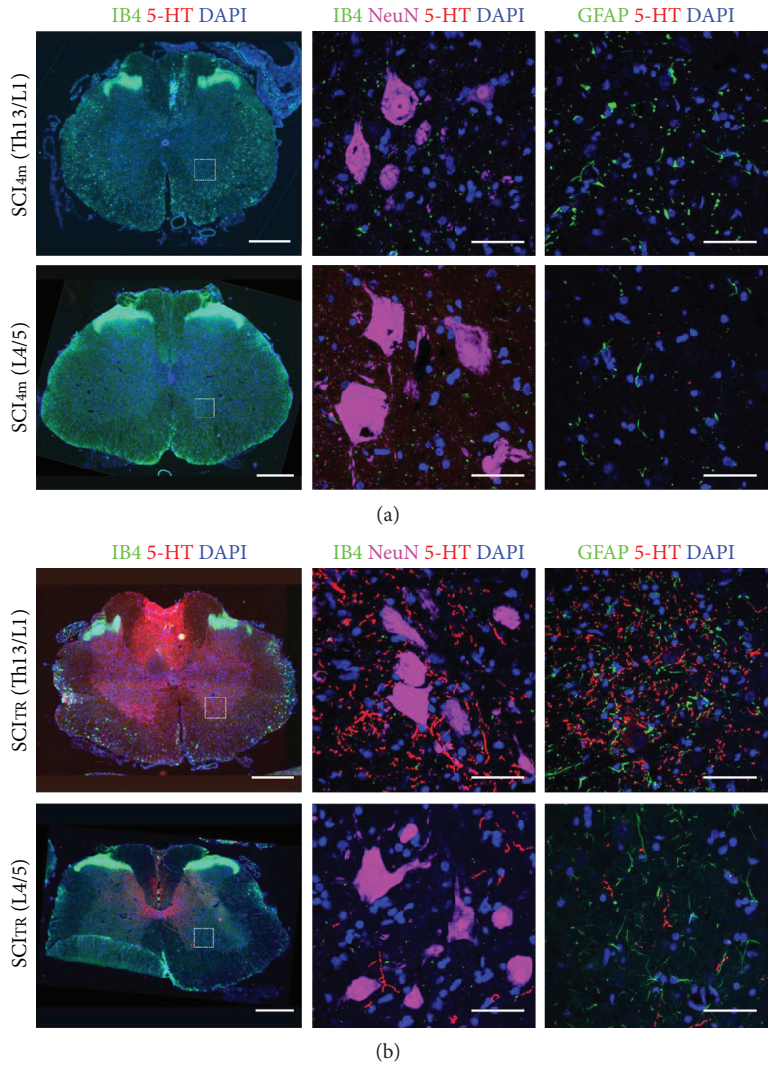

FIGURE 3: Immunofluorescent detection of inflammatory response in control SCI_{4m} (a) and transplanted SCI_{TR} (b) rats at 4 months after total spinal transection and 3 months after transplantation (sham grafting in SCI_{4m}). The first panel shows general view of spinal cord cross section labeled with isolectin B4 (IB4) to visualize activated microglia in low power; the next two panels show boxed area labeled with IB4 (green; left and middle panel) for microglia and GFAP (green; right panel) for astrocytes, reimaged using confocal microscope. Note grafted tissue at Th13/L1 and serotonin-positive fibers (5-HT, red) located closely to ventral horn motoneurons (NeuN; purple) at L4/L5. Representative images: scale bar: 500 μm and 50 μm in low- and high-power images, respectively.

(df: 3, $p = 0.019$) with Conover post hoc test $p < 0.01$) and increased by 103% in ECM MNs (nonparametric Kruskal-Wallis test (df: 3, $p = 0.015$) with Conover post hoc $p < 0.0001$) when normalized to the *Htr2a* gene expression in MNs of INT animals (Figure 5).

In SCI_{4m} rats, the *Htr2a* gene expression was also lower than in INT rats (~45% of INT) in TA MNs (Conover post hoc test $p < 0.001$) and GM MNs (Conover post hoc test $p < 0.05$). There was also a small difference in gene expression in SCI_{4m} rats in comparison to SCI_{1m} rats (Conover post hoc test $p < 0.05$) in MNs of both TA and GM muscles. In SCI_{4m}, the *Htr2a* gene expression in the ECM MNs decreased by ~44% (Conover post hoc $p < 0.001$) in comparison to the gene expression level measured in SCI_{1m} rats. Expression of the *Htr2a* gene in TA and GM MNs of SCI_{4m} rats was still much lower than expression of this gene in INT rats (Figure 5).

Intraspinal grafting of embryonic brainstem serotonergic neurons reversed to some extent changes in the *Htr2a* gene expression observed in the TA and GM MNs of SCI_{1m} rats (Figure 5). Expression of the *Htr2a* gene in TA and in GM MNs in SCI_{TR} rats was significantly higher by 112% and 110%, respectively, than that in SCI_{1m} (Conover post hoc test $p < 0.001$ for both MN populations) and by 52% and 93%, respectively, than that in SCI_{4m} (Conover post hoc test $p < 0.05$ and $p < 0.01$, resp., for both MN populations). However, *Htr2a* gene expression remained ~14% lower in comparison to MNs of INT TA (Conover post hoc test $p < 0.05$) but in the GM MNs was restored to the level of INT (Conover post hoc test $p > 0.05$). The expression of the *Htr2a* gene in ECM MNs of SCI_{TR} rats remained increased by ~25% in comparison to that in MNs of INT rats (Conover post hoc test $p < 0.001$).

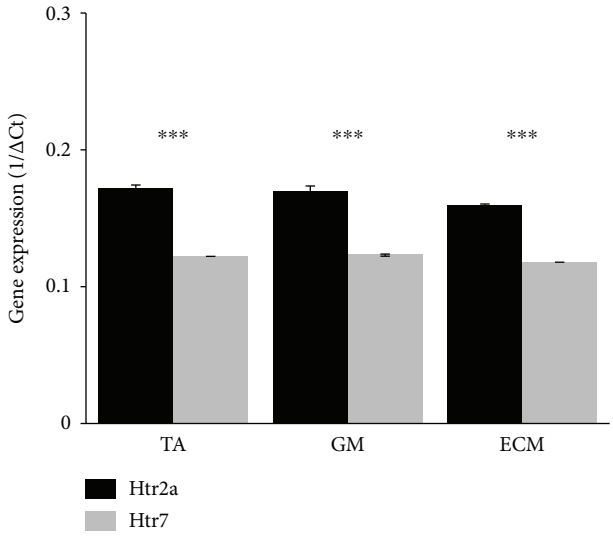

Figure 4: Expression level of *Htr2a* and *Htr7* genes (encoding 5-HT_{2A} and 5-HT_7 receptors, resp.) in motoneuron populations innervating TA, GM, and ECM muscles in intact adult rats. Expression levels of *Htr2a* and *Htr7* genes were normalized to the expression level of the constitutively active *Ppia* (cyclophyline A) gene and was presented as the 1/ΔCt value of the analyzed genes. Student's *t*-test $^{***}p < 0.0001$. Data are presented as mean ± standard deviation (mean ± SD). TA: tibialis anterior muscle; GM: gastrocnemius muscle; ECM: extensor caudae medialis muscle.

3.5. Htr7 Gene Expression in MNs. In SCI_{1m} rats, the *Htr7* gene expression was reduced by ~22% in TA MNs (nonparametric Kruskal-Wallis test (df: 3, $p = 0.015$) with Conover post hoc test $p < 0.001$), by ~50% in GM MNs (nonparametric Kruskal-Wallis test (df: 3, $p = 0.022$) with Conover post hoc test $p < 0.05$), and by ~20% in ECM MNs (nonparametric Kruskal-Wallis test (df: 3, $p = 0.025$) with Conover post hoc test $p < 0.001$) when normalized to the *Htr7* gene expression in MNs of INT animals (Figure 6).

In SCI_{4m} rats, the *Htr7* gene expression was also lower than in INT rats in TA MNs (Conover post hoc test $p < 0.05$) and in GM MNs (Conover post hoc test $p < 0.01$). There was also a small increase in gene expression in SCI_{4m} rats in comparison to SCI_{1m} rats (Conover post hoc test $p < 0.05$) in TA MNs but remained significantly lower in comparison to that of INT ($p < 0.01$). In MNs of GM muscle, *Htr7* gene expression was unchanged (Conover post hoc test $p > 0.05$) in comparison to that of SCI_{1m} rats but remained lower in comparison to that of INT (Conover post hoc test $p < 0.01$). In SCI_{4m}, the *Htr7* gene expression in the ECM MNs increased by ~12% (Conover post hoc test $p < 0.05$) in comparison to the gene expression level measured in SCI_{1m} rats (Figure 6).

Intraspinal grafting of embryonic brainstem serotonergic neurons reversed changes in the *Htr7* gene expression observed in the TA and GM MNs of SCI_{1m} rats (Figure 6). Expression of the *Htr7* gene in the TA MNs (nonparametric Kruskal-Wallis test (df: 3, $p = 0.015$) with post hoc Conover method for multiple comparisons $p < 0.001$) and in the GM MNs (nonparametric Kruskal-Wallis test $p = 0.022$ and Conover post hoc adjusted with FDR method for multiple comparisons $p < 0.05$) in SCI_{TR} rats was higher than that in the INT rats. Expression of the *Htr7* gene in SCI_{TR} significantly increased by ~109% (Conover post hoc $p < 0.01$) and ~215% (Conover post hoc test $p < 0.001$) in the TA and GM MNs, respectively, in comparison to the *Htr7* gene expression in the SCI_{1m} and by ~86% (Conover post hoc $p < 0.001$) and ~215% (Conover post hoc test $p < 0.001$) in the TA and GM MNs, respectively, in comparison to the *Htr7* gene expression in SCI_{4m} rats. On the other hand, in the ECM MNs, expression of the *Htr7* gene in the SCI_{TR} rats was not different in comparison to the *Htr7* expression in the SCI_{4m} rats (nonparametric Kruskal-Wallis (df: 3, $p = 0.025$ with Conover post hoc $p = 0.81$)).

4. Discussion

In our previous papers, we demonstrated that intraspinal grafting of embryonic neurons destined to form the descending 5-HT system of the rat brain stem effectively restores coordinated plantar stepping in adult spinal rats [10, 13, 51, 57]. We also demonstrated that such recovery is mediated by 5-HT_{2A} and 5-HT_7 serotonergic receptors [10, 13].

In the present paper, we confirmed expression of the *Htr2a* and *Htr7* genes in MN populations of intact and paraplegic rats. We showed for the first time that intraspinal transplantation of rat E14 embryo brainstem containing serotonergic neurons increases expression of these genes in the TA and GM hindlimb MNs in comparison to ungrafted spinal animals. We found that 5-HT_7 receptor mRNA was decreased at 1 month and 4 months after spinal cord injury in all 3 types of MNs. In the presence of the grafts, 5-HT_7 mRNA levels increased above those at 1 and 4 months and were significantly different from the intact condition in TA, GM, and ECM MNs. The graft tended to reverse the decrease in 5-HT_7 receptor mRNA in TA and GM MNs, with a sustained increase after 4 months in the grafted rats. The grafts did not have such an effect in ECM (tail) MNs. One month after SCI, 5-HT_{2A} receptor mRNA decreased in flexor and extensor MNs, while it increased in tail MNs. Flexor and extensor MNs had decreased 5-HT_{2A} mRNA after 4 months, while 5-HT_{2A} mRNA in the tail MNs decreased in comparison to that observed one month after SCI but remained slightly higher than that in INT. Grafting resulted in 5-HT_{2A} mRNA levels that did not differ from the intact condition in GM MNs, but 5-HT_{2A} mRNA expression continued to be slightly downregulated in TA MNs and upregulated in ECM MNs. It is possible to conclude that the presence of the grafts tended to normalize the levels of 5-HT receptor mRNA in limb muscle MNs, as predicted by our hypothesis, but not in MNs of tail muscle. A possible mechanism for the effect of the grafts might be that increased *Htr2a* gene expression may be a consequence of the increased presence of 5-HT derived from the graft, which can occur in some cells [62]. The mechanism for regulation of *Htr2a* gene expression in MNs of different types may vary. This is a suitable topic for further research.

Our data showing 5-HT_{2A} mRNA upregulation in ECM is similar to findings on receptor protein upregulation in

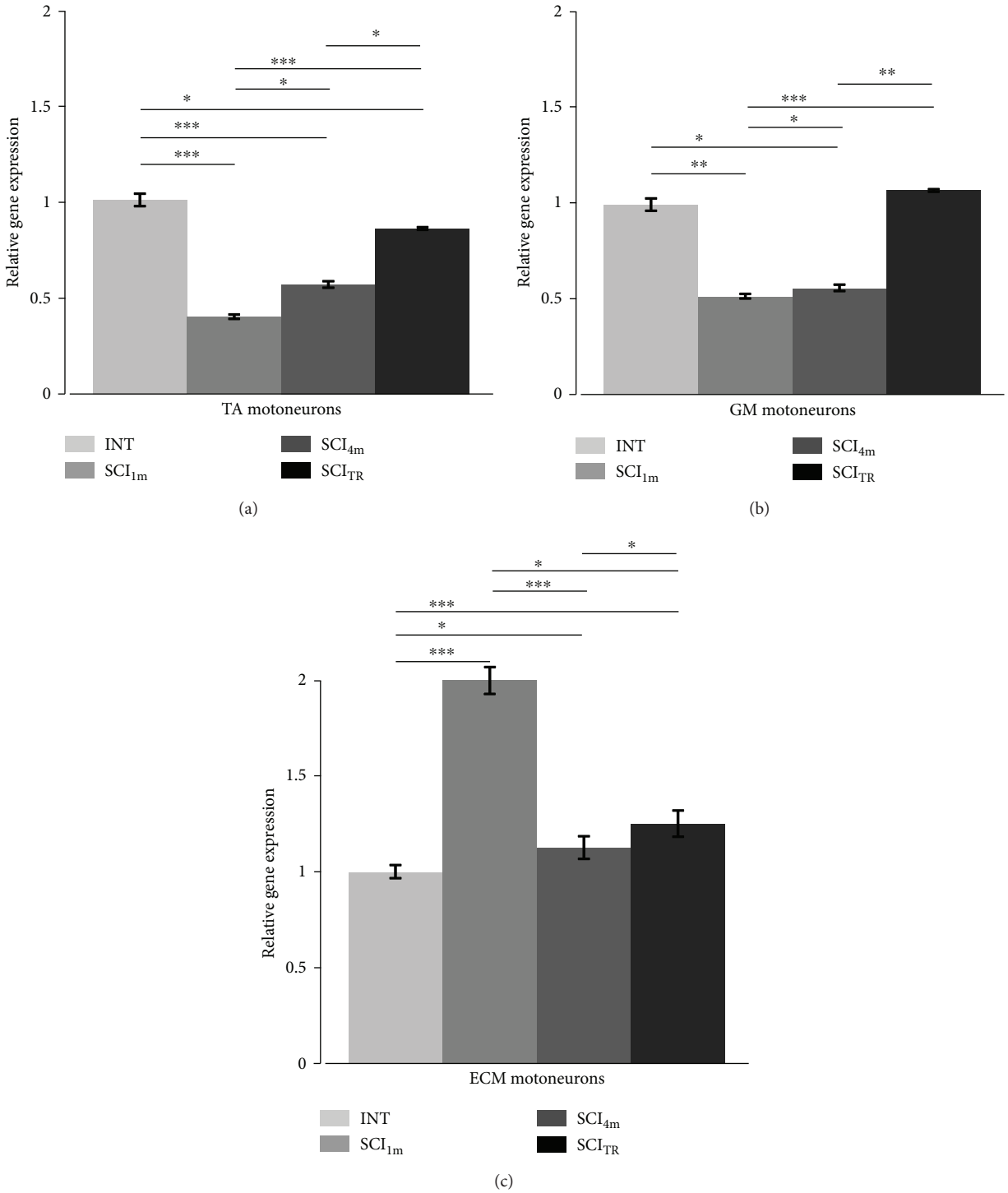

FIGURE 5: Changes in the *Htr2a* gene expression in MNs innervating the TA (a), GM (b), and ECM (c) muscles in rats one and four months after total spinal cord transection and in spinal rats with a graft of 14-day-old rat embryonic brainstem tissue containing serotonergic neurons. INT: intact rats; SCI_{1m}: rats 1 month after spinal cord transection; SCI_{4m}: rats 4 months after spinal cord transection; SCI_{TR}: rats 4 months after spinal cord transection with a graft; TA: tibialis anterior muscle; GM: gastrocnemius muscle; ECM: extensor caudae medialis muscle. Data normalized to the expression of *Htr2a* gene in MNs of INT rats are presented as mean ± SD (standard deviation). Nonparametric Kruskal-Wallis test with Conover post hoc method for multiple comparison ($^{*}p < 0.05$; $^{**}p < 0.01$; $^{***}p < 0.001$).

more distal tail muscle MNs [63–65]. In MNs innervating hindlimb muscles, 5-HT_{2A} receptor protein levels have been observed to be upregulated 4–6 weeks after contusive SCI [66, 67]. Protein levels for this receptor have not been examined at later time points after injury. Absence of an increase in *Htr2a* gene expression after total transection observed here is consistent with in situ hybridization data obtained by Ung and colleagues showing a clear tendency

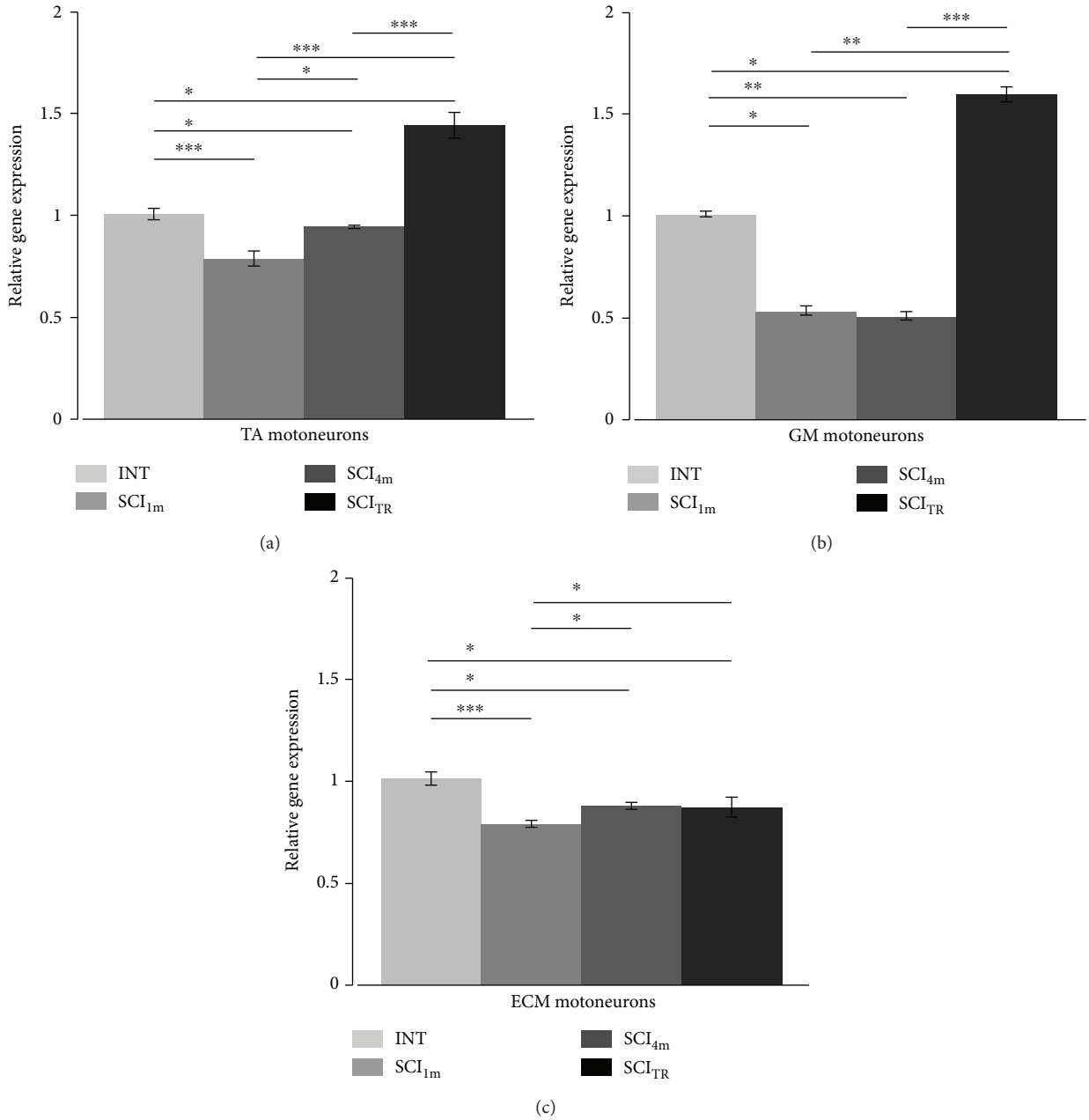

Figure 6: Changes in the *Htr7* gene expression in MNs innervating TA (a), GM (b), and ECM (c) muscles in rats one and four months after total spinal cord transection and in spinal rats with a graft of 14-day-old rat embryonic brainstem tissue containing serotonergic neurons. INT: intact rats; SCI_{1m}: rats 1 month after spinal cord transection; SCI_{4m}: rats 4 months after spinal cord transection; SCI_{TR}: rats 4 months after spinal cord transection with a graft; TA: tibialis anterior muscle; GM: gastrocnemius muscle; ECM: extensor caudae medialis muscle. Data normalized to the expression of *Htr7* gene in MNs of INT rats are presented as mean ± SD (standard deviation). Nonparametric Kruskal-Wallis test with Conover post hoc method for multiple comparison ($^{*}p < 0.05$; $^{**}p < 0.01$; $^{***}p < 0.001$).

of 5-HT_{2A} mRNA to decrease in the ventral horn of lumbar segments 28 days after spinal cord transection in adult mice [68]. Our data on 5-HT_{2A} receptor mRNA are not predictive of the increase in 5-HT_{2A} receptor protein. Maier et al. [69] reviewed the common observation that mRNA and protein expression can be uncorrelated. They conclude that the major posttranslational factor influencing mRNA-protein correlation is the individual half-life of proteins. Our observation of a decrease in mRNA expression at times when increases in protein expression occur [66, 67] can be explained by the relative half-life of the mRNA and the 5-HT_{2A} receptor protein. In situ hybridization results [68] are consistent with a decrease in *Htr2a* gene expression after spinal cord injury in the ventral horn (28 days in their case and one month and 4 months in our case). In the paper by Chopek et al. [42], the samples were taken 3 months after injury. Since mRNA expression is not maintained in a steady state [69], some fluctuation in mRNA expression over time is

to be expected. For example, in laser-captured phrenic motoneurons [70], mRNA for 5-HT_{2A} receptors was upregulated 14 days after cervical hemisection, but had returned to normal or below at 21 days. Fuller et al. [27], in contrast, found upregulation of 5-HT_{2A} protein after 7–14 days in the same preparation (cervical hemisection). The decrease in *Htr2a* gene expression may be an autoregulatory response to increased receptor density [71].

Chopek and others [42] found significant increases in *Htr2a* gene expression in motoneurons innervating hindlimb flexor and extensor muscles after spinal cord transection. This is not surprising given the frequent absence of correlation between gene and protein expression after injury. What might account for the differences between our findings and those of Chopek et al? They might be an effect of different selection of motoneurons for analysis. We compared MNs innervating TA with those innervating GM based upon the fact that these muscles have comparable composition of the three types of motor units, but they are different in function (extensor versus flexor). Chopek and others collected MNs innervating both soleus and gastrocnemius lateralis muscles to the extensor pool and MNs innervating extensor digitorum longus and tibialis anterior muscles to the flexor pool. Soleus is a typical slow muscle, and extensor digitorum longus is a typical fast muscle, so including these MNs in their extensor and flexor pools, respectively, may have influenced the results. MNs of different sizes may express 5-HT_{2A} receptors differently, and they react differently to spinal cord injury [72]. Moreover, Chopek and others [42] use *SDHA* as the reference gene for qPCR analysis, which may have influenced the results, because expression of this gene may be altered by spinal cord injury. This is the case after disuse in microgravity, and it appears to induce changes in *SDHA* expression differently in motoneurons of different sizes [73, 74]. We selected the *Ppia* gene after Navarrett and others [75], who verified it as suitable for use in spinal cord tissue after injury. We also eliminated any effects of 5-HT receptors in blood [76] by perfusing the rat with PBS before dissecting the spinal cord and further preparation for laser capture of the motoneurons, whereas this was not done by others who observed an increase in 5-HT_{2A} mRNA [42, 43]. In the Di Narzo et al. [43] study, the sample was taken from the sacral cord and was not limited to motoneurons. Another possible explanation for the differences between our observations on 5-HT_{2A} mRNA levels after injury and those of Chopek et al. [42] and Di Narzo et al. [43] is that they used Sprague-Dawley rats, while WAG (Wistar Albino Glaxo) rats were used in our study.

Di Narzo et al. [43] described recently that in rat spinal cord, the mRNA expression of *Htr2c* gene is influenced by inflammation caused by total transection at the sacral level (0.6 mm below and above the SCI). Our analysis of the inflammatory responses in the spinal cord of spinal rats with and without a graft revealed that in the ventral horn of the lumbar segments (6 mm below the graft site—the shortest distance below the graft that MNs of TA and GM muscles were collected), there was no increased level of astrocytes and no presence of activated microglia. Thus, inflammation induced by intraspinal grafting is not likely to be responsible for the observed changes in *Htr2a* and *Htr7* gene expression.

There is good evidence for constitutive activity in 5-HT_2 receptors in sacral MNs after S2 spinal cord injury (reviewed in [14]), but the evidence that this is true in MNs innervating limb muscles is less complete. The degree of constitutive activity of 5-HT_{2A} receptors is thought to be dependent upon mRNA expression [75]. The reduction in mRNA after SCI may be interpreted as an indication of decreased constitutive activity in both 5-HT_{2A} and 5-HT_7 receptors. Our finding that limb motoneuron 5-HT_{2A} and 5-HT_7 mRNA expression is increased by the grafts could therefore reflect an increase in constitutive activity in these receptors. Whether this can account for the efficacy of the grafts for improving locomotor recovery in paraplegic rats will require further investigation. These results suggest that the mechanisms regulating 5-HT receptor mRNA expression in limb and tail MNs after SCI might be different.

Our results showing 5-HT_7 receptor mRNA upregulation after grafting provides support for the suggestion that the graft improves locomotion by increasing the role of this receptor in these MNs. Both 5-HT_{2A} and 5-HT_7 receptors are expressed in phrenic MNs, and both receptors facilitate spinal motor plasticity [77, 78]. Their coexistence results in mutual crosstalk inhibition (Fuller and Mitchell respiratory neuroplasticity) due to the downstream effects induced by Gq (5-HT_{2A}) and Gs (5-HT_7) activation. The details of this crosstalk inhibition are not well defined, but this factor needs to be taken into account if the function of neurons expressing both these G protein receptors is to be understood. In the case of limb motoneurons, it is possible that such crosstalk inhibition could result in mutual downregulation of receptor expression. Further investigations of the effects of 5-HT_7 receptors on limb motoneurons are warranted. A description of the mechanisms involved in the increased expression of RNAs for both receptors induced by the grafts will require further investigation.

5-HT_7 receptors appear to be expressed in limb MNs, but their role in controlling motoneuron function has not been established. Zhang [79] found that a 5-HT_7 receptor agonist produced depolarization when applied iontophoretically onto lumbar MNs in cat spinal cord. MN excitability might be increased if 5-HT_7 receptors mediated a reduction in the afterhyperpolarization in limb MNs, which appears to be the case in trigeminal MNs [19]. Limb MN AHPs are reduced by iontophoretically applied 5-HT [80], but the receptor responsible for this effect has not been determined. These issues need to be investigated, along with the possibility of inhibitory crosstalk between 5-HT_{2A} and 5-HT_7 receptors which occurs in phrenic motoneurons [77, 78], when both receptors are present in the same cell.

5. Conclusion

Our results indicate that thoracic spinal cord transection leads to changes in *Htr2a* and *Htr7* gene expression, whereas transplantation of embryonic serotonergic neurons reverses these changes in MNs innervating hindlimb muscles but not those innervating the tail muscle. These differences in *Htr2a* and *Htr7* gene expression between MNs innervating

hindlimb and tail muscles can be a result of the distance from the graft to the motoneurons. The fibers of grafted 5-HT neurons do not extend farther than to the level of L4-L5 lumbar segments [10, 57], so motoneurons innervating the ECM muscle may not be supplied by serotonergic innervation of graft origin. Alternatively, it may be that motoneurons that innervate tail muscles have unique adaptations to spinal injury and the effects of intraspinal grafts of 5-HT neurons, such as reliance on constitutive activity of 5-HT_2 receptors after spinal cord injury. Increased *Htr2a* and *Htr7* gene expression induced by the graft could restore motoneuron excitability and lead to improved motor function, such as we observed in the grafted rats [10, 57]. Here, we show for the first time that changes in gene expression induced by the graft may account for this recovery.

Data Availability

All data used in this study are included in the article. Any additional information required will be provided upon request to the corresponding author.

Conflicts of Interest

The authors declare that there is no conflict of interest regarding the publication of this paper.

Acknowledgments

This work was supported by grants from the Polish National Science Centre (UMO-2013/09/B/NZ4/02885) to Urszula Sławińska and the Operational Programme Human Capital – Priority 8.2.2, engaged in the innovative scientific research in areas considered particularly important for the development of Masovian Voivodeship for Krzysztof Miazga. Research subject was carried out with the use of CePT infrastructure (the Arcturus Laser Microdissection System, Laboratory of Molecular Neurobiology, headed by Professor B. Kamińska) financed by the European Union – the European Regional Development Fund within the Operational Programme "Innovative Economy" for 2007–2013.

References

[1] J. Hounsgaard, "Motor neurons," *Comprehensive Physiology*, vol. 7, no. 2, pp. 463–484, 2017.

[2] J. F. Perrier and F. Cotel, "Serotonergic modulation of spinal motor control," *Current Opinion in Neurobiology*, vol. 33, pp. 1–7, 2015.

[3] B. J. Schmidt and L. M. Jordan, "The role of serotonin in reflex modulation and locomotor rhythm production in the mammalian spinal cord," *Brain Research Bulletin*, vol. 53, no. 5, pp. 689–710, 2000.

[4] A. M. Cabaj, H. Majczyński, E. Couto et al., "Serotonin controls initiation of locomotion and afferent modulation of coordination via 5-HT7 receptors in adult rats," *The Journal of Physiology*, vol. 595, no. 1, pp. 301–320, 2017.

[5] F. Gackiere and L. Vinay, "Serotonergic modulation of postsynaptic inhibition and locomotor alternating pattern in the spinal cord," *Frontiers in Neural Circuits*, vol. 8, 2014.

[6] J. Liu and L. M. Jordan, "Stimulation of the parapyramidal region of the neonatal rat brain stem produces locomotor-like activity involving spinal 5-HT7 and 5-HT2A receptors," *Journal of Neurophysiology*, vol. 94, no. 2, pp. 1392–1404, 2005.

[7] J. Liu, T. Akay, P. B. Hedlund, K. G. Pearson, and L. M. Jordan, "Spinal 5-HT7 receptors are critical for alternating activity during locomotion: in vitro neonatal and in vivo adult studies using 5-HT7 receptor knockout mice," *Journal of Neurophysiology*, vol. 102, no. 1, pp. 337–348, 2009.

[8] M. A. Madriaga, L. C. McPhee, T. Chersa, K. J. Christie, and P. J. Whelan, "Modulation of locomotor activity by multiple 5-HT and dopaminergic receptor subtypes in the neonatal mouse spinal cord," *Journal of Neurophysiology*, vol. 92, no. 3, pp. 1566–1576, 2004.

[9] E. Pearlstein, F. Ben Mabrouk, J. F. Pflieger, and L. Vinay, "Serotonin refines the locomotor-related alternations in the in vitro neonatal rat spinal cord," *European Journal of Neuroscience*, vol. 21, no. 5, pp. 1338–1346, 2005.

[10] U. Sławińska, K. Miazga, A. M. Cabaj et al., "Grafting of fetal brainstem 5-HT neurons into the sublesional spinal cord of paraplegic rats restores coordinated hindlimb locomotion," *Experimental Neurology*, vol. 247, pp. 572–581, 2013.

[11] U. Sławińska, K. Miazga, and L. M. Jordan, "5-HT2 and 5-HT7 receptor agonists facilitate plantar stepping in chronic spinal rats through actions on different populations of spinal neurons," *Frontiers in Neural Circuits*, vol. 8, 2014.

[12] S. Hochman, S. M. Garraway, D. W. Machacek, and B. L. Shay, "5-HT receptors and the neuromodualatory control of spinal cord function," in *Motor Neurobiology of the Spinal Cord*, T. C. Cope, Ed., pp. 48–87, CRC Press, New York, 2001.

[13] H. Majczyński, K. Maleszak, A. Cabaj, and U. Sławińska, "Serotonin-related enhancement of recovery of hind limb motor functions in spinal rats after grafting of embryonic raphe nuclei," *Journal of Neurotrauma*, vol. 22, no. 5, pp. 590–604, 2005.

[14] J. M. D'Amico, E. G. Condliffe, K. J. B. Martins, D. J. Bennett, and M. A. Gorassini, "Recovery of neuronal and network excitability after spinal cord injury and implications for spasticity," *Frontiers in Integrative Neuroscience*, vol. 8, 2014.

[15] M. Zhang, "Normal distribution and plasticity of serotonin receptors after spinal cord injury and their impacts on motor outputs," in *Recovery of Motor Function Following Spinal Cord Injury*, H. Fuller and M. Gates, Eds., InTech, 2016.

[16] M. S. Hoffman and G. S. Mitchell, "Spinal 5-HT7 receptors and protein kinase A constrain intermittent hypoxia-induced phrenic long-term facilitation," *Neuroscience*, vol. 250, pp. 632–643, 2013.

[17] M. S. Hoffman and G. S. Mitchell, "Spinal 5-HT7 receptor activation induces long-lasting phrenic motor facilitation," *The Journal of Physiology*, vol. 589, no. 6, pp. 1397–1407, 2011.

[18] W. Gang, T. Hongjian, C. Jasheng et al., "The effect of the 5-HT7 serotonin receptor agonist, LP44, on micturition in rats with chronic spinal cord injury," *Neurourology and Urodynamics*, vol. 33, no. 7, pp. 1165–1170, 2014.

[19] T. Inoue, S. Itoh, S. Wakisaka, S. Ogawa, M. Saito, and T. Morimoto, "Involvement of 5-HT7 receptors in serotonergic effects on spike afterpotentials in presumed jaw-closing motoneurons of rats," *Brain Research*, vol. 954, no. 2, pp. 202–211, 2002.

[20] K. Matsumoto-Miyai, M. Yoshizumi, and M. Kawatani, "Regulatory effects of 5-hydroxytryptamine receptors on voiding

function," *Advances in Therapy*, vol. 32, Supplement 1, pp. 3–15, 2015.

[21] J. Ogilvie, M. Wigglesworth, L. Appleby, T. O. W. Kingston, and R. W. Clarke, "On the role of 5-HT1B/1D receptors in modulating transmission in a spinal reflex pathway in the decerebrated rabbit," *British Journal of Pharmacology*, vol. 128, no. 3, pp. 781–787, 1999.

[22] A. Dogrul, M. Seyrek, E. O. Akgul, T. Cayci, S. Kahraman, and H. Bolay, "Systemic paracetamol-induced analgesic and antihyperalgesic effects through activation of descending serotonergic pathways involving spinal 5-HT7 receptors," *European Journal of Pharmacology*, vol. 677, no. 1-3, pp. 93–101, 2012.

[23] F. Viguier, B. Michot, M. Hamon, and S. Bourgoin, "Multiple roles of serotonin in pain control mechanisms—implications of 5-HT7 and other 5-HT receptor types," *European Journal of Pharmacology*, vol. 716, no. 1-3, pp. 8–16, 2013.

[24] N. Cao, J. Ni, X. Wang et al., "Chronic spinal cord injury causes upregulation of serotonin (5-HT)2A and 5-HT2C receptors in lumbosacral cord motoneurons," *BJU International*, vol. 121, no. 1, pp. 145–154, 2018.

[25] K. Fouad, M. M. Rank, R. Vavrek, K. C. Murray, L. Sanelli, and D. J. Bennett, "Locomotion after spinal cord injury depends on constitutive activity in serotonin receptors," *Journal of Neurophysiology*, vol. 104, no. 6, pp. 2975–2984, 2010.

[26] P. J. Harvey, X. Li, Y. Li, and D. J. Bennett, "5-HT2 receptor activation facilitates a persistent sodium current and repetitive firing in spinal motoneurons of rats with and without chronic spinal cord injury," *Journal of Neurophysiology*, vol. 96, no. 3, pp. 1158–1170, 2006.

[27] D. D. Fuller, T. L. Baker-Herman, F. J. Golder, N. J. Doperalski, J. J. Watters, and G. S. Mitchell, "Cervical spinal cord injury upregulates ventral spinal 5-HT2A receptors," *Journal of Neurotrauma*, vol. 22, no. 2, pp. 203–213, 2005.

[28] S. Doly, J. Fischer, M. J. Brisorgueil, D. Verge, and M. Conrath, "Pre- and postsynaptic localization of the 5-HT7 receptor in rat dorsal spinal cord: immunocytochemical evidence," *The Journal of Comparative Neurology*, vol. 490, no. 3, pp. 256–269, 2005.

[29] D. P. Fields, S. R. Springborn, and G. S. Mitchell, "Spinal 5-HT7 receptors induce phrenic motor facilitation via EPAC-mTORC1 signaling," *Journal of Neurophysiology*, vol. 114, no. 3, pp. 2015–2022, 2015.

[30] P. Fenik and S. C. Veasey, "Pharmacological characterization of serotonergic receptor activity in the hypoglossal nucleus," *American Journal of Respiratory and Critical Care Medicine*, vol. 167, no. 4, pp. 563–569, 2003.

[31] S. Okabe, M. Mackiewicz, and L. Kubin, "Serotonin receptor mRNA expression in the hypoglossal motor nucleus," *Respiration Physiology*, vol. 110, no. 2-3, pp. 151–160, 1997.

[32] C. H. Gill, E. M. Soffin, J. J. Hagan, and C. H. Davies, "5-HT7 receptors modulate synchronized network activity in rat hippocampus," *Neuropharmacology*, vol. 42, no. 1, pp. 82–92, 2002.

[33] R. M. Brownstone, L. M. Jordan, D. J. Kriellaars, B. R. Noga, and S. J. Shefchyk, "On the regulation of repetitive firing in lumbar motoneurones during fictive locomotion in the cat," *Experimental Brain Research*, vol. 90, no. 3, pp. 441–455, 1992.

[34] B. J. Schmidt, "Afterhyperpolarization modulation in lumbar motoneurons during locomotor-like rhythmic activity in the neonatal rat spinal cord in vitro," *Experimental Brain Research*, vol. 99, no. 2, pp. 214–222, 1994.

[35] P. A. M. ban Dongen, S. Grillner, and T. Hökfelt, "5-Hydroxytryptamine (serotonin) causes a reduction in the afterhyperpolarization following the action potential in lamprey motoneurons and premotor interneurons," *Brain Research*, vol. 366, no. 1-2, pp. 320–325, 1986.

[36] P. Wallén, J. Christenson, L. Brodin, R. Hill, A. Lansner, and S. Grillner, "Chapter 26 Mechanisms underlying the serotonergic modulation of the spinal circuitry for locomotion in lamprey," *Progress in Brain Research*, vol. 80, pp. 321–327, 1989.

[37] S. Doly, A. Madeira, J. Fischer et al., "The 5-HT2A receptor is widely distributed in the rat spinal cord and mainly localized at the plasma membrane of postsynaptic neurons," *The Journal of Comparative Neurology*, vol. 472, no. 4, pp. 496–511, 2004.

[38] V. Cornea-Hebert, M. Riad, C. Wu, S. K. Singh, and L. Descarries, "Cellular and subcellular distribution of the serotonin 5-HT2A receptor in the central nervous system of adult rat," *The Journal of Comparative Neurology*, vol. 409, no. 2, pp. 187–209, 1999.

[39] F. Vult von Steyern and T. Lomo, "Postnatal appearance of 5-HT2A receptors on fast flexor and slow extensor rat motor neurons," *Neuroscience*, vol. 136, no. 1, pp. 87–93, 2005.

[40] J. K. Lee, C. S. Johnson, and J. R. Wrathall, "Up-regulation of 5-HT2 receptors is involved in the increased H-reflex amplitude after contusive spinal cord injury," *Experimental Neurology*, vol. 203, no. 2, pp. 502–511, 2007.

[41] J. W. Chopek, C. W. MacDonell, K. Gardiner, and P. F. Gardiner, "Daily passive cycling attenuates the hyperexcitability and restores the responsiveness of the extensor monosynaptic reflex to quipazine in the chronic spinally transected rat," *Journal of Neurotrauma*, vol. 31, no. 12, pp. 1083–1087, 2014.

[42] J. W. Chopek, P. C. Sheppard, K. Gardiner, and P. F. Gardiner, "Serotonin receptor and KCC2 gene expression in lumbar flexor and extensor motoneurons posttransection with and without passive cycling," *Journal of Neurophysiology*, vol. 113, no. 5, pp. 1369–1376, 2015.

[43] A. F. Di Narzo, A. Kozlenkov, Y. Ge et al., "Decrease of mRNA editing after spinal cord injury is caused by down-regulation of ADAR2 that is triggered by inflammatory response," *Scientific Reports*, vol. 5, no. 1, article 12615, 2015.

[44] I. Giroux, E. M. Kurowska, and K. K. Carroll, "Role of dietary lysine, methionine, and arginine in the regulation of hypercholesterolemia in rabbits," *The Journal of Nutritional Biochemistry*, vol. 10, no. 3, pp. 166–171, 1999.

[45] M. Antri, J. Y. Barthe, C. Mouffle, and D. Orsal, "Long-lasting recovery of locomotor function in chronic spinal rat following chronic combined pharmacological stimulation of serotonergic receptors with 8-OHDPAT and quipazine," *Neuroscience Letters*, vol. 384, no. 1-2, pp. 162–167, 2005.

[46] U. Sławińska, H. Majczyński, Y. Dai, and L. M. Jordan, "The upright posture improves plantar stepping and alters responses to serotonergic drugs in spinal rats," *The Journal of Physiology*, vol. 590, no. 7, pp. 1721–1736, 2012.

[47] E. S. Landry, N. P. Lapointe, C. Rouillard, D. Levesque, P. B. Hedlund, and P. A. Guertin, "Contribution of spinal 5-HT1A and 5-HT7 receptors to locomotor-like movement induced by 8-OH-DPAT in spinal cord-transected mice," *The European Journal of Neuroscience*, vol. 24, no. 2, pp. 535–546, 2006.

[48] R. Bos, K. Sadlaoud, P. Boulenguez et al., "Activation of 5-HT2A receptors upregulates the function of the neuronal K-Cl cotransporter KCC2," *Proceedings of the National*

Academy of Sciences of the United States of America, vol. 110, no. 1, pp. 348–353, 2013.

[49] M. J. Dunbar, M. A. Tran, and P. J. Whelan, "Endogenous extracellular serotonin modulates the spinal locomotor network of the neonatal mouse," *The Journal of Physiology*, vol. 588, no. 1, pp. 139–156, 2010.

[50] M. Antri, C. Mouffle, D. Orsal, and J. Y. Barthe, "5-HT1A receptors are involved in short- and long-term processes responsible for 5-HT-induced locomotor function recovery in chronic spinal rat," *The European Journal of Neuroscience*, vol. 18, no. 7, pp. 1963–1972, 2003.

[51] U. Sławińska, H. Majczyński, and R. Djavadian, "Recovery of hindlimb motor functions after spinal cord transection is enhanced by grafts of the embryonic raphe nuclei," *Experimental Brain Research*, vol. 132, no. 1, pp. 27–38, 2000.

[52] K. C. Murray, A. Nakae, M. J. Stephens et al., "Recovery of motoneuron and locomotor function after spinal cord injury depends on constitutive activity in 5-HT2C receptors," *Nature Medicine*, vol. 16, no. 6, pp. 694–700, 2010.

[53] U. Sławińska, L. M. Jordan, B. Burger, H. Fabczak, and H. Majczyński, "Locomotion of intact adult rats is controlled by 5-HT2A and 5-HT7 but not 5-HT2C receptors; 2012," in *Society of Neuroscience*, Neuroscience Meeting Planner, New Orleans, LA, USA, 2012, Program No. 85.09.

[54] K. L. Wohlpart and P. B. Molinoff, "Regulation of levels of 5-HT2A receptor mRNA," *Annals of the New York Academy of Sciences*, vol. 861, no. 1 ADVANCES IN S, pp. 128–135, 1998.

[55] D. Van Oekelen, W. H. M. L. Luyten, and J. E. Leysen, "5-HT2A and 5-HT2C receptors and their atypical regulation properties," *Life Sciences*, vol. 72, no. 22, pp. 2429–2449, 2003.

[56] K. Miazga, E. Joachimiak, H. Fabczak, and U. Sławińska, "Grafted serotonergic neurons can reverse changes in gene expression in motoneurons produced by spinal cord injury in rats.; 2015. Programm: P9.6," in *12th International Congress of the Polish Neuroscience Society*, Gdańsk, Poland, September 2015.

[57] U. Sławińska, K. Miazga, and L. M. Jordan, "The role of serotonin in the control of locomotor movements and strategies for restoring locomotion after spinal cord injury," *Acta Neurobiologiae Experimentalis*, vol. 74, no. 2, pp. 172–187, 2014.

[58] A. Lev-Tov, A. Etlin, and D. Blivis, "Sensory-induced activation of pattern generators in the absence of supraspinal control," *Annals of the New York Academy of Sciences*, vol. 1198, no. 1, pp. 54–62, 2010.

[59] D. Feraboli-Lohnherr, D. Orsal, A. Yakovleff, M. Gimenez y Ribotta, and A. Privat, "Recovery of locomotor activity in the adult chronic spinal rat after sublesional transplantation of embryonic nervous cells: specific role of serotonergic neurons," *Experimental Brain Research*, vol. 113, no. 3, pp. 443–454, 1997.

[60] M. G. y Ribotta, J. Provencher, D. Feraboli-Lohnherr, S. Rossignol, A. Privat, and D. Orsal, "Activation of locomotion in adult chronic spinal rats is achieved by transplantation of embryonic raphe cells reinnervating a precise lumbar level," *The Journal of Neuroscience*, vol. 20, no. 13, pp. 5144–5152, 2000.

[61] D. M. Basso, M. S. Beattie, and J. C. Bresnahan, "Graded histological and locomotor outcomes after spinal cord contusion using the NYU weight-drop device versus transection," *Experimental Neurology*, vol. 139, no. 2, pp. 244–256, 1996.

[62] R. C. Ferry, C. D. Unsworth, R. P. Artymyshyn, and P. B. Molinoff, "Regulation of mRNA encoding 5-HT2A receptors in P11 cells through a post-transcriptional mechanism requiring activation of protein kinase C," *The Journal of Biological Chemistry*, vol. 269, no. 50, pp. 31850–31857, 1994.

[63] X. Y. Kong, J. Wienecke, M. Chen, H. Hultborn, and M. Zhang, "The time course of serotonin 2a receptor expression after spinal transection of rats: an immunohistochemical study," *Neuroscience*, vol. 177, pp. 114–126, 2011.

[64] X.-Y. Kong, J. Wienecke, H. Hultborn, and M. Zhang, "Robust upregulation of serotonin 2A receptors after chronic spinal transection of rats: an immunohistochemical study," *Brain Research*, vol. 1320, pp. 60–68, 2010.

[65] Y. Zhang, R. X. Zhang, M. Zhang et al., "Electroacupuncture inhibition of hyperalgesia in an inflammatory pain rat model: involvement of distinct spinal serotonin and norepinephrine receptor subtypes," *British Journal of Anaesthesia*, vol. 109, no. 2, pp. 245–252, 2012.

[66] Y. Ryu, T. Ogata, M. Nagao et al., "The swimming test is effective for evaluating spasticity after contusive spinal cord injury," *PLoS One*, vol. 12, no. 2, article e0171937, 2017.

[67] Y. Ryu, T. Ogata, M. Nagao, Y. Sawada, R. Nishimura, and N. Fujita, "Effects of treadmill training combined with serotonergic interventions on spasticity after contusive spinal cord injury," *Journal of Neurotrauma*, vol. 35, no. 12, pp. 1358–1366, 2018.

[68] R. V. Ung, E. S. Landry, P. Rouleau, N. P. Lapointe, C. Rouillard, and P. A. Guertin, "Role of spinal 5-HT2 receptor subtypes in quipazine-induced hindlimb movements after a low-thoracic spinal cord transection," *European Journal of Neuroscience*, vol. 28, no. 11, pp. 2231–2242, 2008.

[69] T. Maier, M. Guell, and L. Serrano, "Correlation of mRNA and protein in complex biological samples," *FEBS Letters*, vol. 583, no. 24, pp. 3966–3973, 2009.

[70] C. B. Mantilla, J. P. Bailey, W. Z. Zhan, and G. C. Sieck, "Phrenic motoneuron expression of serotonergic and glutamatergic receptors following upper cervical spinal cord injury," *Experimental Neurology*, vol. 234, no. 1, pp. 191–199, 2012.

[71] M. Zaniewska, N. Alenina, K. Wydra et al., "Discovering the mechanisms underlying serotonin (5-HT)2A and 5-HT2C receptor regulation following nicotine withdrawal in rats," *Journal of Neurochemistry*, vol. 134, no. 4, pp. 704–716, 2015.

[72] J. Celichowski, W. Mrówczyński, P. Krutki, T. Górska, H. Majczyński, and U. Sławińska, "Changes in contractile properties of motor units of the rat medial gastrocnemius muscle after spinal cord transection," *Experimental Physiology*, vol. 91, no. 5, pp. 887–895, 2006.

[73] A. Ishihara, F. Nagatomo, H. Fujino, H. Kondo, and Y. Ohira, "Decreased succinate dehydrogenase activity of gamma and alpha motoneurons in mouse spinal cords following 13 weeks of exposure to microgravity," *Neurochemical Research*, vol. 38, no. 10, pp. 2160–2167, 2013.

[74] A. Ishihara, R. R. Roy, and V. R. Edgerton, "Succinate dehydrogenase activity and soma size of motoneurons innervating different portions of the rat tibialis anterior," *Neuroscience*, vol. 68, no. 3, pp. 813–822, 1995.

[75] S. Navarrett, L. Collier, C. Cardozo, and S. Dracheva, "Alterations of serotonin 2C and 2A receptors in response to T10 spinal cord transection in rats," *Neuroscience Letters*, vol. 506, no. 1, pp. 74–78, 2012.

[76] N. Herr, C. Bode, and D. Duerschmied, "The effects of serotonin in immune cells," *Frontiers in Cardiovascular Medicine*, vol. 4, p. 48, 2017.

[77] D. P. Fields and G. S. Mitchell, "Divergent cAMP signaling differentially regulates serotonin-induced spinal motor plasticity," *Neuropharmacology*, vol. 113, no. Part A, pp. 82–88, 2017.

[78] D. D. Fuller and G. S. Mitchell, "Respiratory neuroplasticity – overview, significance and future directions," *Experimental Neurology*, vol. 287, Part 2, pp. 144–152, 2017.

[79] L. Zhang, "Effects of 5-hydroxytryptamine on cat spinal motoneurons," *Canadian Journal of Physiology and Pharmacology*, vol. 69, no. 2, pp. 154–163, 1991.

[80] S. R. White and S. J. Fung, "Serotonin depolarizes cat spinal motoneurons in situ and decreases motoneuron afterhyperpolarizing potentials," *Brain Research*, vol. 502, no. 2, pp. 205–213, 1989.

Hindawi
Neural Plasticity
Volume 2018, Article ID 6464896, 12 pages
https://doi.org/10.1155/2018/6464896

Research Article

Testing rTMS-Induced Neuroplasticity: A Single Case Study of Focal Hand Dystonia

Sonia Betti,[1] Andrea Spoto,[1] Umberto Castiello,[1,2] and Luisa Sartori[1,3]

[1]*Dipartimento di Psicologia Generale, Università di Padova, Padova, Italy*
[2]*Centro Beniamino Segre, Accademia Nazionale dei Lincei, Roma, Italy*
[3]*Centro di Neuroscienze Cognitive, Università di Padova, Padova, Italy*

Correspondence should be addressed to Luisa Sartori; luisa.sartori@unipd.it

Received 6 January 2018; Accepted 30 April 2018; Published 30 May 2018

Academic Editor: Toshiyuki Fujiwara

Focal hand dystonia in musicians is a neurological motor disorder in which aberrant plasticity is caused by excessive repetitive use. This work's purposes were to induce plasticity changes in a dystonic musician through five daily thirty-minute sessions of 1 Hz repetitive transcranial magnetic stimulation (rTMS) applied to the left M1 by using neuronavigated stimulation and to reliably measure the effect of these changes. To this aim, the relationship between neuroplasticity changes and motor recovery was investigated using fine-grained kinematic analysis. Our results suggest a statistically significant improvement in motor coordination both in a task resembling the dystonic-inducing symptoms and in a reach-to-grasp task. This single case study supports the safe and effective use of noninvasive brain stimulation in neurologic patients and highlights the importance of evaluating outcomes in measurable ways. This issue is a key aspect to focus on to classify the clinical expression of dystonia. These preliminary results promote the adoption of kinematic analysis as a valuable diagnostic tool.

1. Introduction

Dystonias are a group of disorders characterized by intermittent or sustained muscle contractions causing twisting and repetitive movements (for a review, see [1, 2]). The crucial catalyst behind dystonia is a multifactorial combination of excessive plasticity, intensive training, and failure of limiting plastic changes, as seen through noninvasive neurostimulation studies [3]. Once this abnormal plasticity process is brought under control, it could ultimately result in a clinical improvement [4].

Dystonia may be task-specific producing abnormal motor performance for only a specific task, such as in musician's dystonia (MD). MD affects isolated fingers that perform complex and repetitive motor tasks during actions associated with musical play, but can also lead to impaired adjacent finger flexion [2]. This overflow into adjacent muscles not specifically involved in the particular motor task is due to a loss of inhibition that manifests in the periphery with abnormally long muscle bursts [5]. In MD, abnormally prolonged muscle firing due to selective overtraining of an intended finger may prevent the ability to keep excitability within a useable range (i.e., homeostatic plasticity), a function which is specifically impaired in dystonia [6].

Although its underlying pathophysiology remains unclear, several studies in patients with MD have shown that repeated and prolonged hand use might result in abnormal activity in the cortical representation of the hand [7, 8]. In fact, important neural correlates of task-specific dystonia are the enlarged and partially overlapping fields revealed by brain imaging and transcranial magnetic stimulation (TMS) studies targeting the somatosensory and the motor cortices [8–14]. Whereas a typical homuncular organization reveals a distance of about 2.5 cm between the representations of the thumb and the little finger, these boundaries seem to be blurred for the dystonic fingers [10]. This lack of clearly defined somatosensory and motor cortical representations can lead to involuntary motor control [15]. The loss of control is particularly evident during fast passages, often leading to involuntary flexion or extension of one or more fingers [16]. In particular, stringed instrument players exhibit a use-dependent alteration in the cortical representational

zones of the digits of the hand that engage in the dexterity-demanding task of fingering the strings [17]. While initial MD is only associated with impairment of highly practiced motor tasks, it can subsequently lead to severe deficits, eventually terminating a career for one percent of professional musicians [18].

Although prompt initiation of treatment could rescue some patients, dystonia is often misdiagnosed or neglected since the lack of objective diagnostic criteria and reliable biomarkers prohibits early diagnostic recognition [19]. So far, the extent of motor symptoms has mainly been estimated by means of visual inspection and rating procedures (e.g., [20]), without providing fine resolution (but see [21] for an example of kinematic analysis to assess a flautist performance). In addition, treatment responses are very patient-dependent. A precise quantification tool for objective and reliable diagnosis and for treatment evaluation is therefore needed to acquire highly precise data and to identify subtle differences in the symptomatology.

Given the sparse literature on this topic, there are no clinical practice guidelines on how to recover voluntary motor control. To date, the preferred treatment for dystonia is botulinum toxin injection, but it only transiently works in a minor fraction of patients and its application is limited by the spread of weakness to adjacent muscles, which causes further motor performance impairment [22].

Recently, motor training has been combined with neurostimulation methods in an attempt to normalize brain excitability and recover motor performance [23, 24]. Notably, since the effects of long-term treatment might differ from those of a single session [24], TMS is usually delivered in repeated daily sessions to prolong after effects. Therapeutic procedures with dystonic patients classically adopted daily sessions of low-frequency repetitive TMS (rTMS) over the primary motor cortex (M1; [5, 25–28]) or the premotor cortex (PM; [24, 29, 30]). Siebner and colleagues [25, 26] evaluated the effect of low-frequency (1 Hz) stimulation of M1 to increase inhibition in the motor areas of the cerebral cortex. Low-frequency rTMS set to 10% below the resting motor threshold of the target muscle restored intracortical inhibition. Treatment output on handwriting was quantified by means of a pressure-sensitive digitizing tablet.

Needless to say, the principle of the measurement must be based on the phenomenology of each patient. Motor assessment must be specifically related to the compromised movement (i.e., the particular exercise that most consistently induced the dystonic disorder), rather than to a more general skill (e.g., [21, 31]). As Pujol and colleagues (2000) convincingly demonstrated in an fMRI study, a tailored assessment of patients in the dystonia-inducing situation is necessary [8].

The aim of the present study was to test a multimethodological paradigm based on the combination of single-pulse transcranial magnetic stimulation (spTMS), low-frequency rTMS, and 3D motion analysis in a professional guitarist affected by MD. Single pulses of TMS were used to assess the excitability of synaptic connections within the motor cortex, providing indirect measures of changes produced by neural plasticity. In addition, TMS can also produce long-term changes in excitability if the TMS pulses are applied repetitively [27]. In both cases, changes in excitability were monitored by computing the amplitude of the motor-evoked potential (MEP) in response to a standard TMS pulse. In particular, resting motor threshold MEPs reflect the degree of corticospinal system activation and potentially help in diagnosing motor symptoms and in monitoring treatment progress (i.e., whether interventions are safe and effective in slowing symptoms). Fine-grained 3D movement analysis has been adopted to specifically evaluate the treatment both in terms of improved motor coordination and cortical plasticity. The acquisition of MEPs induced by spTMS to the left M1 and recorded from the contralateral second dorsal interosseous (SDI) muscle before and after five daily sessions of rTMS protocol allowed to measure the variations on the resting motor threshold to obtain a physiological index of *neural plasticity*. Moreover, we considered two behavioral measures of *performance plasticity*: (i) a repetitive sequence of fingers' movement (task 1) and (ii) a reach-to-grasp action (task 2). Since guitar arpeggios involve a rapid succession of fine and isolated finger movements, the finger flexion task was conceived as a realistic attempt to execute the affected flexion pattern. As concerns the grip task, it was specifically chosen to investigate the distinct contribution of the two separate reaching and grasping components [32] on performed movements: the timing dissociation between these two components may in fact give useful hints to the underlying pathological state [33, 34]. Notably, problems to grasp and manipulate objects are frequent in movement disorders and a methodological approach providing highly standardized measures of natural movements is needed [35]. The outputs of both tasks were compared at local and general levels: across daily sessions and throughout the intervention, to provide a consistent measure of plasticity trend.

2. Method

2.1. Participants. A 55-year-old male right-handed classical guitarist (M.C.) diagnosed as suffering from MD in his right hand was recruited at the Neuroscience of Movement (NEMO) Laboratory at the Department of General Psychology, University of Padua. He specifically presented a painless and exaggerated involuntary flexion pattern in his right middle finger's metacarpophalangeal joint, which occurred exclusively in the task-specific context of playing the musical instrument (i.e., plucking the strings). The loss of synergistic muscle control was also evident as a cocontraction of adjacent muscles. The onset of the movement disorder had been three years before this study and had forced him to interrupt his career as a professional musician and especially as a concert performer. He reported no dystonic movement patterns in other activities. There was no evidence of any other neurologic disorder and he was not under medication. An additional guitarist served as control subject in this study. He was right-handed with comparable experience (40 years of practice) and age (50 years).

No adverse effects were reported during the experiment. Informed consent was obtained after they were fully informed, according to the Declaration of Helsinki, about

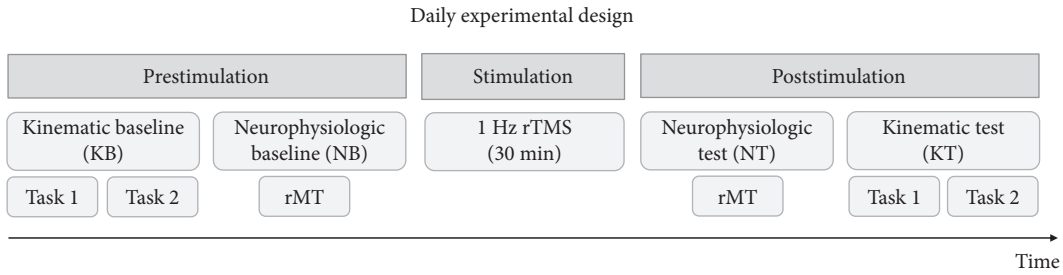

Figure 1: Daily experimental design for both MD patient and control participant. The graph represents the three daily phases of the experiment: behavioral and neurophysiological indexes were measured both before (prestimulation) and after (poststimulation) each stimulation session with low-frequency rTMS (1 Hz) on the left M1 (stimulation). The kinematic behavioral assessment (KB and KT) consisted of two tasks: finger abduction (task 1) and reach-to-grasp (task 2). In the neurophysiological assessment (NB and NT), the resting motor threshold was measured to assess corticospinal excitability variations. This protocol was repeated for five consecutive days.

the study's nature. The experimental protocol was approved by the University of Padua Ethics Review Board.

2.2. General Procedure. A daily protocol (Figure 1) entailing two evaluation sessions (prestimulation) of kinematic and resting motor threshold (rMT) baselines, followed by low-frequency rTMS (stimulation) and kinematic and rMT tests (poststimulation), was repeated for five consecutive days and was designed as follows:

(1) Prestimulation kinematic baseline (KB). A series of alternating finger flexion movements (i.e., the index, middle, and ring fingers, 15 movements per finger; task 1) with the palm upward and a sequence of 15 reach-to-grasp movements (task 2) were performed to test independent movements of the dystonic finger and motor coordination.

(2) Prestimulation neurophysiologic baseline (NB). TMS-induced motor-evoked potentials (MEPs) were recorded from the right second dorsal interosseous (SDI) muscle to measure the rMT, thus assessing corticospinal excitability before intervention.

(3) Stimulation. The participant underwent 30 minutes of rTMS (1 Hz) over the SDI muscle representation on the left primary motor cortex, delivered with intensity of 90% with respect to the rMT.

(4) Poststimulation neurophysiologic test (NT). The same procedure adopted during the prestimulation NB session was implemented for comparison purposes. We performed a trend analysis to evaluate changes in motor cortex plasticity.

(5) Poststimulation kinematic test (KT). The same procedure adopted during preintervention KB session was implemented for comparison purposes. We performed a day-by-day analysis and we compared the first and last day to evaluate both short- and long-term effects in motor coordination.

2.3. Kinematics Recording. A 3D optoelectronic SMART-D system (Bioengineering Technology and Systems, BTS) was used to track the kinematics of the participants' right hand. During the KB and KT phases, the participants were seated in a height-adjustable chair in front of a table (900 mm × 900 mm) with the right hand placed on a designated position on the table surface so as to guarantee the consistency of the start position across participants. Three semispherical infrared-reflective markers (5 mm diameter) were attached to the right hand on the tip of the index, middle, and ring fingers, and one was attached to the radial aspect of the wrist. Six digital video cameras with a frequency of 140 Hz were placed in a semicircle around the table (at 1–1.2 m away) to detect the markers (see Figure 2(a)). Before the experimental sessions, cameras position, roll angle, focus, zoom, brightness, and threshold were adjusted to optimize markers' tracking. Static and dynamic calibrations were then performed. For the static calibration, a three-axis frame of reference at known distance was placed on the center of the table. For the dynamic calibration, a three-marker wand was moved in all directions throughout the workspace of interest for approximately one minute. The spatial resolution of the recording system was 0.3 mm over the field of view. The standard deviation (SD) of the reconstruction error was below 0.2 mm for all the axes (x, y, and z).

During each daily session of the KB and KT phases, the participants took part in two tasks:

(i) Task 1: A series of 45 randomly alternating finger flexion movements of the index, middle, and ring fingers (15 movements per finger) were performed to test independent movements of the dystonic and adjacent fingers. The participants' right wrists were placed over a wooden cylinder (7.5 mm diameter; 11 cm high) with the palm of the hand facing upwards.

(ii) Task 2: In the prehension task, a sequence of 15 reach-to-grasp movements was performed to test motor coordination. At the beginning of each trial, the hand was pronated with the palm resting on a starting platform (60 × 70 mm; 5 mm thick), which was shaped to allow for a comfortable and repeatable posture of all digits, that is, slightly flexed at the

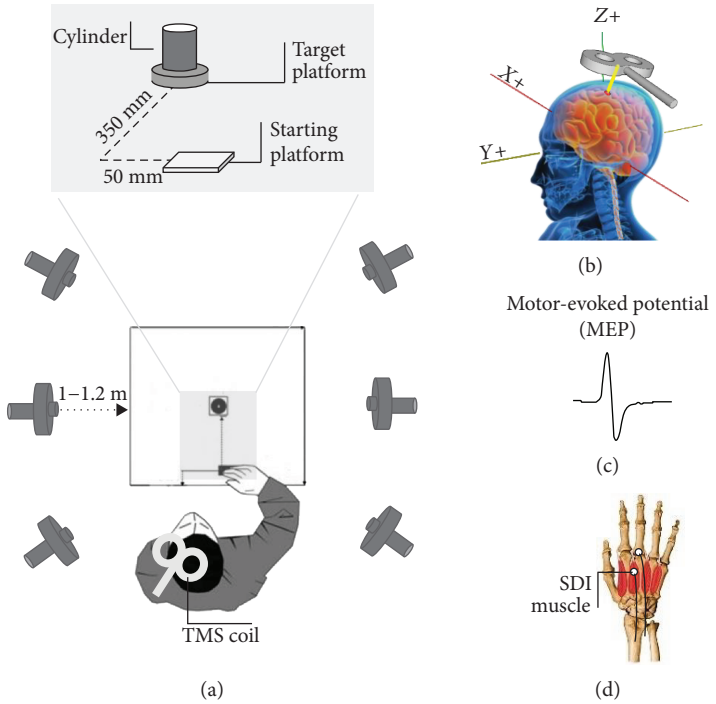

Figure 2: Experiment setup. A 3D optoelectronic SMART-D system was used to track the kinematics of the participant's right hand by means of six video cameras (a). TMS coil placement over the participant's left M1 hand area (b). Example of a TMS-evoked MEP (c). The targeted second dorsal interosseous (SDI) muscle (d).

metacarpal and proximal interphalangeal joints. Then, the participants were asked to reach and grasp the cylinder located frontally with a whole hand grasp (WHG). The starting platform was attached 90 mm away from the edge of the table surface 50 mm away from the midsection. The cylinder was placed on a target platform, located at a distance of 350 mm from the starting platform, for consistent replacing (Figure 2(a)). An affixed colored dot on the cylinder was signaling the required thumb's contact point in order to perform stable and consistent grasps across the experiment. An auditory signal (300 Hz; 200 ms) was adopted as the "go" signal.

2.4. Transcranial Magnetic Stimulation and Electromyographic Recording. During both the MB and the MT phases, each participant was comfortably seated in an armchair with the right hand positioned on a pillow and the head kept stable by a neck pillow. The participant was asked to keep his muscles relaxed and to remain as still as possible during the delivery of the TMS pulses. While TMS pulses were delivered, he was asked to observe a white fixation cross on black background presented in the center of a monitor. TMS-induced MEPs were acquired from the participant's SDI muscle of the right hand (Figure 2(c)). EMG activity was recorded through pairs of surface Ag-AgCl surface electrodes (9 mm diameter) placed in a belly-tendon montage, with the active electrodes over the SDI muscle and the reference electrodes over the corresponding metacarpophalangeal joint (Figure 2(d)). The ground electrode was placed over the dorsal part of the right wrist. Electrodes were connected to an isolable portable ExG input box linked to the main EMG amplifier for signal transmission via a twin fiber optic cable (Professional BrainAmp ExG MR, Munich, Germany). Single-pulse TMS was administered using a 70 mm figure-of-eight coil connected to a Magstim Bistim^2 stimulator (Magstim Co., Whitland, UK). Pulses were delivered to the hand region of the left M1. The coil was placed tangentially on the scalp, with the handle pointing laterally and caudally, so that the flow of induced electrical current in the brain travelled in a posterior-anterior direction [36, 37]. During the first session of the first day, the optimal cortical hotspot of the target muscle (OSP; i.e., the position at which larger and more stable MEPs are recorded from SDI with minimal stimulation intensity) was identified by delivering single TMS pulses at fixed intensity while moving the coil of 0.5 cm around the target area until the position was reached. To maintain an accurate and constant placement of the coil throughout the experimental sessions, it was kept over the OSP by a mechanical arm (Manfrotto, Italy) and its position and orientation were recorded and loaded into a neuronavigation system (SofTaxic Optic, EMS, Bologna, Italy; Figure 2(b)). Once the OSP was found, the individual resting motor threshold (rMT)—defined as the lowest stimulus intensity at which TMS is able to generate MEPs of at least 50 μV in relaxed muscles in 5 out of 10 consecutive pulses [38]—was determined. rMT was then measured every day before and after the rTMS protocol to test possible variations of corticospinal excitability. Repetitive TMS pulses were applied using a Magstim Rapid^2 stimulator (Magstim Co., Whitland, UK) with a figure-of-eight coil (70 mm outer diameter). Each rTMS session consisted of the application

of off-line, low-frequency 1 Hz TMS for 30 min (1800 total pulses) at 90% of each participant's rMT. Both spTMS and rTMS were delivered on the side of the brain contralateral to the participant's dominant (and dystonia-affected) hand.

3. Data Analysis

3.1. Behavioral Measures. Following kinematic data collection, each trial was individually checked for correct marker identification and then run through a low-pass Butterworth filter with a 6 Hz cutoff. The SMART-D Tracker software package (Bioengineering Technology and Systems, BTS) was employed to reconstruct the 3D marker positions as a function of time. In task 1, the amplitude of maximum 3D distance between the dystonic fingertip and adjacent fingers (i.e., index and ring tips) was calculated as an index of abduction independence (AI). The amplitude of minimum distance between the dystonic finger and wrist was calculated as an index of abduction degree (AD) and compared to adjacent fingers' AD (see [21] for a similar approach). In task 2, we selected a set of standard measures universally reported in the literature for reach-to-grasp tasks, possibly enabling a productive comparison of results across participants (MD; control) and across experiments. We first computed movement onset (i.e., the first time point at which the wrist velocity crossed a 5 mm/sec threshold and remained above it for longer than 100 ms) and time of grip offset (i.e., the time at which the grip velocity dropped below a 5 mm/s threshold). Then, the following indexes were measured:

(i) Movement time (i.e., the time interval between onset and offset)

(ii) Maximum grip aperture (MGA, the maximum distance reached by the 3D coordinates of the thumb and index finger)

(iii) Time of maximum grip aperture (TMGA, the time at which the distance between the 3D coordinates of the thumb and index finger was maximum from movement onset)

(iv) Time of maximum grip velocity (TMGV, the time at which the tangential velocity of the 3D coordinates of the thumb and index finger was maximum from movement onset)

(v) Time of maximum wrist height (TMWH, the time at which the 3D coordinates of the wrist were maximum from movement onset)

(vi) Time of maximum wrist deceleration (TMWD, the time at which the deceleration of the 3D coordinates of the wrist was maximum from movement onset)

(vii) Delay grasping (DG, the time interval between the onset of the wrist movement and the onset of fingers' opening)

3.2. Neurophysiological Measures. Motor threshold at rest before (rMT pre) and after (rMT post) rTMS 1 Hz stimulation was evaluated in both MD and control participants.

3.3. Statistical Analyses. Behavioral data were analyzed using the R 3.3.9 statistical package [39]. More specifically, data were analyzed by means of an ad hoc function developed to implement the computation of the Young C test statistics [40]. This test, proposed by Young and Von Neumann, is used to evaluate the presence of a trend into a sequence of data collected on the same subject. It computes the probability that a sequence of data points follows a random, nonoriented distribution. If this probability is low, then the presence of some sort of either increasing or decreasing trend in the data can be argued. More specifically, the C test statistic is computed according to the following formula:

$$C = 1 - \frac{\sum_{i=1}^{N-1} (x_i - x_{i+1})^2}{2\sum_{i=1}^{N-1} (x_i - \bar{x})^2}, \quad (1)$$

where N is the number of observations; x_i and $\bar{x}$ are the average values of the observations. The value of C tends to increase as an inverse function of the ratio between the squared difference of each data point to its subsequent and the squared difference of each point to the mean. The smaller the ratio, the higher the C, the higher the probability that the data do follow some sort of oriented trend (Figure 3).

Given these premises, data analysis was carried out on the two different tasks. More specifically, with respect to task 1, a comparison between the trend of values obtained during the first and the last day of training was carried out separately for the data collected before (pre) and after (post) the administration of the rTMS protocol. Moreover, an analysis of the overall trend along all the five days of training was conducted. This analysis was carried out separately for the pre- and post-rTMS phases and for the variables measured in task 2. A pointwise difference (delta) between the values obtained at the pre- and post-rTMS phases has been computed in order to highlight the presence of any particular daily pattern. As concerns motor threshold at rest, the presence of a significant trend before (rMT pre) and after (rMT post) rTMS 1 Hz stimulation was evaluated by means of the test C in both MD and control participants.

4. Results

4.1. Behavioral Plasticity

4.1.1. Task 1: Finger Flexion Task. The main reference point of the analysis was the movement involving the middle finger. In the MD post phase, a significant increasing trend in the distance between the dystonia-affected finger and the index finger (AI) was observed on the first day of training ($C = .66$; $p < .01$). The evaluation of the overall trend showed that the measures collected throughout all the five days followed a significantly increasing trend ($C = .87$; $p < .01$). Reverse considerations can be referred to the pre-rTMS measures: a significantly increasing trend was not observed at the first day of training ($C = .20$; n.s.); however, the data collected the last day presented a significantly increasing trend ($C = .54$; $p < .05$); the overall trend was significantly increasing ($C = .81$; $p < .01$). Figure 4 shows the increasing

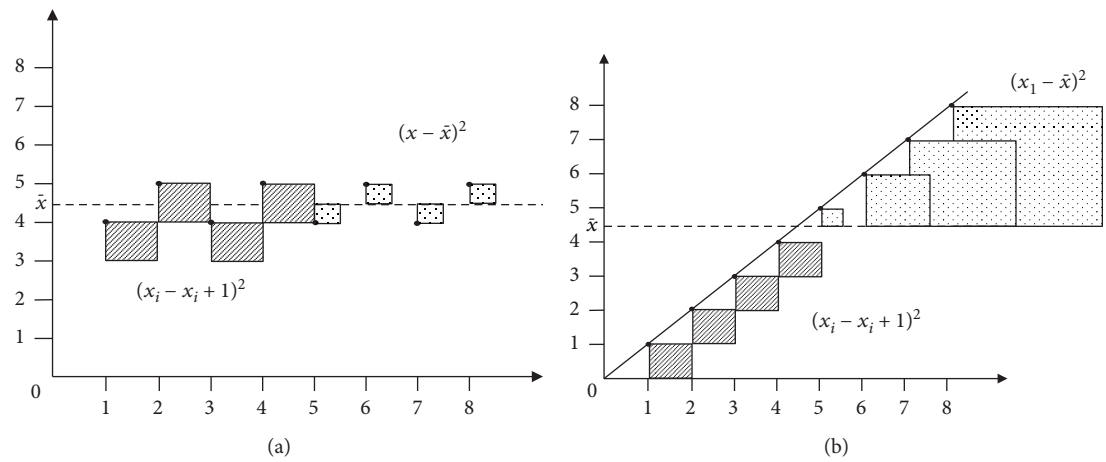

Figure 3: Graphical representation of the squared difference between (i) each data point and its subsequent value in the series (lined squares) and (ii) each data point and the average of the series (dotted squares) in the case of an oriented trend (a) and in the case of stationary data (b).

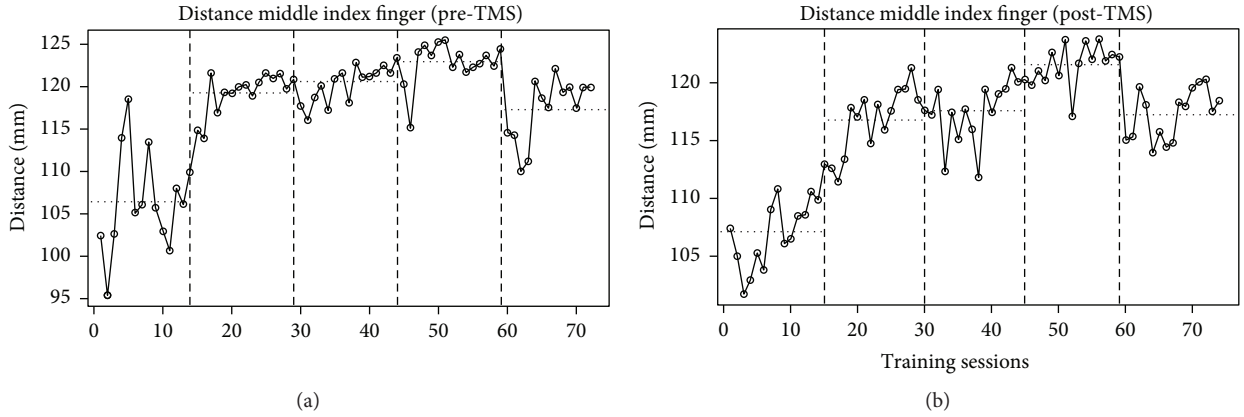

Figure 4: Graphical representation of the trend observed at the pre-rTMS (a) and post-rTMS (b) phases for the distance between the middle and index fingers when the former was flexed.

trend of this measure during the five days of training both at the pre-rTMS phase (a) and at the post-rTMS phase (b).

The same analysis conducted for the distance between the middle finger and the ring finger shows slightly different results. More specifically, while for the post measures the trend observed on the first day was significant (post: $C = .62$; $p < .01$), the measures collected in the pre phase did not show any trend (pre: $C = .33$; n.s.). Moreover, none of the trends were significant in the last days of training (day 5; post: $C = .40$; n.s.; pre: $C = .06$; n.s.). On the other hand, both the overall trends resulted significant (post: $C = .65$; $p < .01$; pre: $C = .64$; $p < .01$), showing an overall increase of the distance between the two fingers throughout the protocol. As concerns the control conditions (i.e., flexion of the adjacent fingers), no significantly increasing trend was observed in the distance between the index finger and the middle finger either at the first day of the training (pre: $C = .30$; n.s.; post: $C = .37$; n.s.) or at the last day (pre: $C = .32$; n.s.; post: $C = .33$; n.s.) when the index finger was flexed. Moreover, the overall analysis showed a significant trend in the pre-rTMS phase ($C = .57$; $p < .01$) while no effect was found in the post ($C = .37$; n.s.). The same results emerged from the analysis of the distance between the index finger and the ring finger when the former was flexed. More precisely no significant trend was observed neither at the first day of the training phases (pre: $C = .28$; n.s.; post: $C = .01$; n.s.) or at the last day of training (pre: $C = .60$; n.s.; post: $C = .03$; n.s.). The overall analysis showed a significant trend in the pre-TMS phase ($C = .62$; $p < .01$) while no effect was found in the post ($C = .37$; n.s.). Finally, when the ring finger was flexed only, some of the overall trends were significantly increasing, namely, the distance between the ring finger and the index finger in the pre-rTMS phase ($C = .75$; $p < .01$) and the distance between the ring finger and the middle finger in both phases (pre: $C = .78$; $p < .01$; post: $C = .85$; $p < .01$). No significant overall trend was observed for the distance between the ring finger and the index finger during the post-rTMS phase ($C = .40$; n.s.). In terms of the middle finger abduction degree, a significant decreasing trend was observed the first day of training at the post-TMS phase ($C = .69$; $p < .01$). Moreover, both the overall trends were strong and significantly decreasing (pre: $C = .71$; $p < .01$; post: $C = .67$; $p < .01$). For the index finger AD, no significant trend was observed during the first day of training either at the pre- or post-TMS phases; similarly, no significant trend was observed the last day of the training. On the contrary,

both the overall trends were significantly decreasing (pre: $C = .68$; $p < .01$; post: $C = .58$; $p < .01$). Finally, only the overall trends were significantly decreasing when considering the distance between the wrist and the ring finger (pre: $C = .82$; $p < .01$; post: $C = .84$; $p < .01$). When considering the control participant, data from day 1 were discarded due to a technical problem. Results showed no significant overall trend when the middle finger, the index finger, and the ring finger were moved. Such stable trends were observed in both the pre-TMS and post-TMS phases.

4.1.2. Task 2: Reach-to-Grasp Task. Several variables were considered during task 2. For such variables, the analysis was conducted by referring to the data collected throughout the five days of training before (pre) and after (post) the TMS stimulation. The results obtained from the selected kinematic variables in MD participant are reported as follows.

Movement time: A significantly decreasing trend was observed for the measures collected both pre-rTMS stimulation ($C = .73$; $p < .01$) and post-rTMS stimulation ($C = .62$; $p < .01$).

Maximum grip aperture: A significantly increasing trend was observed for the measures collected before the stimulation ($C = .64$; $p < .01$). No significant trend was observed for the measures collected after the rTMS ($C = .30$; n.s.).

Time of maximum grip aperture: Two clearly and significantly decreasing trends were observed for this variable. The first one involved the measures collected before the rTMS ($C = .79$; $p < .01$), while the second one involved the measures collected after the stimulation ($C = .62$; $p < .01$).

Time to maximum grip velocity: A clearly significant decreasing trend was observed for the data series collected before the TMS ($C = .72$; $p < .01$). The trend observed for the data series collected after the stimulation was significant, although more noisy ($C = .43$; $p < .01$).

Time of maximum wrist height: A significantly decreasing trend was observed at both the pre-rTMS ($C = .74$; $p < .01$) and the post-rTMS ($C = .69$; $p < .01$) phases.

Time of maximum wrist deceleration: With respect to this variable, a significant although very noisy decreasing trend was observed at both the pre-TMS measures ($C = .49$; $p < .01$) and the post-TMS ones ($C = .50$; $p < .01$).

Delay grasping: A significant decreasing trend was observed for this variable for the measures collected both pre-rTMS stimulation ($C = .57$; $p < .01$) and post-rTMS stimulation ($C = .57$; $p < .01$).

Figure 5 displays the trend of the pointwise delta computed for the main variables measured in task 2. It is noticeable the increase of the negative difference between the pre and the post measures during the first day of training, while an increase in the positive difference between the same values is observed during the second day of training. After these days, the difference tends to remain stable.

As concerns the control participant, no trend resulted statistically significant ($p_s > 0.05$). Figure 6 displays together the trends for the MD patient and the control participant. By the figure, it is clearly seen the difference of the two trends in the movement time variable. Similar results were observed for the remaining variables of task 2.

4.2. Neurophysiological Measures. No significant trend was observed in motor threshold at rest before (rMT pre) and after (rMT post) rTMS 1 Hz stimulation for either the MD ($C = .07$; n.s.; see Table 1) or the control ($C = .17$; n.s.; see Table 1) participant.

5. Conclusions

We set out to investigate neural plasticity in a professional guitarist affected by MD through a multimethodological paradigm. To this end, we combined spTMS, low-frequency rTMS, and 3D motion analysis. Results showed that although rTMS on M1 partially modulated resting motor threshold, a systematic normalization of various kinematic indexes during the 5-day treatment occurred for the MD participant. In particular, as concerns abduction independence, a significant increase in the distance between the dystonia-affected finger and the index and ring fingers was observed on the first day of training during the post-TMS session. The trend significantly increased throughout the five days, showing an overall increase of the distance between the fingers. These data were further confirmed by the distance between the affected finger and the wrist: a decreasing distance (abduction degree) was observed both on the first day of training during the post-TMS session and throughout the treatment's period. These results point to the presence of both a short-term and a long-term trend in the affected finger and not to a general effect of practice.

As regards the reach-to-grasp task, an increase in general motor coordination was hypothesized for the MD participant throughout the five days of training. No significant trend was instead expected for the control participant, since there was no room for improvement (ceiling effect). Results showed an increase in motor coordination only for the MD participant, as indexed by a significant decrease in the movement time. In terms of the reaching component, the time of maximum wrist height and the time of maximum wrist deceleration were anticipated, in line with previous studies demonstrating a significant anticipation when an object is approached more carefully (e.g., [41, 42]). For the grasping component, the amplitude of the maximum grip aperture revealed an increasing pattern of accuracy—as indexed by an appropriate finger scaling—throughout the 5-day training. The time of maximum grip aperture, the time of maximum grip velocity, and the delay grasping were anticipated as well as for the reaching parameters, indicating a temporal coupling between the reaching and the grasping components. These results are consistent with human literature suggesting that task constraints can modulate the proximal and distal components of a coordinated action. The failure to reduce variability as the target is being approached calls for coordination strategies amongst components, which might serve to partially dissipate errors [43].

An intriguing hypothesis points to a malfunctioning in the parietal-premotor pathway of dystonic patients [44]. Parietal-premotor connections are specialized for specific tasks, for example, reach-to-grasp movements, having separate pathways for each of the two components (i.e., reaching and grasping; [45]). Thus, a task-specific deficit

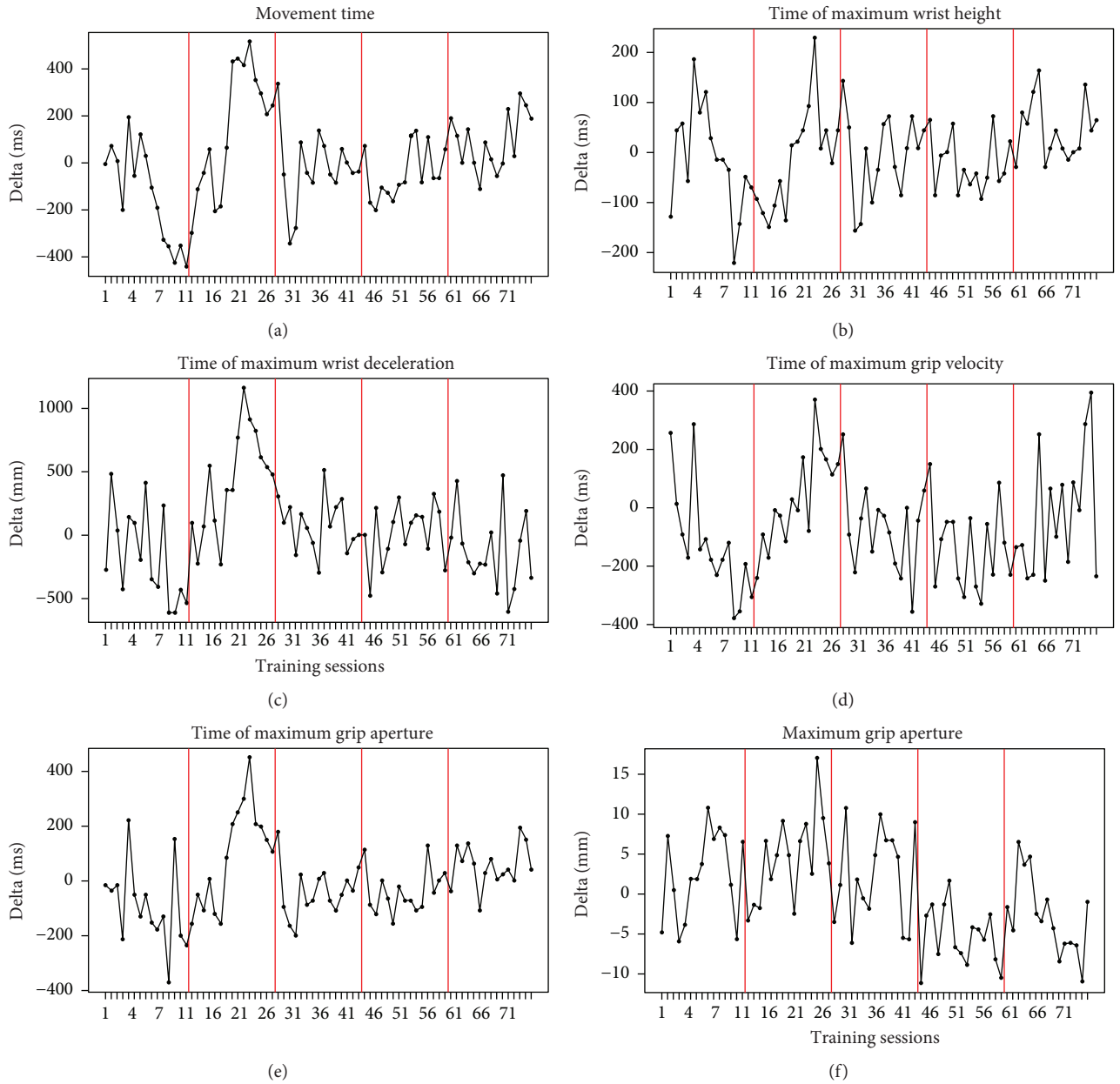

Figure 5: Pointwise delta between the measures, for the main variables of task 2, obtained at pre- and post-rTMS phases by the MD patient. Parameters referring to the reaching component are listed on (a), (b), and (c), whereas parameters for the grasping component are displayed on (d), (e), and (f).

could arise from the combination of excessive motor repetition of a particular task, together with disordered control of neural plasticity in the pathway where that specific task was learned [2]. Based on this hypothesis, we might suggest that future behavioral interventions should be based on restoring specific motor pathways through plasticity processes [22].

Notably, an initial positive outcome was observed during the post-TMS session of day 1, when all the parameters jointly showed a significant improvement. This effect, however, was neutralized and reversed during the post-TMS session of day 2, which was then followed by a stabilization phase for the remaining three days. The convergent oscillation of all these parameters seems to indicate that rTMS inhibitory stimulation might be beneficial in the very short term, but it provides a stable advantage only in the course of a 5-day training. This result might suggest that it takes many days of intervention to rebalance motor activity.

Overall, these results suggest that kinematic assessments of abduction independence, abduction degree, and reaching and grasping components are useful parameters for objective quantification of MD before and after training. Moreover, the reach-to-grasp task might allow studying situations similar to those participants facing in their daily life motor activities. This points to the effectiveness of assessing kinematics in conjunction with individual clinical scores such as the Arm

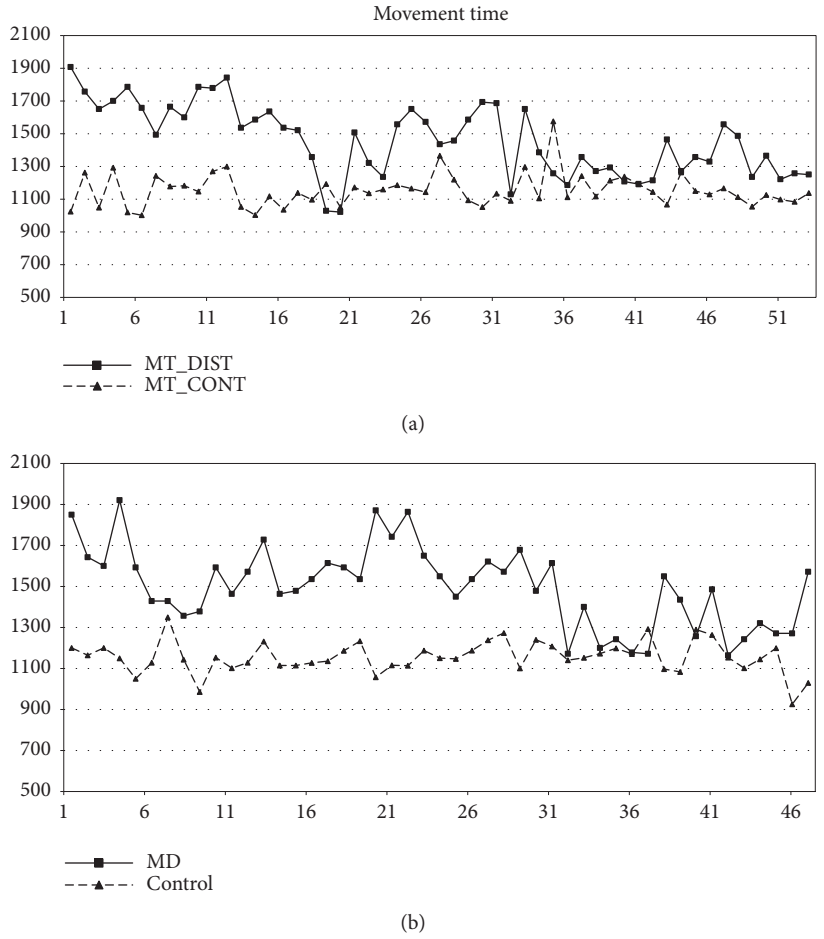

Figure 6: MD and control participant trends on the movement time (task 2).

Table 1: Resting motor threshold variations throughout the five-day protocol, before (rMT pre) and after (rMT post) the rTMS 1 Hz stimulation at the 90 percent of the rMT.

		Day 1	Day 2	Day 3	Day 4	Day 5
MD	rMT pre	43	43	43	44	44
	rMT post	46	44	46	46	46
Control	rMT pre	43	50	44	52	42
	rMT post	48	60	50	53	56

Dystonia Disability Scale (ADDS). Although they probe different aspects of motor impairment and might not correlate with each other [46], they should both be used to supplement the clinical diagnosis for monitoring the treatment and to assess the effectiveness of rehabilitation.

In neural terms, no trend was observed when considering rMT. This is a counterintuitive—though not rare—output. Veugen and colleagues [47] recently found that inhibition of the overactive dorsal premotor cortex partially recovered dystonic symptomatology despite having no influence on surround inhibition (i.e., the mechanism in the motor system which focuses neuronal activity to select the execution of the desired movement; [48]), as indexed by MEP sizes. In particular, stimulation improved writing performance in patients, though there was no significant effect on rMT in either dystonic or control participants.

In this respect, the study described here highlights the importance of evaluating brain stimulation outcomes in a more systematic way, beyond classical measures of neural plasticity such as MEP size. The cause of MD is obscure, but a loss of inhibition in the central nervous system and a loss of the normal regulation of plasticity are classically reported [49–51]. Plasticity generally refers to the ability of the nervous system to change the effectiveness of transmission in neural circuits [3]. An increase of sensory and motor finger representations in musicians is usually described as an adaptive plastic change to conform to the new needs. However, when this change develops too far, brain plasticity might shift from a benefit to a maladaptive mechanism [52]. On the basis of this abnormal plasticity hypothesis, new treatment protocols have been designed aimed at the redifferentiation of the disturbed hand representations. Here, we propose a new procedure to investigate affected muscle activations in individuals with neurologic motor disorders after plastic changes induced by rTMS.

This line of intervention holds several advantages over pharmacologic therapy (e.g., injections of botulinum toxin into the intrinsic arm/hand muscles): It is safe and effective, as demonstrated by kinematic analysis, and there is no risk of impairing movement in adjacent fingers. Moreover, it

can be applied to patients unresponsive to a variety of commonly used medical treatments. Noninvasive brain stimulation can transiently normalize corticospinal excitability to the affected muscles and can improve the degree of motor coordination over time. Objective quantifications of this treatment can be experimentally obtained with EMG and 3D movement analysis, paving the way for developing novel evaluation tools to optimize therapeutic strategies for motor disorders.

As the rehabilitation research in limb dystonia develops, it will be relevant to investigate comparative effectiveness of interventions to understand which approach holds the most promise.

The present results could support three future research aims:

(i) To develop an effective diagnostic tool based on neurophysiologic and behavioral measures for early identification of patients and for quantifying changes in symptoms

(ii) To investigate how dystonia affects the parietal-premotor pathway (reaching and grasping components)

(iii) To determine the best frequency and duration for interventions and after effects following rehabilitation.

A limit of the present study is the small sample adopted. However, according to Kimberley and colleagues [23, 53], studies in this field should utilize robust small *n* methodology such as single subject experimental design studies with repeated measures that allows for detailed analysis of within subject variability. Needless to say that definitive statements cannot yet be made regarding efficacy of this paradigm. Randomized controlled measurements are essential for future studies to compare different outcomes with similar frequency and duration.

Identifying the motor dynamics underlying this disorder will be helpful for moving forward both in diagnosis and in treatment, to optimize therapeutic outcomes. Since the available medical approaches are only moderately effective, preventing dystonia is just as much important.

We argue that an enhanced understanding of how neural plasticity can be assessed in FDH affected patients will provide helpful insights for designing more effective patient-tailored therapies based on noninvasive brain stimulation and for evaluating different treatment approaches.

Data Availability

All related data are included within the article or will be made available upon request.

Conflicts of Interest

The authors declare that there is no conflict of interest regarding the publication of this paper.

Acknowledgments

This work was supported by the Progetto Strategico, Università di Padova (N. 2010XPMFW4) to Umberto Castiello and by the SIR (Scientific Independence of Young Researchers) grant (N. RBSI141QKX) to Luisa Sartori. The authors would like to thank Dr. Paolo Fuschi for his precious advice.

References

[1] E. Altenmüller and H.-C. Jabusch, "Focal dystonia in musicians: phenomenology, pathophysiology and triggering factors," *European Journal of Neurology.*, vol. 17, pp. 31–36, 2010.

[2] S. Pirio Richardson, E. Altenmüller, K. Alter et al., "Research priorities in limb and task-specific dystonias," *Frontiers in Neurology*, vol. 8, p. 170, 2017.

[3] A. Quartarone, H. R. Siebner, and J. C. Rothwell, "Task-specific hand dystonia: can too much plasticity be bad for you?," *Trends in Neurosciences.*, vol. 29, no. 4, pp. 192–199, 2006.

[4] D. Ruge, S. Tisch, M. I. Hariz et al., "Deep brain stimulation effects in dystonia: time course of electrophysiological changes in early treatment," *Movement Disorders*, vol. 26, no. 10, pp. 1913–1921, 2011.

[5] A. Quartarone, S. Bagnato, V. Rizzo et al., "Abnormal associative plasticity of the human motor cortex in writer's cramp," *Brain*, vol. 126, no. 12, pp. 2586–2596, 2003.

[6] A. Quartarone, V. Rizzo, S. Bagnato et al., "Homeostatic-like plasticity of the primary motor hand area is impaired in focal hand dystonia," *Brain*, vol. 128, no. 8, pp. 1943–1950, 2005.

[7] A. Berardelli, J. C. Rothwell, M. Hallett, P. D. Thompson, M. Manfredi, and C. D. Marsden, "The pathophysiology of primary dystonia," *Brain*, vol. 121, no. 7, pp. 1195–1212, 1998.

[8] J. Pujol, J. Roset-Llobet, D. Rosinés-Cubells et al., "Brain cortical activation during guitar-induced hand dystonia studied by functional MRI," *NeuroImage*, vol. 12, no. 3, pp. 257–267, 2000.

[9] W. Bara-Jimenez, M. J. Catalan, M. Hallett, and C. Gerloff, "Abnormal somatosensory homunculus in dystonia of the hand," *Annals of Neurology*, vol. 44, no. 5, pp. 828–831, 1998.

[10] T. Elbert, V. Candia, E. Altenmüller et al., "Alteration of digital representations in somatosensory cortex in focal hand dystonia," *Neuroreport*, vol. 9, no. 16, pp. 3571–3575, 1998.

[11] M. L. Byrnes, G. W. Thickbroom, S. A. Wilson et al., "The corticomotor representation of upper limb muscles in writer's cramp and changes following botulinum toxin injection," *Brain*, vol. 121, no. 5, pp. 977–988, 1998.

[12] M. Sommer, D. Ruge, F. Tergau, W. Beuche, E. Altenmüller, and W. Paulus, "Intracortical excitability in the hand motor representation in hand dystonia and blepharospasm," *Movement Disorders*, vol. 17, no. 5, pp. 1017–1025, 2002.

[13] C. Pantev, A. Engelien, V. Candia, and T. Elbert, "Representational cortex in musicians," *Annals of the New York Academy of Sciences*, vol. 930, no. 1, pp. 300–314, 2001.

[14] A. Pascual-Leone, "The brain that plays music and is changed by it," *Annals of the New York Academy of Sciences*, vol. 930, no. 1, pp. 315–329, 2001.

[15] J. Konczak and G. Abbruzzese, "Focal dystonia in musicians: linking motor symptoms to somatosensory dysfunction," *Frontiers in Human Neuroscience*, vol. 7, p. 297, 2013.

[16] E. Altenmüller, "Focal dystonia: advances in brain imaging and understanding of fine motor control in musicians," *Hand Clinics*, vol. 19, no. 3, pp. 523–538, 2003.

[17] T. Elbert, C. Pantev, C. Wienbruch, B. Rockstroh, and E. Taub, "Increased cortical representation of the fingers of the left hand in string players," *Science*, vol. 270, no. 5234, pp. 305–307, 1995.

[18] E. Altenmüller, V. Baur, A. Hofmann, V. K. Lim, and H.-C. Jabusch, "Musician's cramp as manifestation of maladaptive brain plasticity: arguments from instrumental differences," *Annals of the New York Academy of Sciences*, vol. 1252, no. 1, pp. 259–265, 2012.

[19] S. J. Frucht, "Evaluating the musician with dystonia of the upper limb: a practical approach with video demonstration," *Journal of Clinical Movement Disorders*, vol. 2, no. 1, p. 16, 2015.

[20] N. N. Byl and A. McKenzie, "Treatment effectiveness for patients with a history of repetitive hand use and focal hand dystonia: a planned, prospective follow-up study," *Journal of Hand Therapy*, vol. 13, no. 4, pp. 289–301, 2000.

[21] H.-C. Jabusch and E. Altenmüller, "Three-dimensional movement analysis as a promising tool for treatment evaluation of musicians' dystonia," *Advances in Neurology*, vol. 94, pp. 239–245, 2004.

[22] F. Cogiamanian, S. Barbieri, and A. Priori, "Novel nonpharmacologic perspectives for the treatment of task-specific focal hand dystonia," *Journal of Hand Therapy*, vol. 22, no. 2, pp. 156–162, 2009.

[23] T. J. Kimberley, R. L. S. Schmidt, M. Chen, D. D. Dykstra, and C. M. Buetefisch, "Mixed effectiveness of rTMS and retraining in the treatment of focal hand dystonia," *Frontiers in Human Neuroscience*, vol. 9, p. 385, 2015.

[24] Y.-Z. Huang, C.-S. Lu, J. C. Rothwell et al., "Modulation of the disturbed motor network in dystonia by multisession suppression of premotor cortex," *PLoS One*, vol. 7, no. 10, article e47574, 2012.

[25] H. R. Siebner, J. M. Tormos, A. O. Ceballos-Baumann et al., "Low-frequency repetitive transcranial magnetic stimulation of the motor cortex in writer's cramp," *Neurology*, vol. 52, no. 3, pp. 529–537, 1999.

[26] H. R. Siebner, C. Auer, and B. Conrad, "Abnormal increase in the corticomotor output to the affected hand during repetitive transcranial magnetic stimulation of the primary motor cortex in patients with writer's cramp," *Neuroscience Letters*, vol. 262, no. 2, pp. 133–136, 1999.

[27] H. Siebner and J. Rothwell, "Transcranial magnetic stimulation: new insights into representational cortical plasticity," *Experimental Brain Research*, vol. 148, no. 1, pp. 1–16, 2003.

[28] H. R. Siebner, N. Lang, V. Rizzo et al., "Preconditioning of low-frequency repetitive transcranial magnetic stimulation with transcranial direct current stimulation: evidence for homeostatic plasticity in the human motor cortex," *The Journal of Neuroscience*, vol. 24, no. 13, pp. 3379–3385, 2004.

[29] M. Borich, S. Arora, and T. J. Kimberley, "Lasting effects of repeated rTMS application in focal hand dystonia," *Restorative Neurology and Neuroscience*, vol. 27, no. 1, pp. 55–65, 2009.

[30] N. Murase, J. C. Rothwell, R. Kaji et al., "Subthreshold low-frequency repetitive transcranial magnetic stimulation over the premotor cortex modulates writer's cramp," *Brain*, vol. 128, no. 1, pp. 104–115, 2005.

[31] A. S. Schneider, B. Baur, W. Fürholzer, I. Jasper, C. Marquardt, and J. Hermsdörfer, "Writing kinematics and pen forces in writer's cramp: effects of task and clinical subtype," *Clinical Neurophysiology*, vol. 121, no. 11, pp. 1898–1907, 2010.

[32] M. Jeannerod, "The timing of natural prehension movements," *Journal of Motor Behavior*, vol. 16, no. 3, pp. 235–254, 1984.

[33] D. A. Nowak and J. Hermsdörfer, "Coordination of grip and load forces during vertical point-to-point movements with a grasped object in Parkinson's disease," *Behavioral Neuroscience*, vol. 116, no. 5, pp. 837–850, 2002.

[34] D. A. Nowak and J. Hermsdörfer, "Grip force behavior during object manipulation in neurological disorders: toward an objective evaluation of manual performance deficits," *Movement Disorders*, vol. 20, no. 1, pp. 11–25, 2005.

[35] D. A. Nowak and J. Hermsdörfer, "Objective evaluation of manual performance deficits in neurological movement disorders," *Brain Research Reviews*, vol. 51, no. 1, pp. 108–124, 2006.

[36] J. P. Basil-Neto, L. G. Cohen, M. Panizza, J. Nilsson, B. J. Roth, and M. Hallett, "Optimal focal transcranial magnetic activation of the human motor cortex: effects of coil orientation, shape of the induced current pulse, and stimulus intensity," *Journal of Clinical Neurophysiology*, vol. 9, no. 1, pp. 132–136, 1992.

[37] K. R. Mills, S. J. Boniface, and M. Schubert, "Magnetic brain stimulation with a double coil: the importance of coil orientation," *Electroencephalography and Clinical Neurophysiology/Evoked Potentials Section*, vol. 85, no. 1, pp. 17–21, 1992.

[38] P. M. Rossini, A. T. Barker, A. Berardelli et al., "Non-invasive electrical and magnetic stimulation of the brain, spinal cord and roots: basic principles and procedures for routine clinical application. Report of an IFCN committee," *Electroencephalography and Clinical Neurophysiology*, vol. 91, no. 2, pp. 79–92, 1994.

[39] R Core Team, R: A, *Language and Environment for Statistical Computing*, R Foundation for Statistical Computing, Vienna, Austria, 2014.

[40] L. C. Young, "On randomness in ordered sequences," *The Annals of Mathematical Statistics*, vol. 12, no. 3, pp. 293–300, 1941.

[41] C. Armbrüster and W. Spijkers, "Movement planning in prehension: do intended actions influence the initial reach and grasp movement?," *Motor Control*, vol. 10, no. 4, pp. 311–329, 2006.

[42] A. Schuboe, A. Maldonado, S. Stork, and M. Beetz, "Subsequent actions influence motor control parameters of a current grasping action," in *RO-MAN 2008 - The 17th IEEE International Symposium on Robot and Human Interactive Communication*, pp. 389–394, Munich, Germany, August 2008.

[43] A. M. Wing, A. Turton, and C. Fraser, "Grasp size and accuracy of approach in reaching," *Journal of Motor Behavior*, vol. 18, no. 3, pp. 245–260, 1986.

[44] C. Gallea, S. G. Horovitz, M. 'Ali Najee-Ullah, and M. Hallett, "Impairment of a parieto-premotor network specialized for handwriting in writer's cramp," *Human Brain Mapping*, vol. 37, no. 12, pp. 4363–4375, 2016.

[45] C. Cavina-Pratesi, S. Monaco, P. Fattori et al., "Functional magnetic resonance imaging reveals the neural substrates of arm transport and grip formation in reach-to-grasp actions in humans," *The Journal of Neuroscience*, vol. 30, no. 31, pp. 10306–10323, 2010.

[46] K. E. Zeuner, M. Peller, A. Knutzen et al., "How to assess motor impairment in writer's cramp," *Movement Disorders*, vol. 22, no. 8, pp. 1102–1109, 2007.

[47] L. C. Veugen, B. S. Hoffland, D. F. Stegeman, and B. P. van de Warrenburg, "Inhibition of the dorsal premotor cortex does not repair surround inhibition in writer's cramp patients," *Experimental Brain Research*, vol. 225, no. 1, pp. 85–92, 2013.

[48] S. Beck, S. P. Richardson, E. A. Shamim, N. Dang, M. Schubert, and M. Hallett, "Short intracortical and surround inhibition are selectively reduced during movement initiation in focal hand dystonia," *The Journal of Neuroscience*, vol. 28, no. 41, pp. 10363–10369, 2008.

[49] A. Quartarone and M. Hallett, "Emerging concepts in the physiological basis of dystonia," *Movement Disorders*, vol. 28, no. 7, pp. 958–967, 2013.

[50] P. T. Lin and M. Hallett, "The pathophysiology of focal hand dystonia," *Journal of Hand Therapy*, vol. 22, no. 2, pp. 109–114, 2009.

[51] M. Herrojo Ruiz, P. Senghaas, M. Grossbach et al., "Defective inhibition and inter-regional phase synchronization in pianists with musician's dystonia: an EEG study," *Human Brain Mapping*, vol. 30, no. 8, pp. 2689–2700, 2009.

[52] T. F. Münte, E. Altenmüller, and L. Jäncke, "The musician's brain as a model of neuroplasticity," *Nature Reviews Neuroscience*, vol. 3, no. 6, pp. 473–478, 2002.

[53] T. J. Kimberley and R. P. D. Fabio, "Visualizing the effects of rTMS in a patient sample: small N vs. group level analysis," *PLoS One*, vol. 5, no. 12, article e15155, 2010.

Hindawi
Neural Plasticity
Volume 2018, Article ID 3524960, 14 pages
https://doi.org/10.1155/2018/3524960

Research Article

Laterality of Poststroke Cortical Motor Activity during Action Observation Is Related to Hemispheric Dominance

Sook-Lei Liew[1], **Kathleen A. Garrison**[2], **Kaori L. Ito**[1], **Panthea Heydari**[1], **Mona Sobhani**[1], **Julie Werner**[3,4], **Hanna Damasio**[1], **Carolee J. Winstein**[1], **and Lisa Aziz-Zadeh**[1]

[1]*University of Southern California, Los Angeles, CA, USA*
[2]*Yale University, New Haven, CT, USA*
[3]*California State University, Dominguez Hills, Carson, CA, USA*
[4]*Children's Hospital Los Angeles, Los Angeles, CA, USA*

Correspondence should be addressed to Sook-Lei Liew; sliew@usc.edu

Received 24 February 2018; Revised 5 April 2018; Accepted 19 April 2018; Published 28 May 2018

Academic Editor: Toshiyuki Fujiwara

Background. Increased activity in the lesioned hemisphere has been related to improved poststroke motor recovery. However, the role of the dominant hemisphere—and its relationship to activity in the lesioned hemisphere—has not been widely explored. *Objective.* Here, we examined whether the dominant hemisphere drives the lateralization of brain activity after stroke and whether this changes based on if the lesioned hemisphere is the dominant hemisphere or not. *Methods.* We used fMRI to compare cortical motor activity in the action observation network (AON), motor-related regions that are active both during the observation and execution of an action, in 36 left hemisphere dominant individuals. Twelve individuals had nondominant, right hemisphere stroke, twelve had dominant, left-hemisphere stroke, and twelve were healthy age-matched controls. We previously found that individuals with left dominant stroke show greater ipsilesional activity during action observation. Here, we examined if individuals with nondominant, right hemisphere stroke also showed greater lateralized activity in the ipsilesional, right hemisphere or in the dominant, left hemisphere and compared these results with those of individuals with dominant, left hemisphere stroke. *Results.* We found that individuals with right hemisphere stroke showed greater activity in the dominant, left hemisphere, rather than the ipsilesional, right hemisphere. This left-lateralized pattern matched that of individuals with left, dominant hemisphere stroke, and both stroke groups differed from the age-matched control group. *Conclusions.* These findings suggest that action observation is lateralized to the dominant, rather than ipsilesional, hemisphere, which may reflect an interaction between the lesioned hemisphere and the dominant hemisphere in driving lateralization of brain activity after stroke. Hemispheric dominance and laterality should be carefully considered when characterizing poststroke neural activity.

1. Introduction

Despite intensive research and clinical efforts, stroke remains a leading cause of physical disability worldwide [1], and there is an urgent need for improved poststroke rehabilitation strategies. Many studies have suggested that increased levels of activity in the ipsilesional hemisphere after stroke are associated with enhanced recovery [2–4]. Functional magnetic resonance imaging (fMRI) studies in individuals with stroke suggest that greater blood oxygen level-dependent (BOLD) activity in the contralateral (ipsilesional) hemisphere during a task with the impaired upper limb—a pattern consistent with typical motor control—is associated with better motor outcomes [4–6]. Poststroke therapeutic techniques have therefore aimed at promoting motor recovery by increasing activity in the ipsilesional hemisphere and decreasing activity in the contralesional hemisphere [7–10]. However, poststroke motor

outcomes using such approaches remain variable, suggesting that other factors influence recovery beyond the level of brain activity in the ipsilesional hemisphere.

One factor that has been largely overlooked in stroke studies is the role of motor dominance relative to the lesioned hemisphere. Studies often discuss findings related to the ipsilesional or contralesional hemisphere, without distinguishing whether the ipsilesional hemisphere is the dominant or nondominant hemisphere prior to stroke. However, whether stroke occurs in the dominant or nondominant hemisphere can impact recovery in multiple ways, including impacting the pattern of brain activity achieved in poststroke therapy [11–13]. Research has shown clear hemispheric differences in the specialization of motor control, with differences in the performance of motor actions after stroke related to the lesioned hemisphere. Winstein and Pohl (1995) reported that individuals with left hemisphere stroke showed deficits in open-loop, motor planning aspects of movement, whereas individuals with right hemisphere stroke showed deficits in closed-loop, feedback-based aspects of movement [14]. Another study showed that in an arm-reaching task, individuals with left hemisphere stroke had difficulty controlling the direction of movement, whereas individuals with right hemisphere stroke had a tendency to overshoot their targets [11]. These studies and others suggest that there is hemispheric specialization in a distributed motor control scheme, where the left hemisphere is responsible for optimizing and predicting dynamic aspects of movement, and the right hemisphere is responsible for movement accuracy and stability [15]. There are thus likely differences in task-related brain activity depending on the dominance of the lesioned hemisphere. Better understanding the relationship between motor dominance, hemisphere of stroke, and brain activity is critical because it could enable greater personalization of interventions in stroke neurorehabilitation and allow us to better understand the neural mechanisms underlying deficits following stroke.

Here, we hypothesized that the motor dominant hemisphere might in fact drive poststroke brain activity during action observation more strongly than the side of the stroke lesion. We specifically evaluated brain activity in the action observation network (AON), as it is a brain network typically engaged through both the observation and performance of actions and is comprised of cortical motor regions in the premotor and parietal cortices [16]. Importantly, activity in the AON can be elicited simply through action observation, so even individuals with moderate to severe upper arm paresis can complete the task. Action observation therapy (AOT), in which individuals with stroke observe another person performing actions (e.g., through videos) before or during actual physical practice of those actions, has been proposed as a way to enhance the effects of occupational or physical therapy [17–20]. Behavioral studies examining outcomes of AOT with occupational or physical therapy show modest improvements in poststroke motor recovery when compared to traditional therapy alone [17–19, 21, 22]. Researchers hypothesize that action observation may enhance plasticity in the same motor pathways responsible for action execution [23]. The AON has also been shown to be active during action observation in individuals after stroke [24]. In particular, activity in the AON was found to be lateralized to the ipsilesional, dominant hemisphere in individuals with motor dominant, left hemisphere stroke who observed actions being performed by the counterpart to their own paretic right arm [24]. However, since the left hemisphere was both the ipsilesional and motor dominant hemisphere, it was not possible to distinguish whether action observation drives activity in the ipsilesional hemisphere or in the motor dominant hemisphere.

The present study was designed with a primary aim of improving our understanding of the effects of motor dominance versus side of lesion on AON activity in individuals after stroke. We recruited individuals who were left hemisphere dominant (right handed) prior to stroke and had nondominant, right hemisphere stroke. Using the same fMRI protocol as in the earlier AON stroke study [24], we tested whether individuals with nondominant right hemisphere stroke had greater AON activity during action observation in the ipsilesional (right) hemisphere or in the dominant (left) hemisphere. We compared these data to the dominant left hemisphere stroke group and an age-matched control group from the earlier study [24]. We predicted that if action observation drives activity in the ipsilesional hemisphere, the right hemisphere stroke group should show greater activity in the right hemisphere, whereas if action observation drives activity in the motor dominant hemisphere, the right hemisphere stroke group should show greater activity in the left hemisphere.

2. Methods

2.1. Subjects. The current analysis included 36 individuals who were right-handed (left hemisphere motor dominant) as determined by the Edinburgh Handedness Inventory [25]. There were 24 participants with chronic stroke and moderate-to-severe upper extremity motor impairments and 12 nondisabled, age-matched controls. Both the nondisabled controls and 12 individuals with dominant left hemisphere stroke were included in an earlier study [24]. In the current study, 12 additional individuals with nondominant right hemisphere stroke were recruited from community centers. All participants gave informed consent in accordance with institutional guidelines approved by the University of Southern California Institutional Review Board. All individuals were right handed (prior to stroke), had normal or corrected-to-normal vision, and were safe for MRI. Additional inclusion criteria for individuals with stroke was chronic (>3 months since stroke onset), middle cerebral artery stroke, with no prior history of stroke, moderate-to-severe upper extremity impairment as determined by a phone screening form in which participants indicated difficulty moving their hand or arm for functional tasks, and no apraxia. For all participants, mean age (including nondisabled controls) was 63 ± 13 years and did not differ between groups ($F(2, 33) = 0.94$, $p = 0.40$). For participants with stroke, average time since stroke was 80 ± 58 months and did not differ between right and left

Table 1: Demographics of participants. Fugl-Meyer Assessment, Upper Extremity (FMA-UE; out of 66 points) and Wolf Motor Function Test (WMFT; out of 5 points). Stroke location was characterized as either internal capsule only (IC) or internal capsule plus cerebral cortex (C + IC). "–" indicates missing values.

Subject number	FMA-UE	WMFT	Age (years)	Sex	Time since stroke (months)	Location
			Right hemisphere stroke			
1	5	1	66	F	80	IC
2	17	1	65	F	22	IC
3	10	1	70	M	202	C + IC
4	8	1	59	F	46	C + IC
5	14	—	79	M	168	C + IC
6	16	2	56	F	6	IC
7	18	1.5	52	M	67	IC
8	31	1	33	M	10	C + IC
9	5	0	61	M	118	C + IC
10	31	3.25	71	M	74	IC
11	5	0	65	M	48	IC
12	18	1.25	35	F	21	IC
Mean	**14.83**	**1.18**	**59.33**	**5** F	**71.83**	**7 IC**
SDEV	9.09	0.90	13.81		62.43	
			Left hemisphere stroke			
1	48	3.33	64	F	60	IC
2	13	0.5	64	F	180	C + IC
3	46	3.25	55	M	48	IC
4	18	2	74	M	204	IC
5	40	2	39	M	24	IC
6	13	0.67	73	M	48	IC
7	31	2.5	85	F	96	IC
8	14	0.25	51	F	72	C + IC
9	47	3.33	74	F	108	C + IC
10	15	0.75	68	F	72	C + IC
11	37	2.5	71	M	96	C + IC
12	35	4	71	M	48	C + IC
Mean	**29.75**	**2.09**	**65.75**	**6** F	**88.00**	**6 IC**
SDEV	14.29	1.28	12.34		54.47	

hemisphere stroke groups ($t(22) = -0.17$, $p = 0.61$). Stroke characteristics are described in Table 1.

2.2. fMRI Data Acquisition. All scanning was completed on the same 3T Siemens Trio MRI scanner at the University of Southern California Dornsife Neuroimaging Center, using the scan parameters and task as described in Garrison et al. [24]. Functional images were acquired with a T2*-weighted gradient echo sequence (repetition time [TR]/echo time [TE] = 2000/30 ms, 37 slices, voxel size 3.5 mm isotropic voxels, and flip angle 90°); anatomical images were acquired with a T1-weighted magnetization-prepared rapid gradient-echo (MPRAGE) sequence (TR/TE = 2350/3.09 ms, 208 1 mm slices, 256 × 256 mm, and flip angle 10°).

The fMRI paradigm was a block design in which participants either observed either videos of right hand actions, videos of left hand actions, and images of a still hand (control condition) or rested. For the action observation conditions, videos depicted a mean-age-matched nondisabled control actor grasp objects with either their right hand or their left hand, as previously described [24]. Actions were adapted from the Wolf Motor Function Test (WMFT, Wolf et al. [26]) and included (1) pick up pencil, (2) pick up paperclip, (3) stack checkers, and (4) flip cards (see Supplementary Figure S1 for an example). Each video was 3 s long, and each block consisted of four videos shown in a randomized order for a total block length of 12 s. The control condition (observation of a still hand) was also presented in 12 s blocks with 4 still images of either a left or a right hand shown for 3 s each in a randomized order. All blocks were repeated 15 times and randomized across three 6-minute runs.

Participants were instructed to remain still and watch the actions of the actor as they would be asked to imitate each action after the scanning session. To ensure attention,

participants were asked questions about the videos at the end of each run (e.g., "In the last video you saw, which hand did the actor use?").

2.3. fMRI Analysis

2.3.1. Preprocessing and Analyses. Functional neuroimaging data analysis was carried out using FEAT (FMRI Expert Analysis Tool) Version 6, part of FSL (FMRIB's Software Library, http://www.fmrib.ox.ac.uk/fsl). Registration to high-resolution structural and standard space images was carried out using FLIRT [27, 28]. The following preprocessing steps were applied: semimanual skull stripping of the anatomical image using BET [29], motion correction using MCFLIRT [27], automated nonbrain removal of the fMRI data using BET [29], spatial smoothing using a Gaussian kernel of FWHM 5 mm, grand-mean intensity normalization of the entire 4D dataset by a single multiplicative factor, and high-pass temporal filtering (Gaussian-weighted least-squares straight line fitting, with sigma = 50 s). For each subject, a time-series statistical analysis was carried out using FILM GLM with local autocorrelation correction [30]. These Z (Gaussianized T/F) statistic images were then thresholded using clusters determined by $Z > 3.1$ and a (corrected) cluster significance threshold of $p < 0.05$ [31]. A second-level analysis for each subject was conducted, averaged across the three runs, and carried out using a fixed-effects model by forcing the random-effects variance to zero in FLAME (FMRIB's Local Analysis of Mixed Effects) [32–34]. At the group level, analyses were completed using a mixed-effects model that included both fixed effects and random effects from cross session/subject variance in FLAME. Again, Z (Gaussianized T/F) statistic images were then thresholded using clusters determined by $Z > 3.1$ and a (corrected) cluster significance threshold of $p < 0.05$. Whole brain analyses examined main effects of right hand action observation, main effects of left hand action observation, and contrasts of right hand action observation versus left hand action observation and left hand action observation versus right hand observation.

An additional aim of the current study was to directly compare new data from the right hemisphere stroke group to the data from the left hemisphere stroke group and nondisabled control group from the earlier study [24]. In order to do this, we reanalyzed all of the earlier data using the preprocessing steps described above to ensure that the same, up-to-date analysis techniques were used in all cohorts.

2.3.2. Region of Interest Analyses. A priori regions of interest (ROIs) included regions of the human AON: inferior frontal gyrus pars opercularis (IFGop) and pars triangularis (IFGtri), the supramarginal gyrus (SMG), and the precentral gyrus (PC) [35]. ROIs were defined anatomically using the probabilistic Harvard-Oxford Atlas included in FSL, with a probability threshold of greater than 25% applied for each ROI. The percent signal change (% SC) within each ROI was extracted for each task condition and each participant using Featquery in FSL.

2.3.3. Laterality Index. A laterality index (LI) was calculated to measure lateralization of brain activity during observation of each hand (right, left) for each group (nondisabled control, right hemisphere stroke, and left hemisphere stroke). LI was calculated as the proportion of active voxels in the left versus right ROI averaged across multiple thresholds [36, 37]. We calculated LI using the proportion of active voxels, rather than percent signal change, based on previous work suggesting that this approach is more robust for lesioned brains (Jansen et al. [37]). The cluster tool in FSL was used to set the different threshold values ($Z = 1.0, 1.5, 2.3$); Fslstats was used to determine the number of active voxels. LI was calculated using the classic formula

$$\mathrm{LI} = \frac{(\mathrm{left} - \mathrm{right})}{(\mathrm{left} + \mathrm{right})} \quad (1)$$

at each Z-threshold for each ROI [37], where LI is equal to left hemisphere activity minus right hemisphere activity divided by left hemisphere activity plus right hemisphere activity. The average of the three LIs at different Z-values was then calculated. LI scores range from +1 (all left hemisphere activation only) to −1 (all right hemisphere activation only) and were categorized as either bilateral ($|\mathrm{LI}| \leq 0.1$), hemisphere dominant ($0.1 < |\mathrm{LI}| < 0.2$), or hemisphere lateralized ($|\mathrm{LI}| \geq 0.2$) [37]. Following previous work, the LI and standard error of the mean (SEM) are reported [24]. The complete LI values for each group at each threshold/ROI can be found in Supplementary Table 5 and for each individual at each threshold/ROI in Supplementary Tables 6–9.

2.3.4. ROI-Based Task by Hemisphere by Group Interactions. A three-way ANOVA was carried out in SPSS 22 (IBM Corp., Armonk, NY, USA) to determine the effects of hand observed (right, left), hemisphere of activity (right, left), and group (nondisabled control, right hemisphere stroke, and left hemisphere stroke) for each of our four regions of interest. We applied a Bonferroni correction for multiple comparisons. We also report any significant two-way interactions within the ANOVAs and subsequently tested for simple main effects where appropriate.

2.3.5. Lesion Analyses. Lesions were manually drawn by a trained research assistant following a detailed lesion tracing protocol [38, 39] using MRIcron [40]. Lesion masks were then smoothed using a 2 mm Gaussian kernel. For each subject, a small mask was manually created in the healthy white matter tissue of the contralesional hemisphere. The white matter mask was used to determine the mean and standard deviation of healthy white matter voxel intensities within each subject's anatomical image using fslstats. Each subject's anatomical image was then thresholded at one standard deviation away from the mean white matter intensity, such that voxels with a signal intensity within or above the normal range would be excluded from the final lesion mask. Finally, the volume of the lesion was calculated using fslstats. An independent-sample t-test was conducted to compare lesion size between the right hemisphere stroke group and the left hemisphere stroke group. For each ROI, Pearson product-moment correlations were tested between lesion size and LI for that ROI, for each stroke group.

2.3.6. Percent of Lesion Overlap with ROIs. To examine the percent of lesion overlap with each ROI, each individual's binarized lesion mask was normalized to standard space and masked with each ROI using fslmaths. The number of voxels in the overlapping area was obtained using fslstats. The number of voxels in the overlapping area was then divided by the total number of voxels within the ROI to calculate the percent of overlap between the lesion and the ROI for each subject.

2.4. Behavioral Assessments. Immediately after the scanning session, participants completed a series of behavioral assessments. Due to the small sample size, behavioral correlations with fMRI data were used as secondary, exploratory analyses. Participants were administered the Wolf Motor Function Test (WMFT) to test the function of the upper extremity in the motor domain [26]. Performance on the WMFT was videotaped and scored by a trained, blinded research assistant for a Functional Ability Scale (FAS) score, ranging from 0 to 5, where 0 = does not attempt movement and 5 = movement is normal. Individuals were also assessed with the Fugl-Meyer Assessment, Upper Extremity (FMA-UE) [41], a measure of poststroke motor impairment. Behavioral assessments were performed by graduate research assistants who were trained in the administration of both the WMFT and FMA-UE assessments.

For each ROI, Spearman's rho correlations were tested between ROI activity and motor scores for the WMFT and FMA-UE (both categorical variables) in SPSS 22. We note that these results are exploratory and report results, noting that correcting for multiple comparisons across ROIs results in a corrected p value of $p = 0.00625$ ($p = 0.05$ divided by 8 comparisons).

3. Results

In the current study, we aimed to understand whether individuals with nondominant right hemisphere stroke showed greater ipsilesional right hemisphere activity or greater motor dominant left hemisphere activity during action observation. In order to better generalize our findings, we also compared the nondominant right hemisphere stroke group with a dominant left hemisphere stroke group and a nondisabled control group from our earlier study [24].

3.1. Between-Group Behavioral Comparisons. Individuals with right hemisphere stroke had significantly lower Fugl-Meyer scores than individuals with left hemisphere stroke had ($t(22) = -0.67$, $p = 0.02$), indicating greater poststroke motor impairments of the upper extremity in the right hemisphere stroke group. Fugl-Meyer scores are reported in Table 1. Similarly, on the WMFT, individuals with right hemisphere stroke showed a trend towards lower FAS scores ($t(21) = 1.94$, $p = 0.06$) than did individuals with left hemisphere stroke, again indicating poorer motor performance. WMFT scores are reported in Table 1, along with all participant demographics.

3.2. Whole-Brain fMRI Analyses. Notably, overall, patterns of brain activity during right and left hand action observation were similar between right and left hemisphere stroke groups, despite the groups having motor impairments in opposite hands. Contrasts of right versus left hand action observation, and vice versa, showed similar patterns in the stroke groups and a different pattern in the nondisabled group.

3.2.1. Right Hemisphere Stroke Group. For the right hemisphere stroke group, during *right (corresponding to nonparetic) hand action observation*, activity was found in the left premotor cortex, bilateral precentral gyri, bilateral superior parietal lobules, and bilateral occipital cortices, among other areas (Figure 1; Supplementary Table 1). During *left (corresponding to paretic) hand action observation*, activity was again found in the left supramarginal gyrus, bilateral precentral gyri, bilateral superior parietal lobules, and bilateral occipital cortices (Figure 1; Supplementary Table 2).

Comparing right and left hand action observation directly revealed the following: *Right* versus *left hand action observation* recruited greater activity in the left postcentral gyrus and superior parietal lobule and the right occipital pole. *Left* versus *right hand action observation* more strongly activated the right occipital pole and intracalcarine cortex (Figure 2; Supplementary Tables 3–4).

3.2.2. Left Hemisphere Stroke Group. Despite our reanalysis using a more stringent threshold, for the left hemisphere stroke group, we find results consistent with the findings reported in Garrison et al. [24]. During *right (corresponding to paretic) hand action observation*, activity was found in the left premotor cortex, bilateral precentral gyri, bilateral supramarginal gyri, and bilateral occipital cortices, among other areas, with greater activity in the left hemisphere (Figure 1; Supplementary Table 1).

During *left (corresponding to nonparetic) hand action observation*, a sparser pattern of activity was found in the left supramarginal gyrus, bilateral precentral gyri, bilateral superior parietal lobules, and bilateral occipital cortices among other areas (Figure 1; Supplementary Table 2).

Comparing right and left hand action observation directly revealed the following: *Right* versus *left hand action observation* recruited greater activity in left precentral gyrus and left postcentral gyrus. *Left* versus *right hand action observation* recruited greater activity in right occipital and occipitotemporal regions (Figure 2; Supplementary Figure S2; Supplementary Tables 3–4).

3.2.3. Nondisabled Control Group. Again, consistent with the findings reported in Garrison et al. [24] for the nondisabled control group, during *right (dominant) hand action observation*, activity was found in the right inferior frontal gyrus, right dorsal premotor cortex, right precentral gyrus, bilateral postcentral gyri, bilateral parietal cortices, and bilateral occipital cortices (Figure 3; Supplementary Table 1).

During *left (nondominant) hand action observation*, there was a similar pattern of activity, with activation in the right inferior frontal gyrus, right dorsal premotor cortex, bilateral precentral gyri, bilateral postcentral gyri, bilateral parietal

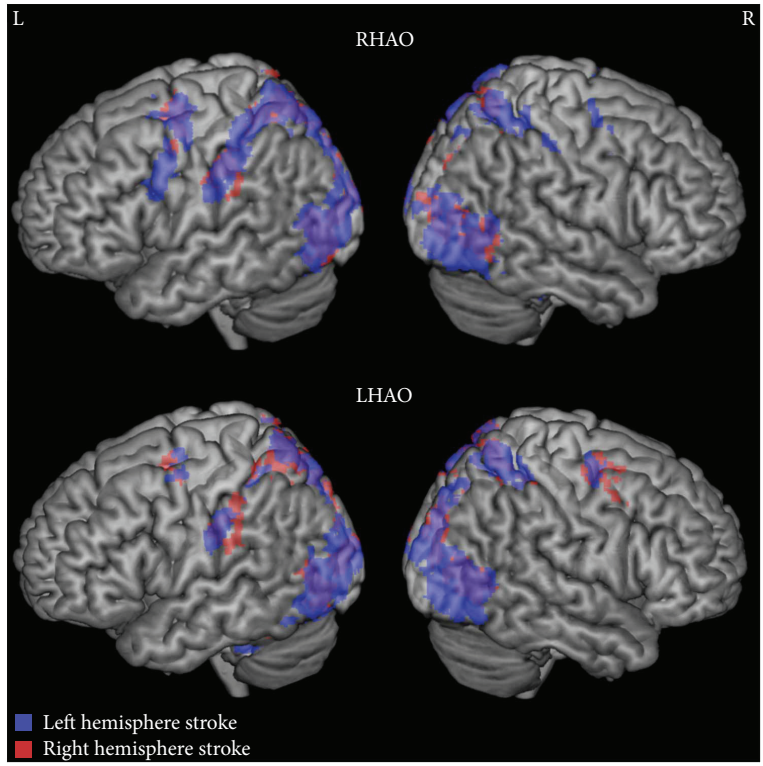

Figure 1: Whole brain activity during right and left action observation for individuals with stroke. While both stroke groups show bilateral activity during right and left hand action observation, activity in the left hemisphere was more extensive regardless of hemisphere of lesion. Top: right hand action observation (RHAO), bottom: left hand action observation (LHAO). Participants with left hemisphere stroke are represented in blue; participants with right hemisphere stroke are represented in red. Overlap between stroke groups is represented in purple. Thresholded at $Z > 3.1$, corrected for multiple comparisons at $p < 0.05$.

cortices, and bilateral occipital cortices, as well as the right posterior superior temporal sulcus at the temporoparietal junction (Figure 3; Supplementary Table 2).

Comparing right and left hand action observation directly revealed the following: *Right* versus *left hand action observation* revealed no significant activity (Figure 4; Supplementary Table 3). In contrast, *left* versus *right hand action observation* recruited more activity in the right hemisphere, particularly in the right postcentral gyrus, right superior parietal lobule, and right occipital cortex (Figure 4; Supplementary Table 4).

3.2.4. Interim Summary. Whole brain patterns in both stroke groups primarily showed greater left hemisphere activity during *right hand action observation*, while whole brain patterns in nondisabled controls were largely right lateralized during *left hand action observation*. Results here were reported at a relatively stringent threshold of $Z > 3.1$, cluster corrected at $p < 0.05$. Given our smaller group sample sizes and heterogeneity of lesion locations, we also wished to visualize this data at a more lenient threshold ($Z > 2.3$, cluster corrected at $p < 0.05$) to examine whether these laterality trends expanded. At this more lenient threshold, we found the same laterality patterns reported above, but they were extended to much wider regions of the AON (see Supplementary Figure S2).

3.3. Laterality Index. LI scores range from +1 (all left hemisphere activation only) to −1 (all right hemisphere activation only) and are typically categorized as either bilateral ($|LI| \leq 0.1$), hemisphere dominant ($0.1 < |LI| < 0.2$), or hemisphere lateralized ($|LI| \geq 0.2$; Jansen et al. [37]). Participants in both the right and left hemisphere stroke groups demonstrated a left hemisphere dominant/lateralized pattern of activation across ROIs during *right hand action observation*, independently of which limb was affected by stroke (Figure 5; Supplementary Tables 5–9). For participants with right hemisphere stroke, LI values were as follows: inferior frontal gyrus pars opercularis (LI = 0.33, SEM = 0.17), pars triangularis (LI = 0.16, SEM = 0.19), precentral gyrus (LI = 0.22, SEM = 0.09), and supramarginal gyrus (LI = 0.40, SEM = 0.08). For participants with left hemisphere stroke, LI values were as follows: inferior frontal gyrus pars opercularis (LI = 0.28, SEM = 0.17), pars triangularis (LI = 0.24, SEM = 0.21), precentral gyrus (LI = 0.15, SEM = 0.08), and supramarginal gyrus (LI = 0.32, SEM = 0.12).

Participants in both the right and left hemisphere stroke groups demonstrated a largely bilateral pattern of activation in most ROIs during *left hand action observation*, independent of the limb that was affected by stroke (Figure 5; Supplementary Tables 5–9). Participants with right hemisphere stroke showed bilateral results in the inferior frontal gyrus pars opercularis (LI = −0.10, SEM =

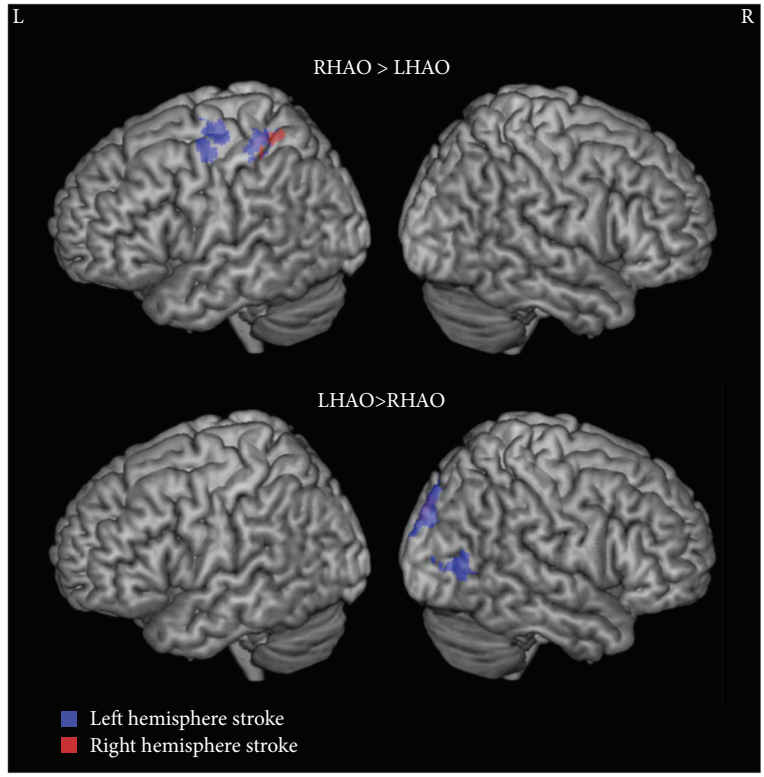

Figure 2: Whole brain activity contrasted between right and left action observation for individuals with stroke. Top: right hand action observation (RHAO) compared to left hand action observation (LHAO), bottom: Left hand action observation (LHAO) compared to right hand action observation (RHAO). Participants with left hemisphere stroke are represented in cool colors (blue); participants with right hemisphere stroke are represented in warm colors (red). Overlap between stroke groups is represented in purple. Thresholded at $Z > 3.1$, corrected for multiple comparisons at $p < 0.05$.

0.19), inferior frontal gyrus pars triangularis (LI = −0.08, SEM = 0.22), right hemisphere lateralization in the precentral gyrus (LI = −0.17, SEM = 0.10), and left hemisphere dominant in the supramarginal gyrus (LI = 0.21, SEM = 0.17). Participants with left hemisphere stroke showed bilateral results in the inferior frontal gyrus pars opercularis (LI = −0.05, SEM = 0.18), pars triangularis (LI = 0.01, SEM = 0.22), and supramarginal gyrus (LI = 0.07, SEM = 0.14) and right hemisphere lateralization in the precentral gyrus (LI = −0.23, SEM = 0.10; Figure 5; Supplementary Tables 5–9). We note that one difference in the LI pattern between stroke groups was that for the right hemisphere stroke group, activity in the supramarginal gyrus was left hemisphere dominant compared to bilateral in the left hemisphere stroke group.

For the nondisabled control group, regions in the AON demonstrated either right hemisphere dominant/lateralized or bilateral activity during both right and left hand action observation (Figure 5; Supplementary Tables 5–9). For *right hand action observation*, LI values are as follows: inferior frontal gyrus pars opercularis (LI = −0.15, SEM = 0.17), pars triangularis (LI = −0.21, SEM = 0.18), precentral gyrus (LI = −0.08, SEM = 0.11), and supramarginal gyrus (LI = −0.07, SEM = 0.14). For *left hand action observation*, LI values are as follows: inferior frontal gyrus pars opercularis (LI = −0.17, SEM = 0.14), pars triangularis (LI = −0.11, SEM = 0.12), precentral gyrus (LI = −0.15, SEM = 0.04), and supramarginal gyrus (LI = 0.05, SEM = 0.09). Importantly, the laterality patterns seen in the nondisabled control group, particularly for right hand action observation, differ from those of the two stroke groups.

3.4. Task by Hemisphere by Group Interactions in ROI Activity

3.4.1. Right Hemisphere Stroke Group versus Nondisabled Controls. No three-way interactions were found between group (nondisabled control, right hemisphere stroke), hand observed (right, left), and hemisphere of activity (right, left) for any ROI. A significant two-way interaction was found for group (nondisabled control versus right hemisphere stroke) and hemisphere of activity (right, left) in the supramarginal gyrus ($F(1, 22) = 7.17$, $p = 0.01$, partial $\eta^2 = 0.25$; Bonferroni-corrected p value: $p = 0.04$). We then tested for simple main effects. For hemisphere of activity, there was a statistically significant difference between the left and right SMG in the right hemisphere stroke group ($F(1, 23) = 13.14$, $p = 0.001$, partial $\eta^2 = 0.36$), with greater activity in the left compared to right hemisphere (mean ± standard deviation reported for all analyses; left hemisphere: 0.20 ± 0.16, right hemisphere: 0.10 ± 0.19). There were no

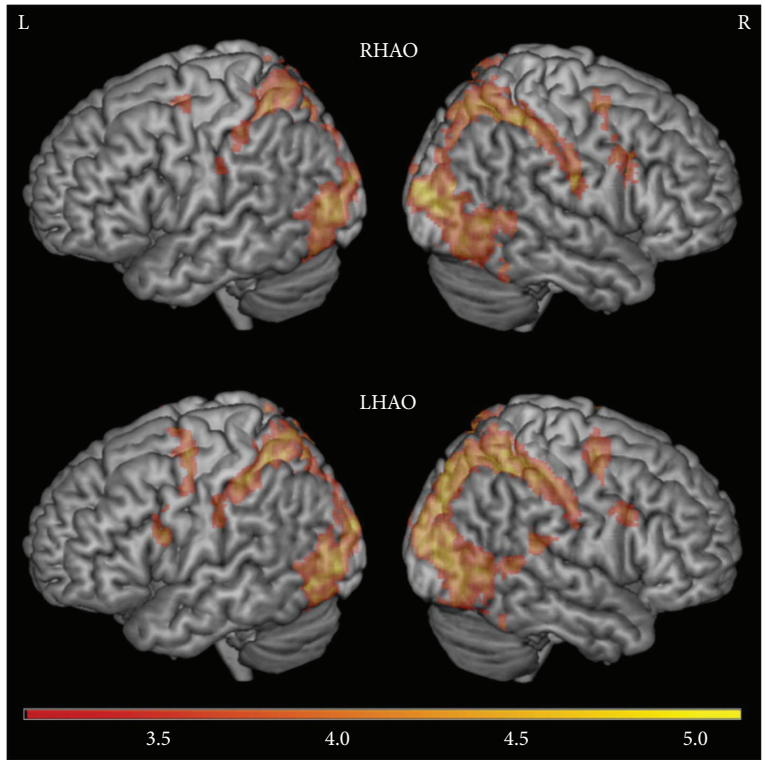

Figure 3: Whole brain activity during right and left action observation for the nondisabled control group. Unlike the two stroke groups, the nondisabled group did not show greater activity on the left hemisphere during right and left hand action observation. Top: right hand action observation (RHAO), bottom: left hand action observation (LHAO). Thresholded at $Z > 3.1$, corrected for multiple comparisons at $p < 0.05$.

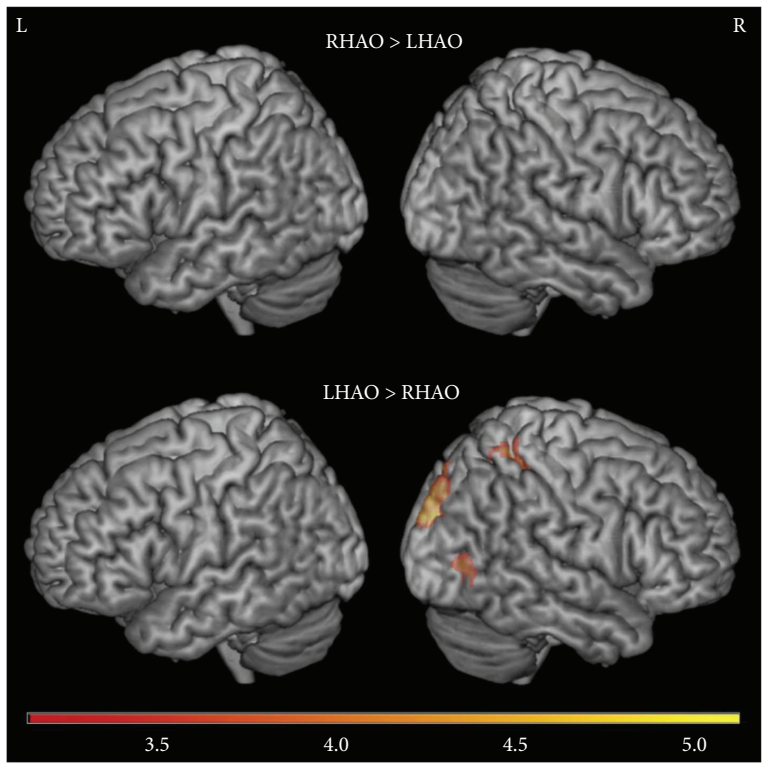

Figure 4: Whole brain activity contrasted between right and left action observation for the nondisabled control group. Top: right hand action observation (RHAO) compared to left hand action observation (LHAO), bottom: left hand action observation (LHAO) compared to right hand action observation (RHAO). Thresholded at $Z > 3.1$, corrected for multiple comparisons at $p < 0.05$.

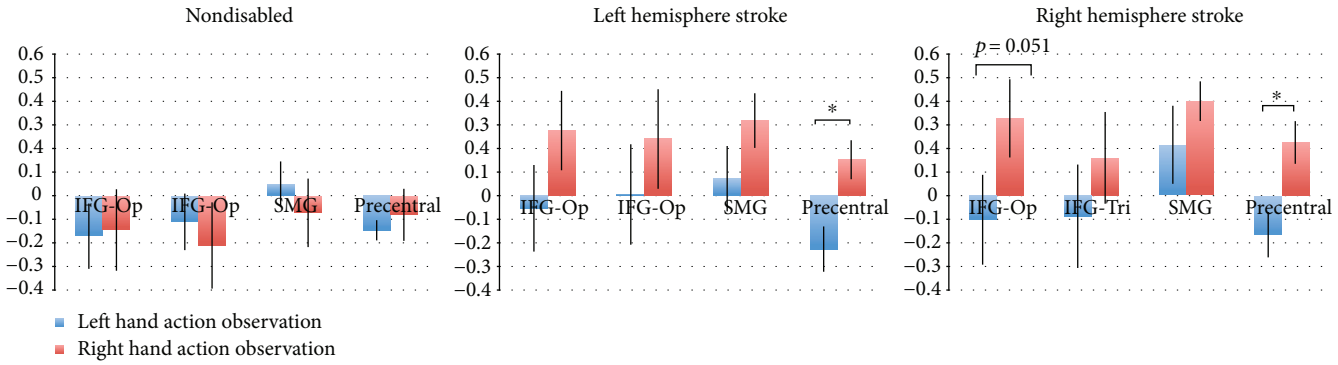

Figure 5: Laterality index in regions of interest. Left: nondisabled participants, middle: participants with left hemisphere stroke, right: participants with right hemisphere stroke; each during left hand (blue) and right hand (red) action observation; in the inferior frontal gyrus pars opercularis (IFG-Op), inferior frontal gyrus pars triangularis (IFG-Tri), supramarginal gyrus (SMG), and precentral gyrus (Precentral). $^*p < 0.05$. Positive values indicate left hemisphere laterality; negative values indicate right hemisphere laterality.

differences in left and right SMG activity in the ND group ($F(1, 23) = 2.35$, $p = 0.14$). For group, there was a statistically significant difference between groups in the right SMG ($F(1, 46) = 6.60$, $p = 0.01$, partial $\eta^2 = 0.13$), with greater activity for the nondisabled control group compared to the right hemisphere stroke group (nondisabled controls: 0.24 ± 0.19; right hemisphere stroke: 0.10 ± 0.19). No differences in activity were found between ND and RHS groups in the left SMG ($F(1, 46) = 0.04$, $p = 0.85$). Put together, this suggests that the nondisabled control group had more activity in the right compared left supramarginal gyrus, whereas the right hemisphere stroke group had more activity in the left compared to right supramarginal gyrus.

A significant two-way interaction was also found for the hemisphere of activity (right, left) and side of hand observed (right, left) in the precentral gyrus ($F(1, 22) = 14.78$, $p = 0.001$, partial $\eta^2 = 0.40$; Bonferroni-corrected p value: $p = 0.004$). We then tested for simple main effects. We did not find a simple main effect for hand observed (i.e., no difference in activity between right and left hand observation for either hemisphere (right hemisphere: $F(1, 23) = 0.19$, $p = 0.67$; left hemisphere: $F(1, 23) = 3.15$, $p = 0.09$)). We found a simple main effect of hemisphere of activity during right hand action observation, with greater activity in the left versus right precentral gyrus ($F(1, 23) = 7.3$, $p = 0.01$; left hemisphere: 0.09 ± 1.5, right hemisphere: 0.04 ± 0.13). Put another way, for both groups, during right hand action observation, activity was greater in the left precentral gyrus.

3.4.2. Right versus Left Hemisphere Stroke Group. We then compared the two stroke groups to one another directly. No three-way interactions were found between the side of the stroke (right, left), hand observed (right, left), and hemisphere of activity (right, left) in any ROI. A significant two-way interaction was found between the hemisphere of activity (right, left) and hand observed (right, left) in the precentral gyrus ($F(1, 22) = 18.73$, $p < 0.001$, partial $\eta^2 = 0.46$; Bonferroni-corrected p value: $p < 0.004$); this same interaction was also marginally significant in the inferior frontal gyrus pars opercularis after correcting for multiple comparisons ($F(1), 22 = 5.74$, $p = 0.025$, partial $\eta^2 = 0.21$; Bonferroni-corrected p value: $p = 0.1$). We then tested for simple main effects for each interaction. In the precentral gyrus, for effect of hand observed, there was a statistically significant difference in the left precentral gyrus, with greater activity during right hand action observation than during left hand action observation ($F(1, 23) = 13.78$, $p = 0.001$; partial $\eta^2 = 0.38$; left hand action observation: 0.01 ± 0.10, right hand action observation: 0.08 ± 0.11). There was no statistically significant main effect in the right precentral gyrus ($F(1, 23) = 0.37$, $p = 0.55$). For simple main effect of hemisphere of activity, there was a statistically significant difference during right hand action observation ($F(1, 23) = 11.27$, $p = 0.003$, partial $\eta^2 = 0.33$), with greater activity in the left compared to right precentral gyrus (left hemisphere: 0.08 ± 0.11, right hemisphere: 0.03 ± 0.13). There were no significant simple main effects for hemisphere during left hand action observation ($F(1, 23) = 3.14$, $p = 0.09$).

For the inferior frontal gyrus pars opercularis, we found a similar simple main effect for hand observed in the left hemisphere with greater activity during right hand action observation compared to left hand action observation ($F(1, 23) = 8.1$, $p = 0.009$, partial $\eta^2 = 0.26$; right hand action observation: 0.08 ± 0.14, left hand action observation: 0.02 ± 0.14). There were no simple main effects for hand observed in the right hemisphere ($F(1, 23) = 0.002$, $p = 0.97$) and no simple main effects for hemisphere during either right hand action observation ($F(1, 23) = 2.07$, $p = 0.16$) or left hand action observation ($F(1, 23) = 1.17$, $p = 0.29$). Overall, these results suggest there was more left hemisphere activity during *right hand action observation* for both stroke groups. Both stroke groups showed similar hemispheres by hand observed interactions, with brain activity lateralized toward the left motor dominant hemisphere, despite having lesions in different hemispheres.

3.5. Lesion Analyses

3.5.1. Lesion Volume Compared between Groups. No significant difference in lesion size was found between the

right hemisphere stroke group ($M = 35593.08\,\text{mm}^3$, SD = 55942.81) and the left hemisphere stroke group ($M = 23196.64\,\text{mm}^3$, SD = 33296.69; $t(22) = -0.660$, $p = 0.52$). This suggests that, despite varying lesion sizes across individuals, reported results were not driven by a difference in overall lesion size between groups. Lesion overlap maps can be found in Supplementary Material Figures S3–S7.

3.5.2. ROI-Lesion Overlap. Overlap between the individual lesions and the AON ROIs (measured as greater than 5% overlap) occurred in only 4 of the individuals in the left hemisphere stroke group and 3 of the individuals in the right hemisphere stroke group. While we had considered also examining the relationship between lesion overlap and laterality index, to examine whether lesion overlap with critical AON regions influenced laterality results, the resulting sample of individuals with lesion overlap was too limited to make an accurate calculation.

3.6. Brain Behavior Analyses. Finally, as an exploratory analysis, we examined correlations between ROI activity and motor scores.

3.6.1. Correlations between ROI Activity and WMFT FAS Scores. For participants with right hemisphere stroke, there were no significant correlations between WMFT motor scores and ROI activity. For participants with left hemisphere stroke, nonsignificant trends showing negative correlations between WMFT scores and ROI activity during right hand action observation were found in the inferior frontal gyrus, pars opercularis ($\rho = -0.51$, $p = 0.091$), and pars triangularis ($\rho = -0.534$, $p = 0.074$). In addition, trends in negative correlations between WFMT scores and ROI activity during left hand action observation were found in the right inferior frontal gyrus ($\rho = -0.545$, $p = 0.067$) and precentral gyrus ($\rho = -0.517$, $p = 0.085$). Notably, however, none of these relationships meets the significance threshold after correcting for multiple comparisons ($p = 0.00625$).

3.6.2. Correlations between ROI Activity and Fugl-Meyer Scores. For participants with right hemisphere stroke, no significant correlations were found between Fugl-Meyer scores and ROI activity. For participants with left hemisphere stroke, activity in the right precentral gyrus during right hand action observation demonstrated a trend towards a negative correlation with Fugl-Meyer scores ($\rho = -0.53$, $p = 0.077$), although this again was not significant.

4. Discussion

In this study, our primary aim was to examine whether cortical motor activity in the action observation network was lateralized more towards the ipsilesional hemisphere or the motor dominant hemisphere during action observation after a stroke. In both individuals with nondominant right hemisphere stroke and individuals with dominant left hemisphere stroke, AON activity was lateralized toward the left motor dominant hemisphere. There were no significant differences in the lateralization of AON activity between the two stroke groups, despite having lesions in different hemispheres. These results suggest that action observation after stroke may drive greater activity in the motor dominant rather than the ipsilesional hemisphere, at least in our sample of individuals who were right-handed prior to stroke. These findings also differed from our nondisabled control group, in which AON activity was either bilateral or slightly lateralized toward the right nondominant hemisphere.

As mentioned in the Introduction, hemispheric specialization could be an underlying cause of these results in stroke patients. That is, greater AON activity in the dominant left hemisphere may reflect hard-wired properties of the left hemisphere for motor control such as left hemisphere specialization for motor planning, and by extension, action observation, compared to the right hemisphere, regardless of which hemisphere is affected after stroke. This may mean that the motor dominant hemisphere may also play a role in the effectiveness of action observation therapy. While not tested here, it is possible that driving activity in the motor dominant hemisphere via action observation could help to promote motor recovery after stroke. Future studies could examine whether dominant hemisphere activation during action observation relates to changes in motor recovery following poststroke action observation therapy.

In addition, previous work has shown that the motor dominant hemisphere has greater descending motor pathways than the nondominant hemisphere has [42, 43]. Additionally, the typically motor dominant left precentral gyrus receives inputs from both the contralateral and ipsilateral hand, whereas the nondominant right precentral gyrus receives the majority of inputs solely from the contralateral left hand [44]. After a stroke, this imbalance in motor pathways may be accentuated to more strongly engage left-lateralized activity during right hand action observation and bilateral activity during left hand action observation. Likewise, individuals with dominant left hemisphere stroke have been shown to experience some motor deficits in both hands, whereas those with right hemisphere stroke typically only experience motor deficits in the contralateral left hand [45]. Again, while it remains to be tested in a future study, it is possible that individuals with nondominant right hemisphere stroke are able to continue to use their dominant (nonparetic) hand, and individuals with dominant left hemisphere stroke may place more emphasis on using their dominant (paretic) hand in spite of its impairments. Therefore, both groups may place greater emphasis on the dominant hand when asked to observe and later imitate actions, explaining the greater activation in the dominant left hemisphere in both groups.

Based on this logic, we might expect individuals with nondominant hand paresis to experience poorer motor recovery due to the ability to rely on the nonparetic dominant hand. Although results across studies vary, there is indeed evidence that individuals with right hemisphere stroke show poorer motor recovery of the affected nondominant left hand than those with left hemisphere stroke and an affected dominant right hand [46, 47]. Related, a limitation of the current study is the fact that the nondominant right hemisphere stroke group also had greater motor impairments (lower Fugl-Meyer and Wolf Motor Function Test scores) of the

affected hand than the dominant left hemisphere stroke group, despite both groups falling within the eligibility range of moderate-to-severe motor impairments and having no differences in lesion volumes. While this may be reflective of trends in the general stroke population, this difference does introduce a potential confound, as the level of impairment could also drive patterns of cortical activity. However, importantly, there was no significant relationship between the level of impairment and brain activity within the right hemisphere stroke group, suggesting that the level of impairment for individuals with right hemisphere stroke does not influence AON activity. Given the small sample size, we further visually inspected the subject-level correlation data between brain activity and motor impairment, in case there were potential trends that were not significant. However, there were no relationships or trends between level of motor impairment and brain activity across this sample, such that individuals with less severe stroke did not show any differences in laterality index than individuals with more severe stroke. This suggests that between-group differences in level of motor impairment did not drive these left-lateralized results. Regardless, further research with a larger sample of nondominant, right hemisphere stroke patients, with a wider range from mild to severe impairments, is needed to confirm these findings.

In addition, although both right and left hemisphere stroke groups had *stronger* activations in the left hemisphere during action observation, it should be noted that there was still significant activity observed in the right hemisphere in all groups, including the two stroke groups (see Figure 1; Tables S1 and S2). General whole brain activity during action observation was bilateral for all groups, and the lateralization results emerged primarily when examining the laterality index, which calculates a ratio of left to right hemisphere activity. Thus, while we emphasize the role of the dominant left hemisphere because AON activity examined using the laterality index calculation was lateralized to the dominant left hemisphere more in both stroke groups compared to the control group, there is likely also a role of right hemisphere activity for all groups during action observation.

Finally, in line with this, we note that the healthy, age-matched control group showed bilateral or slightly right-lateralized activity. Although this is in line with many previous studies showing that AON activity in healthy right-handed individuals is typically bilateral [35, 48, 49], a previous study specifically examining the laterality index in healthy individuals showed left-lateralized AON patterns [50]. In reconciling our current findings with the previous literature, we first note that in that study, the laterality index was performed on entire lobes (e.g., LI of the frontal lobe was left-lateralized) whereas here we calculated the LI within specific AON nodes. This specificity may have affected results. In addition, a primary factor that may contribute to these disparate results is age. The previous study examining the laterality index of the AON in healthy individuals used healthy younger adults, while in our study, we used healthy older adults (age-matched to our stroke population). Research has shown that older adults typically recruit additional and broader regions of the AON compared to younger adults [51–54]. While further research is needed to specifically examine the laterality of the AON in healthy younger versus older adults, it is possible that our healthy older adult control group shows more bilateral or slightly right-lateralized AON activity, instead of left-lateralized AON activity, due to age-related changes in the AON.

4.1. Limitations and Future Directions. Our results support the idea that hemispheric dominance affects patterns of neural activity induced by action observation after stroke. While the current sample size was small (12 participants per group), both right and left hemisphere stroke groups (24 participants in total) showed similar patterns of left-lateralized AON activity during observation of right hand actions and bilateral AON activity during observation of left hand actions, which was different from nondisabled individuals. However, as noted in the Discussion, the functional abilities of the two groups were significantly different. Notably, we did not find a relationship between the level of impairment and lateralization of AON activity within the right hemisphere group, suggesting that the differing functional levels were not associated with different brain activation patterns. However, we acknowledge that this group difference still provides a possible confounding factor as previous work has shown that degree of motor severity influences cortical recruitment [55]. In addition, previous work has shown that patients with greater corticospinal tract (CST) damage also show greater recruitment of cortical areas [56, 57]. Although lesion volumes were similar between groups, the current study did not specifically examine overlap of the lesion with the CST. Thus, a replication of these patterns in a larger, more diverse sample, with individuals across a range of motor impairment levels (mild, moderate, severe), and examining the overlap of the lesion with the CST, would improve our understanding of how the current findings relate to a diverse population of individuals after stroke.

Our findings support a possible specialization of the motor dominant hemisphere during action observation following stroke. However, the functional implications of this activation are unclear. An important question is whether and how these results, and recovery from nondominant (right hemisphere) stroke, may relate to real-world hand usage. Future studies might examine real-world hand usage during daily activities (e.g., using accelerometers [58, 59]), and relate that to laterality patterns in brain activity following stroke.

In addition, here we showed that action observation engages the motor dominant hemisphere in individuals who are right hemisphere dominant (left-handed) prior to stroke. Right hemisphere dominance is less common, and therefore, the population with stroke will be smaller and less is known about motor control in this group. However, given our findings' interpretations, we might expect AON activity to be lateralized toward the dominant right hemisphere in that group. A more complete understanding of the relationship between motor dominance, hemisphere of stroke, and AON activity should be studied to enable personalized interventions in stroke neurorehabilitation.

Finally, given the conventional wisdom that activity in the ipsilesional hemisphere promotes recovery of motor function after stroke [2–4], a logical next step is to evaluate what our findings may mean for stroke rehabilitation. Our findings, and those of others, suggest that optimal recovery of motor function may depend on the hemisphere of the lesion [20]. As such, parameters of AOT, such as whether individuals with stroke observe actions corresponding to their paretic limb only, versus observation of bilateral movements, may yield different results for different participants. While few stroke neuroimaging studies have been adequately powered to compare between right and left hemisphere stroke groups, it may be a critical difference that affects stroke rehabilitation and motor recovery. Future large-scale studies should examine whether and how the hemispheric dominance of the lesioned hemisphere affects neural activity during different types of therapy and subsequent motor recovery.

Data Availability

The authors are happy to share their data. However, due to IRB regulations, the authors may share only deidentified subsets of the data from this study upon request.

Disclosure

The contents of the study are solely the responsibility of the author and do not necessarily represent the official views of the NIH.

Conflicts of Interest

The authors have no conflicts of interest to declare.

Acknowledgments

The authors thank the research participants and Alicia Johnson and Matthew Konersman, DPT, for their contributions. This work was supported by the American Heart Association (10SDG3510062, 14CRP18200010, and 16IRG26960017), the National Institute on Drug Abuse (K12DA00167), the National Institutes of Health, Eunice Kennedy Shriver National Institute of Child Health and Human Development (R03HD067475 and K01HD091283), the National Institutes of Health (NIH) National Institute of Neurological Disorders and Stroke (NINDS) Intramural Competitive Fellowship Award, and the NIH Rehabilitation Research Career Development Program Grant K12 (HD055929).

Supplementary Materials

Figure S1: Example from video stimuli during fMRI. Figure S2: Whole brain activity contrasted between right and left action observation compared between stroke and control groups at a more lenient threshold. Figure S3: Lesion overlap heat map (whole group). Figure S4: Lesion overlap heat map for cortical left hemisphere strokes ($n = 6$). Figure S5: Lesion overlap heat map for subcortical left hemisphere strokes ($n = 6$). Figure S6: Lesion overlap heat map for cortical right hemisphere stroke ($n = 5$). Figure S7: Lesion overlap heat map for subcortical right hemisphere stroke ($n = 7$). Table S1: Main effect of right hand action observation. Table S2: Main effect of left hand action observation. Table S3: Brain activity during right hand action observation versus left hand action observation (RHAO > LHAO). Table S4: Brain activity during left hand action observation versus right hand action observation (LHAO > RHAO). Table S5: Group laterality index values. Table S6: Individual laterality index values—inferior frontal gyrus and pars opercularis. Table S7: Individual laterality index values—inferior frontal gyrus and pars triangularis. Table S8: Individual laterality index values—supramarginal gyrus. Table S9: Individual laterality index values—precentral gyrus. *(Supplementary Materials)*

References

[1] D. Mozaffarian, E. J. Benjamin, A. S. Go et al., "Heart disease and stroke statistics-2016 update a report from the American Heart Association," *Circulation*, vol. 133, no. 4, pp. e38–e360, 2016.

[2] R. S. Marshall, G. M. Perera, R. M. Lazar, J. W. Krakauer, R. C. Constantine, and R. L. DeLaPaz, "Evolution of cortical activation during recovery from corticospinal tract infarction," *Stroke*, vol. 31, no. 3, pp. 656–661, 2000.

[3] R. J. Nudo, "Mechanisms for recovery of motor function following cortical damage," *Current Opinion in Neurobiology*, vol. 16, no. 6, pp. 638–644, 2006.

[4] N. S. Ward and L. G. Cohen, "Mechanisms underlying recovery of motor function after stroke," *Archives of Neurology*, vol. 61, no. 12, pp. 1844–1848, 2004.

[5] N. S. Ward, M. M. Brown, A. J. Thompson, and R. S. J. Frackowiak, "Neural correlates of outcome after stroke: a cross-sectional fMRI study," *Brain*, vol. 126, no. 6, pp. 1430–1448, 2003.

[6] K. J. Werhahn, A. B. Conforto, N. Kadom, M. Hallett, and L. G. Cohen, "Contribution of the ipsilateral motor cortex to recovery after chronic stroke," *Annals of Neurology*, vol. 54, no. 4, pp. 464–472, 2003.

[7] F. Fregni, P. S. Boggio, C. G. Mansur et al., "Transcranial direct current stimulation of the unaffected hemisphere in stroke patients," *Neuroreport*, vol. 16, no. 14, pp. 1551–1555, 2005.

[8] S.-L. Liew, E. Santarnecchi, E. R. Buch, and L. G. Cohen, "Non-invasive brain stimulation in neurorehabilitation: local and distant effects for motor recovery," *Frontiers in Human Neuroscience*, vol. 8, p. 77, 2014.

[9] R. Lindenberg, V. Renga, L. L. Zhu, D. Nair, and G. Schlaug, "Bihemispheric brain stimulation facilitates motor recovery in chronic stroke patients," *Neurology*, vol. 75, no. 24, pp. 2176–2184, 2010.

[10] N. Takeuchi, T. Chuma, Y. Matsuo, I. Watanabe, and K. Ikoma, "Repetitive transcranial magnetic stimulation of contralesional primary motor cortex improves hand function after stroke," *Stroke*, vol. 36, no. 12, pp. 2681–2686, 2005.

[11] S. Mani, P. K. Mutha, A. Przybyla, K. Y. Haaland, D. C. Good, and R. L. Sainburg, "Contralesional motor deficits after unilateral stroke reflect hemisphere-specific control mechanisms," *Brain*, vol. 136, no. 4, pp. 1288–1303, 2013.

[12] R. L. Sainburg and S. V. Duff, "Does motor lateralization have implications for stroke rehabilitation?," *Journal of*

Rehabilitation Research and Development, vol. 43, no. 3, pp. 311–322, 2006.

[13] S. Y. Schaefer, K. Y. Haaland, and R. L. Sainburg, "Ipsilesional motor deficits following stroke reflect hemispheric specializations for movement control," *Brain*, vol. 130, no. 8, pp. 2146–2158, 2007.

[14] C. J. Winstein and P. S. Pohl, "Effects of unilateral brain damage on the control of goal-directed hand movements," *Experimental Brain Research*, vol. 105, no. 1, pp. 163–174, 1995.

[15] V. Yadav and R. L. Sainburg, "Limb dominance results from asymmetries in predictive and impedance control mechanisms," *PLoS One*, vol. 9, no. 4, article e93892, 2014.

[16] G. Rizzolatti and L. Craighero, "The mirror-neuron system," *Annual Review of Neuroscience*, vol. 27, no. 1, pp. 169–192, 2004.

[17] P. Celnik, B. Webster, D. M. Glasser, and L. G. Cohen, "Effects of action observation on physical training after stroke," *Stroke*, vol. 39, no. 6, pp. 1814–1820, 2008.

[18] D. Ertelt, S. Small, A. Solodkin et al., "Action observation has a positive impact on rehabilitation of motor deficits after stroke," *NeuroImage*, vol. 36, pp. T164–T173, 2007.

[19] M. Franceschini, M. G. Ceravolo, M. Agosti et al., "Clinical relevance of action observation in upper-limb stroke rehabilitation: a possible role in recovery of functional dexterity. A randomized clinical trial," *Neurorehabilitation and Neural Repair*, vol. 26, no. 5, pp. 456–462, 2012.

[20] P. Sale, M. G. Ceravolo, and M. Franceschini, "Action observation therapy in the subacute phase promotes dexterity recovery in right-hemisphere stroke patients," *BioMed Research International*, vol. 2014, Article ID 457538, 7 pages, 2014.

[21] S. Sarasso, S. Määttä, F. Ferrarelli, R. Poryazova, G. Tononi, and S. L. Small, "Plastic changes following imitation-based speech and language therapy for aphasia: a high-density sleep EEG study," *Neurorehabilitation and Neural Repair*, vol. 28, no. 2, pp. 129–138, 2014.

[22] K. Sugg, S. Müller, C. Winstein, D. Hathorn, and A. Dempsey, "Does Action Observation Training with Immediate Physical Practice Improve Hemiparetic Upper-Limb Function in Chronic Stroke?," *Neurorehabilitation and Neural Repair*, vol. 29, no. 9, pp. 807–817, 2015.

[23] K. A. Garrison, C. J. Winstein, and L. Aziz-Zadeh, "The mirror neuron system: a neural substrate for methods in stroke rehabilitation," *Neurorehabilitation and Neural Repair*, vol. 24, no. 5, pp. 404–412, 2010.

[24] K. A. Garrison, L. Aziz-Zadeh, S. W. Wong, S. L. Liew, and C. J. Winstein, "Modulating the motor system by action observation after stroke," *Stroke*, vol. 44, no. 8, pp. 2247–2253, 2013.

[25] R. C. Oldfield, "The assessment and analysis of handedness: the Edinburgh inventory," *Neuropsychologia*, vol. 9, no. 1, pp. 97–113, 1971.

[26] S. L. Wolf, P. A. Catlin, M. Ellis, A. L. Archer, B. Morgan, and A. Piacentino, "Assessing Wolf motor function test as outcome measure for research in patients after stroke," *Stroke*, vol. 32, no. 7, pp. 1635–1639, 2001.

[27] M. Jenkinson, P. Bannister, M. Brady, and S. Smith, "Improved optimization for the robust and accurate linear registration and motion correction of brain images," *NeuroImage*, vol. 17, no. 2, pp. 825–841, 2002.

[28] M. Jenkinson and S. Smith, "A global optimisation method for robust affine registration of brain images," *Medical Image Analysis*, vol. 5, no. 2, pp. 143–156, 2001.

[29] S. M. Smith, "Fast robust automated brain extraction," *Human Brain Mapping*, vol. 17, no. 3, pp. 143–155, 2002.

[30] M. W. Woolrich, B. D. Ripley, M. Brady, and S. M. Smith, "Temporal autocorrelation in univariate linear modeling of FMRI data," *NeuroImage*, vol. 14, no. 6, pp. 1370–1386, 2001.

[31] K. J. Worsley, "Statistical analysis of activation images," *Functional Magnetic Resonance Imaging*, vol. 14, pp. 251–270, 2001.

[32] C. F. Beckmann, M. Jenkinson, and S. M. Smith, "General multilevel linear modeling for group analysis in FMRI," *NeuroImage*, vol. 20, no. 2, pp. 1052–1063, 2003.

[33] M. Woolrich, "Robust group analysis using outlier inference," *NeuroImage*, vol. 41, no. 2, pp. 286–301, 2008.

[34] M. W. Woolrich, T. E. J. Behrens, C. F. Beckmann, M. Jenkinson, and S. M. Smith, "Multilevel linear modelling for FMRI group analysis using Bayesian inference," *NeuroImage*, vol. 21, no. 4, pp. 1732–1747, 2004.

[35] S. Caspers, K. Zilles, A. R. Laird, and S. B. Eickhoff, "ALE meta-analysis of action observation and imitation in the human brain," *NeuroImage*, vol. 50, no. 3, pp. 1148–1167, 2010.

[36] K. L. Ito and S.-L. Liew, "Calculating the laterality index using FSL for stroke neuroimaging data," *GigaScience*, vol. 5, Supplement 1, pp. 14-15, 2016.

[37] A. Jansen, R. Menke, J. Sommer et al., "The assessment of hemispheric lateralization in functional MRI-robustness and reproducibility," *NeuroImage*, vol. 33, no. 1, pp. 204–217, 2006.

[38] J. D. Riley, V. le, L. der-Yeghiaian et al., "Anatomy of stroke injury predicts gains from therapy," *Stroke*, vol. 42, no. 2, pp. 421–426, 2011.

[39] S.-L. Liew, J. M. Anglin, N. W. Banks et al., "A large, open source dataset of stroke anatomical brain images and manual lesion segmentations," *Scientific Data*, vol. 5, article 180011, 2018.

[40] C. Rorden and M. Brett, "Stereotaxic display of brain lesions," *Behavioural Neurology*, vol. 12, no. 4, pp. 191–200, 2000.

[41] A. R. Fugl-Meyer, L. Jääskö, I. Leyman, S. Olsson, and S. Steglind, "The post-stroke hemiplegic patient. 1. A method for evaluation of physical performance," *Scandinavian Journal of Rehabilitation Medicine*, vol. 7, no. 1, pp. 13–31, 1975.

[42] G. Hammond, "Correlates of human handedness in primary motor cortex: a review and hypothesis," *Neuroscience & Biobehavioral Reviews*, vol. 26, no. 3, pp. 285–292, 2002.

[43] J. Rademacher, U. Bürgel, S. Geyer et al., "Variability and asymmetry in the human precentral motor system: a cytoarchitectonic and myeloarchitectonic brain mapping study," *Brain*, vol. 124, no. 11, pp. 2232–2258, 2001.

[44] S. Kim, J. Ashe, K. Hendrich et al., "Functional magnetic resonance imaging of motor cortex: hemispheric asymmetry and handedness," *Science*, vol. 261, no. 5121, pp. 615–617, 1993.

[45] K. Y. Haaland and D. L. Harrington, "Hemispheric asymmetry of movement," *Current Opinion in Neurobiology*, vol. 6, no. 6, pp. 796–800, 1996.

[46] J. E. Harris and J. J. Eng, "Individuals with the dominant hand affected following stroke demonstrate less impairment than those with the nondominant hand affected," *Neurorehabilitation and Neural Repair*, vol. 20, no. 3, pp. 380–389, 2006.

[47] J. E. Ween, M. P. Alexander, M. D'Esposito, and M. Roberts, "Factors predictive of stroke outcome in a rehabilitation setting," *Neurology*, vol. 47, no. 2, pp. 388–392, 1996.

[48] L. Aziz-Zadeh, L. Koski, E. Zaidel, J. Mazziotta, and M. Iacoboni, "Lateralization of the human mirror neuron system," *Journal of Neuroscience*, vol. 26, no. 11, pp. 2964–2970, 2006.

[49] L. Aziz-Zadeh, F. Maeda, E. Zaidel, J. Mazziotta, and M. Iacoboni, "Lateralization in motor facilitation during action observation: a TMS study," *Experimental Brain Research*, vol. 144, no. 1, pp. 127–131, 2002.

[50] M. Cabinio, V. Blasi, P. Borroni et al., "The shape of motor resonance: right- or left-handed?," *NeuroImage*, vol. 51, no. 1, pp. 313–323, 2010.

[51] M. C. Costello and E. K. Bloesch, "Are older adults less embodied? A review of age effects through the lens of embodied cognition," *Frontiers in Psychology*, vol. 8, p. 267, 2017.

[52] N. Diersch, K. Mueller, E. S. Cross, W. Stadler, M. Rieger, and S. Schütz-Bosbach, "Action prediction in younger versus older adults: neural correlates of motor familiarity," *PLoS One*, vol. 8, no. 5, article e64195, 2013.

[53] E. Kuehn, M. B. Perez-Lopez, N. Diersch, J. Döhler, T. Wolbers, and M. Riemer, "Embodiment in the aging mind," *Neuroscience & Biobehavioral Reviews*, vol. 86, no. 4, pp. 207–225, 2017.

[54] G. Léonard and F. Tremblay, "Corticomotor facilitation associated with observation, imagery and imitation of hand actions: a comparative study in young and old adults," *Experimental Brain Research*, vol. 177, no. 2, pp. 167–175, 2007.

[55] A. K. Rehme, G. R. Fink, D. Y. von Cramon, and C. Grefkes, "The role of the contralesional motor cortex for motor recovery in the early days after stroke assessed with longitudinal FMRI," *Cerebral Cortex*, vol. 21, no. 4, pp. 756–768, 2010.

[56] N. S. Ward, J. M. Newton, O. B. C. Swayne et al., "The relationship between brain activity and peak grip force is modulated by corticospinal system integrity after subcortical stroke," *European Journal of Neuroscience*, vol. 25, no. 6, pp. 1865–1873, 2007.

[57] N. S. Ward, J. M. Newton, O. B. C. Swayne et al., "Motor system activation after subcortical stroke depends on corticospinal system integrity," *Brain*, vol. 129, no. 3, pp. 809–819, 2006.

[58] R. R. Bailey, J. W. Klaesner, and C. E. Lang, "An accelerometry-based methodology for assessment of real-world bilateral upper extremity activity," *PLoS One*, vol. 9, no. 7, article e103135, 2014.

[59] C. E. Lang, J. M. Wagner, D. F. Edwards, and A. W. Dromerick, "Upper extremity use in people with hemiparesis in the first few weeks after stroke," *Journal of Neurologic Physical Therapy*, vol. 31, no. 2, pp. 56–63, 2007.

Hindawi
Neural Plasticity
Volume 2018, Article ID 3846593, 10 pages
https://doi.org/10.1155/2018/3846593

Review Article

State-of-the-Art Techniques to Causally Link Neural Plasticity to Functional Recovery in Experimental Stroke Research

Anna-Sophia Wahl [1,2,3]

[1]*Brain Research Institute, University of Zurich, Winterthurerstr. 190, 8057 Zurich, Switzerland*
[2]*Department of Health Sciences and Technology, ETH Zurich, Winterthurerstr. 190, 8057 Zurich, Switzerland*
[3]*Central Institute of Mental Health, University of Heidelberg, J5, 68159 Mannheim, Germany*

Correspondence should be addressed to Anna-Sophia Wahl; wahl@hifo.uzh.ch

Received 23 January 2018; Revised 12 April 2018; Accepted 2 May 2018; Published 27 May 2018

Academic Editor: Surjo R. Soekadar

Current experimental stroke research faces the same challenge as neuroscience: to transform correlative findings in causative ones. Research of recent years has shown the tremendous potential of the central nervous system to react to noxious stimuli such as a stroke: Increased plastic changes leading to reorganization in form of neuronal rewiring, neurogenesis, and synaptogenesis, accompanied by transcriptional and translational turnover in the affected cells, have been described both clinically and in experimental stroke research. However, only minor attempts have been made to connect distinct plastic remodeling processes as causative features for specific behavioral phenotypes. Here, we review current state-of the art techniques for the examination of cortical reorganization and for the manipulation of neuronal circuits as well as techniques which combine anatomical changes with molecular profiling. We provide the principles of the techniques together with studies in experimental stroke research which have already applied the described methodology. The tools discussed are useful to close the loop from our understanding of stroke pathology to the behavioral outcome and may allow discovering new targets for therapeutic approaches. The here presented methods open up new possibilities to assess the efficiency of rehabilitative strategies by understanding their external influence for intrinsic repair mechanisms on a neurobiological basis.

1. Introduction

Although huge efforts have been made in recent years, both by clinicians and basic researchers, we have still gained limited insights into a neurological disease such as stroke preventing us from developing specific cures and resulting in poor statistical numbers: Of 15 million people suffering from an ischemic brain attack every year, a third dies, a third remains permanently disabled, and a third recovers as the stroke itself has not been too devastating. On the clinical side, stroke units have been created, which combine experts in intensive care medicine, neurology, physiotherapy, and speech therapy, to accelerate and coordinate the diagnostic and therapeutical processes aiming at improving recovery rates for patients. According to the neurologists' saying "time is brain," even mobile units have been established to bring the hospital to the patient [1]. These efforts aim at increasing the number of patients being eligible for the only currently approved acute treatment—thrombolysis or thrombectomy—within a very early time window of 4.5 h after stroke [2, 3].

On the side of basic research, we study the neurobiology of stroke, but seem to be stuck in a "black box" situation: We have accumulated data showing the tremendous capacities of the brain to reorganize by synaptogenesis and even neurogenesis and by neuronal circuit rewiring and new circuit formation. We find cortical map shifts and hyperactive brain regions after stroke; we detect genetic and proteomic turnover within a distinct spatiotemporal profile and sequence of events [4]. However, only minor attempts have been made to transform pure correlative data into causative ones, which would enable a causal connection of plastic remodeling processes in the brain with distinct behavioral outcomes. Not only would this allow us to form a new understanding of the functional brain status after stroke, but also it opens up possibilities to develop and test the efficiency of new

therapeutic approaches. Today's basic stroke research is part of neuroscience that faces the challenges to first describe the broad morphological features, then study fine cellular and molecular events, find genes which are active in a specific neuron or cell type, and link it to the behavioral phenotype. But as the philosopher of science Karl Popper might have argued: Before we can provide answers, we need the power to ask new questions.

In recent years, new technology has been designed which is starting to fill the gap between correlative and causative research.

The aim of this review is to first discuss current state-of-the-art technology of experimental stroke research which enables a deeper understanding of neuronal reorganization and circuit formation. In the second part, techniques for distinct neuronal circuit manipulation are introduced which help to reveal causal relationships between anatomy and behavior. Finally, new approaches combining cytology with molecular profiles are provided which elucidate the underlying molecular mechanisms of neuronal rewiring and repair. The principles of the techniques are explained together with exemplary studies in experimental stroke research which have already applied the described methodology. The here discussed tools may not only enhance our understanding of stroke pathology but also help to identify crucial anchor points for new therapeutic interventions.

2. State-of-the-Art Techniques to Study Neuronal Reorganization and Circuit Formation after Experimental Stroke

2.1. Approaches to Examine Brain-Wide Remodeling. A classical approach to study reorganizational processes across the whole brain is functional resonance imaging (fMRI), allowing the monitoring of neuronal rewiring processes on a macroanatomical level within the same animal. However, although significant contributions to the understanding of the interplay between altered functional status and structural connectivity have been made in stroke models [5, 6] using this technique, the spatial and temporal resolution level remains low.

In contrast, intrinsic optical imaging sticks out by a high spatial resolution enabling the visualization of small domains within larger brain areas demonstrating the functional organization and the spatial relationships among those smaller domains, for example, in the barrel or visual cortex [7]. Intrinsic optical imaging uses the effect that more active brain tissue reflects less light than does less active tissue. Thus, the most active areas appear as the darkest ones. Optical imaging has been used to show disrupted functional connectivity in rodent mouse models of stroke [8, 9].

Another technique to study in particular sensory map shifts is millisecond-timescale voltage-sensitive dye (VSD) imaging which unlike functional fMRI and intrinsic optical signal imaging measures electrical activity with relatively high spatial and temporal resolution [10]. VSD imaging has recently been applied to measure spontaneous activity over large regions of the mouse cortex to reveal fast, complex, localized, and bilaterally synchronized patterns of depolarization [10]. In a study by Gosh et al. [11], VSD imaging was used to show the expansion of the forelimb sensory map towards parts of the hindlimb cortex after a large thoracic spinal cord injury, indicating incorporation of axotomized hindlimb neurons into sensory circuits of the forelimb. In another study by Brown et al. [12], the function of the sensorimotor cortex was visualized with VSD imaging. The mouse forelimb sensory cortex was targeted by stroke leading to a new sensory representation in the territory previously occupied by the forelimb motor cortex. VSD imaging revealed slower kinetics in remapped sensory circuits accompanied by high levels of dendritic spines as visualized with two-photon microscopy.

While VSD imaging was the first demonstration of wide-field optical imaging of neural activity [13], the necessity to apply VSDs prior to imaging, their very fast response time, and their very small signal ratios made them difficult to use. However, recent developments of exogenous and in particular genetically encoded fluorescent indicators of neuronal activity such as GCaMP and YC-Nano have revolutionized the targeted expression of fluorescence with much higher signal levels. And even transgenetic lines exist [14]. Furthermore, recent work has shown that the dynamics of flavoprotein fluorescence can be optically mapped in wild-type CNS tissue as an indicator of oxidative metabolism [15, 16], which might be also a useful tool in experimental stroke research. As wide-field neuroimaging methods are also relatively easily combined with optogenetics to modify brain activity in the behaving animal, studies have been conducted using camera-based "mesoscopic" optical recording of neuronal activity examining a large part of the cortical surface. These mesoscopic optical recordings became possible by extensive chronic window implantations [17] and improved high-speed sensitive camera technology. Vanni et al. [18] measured cortical functional connectivity using wide-field imaging in lightly anesthetized GCaMP3 mice and correlated calcium signals recoded in the primary sensory cortex to the other sensorimotor areas bilaterally. The coactivation of areas was interpreted as an indication that areas might be functionally connected. However, a final proof for a functional connection, shutting-off correlated areas, was missing in this study. Balbi et al. [19] used the same approach in awake GCaMP6 mice studying mososcopic functional connectivity longitudinally in a microinfarct model.

That wide-field calcium imaging might be also a powerful tool to study brain-wide cortical reorganization on a high-resolution level over time in animals monitoring their rehabilitative courses or recording rehabilitative training after stroke was demonstrated by Murphy et al. [20]. His lab presented a home cage system, where mice could initiate mesoscopic functional imaging by themselves over days being unsupervised.

2.2. Methods to Understand Regional Reorganization. Intracortical microstimulation (ICMS) and surface stimulation with electrode arrays have been used for many years to map cortical regions, to study cortical reorganization, and to find first hints if projections in the motor cortex are functionally

relevant. This technique applies electrical stimulation of cortical sites to induce, for example, stimulus-evoked movement responses, which can be detected visually, by EMG responses or by the usage of accelerometers. Several studies have used this technique to either examine cortical map shifts in sensorimotor areas after spontaneous recovery or different therapeutical applications [21–24] or used the stimulation itself as a method to increase plastic processes [25]. However, ICMS has its disadvantages such as the inability to selectively target neuronal subtypes as well as the indiscriminate activation of axons of passage. Furthermore, due to electrode penetration, intracortical electric stimulation remains an invasive procedure causing tissue damage [26]. ICMS is also limited to perform cortical representation of body function at a distinct time point after stroke constraining longitudinal experiments within the same animal.

A new noninvasive strategy to study the reorganization of the motor cortex after stroke in the same animal over time is light-based motor mapping: This technique makes usage of the possibility to stimulate neurons by light, either by uncaging neurotransmitters [27, 28] or by directly activating light-sensitive channels, such as channelrhodopsin-2 (ChR-2). Ayling et al. [26] used transgenic channelrhodopsin-2 mice which express ChR-2 in layer 5B pyramidal neurons of the motor cortex. Thus, light-based stimulation directly targets corticofugal cells, enabling the analysis of their contribution to motor cortex topography. Light-based motor mapping has the advantage of sampling stimulus-evoked movements at hundreds of cortical locations in mere minutes objectively and in a reproducible manner [29]. It is faster and less invasive than electrode-based mapping and can be combined with intrinsic signal imaging in animals with cranial window preparations [30]. In addition, it enables repeated mapping of the motor cortex over a timescale of minutes to months, opening up possibilities to examine the dynamics of movement representations at distinct conditions such as learning over time, pharmacological intervention or reorganization before, during, and after cortical damage. In a first study by Harrison et al. [29] light-based motor mapping revealed a functional subdivision of the forelimb motor cortex based on the direction of movements evoked by brief light pulses (10 ms), while prolonged stimulation (100–500 ms) resulted in complex movements of the forelimb to specific positions in space. In a follow-up study [30], light-based mapping was for the first time used to perform a longitudinal experiment studying the reorganization of the sensorimotor cortex after a focal sensory stroke. The sensory stroke caused the establishment of a new sensory map in prior parts of the forelimb motor cortex, which preserved its center position but became more dispersed.

2.3. Studying Poststroke Neuronal Circuit Formation and Network Activity. However, although all described mapping approaches are powerful tools, they can only provide information about map shifts and representation of general movement dynamics. They stay far beyond cellular resolution and do not allow studying local neuronal circuitry or single neuron contribution to neuronal networks. In particular after stroke, it is not clear how activity in single neurons changes in relation to cortical map shifts. The analysis of single neurons in relation to the neuronal circuit in which they are embedded may elucidate whether stroke-induced plasticity is a result of the capacity of surviving neurons to process multiple functional streams. In vivo two-photon calcium imaging is a potent method which not only allows studying activity of a single neuron or ensembles of neurons in a network but also enables cell type and neuronal subtype-specific analysis. Only a few in vivo two-photon calcium imaging studies focusing on neuronal reorganization and circuit rewiring after stroke have been conducted so far. In an acute in vivo calcium imaging experiment during the induction of a transient global ischemia model in mice, Murphy et al. [31] saw a widespread loss of mouse somatosensory cortex apical dendritic structure during the phase of ischemic depolarization. This was accompanied by increased intracellular calcium levels which coincidently occurred with the loss of dendritic structure. In a second study [32], in vivo two-photon calcium imaging was used to examine how response properties of individual neurons and glial cells in reorganized forelimb and hindlimb functional somatosensory maps modified during the recovery period from ischemic damage in the sensory cortex. However, all studies have been conducted in animals under anesthesia which itself influences neuronal activity. An experiment which examines single neuron activity in the behaving animal before stroke and during the recovery phase after insult is lacking so far.

Two-photon calcium imaging enables recordings of individual neuronal activity within a neuronal network and allows subtype-specific functional analysis of brain tissue. However, neuronal activity with cellular resolution level can only be examined in small (<1 millimeter) fields of view. Collective dynamics across different brain regions are inaccessible. Recent advances in two-photon microscopy allow the simultaneous imaging of neuronal networks with cellular resolution level in the active animal in multiple areas, which are even not directly connected [33–35]. This technological progress also provides new promises for experimental stroke research.

3. State-of-the-Art Techniques for Manipulating Neuronal Circuits

In a 1979 Scientific American article, Nobel laureate Francis Crick stated that the major challenge facing neuroscience was the need to control one type of cell in the brain while leaving others unaltered. In a lecture from 1999, he further confined: "One of the next requirements is to be able to turn the firing of one or more types of neuron on and off in the alert animal in a rapid manner. The ideal signal would be light, probably at an infrared wavelength to allow the light to penetrate far enough. This seems rather farfetched but it is conceivable that molecular biologists could engineer a particular cell type to be sensitive to light in this way" [36].

Manipulation of neuronal circuits or single neurons has two prerequisites: Manipulation has to be quick and very specific. Over the years, a very diverse set of tools has been developed to manipulate whole brain regions as

well as the activity of individual cells and subtypes in the alert behaving animal.

3.1. Manipulating with Specific Spatial Control. The first constraint for specific manipulation implies a high spatial control allowing the selective modulation of a whole brain area, a distinct anatomical sub region (e.g., layer 5 pyramidal cells in the sensorimotor cortex) or a particular cell type (e.g., a parvalbumin-positive interneuron).

For inhibiting neuronal activity in whole brain regions, agents such as the GABA agonist muscimol have been used [37, 38] resulting in a loss of motor function, indicating a causal relationship between anatomy and behavior. Other approaches block synapse remodeling through protein synthesis inhibitors such as anisomycin, for example, inducing the disruption of synapses and motor maps in a rat forelimb stroke model [39]. However, for a better spatial control to target distinct circuits and individual cell types, researchers have either created transgenic mouse lines or locally injected viruses with cell-type specific promotors [40]. These promotors induce gene expression directly—as in the case of transgenic mice—or indirectly via, for example, Tet- (tetracycline-controlled transcriptional activation-) on/off or Cre-flox systems.

The Tet system uses at least two viral vectors plus an antibiotic drug which in a sequential way activate each other to induce the transcription and translation of the gene of interest: A tissue-specific promoter initiates the expression of a transcription factor, either the tetracycline transactivator (tTA) or the reverse tetracycline transactivator (rtTA). The tTA or rtTA then becomes the key player for the transcription of a tetracycline response element (TRE) promotor, which in dependence of the presence of tetracycline or doxycycline drives the expression of the gene of interest. Expression of the gene of interest is fully reversible as administration or removal of tetracycline or doxycycline will turn its expression on or off. In a study by Kinoshita et al. [41] a Tet-on system was used to selectively express the synaptotoxin tetanus toxin in propriospinal (PN) neurons innervated by the motor cortex. The researchers could show that upon doxycycline administration in the drinking water reaching performance of monkeys significantly declined due to temporal blockade of the motor cortex–PN–motor neuron pathway. The same Tet-on system was used by Wahl et al. [42] in a rat stroke model to selectively shut off rewired corticospinal fibers originating in the contralesional pre- and motor cortex and targeting the stroke-denervated hemispinal cord: When doxycycline was administered to the rats in the drinking water after the rehabilitative treatment for impaired skilled motor function, the recovered grasping skills of the impaired paw decreased again over time. The effect was reversible, when doxycycline was removed from the drinking water. This study showed for the first time the specific and reversible inactivating of newly out-sprouting corticospinal fibers after stroke. In another study by Ishida et al. [43] ipsilesional corticorubral fibers were shut off after forced rehabilitation in a rat stroke model revealing the functional importance of the red nucleus for the recovery of impaired motor function.

Similar to the Tet system, the Cre-flox system also requires two transgenes: A tissue-specific promotor regulates the expression of Cre recombinase, a bacteriophage enzyme which recombines DNA at specific recognition sequences called loxP sites. Cre recombinase then excises DNA within two loxP sites ("floxed"). As in most cases, floxed-stop constructs are knocked in by homologous recombination to a gene of interest [40]; the stop signal is excised in the presence of Cre and the transgene expression can be initiated. Cre-mediated expression only occurs in cells expressing Cre, which are also those cells in which the tissue-specific promotor is active, indicating the high cell-type specificity of this technique.

3.2. Manipulating with High Spatial and Temporal Control

3.2.1. DREADDs. As the second prerequisite for specific neuronal manipulation in addition to a high degree of spatial resolution, temporal resolution and directional modulation of signaling are required for remotely controlling neuronal firing. Temporal resolution implies the precise control when a receptor or pathway is active or inactive and for how long it should be in a specific active status. Temporal resolution can vary from milliseconds (see "opsins" described below) to hours (e.g., designer receptors exclusively activated by designer drugs, DREADDs). Important are also "onset" kinetics (the time between the experimental manipulation and the modulation of the receptor or signaling pathway) and "offset" kinetics (the time between the initiation of the signaling modulation and the termination of the modulation [40]). Directional regulation describes the effect of the tool on neuronal activity (either activating or inhibiting), while bidirectional control would be the optimal case: Turning on and off the same cell population would elucidate the full spectrum of function that a cell provides within a particular network for perception or execution of a distinct behavior.

For manipulation of neuronal networks for minutes to hours, designer G protein-coupled receptors have been developed. G protein-coupled receptor pathways are involved in a multitude of cellular functions. Unlike opsins, which are functionally silent without excitation in vivo as they are not directly activated by endogenous compounds, G protein-coupled receptors (GCPRs) are constantly modulated by endogenous ligands in vivo or reveal ligand-independent activity [44, 45]. In vitro and in vivo pharmacological studies have described GPCRs as the most important class of druggable targets in the human genome [46], through which 50% of prescribed therapeutics act [47]. These facts made the development of highly selective orthologous ligand-receptor pairs, which would enable a high spatiotemporal control over GPCR signaling pathways in vivo challenging [48]. In recent years, mutations to more than a dozen native GPCRs have opened the field for the development of selectively activated designer receptors. Most of these receptors are divided in two classes: the first-generation RASSLs (receptors activated solely by synthetic ligands) and the second-generation DREADDs (designer receptors exclusively activated by designer drugs), which were evolved through directed molecular evolution in yeast [40]. RASSLs

were first engineered on the basis of serotonin receptors [49], histamine receptors [50], and melanocortin-4 receptors [51]. However, the first generation of orthologous ligand-GPCR pairs revealed potential shortcomings: Although the receptors were activated solely by the synthetic ligands, the ligands themselves did not solely activate the designer receptors (as reviewed by Rogan and Roth [40]). Thus, for the development of second-generation DREADDs, Armbruster et al. took a designer ligand, clozapine n-oxide (CNO), which was known to be inert at endogenous targets and highly bioavailable and blood-brain barrier-permeant in both humans and mice [52, 53]. As CNO had a modified structure of clozapine, which is known to be a weak partial agonist at muscarinic receptors, [54] mutations were induced in the five members of the muscarinic cholinergic receptor family and tested upon their selective responsiveness to the CNO application. Introducing two mutations transformed the hM3 receptor into a designer receptor which was insensitive to its native ligands, but highly sensitive to the designer ligand CNO. In smooth muscles cells the G_q-coupled hM3 DREADD receptor stimulated a cascade of inositol phosphate hydrolysis, calcium release and ERK1/2 activation, while the hM4Di DREADD receptor, derived from the G_i-coupled human muscarinic M4 receptor, inhibited forskolin-induced cAMP formation and activation of GIRK causing hyperpolarization and inhibition of neuronal firing [54].

Since the first development of DREADD receptors, reports of their usage in vivo are now appearing: The pharmacokinetic properties of the DREADD ligands and the particular route of administration (oral administration, subcutaneous, intraperitoneal, or even local stereotaxic infusion) determine how quickly neurons response to experimental manipulation by ligand application. Responses typically emerge 5 to 15 min after systematic application, for example, of CNO and usually last for 2 h—but this time period can be further enlarged upon dose-dependent increase of CNO [55]. When Ferguson et al. [56] used virus-mediated expression of the hM4Di receptor in the direct and indirect pathway neurons of the striatum, they found altered behavioral plasticity associated with repeated drug treatment. In particular, decreasing striatopallidal neuronal activity facilitated behavioral sensitization to drug treatment. Expression of the hM4Di receptor in rewired corticospinal projecting neurons was recently used to shut off regained grasping function in rats which had gained nearly full recovery of impaired skilled forelimb function due to a large stroke after the sequential application of a growth-promoting therapy and intense rehabilitative training [42].

3.2.2. Optogenetics. Although manipulation of GPCR signaling pathways by DREADD receptor induction and activation is highly efficient and shows a very specific spatial resolution (depending on the constructs or transgenic mouse lines used), the temporal resolution remains limited to an activation within minutes—due to the slower nature of GPCR signaling—and the necessary ligand delivery to the location of neuronal manipulation. In contrast, high-temporal (milliseconds) and cellular precision within intact mammalian neural tissue for fast, specific excitation or inhibition even within a freely moving animal can only be achieved with optogenetics [57].

Early approaches to use light to stimulate neuron activity included the selective photostimulation of neurons in *Drosophila* by coexpression of the drosophila photoreceptor genes encoding arrestin-2, rhodopsin, and the alpha subunit of the cognate heterotrimeric G protein which enabled the sensitization of neurons to light [58]. In a second approach, action potentials in hippocampal neurons were induced in a reliable and temporarily precise manner by uncaging a caged capsaicin derivate by light [59]. However, depolarization occurred within 5 s after a 1 s light pulse, lasting for 2–3 s and did not attenuate with multiple light pulses. Other approaches such as UV light-isomerizable chemicals linked to genetically encoded channels [60, 61] had also shown limitations due to reduced speed, targeting, tissue penetration, or applicability because of their multicomponent nature [57]. In 2003, Nagel et al. [62] cloned channelrhodopsin-2 (ChR2), a cation channel from the green alga *Chlamydomonas reinhardtii* which depicted similarities to the vertebrate rhodopsin which opens in response to blue light allowing potassium ions to enter the cell. Two years later, the first optogenetic experiment in neuroscience was conducted by expressing ChR2 using a lentiviral vector in cultured rat hippocampal neurons [63]. Illumination of these cultures with shorter wavelength blue light (450–490 nm) initiated large and rapid depolarization, while light with longer wavelengths (490–510 nm) induced smaller currents. Light stimulation of neurons was selective to those neurons expressing ChR2. Since then, neuroscientists rapidly adapted the possibilities of this new technology to in vivo experiments. In addition, the palette of available light-sensitive channels and ion pumps for neuronal inhibition and activation, for fast- and slow-acting opsins, and for opsins activated at distinct wavelengths has been extensively augmented in recent years [64–68].

However, although the numerous advantages of optogenetics are evident—such as the highest specificity, the ultrafast millisecond time scale dissection, and basically no adverse effects due to the light (unless the light source is not too strong or applied too long)—optogenetics stays an invasive procedure for many in vivo experiments: As the light source has to be brought close to the neuronal tissue, targeting deep brain areas or diffuse neuronal populations remains challenging. New development of step function or bistable opsins and opsins such as Jaws—an inhibitory opsin, which is activated by light of infrared wavelength [66]—opens up new possibilities for noninvasive manipulation in-vivo.

Only very few studies have applied optogenetics in experimental stroke research so far: Optogenetics was mainly used in the context of light-based motor mapping as described above [30]. Other studies used optogenetics as a therapeutic approach to increase neuronal activity aiming at enhancing functional recovery: In a first study by Cheng et al. [69], optogenetic stimulation of the ipsilateral primary motor cortex in ChR2 transgenic mice promoted functional recovery and the induction of growth-promoting genes after stroke induction in the striatum and somatosensory cortex. Shah et al. [70]

could furthermore show that selectively stimulating neurons in the lateral cerebellar nucleus (LCN), a deep cerebellar nucleus that sends major excitatory output to multiple motor and sensory areas in the forebrain, results in persistent recovery on the rotating beam after stroke in a transgenic mouse line (Thy1-ChR2-YFP-channelrhodopsin fused to yellow fluorescent protein under the Thy1 pan-neuronal promoter). Tennant et al. [71] revealed that optogenetic stimulation of thalamocortical axons could facilitate recovery. In another study [72], optogenetic stimulation of the intact corticospinal tract was sufficient to promote functional recovery after a large photothrombotic stroke in rats. Optogenetics were also used to drive the excitatory outputs of the grafted neural stem cells and increase forelimb use on the stroke-affected side and motor activity in a rat stroke model [73]. Reducing the inhibitory striatal output by optogenetics enhanced neurogenesis in the subventribular zone and behavioral recovery in mice after middle cerebral artery occlusion [74–76].

That optogenetics can also be used to demonstrate a causal relationship between a rewiring neuronal circuit and recovery of a specific (sensorimotor) behavior was demonstrated by Wahl et al. [72]: The authors used the inhibitory light-sensitive proton pump ArchT to reveal the functional relevance and regionalized organization of rewired corticospinal circuitry for the recovery of distinct grasping features.

New advanced technology in microscopy allows the precise optogenetic stimulation of individual neurons [77] and even dendritic spines and nerve cell somata [78, 79] using holographic photostimulation. In addition, the development of parallel illumination methods [80] which combine the preservation of the spatial targeting capability of beam-scanning systems and the rapid stimulation of multiple neurons now enable the simultaneous excitation of neurons in selected target regions.

3.2.3. Magnetogenetics. Although optogenetics have revolutionized the field of neuroscience, the examination of deeper, subcortical brain regions remains a challenge, as the light has to be somehow delivered to the tissue often requiring invasive implantation of fiber optics causing collateral damage of the surrounding brain tissue. A new emerging method which overcomes the spatial limitations is magnetogenetics: It relies on a principle known as thermal relaxation [81], implying that an alternating magnetic field is able to heat up small magnetic nanoparticles. As key elements the specific frequency of the magnetic field, the size and composition of the nanoparticles are required. Huang et al. [82] activated a heat-sensitive TRPV1 channel expressed in human embryonic kidney (HEK) cells by induction of thermal relaxation of manganese oxide nanoparticles, which enhanced the temperature at the plasma membrane and initiated the calcium influx through the heat-sensitive ion channels. Chen et al. [83] used this technique to stimulate a defined neuronal population activity in the ventral tegmental area in behaving mice demonstrating the potential of magnetogenetics for deep brain stimulation.

However, although individual neuron and specific neuronal circuit manipulation with high spatial and temporal control is possible as discussed above, there still is a need for good behavioral readouts: In particular, in experimental stroke research studying, for example, motor impairment and recovery, it is crucial to quantitatively understand true recovery versus compensation of impaired function [84]: While analyzing video recordings of motor behavior using scores is not only time consuming but also often very subjective, even the analysis of movement trajectories might not provide the full picture [72]: When manipulating with high precision control on a cellular and even subcellular level on the neurobiological side, there is a need for precise analysis of the behavioral phenotype. The dramatic development of Computer Vision algorithms and artificial intelligence may allow further steps beyond for a detailed analysis of kinematics including the sequence of postures, shape and trajectories, which is missed by the human eye.

4. State-of-the-Art Techniques to Combine Anatomy and Molecular Biology

So far, we have discussed how stroke reorganization can be examined on the macrolevel of map shifts or by studying single neurons in neuronal circuits using 2-photon calcium imaging approaches. We have reviewed how individual neurons and whole neuronal populations can be manipulated with high spatiotemporal resolution disclosing new possibilities of causally linking individual neuronal activity with a distinct behavioral phenotype. However, an understanding of the underlying molecular crosstalk which induces anatomical and behavioral changes is still lacking. Classically, tracing techniques (e.g., dextran tracers) have been applied to visualize cells involved in structural reorganization after stroke [22, 23]. Li et al. [85] found a way to exclusively study molecular changes in newly out-sprouting neurons ("the sprouting transcriptome") in the peri-infarct cortex by injecting two different fluorescent conjugates of the tracer cholera toxin B (CTB) into forelimb sensorimotor cortex at different times points: One CTB tracer was injected at the time of stroke, the second differently labeled one either 7 or 21 days afterwards. Neurons which expressed only the second tracer were those which missed an axonal projection to the injection site at the time of the injection of the first tracer and thus represented neurons which established a new projection pattern after stroke. Both neuron types (single- and double-labeled ones) were laser captured to identify the distinct transcriptional profile of an out-sprouting neuron in the peri-infarct cortex.

In addition, new constructs have been recently developed for molecular profiling of projecting neurons and thus bridging the gap between anatomical modifications and underlying molecular mechanisms. Using, for example, bacterial artificial chromosome (BAC) transgenic mice which express EGFP-tagged ribosomal protein L10a in defined cell populations allowed purification of polysomal mRNAs from genetically defined cell populations in the brain [86, 87]. In another study by Ekstrand et al. [88], ribosomes were tagged with a camelid nanobody raised against GFP enabling the selective capture of translating mRNAs in projecting neurons.

5. Conclusion

Here, we have reviewed current and new promising state-of-the-art techniques for studying reorganization after stroke, for the identification and manipulation of distinct neuronal populations and approaches which allow examining molecular profiles of neurons being part of the cortical reorganization process. While for decades studies in basic stroke research have only described and reported correlative findings, these techniques open up tremendous possibilities to analyze plastic processes and identify and target key players for the development of new therapies in stroke.

Conflicts of Interest

The author excludes any competing interest.

Funding

This work was supported by the Swiss National Science Foundation Grant no. 31003A-149315-1.

References

[1] S. Walter, P. Kostopoulos, A. Haass et al., "Diagnosis and treatment of patients with stroke in a mobile stroke unit versus in hospital: a randomised controlled trial," *The Lancet Neurology*, vol. 11, no. 5, pp. 397–404, 2012.

[2] O. A. Berkhemer, P. S. Fransen, D. Beumer et al., "A randomized trial of intraarterial treatment for acute ischemic stroke," *The New England Journal of Medicine*, vol. 372, no. 1, pp. 11–20, 2015.

[3] W. Hacke, M. Kaste, E. Bluhmki et al., "Thrombolysis with alteplase 3 to 4.5 hours after acute ischemic stroke," *The New England Journal of Medicine*, vol. 359, no. 13, pp. 1317–1329, 2008.

[4] S. T. Carmichael, I. Archibeque, L. Luke, T. Nolan, J. Momiy, and S. Li, "Growth-associated gene expression after stroke: evidence for a growth-promoting region in peri-infarct cortex," *Experimental Neurology*, vol. 193, no. 2, pp. 291–311, 2005.

[5] M. P. van Meer, K. van der Marel, W. M. Otte, J. W. Berkelbach van der Sprenkel, and R. M. Dijkhuizen, "Correspondence between altered functional and structural connectivity in the contralesional sensorimotor cortex after unilateral stroke in rats: a combined resting-state functional MRI and manganese-enhanced MRI study," *Journal of Cerebral Blood Flow & Metabolism*, vol. 30, no. 10, pp. 1707–1711, 2010.

[6] M. P. A. van Meer, W. M. Otte, K. van der Marel et al., "Extent of bilateral neuronal network reorganization and functional recovery in relation to stroke severity," *The Journal of Neuroscience*, vol. 32, no. 13, pp. 4495–4507, 2012.

[7] R. D. Frostig and C. H. Chen-Bee, "Visualizing adult cortical plasticity using intrinsic signal optical imaging," in *In Vivo Optical Imaging of Brain Function*, R. D. Frostig, Ed., CRC Press, Boca Raton, FL, USA, 2009.

[8] A. Q. Bauer, A. W. Kraft, P. W. Wright, A. Z. Snyder, J. M. Lee, and J. P. Culver, "Optical imaging of disrupted functional connectivity following ischemic stroke in mice," *NeuroImage*, vol. 99, pp. 388–401, 2014.

[9] J. Hakon, M. J. Quattromani, C. Sjölund et al., "Multisensory stimulation improves functional recovery and resting-state functional connectivity in the mouse brain after stroke," *NeuroImage: Clinical*, vol. 17, pp. 717–730, 2018.

[10] M. H. Mohajerani, A. W. Chan, M. Mohsenvand et al., "Spontaneous cortical activity alternates between motifs defined by regional axonal projections," *Nature Neuroscience*, vol. 16, no. 10, pp. 1426–1435, 2013.

[11] A. Ghosh, F. Haiss, E. Sydekum et al., "Rewiring of hindlimb corticospinal neurons after spinal cord injury," *Nature Neuroscience*, vol. 13, no. 1, pp. 97–104, 2010.

[12] C. E. Brown, K. Aminoltejari, H. Erb, I. R. Winship, and T. H. Murphy, "*In vivo* voltage-sensitive dye imaging in adult mice reveals that somatosensory maps lost to stroke are replaced over weeks by new structural and functional circuits with prolonged modes of activation within both the peri-infarct zone and distant sites," *The Journal of Neuroscience*, vol. 29, no. 6, pp. 1719–1734, 2009.

[13] Y. Ma, M. A. Shaik, S. H. Kim et al., "Wide-field optical mapping of neural activity and brain haemodynamics: considerations and novel approaches," *Philosophical Transactions of the Royal Society of London Series B, Biological Sciences*, vol. 371, no. 1705, p. 20150360, 2016.

[14] K. Horikawa, "Recent progress in the development of genetically encoded Ca^{2+} indicators," *The Journal of Medical Investigation*, vol. 62, no. 1.2, pp. 24–28, 2015.

[15] M. Kozberg and E. Hillman, "Chapter 10 - neurovascular coupling and energy metabolism in the developing brain," *Progress in Brain Research*, vol. 225, pp. 213–242, 2016.

[16] M. G. Kozberg, Y. Ma, M. A. Shaik, S. H. Kim, and E. M. C. Hillman, "Rapid postnatal expansion of neural networks occurs in an environment of altered neurovascular and neurometabolic coupling," *The Journal of Neuroscience*, vol. 36, no. 25, pp. 6704–6717, 2016.

[17] G. Silasi, D. Xiao, M. P. Vanni, A. C. N. Chen, and T. H. Murphy, "Intact skull chronic windows for mesoscopic wide-field imaging in awake mice," *Journal of Neuroscience Methods*, vol. 267, pp. 141–149, 2016.

[18] M. P. Vanni and T. H. Murphy, "Mesoscale transcranial spontaneous activity mapping in GCaMP3 transgenic mice reveals extensive reciprocal connections between areas of somatomotor cortex," *The Journal of Neuroscience*, vol. 34, no. 48, pp. 15931–15946, 2014.

[19] M. Balbi, M. P. Vanni, M. J. Vega et al., "Longitudinal monitoring of mesoscopic cortical activity in a mouse model of microinfarcts reveals dissociations with behavioral and motor function," *Journal of Cerebral Blood Flow & Metabolism*, 2018.

[20] T. H. Murphy, J. D. Boyd, F. Bolaños et al., "High-throughput automated home-cage mesoscopic functional imaging of mouse cortex," *Nature Communications*, vol. 7, article 11611, 2016.

[21] A. J. Emerick, E. J. Neafsey, M. E. Schwab, and G. L. Kartje, "Functional reorganization of the motor cortex in adult rats after cortical lesion and treatment with monoclonal antibody IN-1," *The Journal of Neuroscience*, vol. 23, no. 12, pp. 4826–4830, 2003.

[22] N. T. Lindau, B. J. Bänninger, M. Gullo et al., "Rewiring of the corticospinal tract in the adult rat after unilateral stroke and anti-Nogo-A therapy," *Brain*, vol. 137, no. 3, pp. 739–756, 2014.

[23] M. L. Starkey, C. Bleul, B. Zörner et al., "Back seat driving: hindlimb corticospinal neurons assume forelimb control following ischaemic stroke," *Brain*, vol. 135, no. 11, pp. 3265–3281, 2012.

[24] K. A. Tennant, D. A. L. Adkins, N. A. Donlan et al., "The organization of the forelimb representation of the C57BL/6 mouse motor cortex as defined by intracortical microstimulation and cytoarchitecture," *Cerebral Cortex*, vol. 21, no. 4, pp. 865–876, 2011.

[25] M. Brus-Ramer, J. B. Carmel, S. Chakrabarty, and J. H. Martin, "Electrical stimulation of spared corticospinal axons augments connections with ipsilateral spinal motor circuits after injury," *The Journal of Neuroscience*, vol. 27, no. 50, pp. 13793–13801, 2007.

[26] O. G. S. Ayling, T. C. Harrison, J. D. Boyd, A. Goroshkov, and T. H. Murphy, "Automated light-based mapping of motor cortex by photoactivation of channelrhodopsin-2 transgenic mice," *Nature Methods*, vol. 6, no. 3, pp. 219–224, 2009.

[27] G. M. G. Shepherd, T. A. Pologruto, and K. Svoboda, "Circuit analysis of experience-dependent plasticity in the developing rat barrel cortex," *Neuron*, vol. 38, no. 2, pp. 277–289, 2003.

[28] L. Luo, E. M. Callaway, and K. Svoboda, "Genetic dissection of neural circuits," *Neuron*, vol. 57, no. 5, pp. 634–660, 2008.

[29] T. C. Harrison, O. G. S. Ayling, and T. H. Murphy, "Distinct cortical circuit mechanisms for complex forelimb movement and motor map topography," *Neuron*, vol. 74, no. 2, pp. 397–409, 2012.

[30] T. C. Harrison, G. Silasi, J. D. Boyd, and T. H. Murphy, "Displacement of sensory maps and disorganization of motor cortex after targeted stroke in mice," *Stroke*, vol. 44, no. 8, pp. 2300–2306, 2013.

[31] T. H. Murphy, P. Li, K. Betts, and R. Liu, "Two-photon imaging of stroke onset *in vivo* reveals that NMDA-receptor independent ischemic depolarization is the major cause of rapid reversible damage to dendrites and spines," *The Journal of Neuroscience*, vol. 28, no. 7, pp. 1756–1772, 2008.

[32] I. R. Winship and T. H. Murphy, "*In vivo* calcium imaging reveals functional rewiring of single somatosensory neurons after stroke," *The Journal of Neuroscience*, vol. 28, no. 26, pp. 6592–6606, 2008.

[33] N. J. Sofroniew, D. Flickinger, J. King, and K. Svoboda, "A large field of view two-photon mesoscope with subcellular resolution for in vivo imaging," *eLife*, vol. 5, 2016.

[34] J. Lecoq, J. Savall, D. Vučinić et al., "Visualizing mammalian brain area interactions by dual-axis two-photon calcium imaging," *Nature Neuroscience*, vol. 17, no. 12, pp. 1825–1829, 2014.

[35] J. L. Chen, F. F. Voigt, M. Javadzadeh, R. Krueppel, and F. Helmchen, "Long-range population dynamics of anatomically defined neocortical networks," *eLife*, vol. 5, 2016.

[36] F. Crick, "The impact of molecular biology on neuroscience," *Philosophical Transactions of the Royal Society of London Series B, Biological Sciences*, vol. 354, no. 1392, pp. 2021–2025, 1999.

[37] J. B. Carmel, H. Kimura, and J. H. Martin, "Electrical stimulation of motor cortex in the uninjured hemisphere after chronic unilateral injury promotes recovery of skilled locomotion through ipsilateral control," *The Journal of Neuroscience*, vol. 34, no. 2, pp. 462–466, 2014.

[38] B. K. Mansoori, L. Jean-Charles, B. Touvykine, A. Liu, S. Quessy, and N. Dancause, "Acute inactivation of the contralesional hemisphere for longer durations improves recovery after cortical injury," *Experimental Neurology*, vol. 254, pp. 18–28, 2014.

[39] S. Y. Kim, J. E. Hsu, L. C. Husbands, J. A. Kleim, and T. A. Jones, "Coordinated plasticity of synapses and astrocytes underlies practice-driven functional vicariation in peri-infarct motor cortex," *The Journal of Neuroscience*, vol. 38, no. 1, pp. 93–107, 2018.

[40] S. C. Rogan and B. L. Roth, "Remote control of neuronal signaling," *Pharmacological Reviews*, vol. 63, no. 2, pp. 291–315, 2011.

[41] M. Kinoshita, R. Matsui, S. Kato et al., "Genetic dissection of the circuit for hand dexterity in primates," *Nature*, vol. 487, no. 7406, pp. 235–238, 2012.

[42] A. S. Wahl, W. Omlor, J. C. Rubio et al., "Neuronal repair. Asynchronous therapy restores motor control by rewiring of the rat corticospinal tract after stroke," *Science*, vol. 344, no. 6189, pp. 1250–1255, 2014.

[43] A. Ishida, K. Isa, T. Umeda et al., "Causal link between the cortico-rubral pathway and functional recovery through forced impaired limb use in rats with stroke," *The Journal of Neuroscience*, vol. 36, no. 2, pp. 455–467, 2016.

[44] R. Seifert and K. Wenzel-Seifert, "Constitutive activity of G-protein-coupled receptors: cause of disease and common property of wild-type receptors," *Naunyn-Schmiedeberg's Archives of Pharmacology*, vol. 366, no. 5, pp. 381–416, 2002.

[45] M. J. Smit, H. F. Vischer, R. A. Bakker et al., "Pharmacogenomic and structural analysis of constitutive G protein-coupled receptor activity," *Annual Review of Pharmacology and Toxicology*, vol. 47, no. 1, pp. 53–87, 2007.

[46] P. M. Giguere, W. K. Kroeze, and B. L. Roth, "Tuning up the right signal: chemical and genetic approaches to study GPCR functions," *Current Opinion in Cell Biology*, vol. 27, pp. 51–55, 2014.

[47] J. P. Overington, B. Al-Lazikani, and A. L. Hopkins, "How many drug targets are there?," *Nature Reviews Drug Discovery*, vol. 5, no. 12, pp. 993–996, 2006.

[48] B. R. Conklin, E. C. Hsiao, S. Claeysen et al., "Engineering GPCR signaling pathways with RASSLs," *Nature Methods*, vol. 5, no. 8, pp. 673–8, 2008.

[49] K. Kristiansen, W. K. Kroeze, D. L. Willins et al., "A highly conserved aspartic acid (Asp-155) anchors the terminal amine moiety of tryptamines and is involved in membrane targeting of the 5-HT_{2A} serotonin receptor but does not participate in activation via a "salt-bridge disruption" mechanism," *The Journal of Pharmacology and Experimental Therapeutics*, vol. 293, no. 3, pp. 735–746, 2000.

[50] M. Bruysters, A. Jongejan, A. Akdemir, R. A. Bakker, and R. Leurs, "A $G_{q/11}$-coupled mutant histamine H_1 receptor F435A activated solely by synthetic ligands (RASSL)," *Journal of Biological Chemistry*, vol. 280, no. 41, pp. 34741–34746, 2005.

[51] S. Srinivasan, C. Vaisse, and B. R. Conklin, "Engineering the melanocortin-4 receptor to control G_s signaling *in vivo*," *Annals of the New York Academy of Sciences*, vol. 994, no. 1, pp. 225–232, 2003.

[52] W. H. Chang, S. K. Lin, H. Y. Lane et al., "Reversible metabolism of clozapine and clozapine N-oxide in schizophrenic patients," *Progress in Neuro-Psychopharmacology & Biological Psychiatry*, vol. 22, no. 5, pp. 723–739, 1998.

[53] D. M. Weiner, H. Y. Meltzer, I. Veinbergs et al., "The role of M1 muscarinic receptor agonism of *N*-desmethylclozapine in the unique clinical effects of clozapine," *Psychopharmacology*, vol. 177, no. 1-2, pp. 207–216, 2004.

[54] B. N. Armbruster, X. Li, M. H. Pausch, S. Herlitze, and B. L. Roth, "Evolving the lock to fit the key to create a family of G protein-coupled receptors potently activated by an inert ligand," *Proceedings of the National Academy of Sciences of the United States of America*, vol. 104, no. 12, pp. 5163–5168, 2007.

[55] J. M. Guettier, D. Gautam, M. Scarselli et al., "A chemical-genetic approach to study G protein regulation of β cell function in vivo," *Proceedings of the National Academy of Sciences of the United States of America*, vol. 106, no. 45, pp. 19197–19202, 2009.

[56] S. M. Ferguson, D. Eskenazi, M. Ishikawa et al., "Transient neuronal inhibition reveals opposing roles of indirect and direct pathways in sensitization," *Nature Neuroscience*, vol. 14, no. 1, pp. 22–24, 2011.

[57] L. Fenno, O. Yizhar, and K. Deisseroth, "The development and application of optogenetics," *Annual Review of Neuroscience*, vol. 34, no. 1, pp. 389–412, 2011.

[58] B. V. Zemelman, G. A. Lee, M. Ng, and G. Miesenböck, "Selective photostimulation of genetically chARGed neurons," *Neuron*, vol. 33, no. 1, pp. 15–22, 2002.

[59] B. V. Zemelman, N. Nesnas, G. A. Lee, and G. Miesenbock, "Photochemical gating of heterologous ion channels: remote control over genetically designated populations of neurons," *Proceedings of the National Academy of Sciences of the United States of America*, vol. 100, no. 3, pp. 1352–1357, 2003.

[60] S. Szobota, P. Gorostiza, F. del Bene et al., "Remote control of neuronal activity with a light-gated glutamate receptor," *Neuron*, vol. 54, no. 4, pp. 535–545, 2007.

[61] P. Gorostiza and E. Y. Isacoff, "Optical switches for remote and noninvasive control of cell signaling," *Science*, vol. 322, no. 5900, pp. 395–399, 2008.

[62] G. Nagel, T. Szellas, W. Huhn et al., "Channelrhodopsin-2, a directly light-gated cation-selective membrane channel," *Proceedings of the National Academy of Sciences of the United States of America*, vol. 100, no. 24, pp. 13940–13945, 2003.

[63] E. S. Boyden, F. Zhang, E. Bamberg, G. Nagel, and K. Deisseroth, "Millisecond-timescale, genetically targeted optical control of neural activity," *Nature Neuroscience*, vol. 8, no. 9, pp. 1263–1268, 2005.

[64] O. Yizhar, L. Fenno, F. Zhang, P. Hegemann, and K. Diesseroth, "Microbial opsins: a family of single-component tools for optical control of neural activity," *Cold Spring Harbor Protocols*, vol. 2011, no. 3, article top102, 2011.

[65] D. Schmidt, P. W. Tillberg, F. Chen, and E. S. Boyden, "A fully genetically encoded protein architecture for optical control of peptide ligand concentration," *Nature Communications*, vol. 5, p. 3019, 2014.

[66] A. S. Chuong, M. L. Miri, V. Busskamp et al., "Noninvasive optical inhibition with a red-shifted microbial rhodopsin," *Nature Neuroscience*, vol. 17, no. 8, pp. 1123–1129, 2014.

[67] N. C. Klapoetke, Y. Murata, S. S. Kim et al., "Independent optical excitation of distinct neural populations," *Nature Methods*, vol. 11, no. 3, pp. 338–346, 2014.

[68] C. K. Kim, A. Adhikari, and K. Deisseroth, "Integration of optogenetics with complementary methodologies in systems neuroscience," *Nature Reviews Neuroscience*, vol. 18, no. 4, pp. 222–235, 2017.

[69] M. Y. Cheng, E. H. Wang, W. J. Woodson et al., "Optogenetic neuronal stimulation promotes functional recovery after stroke," *Proceedings of the National Academy of Sciences of the United States of America*, vol. 111, no. 35, pp. 12913–12918, 2014.

[70] A. M. Shah, S. Ishizaka, M. Y. Cheng et al., "Optogenetic neuronal stimulation of the lateral cerebellar nucleus promotes persistent functional recovery after stroke," *Scientific Reports*, vol. 7, article 46612, 2017.

[71] K. A. Tennant, S. L. Taylor, E. R. White, and C. E. Brown, "Optogenetic rewiring of thalamocortical circuits to restore function in the stroke injured brain," *Nature Communications*, vol. 8, article 15879, 2017.

[72] A. S. Wahl, U. Büchler, A. Brändli et al., "Optogenetically stimulating intact rat corticospinal tract post-stroke restores motor control through regionalized functional circuit formation," *Nature Communications*, vol. 8, no. 1, p. 1187, 2017.

[73] M. M. Daadi, J. Q. Klausner, B. Bajar et al., "Optogenetic stimulation of neural grafts enhances neurotransmission and downregulates the inflammatory response in experimental stroke model," *Cell Transplantation*, vol. 25, no. 7, pp. 1371–1380, 2016.

[74] L. Jiang, W. Li, M. Mamtilahun et al., "Optogenetic inhibition of striatal GABAergic neuronal activity improves outcomes after ischemic brain injury," *Stroke*, vol. 48, no. 12, pp. 3375–3383, 2017.

[75] Y. Lu, L. Jiang, W. Li et al., "Optogenetic inhibition of striatal neuronal activity improves the survival of transplanted neural stem cells and neurological outcomes after ischemic stroke in mice," *Stem Cells International*, vol. 2017, Article ID 4364302, 11 pages, 2017.

[76] M. Song, S. P. Yu, O. Mohamad et al., "Optogenetic stimulation of glutamatergic neuronal activity in the striatum enhances neurogenesis in the subventricular zone of normal and stroke mice," *Neurobiology of Disease*, vol. 98, pp. 9–24, 2017.

[77] O. A. Shemesh, D. Tanese, V. Zampini et al., "Temporally precise single-cell-resolution optogenetics," *Nature Neuroscience*, vol. 20, no. 12, pp. 1796–1806, 2017.

[78] A. M. Packer, D. S. Peterka, J. J. Hirtz, R. Prakash, K. Deisseroth, and R. Yuste, "Two-photon optogenetics of dendritic spines and neural circuits," *Nature Methods*, vol. 9, no. 12, pp. 1202–1205, 2012.

[79] A. M. Packer, L. E. Russell, H. W. P. Dalgleish, and M. Häusser, "Simultaneous all-optical manipulation and recording of neural circuit activity with cellular resolution *in vivo*," *Nature Methods*, vol. 12, no. 2, pp. 140–146, 2015.

[80] V. Emiliani, A. E. Cohen, K. Deisseroth, and M. Hausser, "All-optical interrogation of neural circuits," *The Journal of Neuroscience*, vol. 35, no. 41, pp. 13917–13926, 2015.

[81] S. Nimpf and D. A. Keays, "Is magnetogenetics the new optogenetics?," *The EMBO Journal*, vol. 36, no. 12, pp. 1643–1646, 2017.

[82] H. Huang, S. Delikanli, H. Zeng, D. M. Ferkey, and A. Pralle, "Remote control of ion channels and neurons through magnetic-field heating of nanoparticles," *Nature Nanotechnology*, vol. 5, no. 8, pp. 602–606, 2010.

[83] R. Chen, G. Romero, M. G. Christiansen, A. Mohr, and P. Anikeeva, "Wireless magnetothermal deep brain stimulation," *Science*, vol. 347, no. 6229, pp. 1477–1480, 2015.

[84] T. A. Jones, "Motor compensation and its effects on neural reorganization after stroke," *Nature Reviews Neuroscience*, vol. 18, no. 5, pp. 267–280, 2017.

[85] S. Li, J. J. Overman, D. Katsman et al., "An age-related sprouting transcriptome provides molecular control of axonal sprouting after stroke," *Nature Neuroscience*, vol. 13, no. 12, pp. 1496–1504, 2010.

[86] J. P. Doyle, J. D. Dougherty, M. Heiman et al., "Application of a translational profiling approach for the comparative analysis of CNS cell types," *Cell*, vol. 135, no. 4, pp. 749–762, 2008.

[87] M. Heiman, A. Schaefer, S. Gong et al., "A translational profiling approach for the molecular characterization of CNS cell types," *Cell*, vol. 135, no. 4, pp. 738–748, 2008.

[88] M. I. Ekstrand, A. R. Nectow, Z. A. Knight, K. N. Latcha, L. E. Pomeranz, and J. M. Friedman, "Molecular profiling of neurons based on connectivity," *Cell*, vol. 157, no. 5, pp. 1230–1242, 2014.

Hindawi
Neural Plasticity
Volume 2018, Article ID 2651918, 12 pages
https://doi.org/10.1155/2018/2651918

Review Article

Neurorehabilitation in Parkinson's Disease: A Critical Review of Cognitive Rehabilitation Effects on Cognition and Brain

María Díez-Cirarda, Naroa Ibarretxe-Bilbao, Javier Peña, and Natalia Ojeda

Department of Methods and Experimental Psychology, Faculty of Psychology and Education, University of Deusto, Bilbao, Spain

Correspondence should be addressed to Naroa Ibarretxe-Bilbao; naroa.ibarretxe@deusto.es

Received 20 February 2018; Accepted 29 March 2018; Published 6 May 2018

Academic Editor: Toshiyuki Fujiwara

Background. Parkinson's disease (PD) patients experience cognitive impairment which has been related to reduced quality of life and functional disability. These symptoms usually progress until dementia occurs. Some studies have been published assessing the efficacy of cognitive treatments on improving cognition, functional outcome, and producing changes in brain activity. *Objective*. A critical review was performed to present up-to-date neurorehabilitation effects of cognitive rehabilitation in PD, with special emphasis on the efficacy on cognition, quality of life aspects, brain changes, and the longitudinal maintenance of these changes. *Results*. After exclusions, 13 studies were reviewed, including 6 randomized controlled trials for the efficacy on cognition, 2 randomized controlled trials regarding the brain changes after cognitive training, and 5 studies which evaluated the long-term effects of cognitive treatments. *Conclusions*. Cognitive rehabilitation programs have demonstrated to be effective on improving cognitive functions, but more research is needed focusing on the efficacy on improving behavioral aspects and producing brain changes in patients with PD. Moreover, there is a need of randomized controlled trials with long-term follow-up periods.

1. Introduction

Parkinson's disease (PD) is a common neurodegenerative disease, being most of the cases diagnosed at around 60 years [1]. Traditionally, PD has been considered a motor disorder, and the core motor symptoms are rigidity, tremor, bradykinesia (akinesia), and postural instability. In addition, freezing of gait (difficulty to initiate or continue walking) and flexed posture have been included in the cardinal motor symptoms of the disease [2]. Nowadays, it is known that this neurodegenerative process produces a wide range of motor and nonmotor symptoms in PD patients; hence, PD is considered a multiple system neurodegenerative disorder [3]. Among these nonmotor symptoms, cognitive impairment is an important nonmotor symptom due to its prevalence among PD patients (20–50%) [4, 5]. In addition, PD patients might develop cognitive impairment from the early stages of the disease [4, 5]. These cognitive deficits may deteriorate with the progression of the disease until dementia occurs [6, 7]. The analysis of cognitive impairment and dementia in PD patients is relevant because both have shown relationship with reduced quality of life and functional disability in PD patients [8, 9].

These cognitive impairments in PD have been related to grey matter (GM) atrophy, white matter (WM) alterations, brain functional connectivity (FC), and brain activation alterations. PD patients with Mild Cognitive Impairment (MCI) diagnosis have shown GM volume reduction in the frontal, temporal, and parietal lobes, but also in the hippocampus, amygdala, and putamen [10, 11]. Additionally, PD patients with MCI have shown widespread cerebral WM deterioration [11–13]. Interestingly, WM alterations have been found to appear before GM volume reduction in PD patients, which highlights the importance to explore the relationship between WM indexes and cognitive impairment [14]. In addition, cognitive deficits have also been related to functional brain alterations, showing altered FC and brain activation values both during resting state and during cognitive tasks inside the scanner [15, 16].

With the progression of the disease, cognitive deficits usually deteriorate until dementia occurs after 10 to 20 years [6, 17]. A study followed newly diagnosed PD patients over time and found that after 20 years, dementia was present in up to 80% of PD patients [6]. In addition, recent studies showed that the presence of MCI diagnosis in PD patients contributes to the development of dementia [7], and results support that MCI could be considered as a prodromal stage for dementia in PD [18]. Cognitive deterioration is accompanied by GM volume loss [19], WM alterations [20], and functional brain changes [21, 22]. When dementia occurs in PD patients, cortical degeneration has been extended to frontal, temporal, parietal, and occipital areas [23].

Due to the relevance of cognitive deficits, therapeutic strategies are needed to treat cognitive decline. A common cognitive rehabilitation program could be described as a behavioral treatment for cognitive impairment which focused on cognitive abilities and daily living activities, which is based on the restoration, compensation, and optimization of the cognitive functions [24, 25]. Cognitive rehabilitation programs have demonstrated their efficacy on improving cognition in different studies in PD. Several reviews [26–28] and meta-analyses [29, 30] have been published in the field. The efficacy of cognitive rehabilitation on improving cognition has been shown, but these reviews and meta-analyses highlight the importance of continuing with research focused on the efficacy of the cognitive rehabilitation approach in PD.

The main objective of the present study is to perform a critical review to present up-to-date neurorehabilitation effects of cognitive rehabilitation in PD. The first objective was to examine the efficacy of cognitive rehabilitation programs on cognition and behavioral aspects. The second objective was to review the evidence of the brain changes found after cognitive treatments. Finally, the present study analyzed the long-term effects of cognitive rehabilitation in PD.

2. Methods

2.1. Review Strategy. Studies were included from inception to December 2017. Focusing on the first objective of this critical review, which was to analyze those randomized controlled trials focused on the efficacy of cognitive rehabilitation programs on cognition, we selected only those studies that fulfilled the following criteria: (1) randomized controlled trials; (2) PD patients underwent a cognitive rehabilitation program; (3) the main objective was to investigate the change in cognition; and (4) studies including a PD control group. Among the studies that fulfilled these specific criteria, we also reported (if included in the studies) the results of the efficacy on behavioral or mood aspects, such as depression, apathy, functional disability, and quality of life aspects.

Regarding the second objective of the present review, the efficacy of cognitive rehabilitation programs in producing brain changes in PD was determined based on the following criteria: (1) randomized controlled trials; (2) PD patients underwent a cognitive rehabilitation program; (3) studies including a PD control group; and (4) brain changes were evaluated.

Finally, focusing on the last objective of the present study, the review about the long-term effects of cognitive rehabilitation programs was based on the following criteria: (1) PD patients underwent a cognitive rehabilitation program; (2) a longitudinal follow-up evaluation was performed; and (3) the main objective was to investigate the change in cognition at follow-up. In this specific section, we included both randomized controlled trials and nonrandomized trials, due to the scarce number of published studies and to have a wider perspective.

Databases included were PubMed, Medline, and Google Scholar. The search terms were specified to be found in the title of the studies. The terms were (1) Parkinson's disease/Parkinson disease; (2) cognitive rehabilitation/cognitive training/cognitive remediation; (3) attention rehabilitation/attention training/attention remediation; (4) executive training/executive rehabilitation/executive remediation; (5) memory training/memory rehabilitation/memory remediation; (6) randomized controlled trial/randomized controlled trial; and (7) cognition. The search term combinations in the databases were (1) + (2); (1) + (3); (1) + (4); (1) + (5); and (1) + (6) + (7).

A summary of study selection is shown in Figure 1. The results of the selected studies were divided into 3 different sections. First, the studies evaluating the cognitive and behavioral changes are shown in Table 1. Then, Table 2 shows the studies that assessed the brain changes after cognitive rehabilitation in PD. In addition, the longitudinal effects of cognitive rehabilitation programs are shown in Table 3. In Tables 1 and 3, different characteristics of the studies are shown, such as the sample size, characteristics of the cognitive rehabilitation program used, cognitive domains analyzed, significant results found, and limitations of each study. In Table 2, MRI acquisition, preprocessing, and analysis specifications are included for each study, along with the brain significant results and the study limitations.

3. Results

3.1. Efficacy on Improving Cognition and Behavioral Aspects. A summary of the included cognitive rehabilitation studies in PD is shown in Table 1. Studies were included if they followed guidelines for randomized controlled trials, the intervention was a cognitive rehabilitation program, and the main objective of the study was to improve cognition. As previously reported in other reviews and meta-analyses, cognitive rehabilitation improves cognition in PD [27, 29, 30]. However, there is a need for studies with larger samples and double-blind randomized controlled trials to reach generalized conclusions in PD.

A less studied aspect of cognitive rehabilitation is its efficacy on improving mood symptoms or functional disability related to the disease. Following the review-specific criteria, among the randomized controlled trials in PD, only five studies have evaluated the change in functionality and mood aspects [31–35] and two of them found positive effects [31, 32] (Table 1). Petrelli et al. compared a structured and a nonstructured cognitive training program in PD patients and found that the symptoms of depression were reduced only in those PD patients that attended the nonstructured cognitive program [32]. Peña et al. found that functional disability scores were reduced in the experimental group (3 months of cognitive training) compared to the

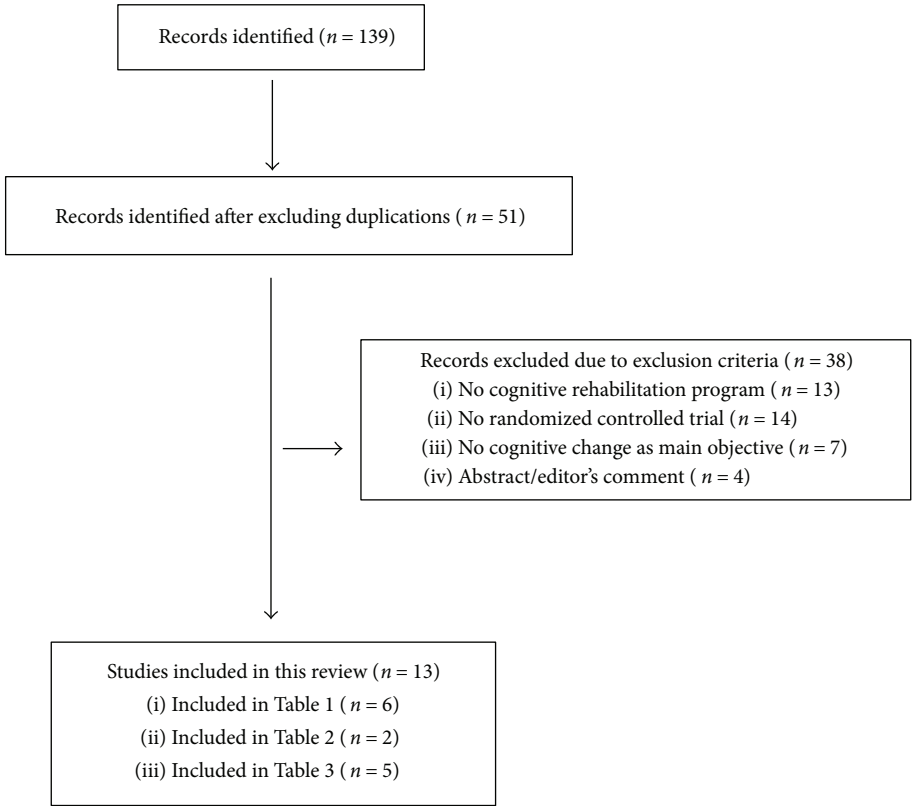

Figure 1: Summary of studies identified and included in the review.

active control group [31]. On the contrary, París et al. evaluated the change in quality of life, depressive symptoms, and activities of daily life after attending a cognitive rehabilitation program [35]. No significant changes were found in any scale, and authors related the absence of significant changes in quality of life to the short time of training (12 sessions in 1 month). In the same line, PD patients in the study of Cerasa et al. also attended a cognitive training program during 12 sessions and showed no significant changes in mood status [33]. However, in the study of Edwards et al., PD patients attended a cognitive training program during a longer period of time (3 months), but patients showed no changes in behavioral measures [34]. Among clinical symptoms of the disease, the change in depressive symptoms has been usually assessed in cognitive training studies in PD, but despite some significant changes, the overall results point to the absence of efficacy in reducing depression symptomatology after treatment [30]. However, these studies excluded patients with depression diagnosis or with severe symptoms of depression prior to participation. Therefore, this criterion could have influenced the absence of significant changes. With all, the mechanisms that make possible the improvement in quality of life aspects after a cognitive rehabilitation program are not clear. The duration of treatment and degree of structuration of the sessions could be two relevant variables to take into account when assessing transfer effects to clinical variables, but other variables seem to influence this process. Interestingly, in schizophrenia studies, the presence of a therapist during the training sessions and the group format of the training program have been suggested to influence the results on mood symptoms [36]. The cognitive sessions carried in a group format enhance social interactions between participants, and the presence of a therapist may increase the motivation and give positive feedback to the patients, which could have an impact in the affective state of patients. In fact, the two PD studies that found transfer effects to functional aspects or depressive symptoms performed a group-based cognitive training, and the training was guided by a qualified therapist [31, 32].

Moreover, detecting variables that predict the efficacy of cognitive treatments is an important aspect to take into account in order to understand the cognitive rehabilitation process, which could guide researchers to develop more effective programs and clinicians to personalize treatments for patients (Table 1). Despite the large amount of studies assessing the efficacy of cognitive rehabilitation in PD, few studies have investigated the predictors of the efficacy of cognitive treatments in PD. These PD studies found that lower age at diagnosis and longer disease duration were predictors of higher degree of cognitive improvements after rehabilitation [34], but higher scores in working memory and flexibility at baseline were related with lower degree of improvements after rehabilitation [37].

3.2. Changes in Brain Activity after Cognitive Rehabilitation. Little is known about the neurobiological effects of cognitive rehabilitation programs in PD. To date, literature is scarce about the presence of cerebral changes associated with cognitive rehabilitation programs assessed with structural and functional MRI techniques in PD. Table 2 summarized the main findings of the two randomized controlled trials in

Table 1: Summary of the randomized controlled trials in assessing the efficacy of cognitive rehabilitation programs in PD.

Authors	Sample	H&Y	Cognitive rehabilitation program				Tests[1]	Predictors of greater improvement	MRI (Table 2)	Results	Long-term follow-up (Table 3)	Limitations/ risk of bias
			Duration	Paper-pencil—P Computerized—C	Cogn. domains trained	Format						
París et al. [35]	**28 PD** 16 CR 12 ACG	1–3	**12 sessions** 4 weeks 3 times/ week 45 min/ session	CR—"SmartBrain tool" (P + C) ACG—speech therapy	(i) Attention (ii) WM (iii) Memory (iv) Psychomotor speed (v) EF (vi) Visuospatial ability (vii) Language (viii) Calculation skills (ix) Culture	Group + home	(i) Attention (ii) WM (iii) EF (iv) Processing speed (v) Verbal memory (vi) Visual memory (vii) Visuoconstruction (viii) Visuospatial ability (ix) Verbal fluency (x) *Depression* (xi) *Quality of life* (xii) *Daily living activities*	—	—	**Improvements** (i) Attention/WM (ii) Information processing speed (iii) Visual memory (iv) Visuospatial ability (v) Visuoconstructive ability (vi) Semantic fluency (vii) EF	—	Small sample size
Edwards et al. [34]	**74 PD** 32 CR 42 CG	1–3	**36 sessions** 3 months 3 times/ week 1 h/session	CR—"InSight version of SOPT" (C)	(i) Information processing speed	Home	(i) Speed of processing (self-reported) (ii) Perception of cognitive and everyday functioning (self-reported) (iii) *Depression*	<Age at PD diagnosis >Disease duration	—	**Improvements** (i) Speed of processing	—	No ACG Only 1 domain trained Self-reported test for cognition and functionality
Cerasa et al. [33]	**15 PD** 8 CR 7 ACG	1–3	**12 sessions** 6 weeks 2 times/ week 1 h/session	CR—"RehaCom" (C) ACG—visuomotor coordination tapping task. In-house software (C)	(i) Attention (ii) Information processing	Group	(i) Attention/ processing speed (ii) EF (iii) WM (iv) Spatial memory (v) Verbal memory (vi) Visuospatial orientation (vii) Verbal fluency (viii) *Depression* (ix) *Anxiety* (x) *Quality of life*	—	Yes	**Improvements** (i) Attention/ processing speed (ii) WM	—	Small sample size
Zimmermann et al. [37]	**39 PD** 19 CR 20 ACG	2[a]	**12 sessions** 4 weeks 3 times/ week	CR—"CogniPlus" (C) ACG—"Nintendo Wii" (C)	(i) Attention (ii) Working memory (iii) EF	Group	(i) Attention (ii) WM (iii) EF (iv) Episodic memory (v) Visuoconstruction	(i) WM score (ii) Flexibility score	—	(i) ACG improved attention compared to CR	—	Small sample size No change in functionality evaluated

Table 1: Continued.

Authors	Sample	H&Y	Cognitive rehabilitation program					Predictors of greater improvement	MRI (Table 2)	Results	Long-term follow-up (Table 3)	Limitations/ risk of bias
			Duration	Paper-pencil—P Computerized—C	Cogn. domains trained	Format	Tests[1]					
Petrelli et al. [32]	**65 PD** 22 CR-NV 22 CR-MT 21 CG	1–3	12 sessions 6 weeks 2 times/ week 90 min/ session	P "NEUROvitalis"—NV P "mentally fit"—MF	**NV** (i) Attention (ii) Memory (iii) EF **MF** (i) Attention (ii) Memory (iii) Creativity	Group + individual	(i) Attention (ii) Memory (iii) EF (iv) Visuoconstruction (v) *Depression* (vi) *Quality of life*	—	—	**Improvements NV versus CG** (i) Working memory (ii) Short-term memory **Improvements MF versus CG** (i) *Depression* **Improvements NV versus MT** (i) Working memory	12 months	Small sample size No ACG
Peña et al. [31]	**42 PD** 20 PD-CR 22 PD-ACG	1–3	39 sessions 13 weeks 3 times/ week 1 h/session	CR—"REHACOP" (P) ACG—occupational activities (P)	(i) Attention (ii) Memory (iii) Language (iv) EF (v) Social cognition (vi) PS	Group	(i) Processing speed (ii) Memory (iii) Executive functions (iv) Social cognition (v) *Functional disability* (vi) *Apathy* (vii) *Depression*	—	Yes	**Improvements PD-CR versus PD-ACG** (i) Processing speed (ii) Visual memory (iii) Social cognition (iv) *Functional disability*	18 months	Small sample size

ACG = active control group; CG = control group; CR = cognitive rehabilitation; EF = executive functions; HC = healthy controls; H&Y = Hoehn and Yahr; MRI = magnetic resonance image; PD = Parkinson's disease; WM = working memory. [1]Tests assessing mood, clinical, and functionality aspects are shown in *italics*. [a]Median.

Table 2: Summary of randomized controlled trials in assessing brain changes related to cognitive rehabilitation programs in PD.

Authors	MRI sample	H&Y	Cognitive rehabilitation program	MRI acquisition/ preprocessing/analysis	MRI statistical analysis	MRI results	Correlation with cognitive measures	Limitations/risk of bias
Cerasa et al. [33]	**15 PD** 8 CR 7 ACG	1–3	RehaCom computer program Training: (i) Attention (ii) Information processing	Resting-state fMRI/ICA in FSL/FC analysis	ANOVA (group × time) Region of interests Dorsolateral PFC Ventrolateral PFC ACC Sup + inf parietal left Caudate Cerebellum	Increased functional activity: (i) Left dorsolateral PFC (executive network) (ii) Superior parietal left (attention network)	—	Small sample size Only one type of MRI acquisition
Díez-Cirarda et al. [38] (cognitive results in [31])	**30 PD** 15 CR 15 ACG	1–3	"REHACOP" program Training: (i) Attention (ii) Memory (iii) Language (iv) EF (v) Social cognition	Resting-state fMRI/ROI-to-ROI approach in CONN toolbox	ANOVA (group × time) Paired *t*-test Whole brain	Increased FC between BA9L-BA20L and BA9R-BA20L	Yes	Small sample size and reduced at long-term follow-up Memory fMRI paradigm results at FWE uncorrected
				Memory fMRI paradigm/ model-based approach in SPM		Increased brain activation Learning task: left frontal inferior lobe Increased brain activation Memory task: left middle temporal lobe		
				Diffusion weighted/TBSS in FSL		—		
				T1 weighted/VBM in FSL		—		

ACC = anterior cingulate cortex; ACG = active control group; BA = Brodmann area; CR = cognitive rehabilitation; EF = executive functions; FC = functional connectivity; fMRI = functional magnetic resonance imaging; FSL = FMRIB Software Library; H&Y = Hoehn and Yahr; ICA = independent component analysis; MRI = magnetic resonance image; PD = Parkinson's disease; PFC = prefrontal cortex; TBSS = tract-based spatial statistics; VBM = voxel-based morphometry.

Table 3: Summary of cognitive rehabilitation studies in PD with longitudinal follow-up evaluation.

Authors	Sample	H&Y	Duration	Cognitive rehabilitation program Paper-pencil—P Computerized—C	Cogn. domains trained	Format	Tests[1]	MRI (Table 2)	Results (pre- and posttreatment)	Long-term follow-up (T0/T1/T2)	Limitations/ risk of bias
Nonrandomized/noncontrolled trials											
Sinforiani et al. [39]	**20 PD**	1.5 ± 0.6	**12 sessions** 6 weeks + 12 h MT	C "TNP"	(i) Attention (ii) Abstract reasoning (iii) Visuospatial	Group	(i) MMSE (ii) Digit span (iii) Corsi's test (iv) Babcock's story (v) FAS phonetic (vi) Raven matrix (vii) WCST (viii) Stroop test	—	**Improvements:** (i) Babcock (recall) (ii) FAS phonetic (iii) Raven matrix	**6 months without training: maintenance (no statistical data)** (i) Babcock (recall) (ii) FAS phonetic (iii) Raven matrix	No CG No differentiation of the efficacy of motor or cognitive training No statistical data at follow-up
Reuter et al. [40]	**222 PD** Gr A—CR = 71 Gr B—CR-TT = 75 Gr C—CR-TT-MT = 76 (plus psychoeducation with caregivers)	2–4	**14 sessions** 4 weeks 4 times/week 60 min/session	P + C Group A: cognitive training Group B: cognitive + transfer training Group C: cognitive + transfer + motor training	(i) Attention (ii) Concentration (iii) EF (iv) WM (v) Memory (vi) Processing speed	Individual	(i) ADAS-Cog (ii) SCOPA-Cog (iii) EF-BADS (iv) PS-PASAT (v) *Depression* (vi) *Anxiety* (vii) *PDQ-39*	—	**Improvements in all groups:** (i) ADAS-Cog (ii) BADS (iii) PASAT **Greater improvements in group C:** (i) ADAS-Cog (ii) SCOPA-Cog (iii) BADS (iv) PASAT	**6 months with home training: group C performed more training sessions (T2 > T0)** (i) ADAS-Cog (ii) SCOPA-Cog (iii) BADS (iv) PASAT	No ACG No PDQ-39 scores at baseline Different number of sessions between posttreatment and long-term evaluation
Adamski et al. [45]	**6 PD-CR** **12 HC-CR** **7 HC-CG**	—	**16 sessions** 4 weeks 4 times/week 45 min/session	C "BrainStim"	(i) WM (ii) Encoding (iii) Recall (iv) EF (v) Visuospatial ability	Group	(i) Attention (ii) WM (iii) Short-term memory (iv) Long-term memory (v) PS (vi) EF (vii) *Depression* (viii) *Fatigue*	—	**Improvements in PD group:** (i) Short-term memory (ii) Long-term memory **Improvements in HC groups:** (iii) Diverse cognitive domains	**3 months without training: PD group increased (T2 > T0)** (i) Short-term memory	Small sample size No PD-ACG Baseline differences between groups

Table 3: Continued.

Authors	Sample	H&Y	Duration	Cognitive rehabilitation program Paper-pencil—P Computerized—C	Cogn. domains trained	Format	Tests[1]	MRI (Table 2)	Results (pre- and posttreatment)	Long-term follow-up (T0/T1/T2)	Limitations/ risk of bias
Randomized controlled trials											
Petrelli et al. [42]	**65 PD** 22 CR-NV 22 CR-MF 21 CG	1–3	**12 sessions** 6 weeks 2 times/ week 90 min/ session	P "NEUROvitalis"—NV P "mentally fit"—MF	**NV** (i) Attention (ii) Memory (iii) EF **MF** (i) Attention (ii) Memory (iii) Creativity	Group + individual	(i) Attention (ii) Memory (iii) EF (iv) Visuoconstruction (v) *Depression* (vi) *Quality of life*	—	**Improvements in NV versus CG:** (i) Working memory (ii) Short-term memory **Improvements in MF versus CG:** (i) *Depression* **Improvements in NV versus MT:** (i) Working memory	**12 months without training: NV group maintenance (T2 = T0)** (i) MMSE (ii) DemTect	Small sample size No ACG Long-term evaluation with screening tests
Díez-Cirarda et al. [41]	**42 PD** 20 PD-CR 22 PD-ACG	1–3	**39 sessions** 13 weeks 3 times/ week 60 min/ session	CR—"REHACOP" (P) ACG—occupational activities (P)	(i) Attention (ii) Memory (iii) Language (iv) EF (v) Social cognition (vi) PS	Group	(i) PS (ii) Memory (iii) Executive functions (iv) Social cognition (v) *Functional disability* (vi) *Apathy* (vii) *Depression*	Yes	**Improvements in PD-CR versus PD-ACG:** (i) PS (ii) Visual memory (iii) Social cognition (iv) *Functional disability* (v) Brain functional changes	**18 months without training: PD-CR increased (T2 > T0):** (i) Verbal memory (ii) Visual memory (iii) EF (iv) ToM (v) *Functional disability* (vi) Brain functional activity	Small sample size Absence of CG at follow-up

ACG = active control group; CG = control group; CR = cognitive rehabilitation; EF = executive functions; FAS = phonetic fluency test; HC = healthy controls; H&Y = Hoehn and Yahr; MMSE = minimental state examination; MRI = magnetic resonance image; MT = motor training; TT = transfer training; PD = Parkinson's disease; PS = processing speed; WCST = Wisconsin card sorting task; WM = working memory.
[1]Tests assessing mood, clinical, and functionality aspects are shown in *italics*.

evaluating brain changes after a cognitive rehabilitation program in PD.

One study evaluated the effects of group-based attention rehabilitation on brain functional activity in PD patients [33]. PD patients were included in the trial if they had attention impairment but no other cognitive domain impaired. At pre- and post-treatment assessments, patients underwent an extensive neuropsychological assessment and resting-state fMRI were acquired. PD patients were randomly divided into experimental group and active control group. The experimental group received attention rehabilitation using "RehaCom" computer program, while the control group attended in-house software which focused on visuomotor coordination. The attention rehabilitation consisted in computer-assisted tasks which trained attention and information processing during 6 weeks. Specifically, attention rehabilitation tasks were focused on concentration and attention tasks and vigilance program and divided attention from the RehaCom software. After rehabilitation, PD patients showed improvements in attention and processing speed tasks and increased brain activation in the left dorsolateral prefrontal cortex (part of the executive resting-state network) and the left superior parietal cortex (part of the attentional resting-state network) [33] (Table 2).

A later study in PD patients evaluated the changes in brain activity after a 3-month integrative cognitive rehabilitation program [38]. PD patients underwent an extensive neuropsychological assessment at pre- and post-treatment. Regarding MRI acquisition, GM and WM changes were analyzed as well as brain activity changes during resting-state and during a memory paradigm. The cognitive rehabilitation program used was the REHACOP, a paper/pencil rehabilitation program, which trained attention, processing speed, memory, language, executive functions, and social cognition during 3 months. PD patients after cognitive rehabilitation showed increased brain FC between frontal and temporal lobes and increased brain activation during the memory paradigm in frontal and temporal areas (see Table 2). No brain structural changes were found after rehabilitation. These brain FC and activation values at post-treatment showed correlations with post-treatment cognitive performance in PD patients from the experimental group. Specifically, during resting state, FC values between frontal and temporal lobes at post-treatment correlated with executive function performance at post-treatment. Additionally, during the learning fMRI task, the brain activation values after treatment correlated with the visual memory performance at post-treatment [38].

These studies suggest that brain activity changes are possible after a cognitive rehabilitation program in PD. Further studies are needed to replicate and complement these findings.

3.3. Long-Term Effects of Cognitive Rehabilitation. Furthermore, the ultimate goal of cognitive treatments is to ensure that benefits are maintained over long periods of time, but little is known about the maintenance of cognitive improvements over time in PD patients, and a few studies have evaluated it [39–42, 45]. A summary of these studies is shown in Table 3.

The first study to evaluate the long-term effects of cognitive rehabilitation was published in 2004 by Sinforiani et al. and showed that PD patients attending a cognitive training program combined with motor training during one month showed maintenance of the cognitive benefits after 6 months [39]. However, the study did not include statistical analyses for the follow-up period. Moreover, this study did not include a control group; therefore, we cannot conclude that these possible benefits were related to the cognitive or motor training or the combination of treatments.

Another study in PD compared three training groups: "group A" which attended cognitive training, "group B" which attended cognitive training and transfer training, and "group C" which attended cognitive, transfer, and motor training [40] (Table 3). The authors found that the three groups benefited from training, but those PD patients that attended cognitive training combined with transfer training and physical activity benefited significantly more in the short term. Moreover, over the next 6 months, patients from "group C" were more motivated to spend more time training at home compared to the other groups and showed greater maintenance of cognitive improvements after 6 months [40]. However, because patients from group C spent more hours in training at home over the next 6 months compared to the other groups, these results may be influenced by the difference of hours spent in training. Finally, this study also included an intervention therapy with caregivers focusing on psychoeducation, which helped the patients to continue the training tasks at home [40] (Table 3).

A later study in PD assessed the long-term effects of cognitive rehabilitation for a longer period of time (12 months) [42]. At baseline, these PD patients were randomized to a structured cognitive rehabilitation program (NEUROvitalis), to a nonstructured cognitive rehabilitation program (mentally fit), or to a control group. After 12 months from post-treatment, PD patients that attended NEUROvitalis training program showed reduced cognitive performance compared to post-treatment, but scores were similar compared to baseline. Moreover, the risk of conversion to MCI was found higher in the control group than in any of the cognitive training groups. Regarding depression, the "mentally fit" group was the only group that showed significant reduction in depressive symptoms after training, but these changes were not maintained at follow-up (Table 3). With all, the authors concluded that a structured cognitive treatment could prevent cognitive decline [42].

Regarding the maintenance of neuroimaging changes, to date, only one study has been published assessing the longitudinal effects of cognitive rehabilitation [41]. PD patients attended a 3-month cognitive rehabilitation program and showed increased brain connectivity and activation in the frontal and temporal lobes after treatment. These patients underwent a neuropsychological and neuroimaging assessment after 18 months from post-treatment. The results showed that not only improvements in cognitive performance and functionality were maintained after 18 months but also increased FC was found at follow-up [41]. In addition, PD patients also showed maintenance of the increased brain activation during the memory paradigm at long-term

compared to baseline, but the level of activation at long-term was reduced compared to post-treatment. This study showed promising findings regarding the maintenance of brain changes in a neurodegenerative disease; however, the sample size was small, and the control group was not evaluated in the long term. The results need to be replicated.

These few studies suggest the maintenance of cognitive improvements after attending a cognitive rehabilitation program in PD patients (Table 3). However, literature is scarce in this pathology and more research needs to be done, especially including neuroimaging assessment at follow-up.

4. Discussion

The studies on the efficacy of cognitive rehabilitation programs in PD suggest that cognitive rehabilitation programs are effective in improving cognition but further research is needed in this field to clarify its efficacy on functional disability and brain activity changes. Also, very little is known about the long-term maintenance of cognitive changes after rehabilitation. There are few cognitive rehabilitation studies in PD which followed the Consolidated Standards of Reporting Trials (CONSORT) guidelines for randomized controlled trials. These make more difficult to find conclusive findings. Future studies should implement these guidelines in order to improve the research quality and validity of findings.

All randomized controlled trials in PD for cognitive rehabilitation programs point to the efficacy in improving cognition. However, most of them highlighted the small sample size as a limitation, which makes it difficult to generalize the findings. Additionally, all of them used different types of cognitive training programs, with different duration and type of exercises. One of the future steps to be taken towards understanding the efficacy of cognitive rehabilitation is identifying the characteristics that make an integrative cognitive rehabilitation program effective against cognitive impairment. A review of cognitive rehabilitation concluded that better results may be obtained in a group-based format compared to an individual format [28]. However, while most of the rehabilitation studies in PD are group-based, this question has not been directly addressed. In addition, a recent meta-analysis compared the efficacy of standardized with tailored (individualized) cognitive interventions, but found that there were insufficient studies for a statistical comparison [29]. Furthermore, other variables are also to be defined, such as the most appropriate number of sessions, their frequency, and the duration of the treatment. Also, the number of cognitive domains trained may also influence the results. Moreover, predictors of the efficacy of cognitive treatments are useful in the disease to adequate cognitive treatment to the patient. Very few studies have evaluated this aspect, and research is needed in the field.

Regarding patients' characteristics, most of the randomized controlled trials in PD have been performed with PD patients at the early Hoehn and Yahr stages of the disease. Future studies should also include PD patients at more advanced stages to evaluate whether cognitive treatments could also benefit these patients. Interestingly, a study protocol was recently published addressing the efficacy of a cognitive rehabilitation in PD patients with dementia, but results are pending [43].

Moreover, transfer effects to clinical aspects have been found in some cognitive rehabilitation studies in PD; however, other studies found no significant changes. The mechanisms that make possible to transfer benefits to clinical variables are unknown. There is an urgent need of studies analyzing this subject. The last goal of cognitive rehabilitation programs is to improve quality of life of patients. Future studies should also include clinical and functionality scales in pre- and post-treatment neuropsychological assessments.

On the other hand, promising findings have been found regarding brain changes after treatment in PD, which support the efficacy of cognitive rehabilitation programs in the disease. Results showing brain connectivity and activation increments after a cognitive treatment of less than 3 months in patients with a neurodegenerative disease are relevant in the field of neurorehabilitation. Future studies should include the MRI acquisition as part of the protocol assessment to evaluate brain changes after treatment and replicate the findings.

All these changes have been analyzed at follow-up, and some studies found maintenance of these improvements. Future randomized controlled trials should include follow-up periods in order to replicate previous findings and assess whether the improvements after training could be maintained over time. It would be also interesting to examine the maintenance of these changes in PD patients with and without booster sessions.

Another aspect to be taken into account during the rehabilitation process of the patient is the role of the caregiver. Some cognitive rehabilitation studies have included an intervention which focused on psychoeducation with the caregivers of the PD patients [40, 44]. The psychoeducation usually addresses aspects of the disease, patients' care management, information about help aids, and the importance of the self-care [40, 44]. These studies found that the caregivers gain self-confidence and felt more confident to take care of the person with the disease.

In conclusion, cognitive rehabilitation programs have demonstrated to be effective in improving cognitive functions and may also improve functional disability and produce brain changes in patients with PD. In addition, to provide a complete or integrative treatment, the combination of cognitive training with other types of trainings or the intervention with the caregivers should be further analyzed. More research should be performed in the field, with a view to reaching generalized conclusions and including cognitive rehabilitation in the standard of care of PD patients.

Disclosure

This article is a contribution to the special issue entitled Neurorehabilitation: Neural Plasticity and Functional Recovery 2018.

Conflicts of Interest

Natalia Ojeda and Javier Peña are coauthors and copyright holders of the REHACOP cognitive rehabilitation

program, published by Parima Digital, S.L. (Bilbao, Spain). María Díez-Cirarda and Naroa Ibarretxe-Bilbao have no conflicts of interest to report.

Acknowledgments

The authors thank ASPARBI (Parkinson's Disease Association in Biscay) and all the patients involved in the study. This study was supported by the Department of Health of the Basque Government (2011111117), the Ministerio de Economía y Competitividad (PSI2012-32441), and the Department of Education and Science of the Basque Government (Equipo A) (IT946-16).

References

[1] L. Hirsch, N. Jette, A. Frolkis, T. Steeves, and T. Pringsheim, "The incidence of Parkinson's disease: a systematic review and meta-analysis," *Neuroepidemiology*, vol. 46, no. 4, pp. 292–300, 2016.

[2] R. Xia and Z.-H. Mao, "Progression of motor symptoms in Parkinson's disease," *Neuroscience Bulletin*, vol. 28, no. 1, pp. 39–48, 2012.

[3] E. Tolosa, C. Gaig, J. Santamaria, and Y. Compta, "Diagnosis and the premotor phase of Parkinson disease," *Neurology*, vol. 72, no. 7, Supplement 2, pp. S12–S20, 2009.

[4] D. Muslimovic, B. Post, J. D. Speelman, and B. Schmand, "Cognitive profile of patients with newly diagnosed Parkinson disease," *Neurology*, vol. 65, no. 8, pp. 1239–1245, 2005.

[5] A. J. Yarnall, D. P. Breen, G. W. Duncan et al., "Characterizing mild cognitive impairment in incident Parkinson disease: the ICICLE-PD study," *Neurology*, vol. 82, no. 4, pp. 308–316, 2014.

[6] M. A. Hely, W. G. J. Reid, M. A. Adena, G. M. Halliday, and J. G. L. Morris, "The Sydney multicenter study of Parkinson's disease: the inevitability of dementia at 20 years," *Movement Disorders*, vol. 23, no. 6, pp. 837–844, 2008.

[7] J. Hoogland, J. A. Boel, R. M. A. de Bie et al., "Mild cognitive impairment as a risk factor for Parkinson's disease dementia," *Movement Disorders*, vol. 32, no. 7, pp. 1056–1065, 2017.

[8] I. Leroi, K. McDonald, H. Pantula, and V. Harbishettar, "Cognitive impairment in Parkinson disease: impact on quality of life, disability, and caregiver burden," *Journal of Geriatric Psychiatry and Neurology*, vol. 25, no. 4, pp. 208–214, 2012.

[9] E. Rosenthal, L. Brennan, S. Xie et al., "Association between cognition and function in patients with Parkinson disease with and without dementia," *Movement Disorders*, vol. 25, no. 9, pp. 1170–1176, 2010.

[10] T. R. Melzer, R. Watts, M. R. MacAskill et al., "Grey matter atrophy in cognitively impaired Parkinson's disease," *Journal of Neurology, Neurosurgery, & Psychiatry*, vol. 83, no. 2, pp. 188–194, 2012.

[11] G. W. Duncan, M. J. Firbank, A. J. Yarnall et al., "Gray and white matter imaging: a biomarker for cognitive impairment in early Parkinson's disease?," *Movement Disorders*, vol. 31, no. 1, pp. 103–110, 2016.

[12] Z. Zheng, S. Shemmassian, C. Wijekoon, W. Kim, S. Y. Bookheimer, and N. Pouratian, "DTI correlates of distinct cognitive impairments in Parkinson's disease," *Human Brain Mapping*, vol. 35, no. 4, pp. 1325–1333, 2014.

[13] H. Matsui, K. Nishinaka, M. Oda, H. Niikawa, T. Kubori, and F. Udaka, "Dementia in Parkinson's disease: diffusion tensor imaging," *Acta Neurologica Scandinavica*, vol. 116, no. 3, pp. 177–181, 2007.

[14] I. Rektor, A. Svátková, L. Vojtíšek et al., "White matter alterations in Parkinson's disease with normal cognition precede grey matter atrophy," *PLoS One*, vol. 13, no. 1, article e0187939, 2018.

[15] R. Cabeza and L. Nyberg, "Imaging cognition II: an empirical review of 275 PET and fMRI studies," *Journal of Cognitive Neuroscience*, vol. 12, no. 1, pp. 1–47, 2000.

[16] L. Christopher and A. P. Strafella, "Neuroimaging of brain changes associated with cognitive impairment in Parkinson's disease," *Journal of Neuropsychology*, vol. 7, no. 2, pp. 225–240, 2013.

[17] C. H. Williams-Gray, S. L. Mason, J. R. Evans et al., "The CamPaIGN study of Parkinson's disease: 10-year outlook in an incident population-based cohort," *Journal of Neurology, Neurosurgery, & Psychiatry*, vol. 84, no. 11, pp. 1258–1264, 2013.

[18] D. K. Johnson, Z. Langford, M. Garnier-Villarreal, J. C. Morris, and J. E. Galvin, "Onset of mild cognitive impairment in Parkinson disease," *Alzheimer Disease & Associated Disorders*, vol. 30, no. 2, pp. 127–133, 2016.

[19] B. Ramírez–Ruiz, M. J. Martí, E. Tolosa et al., "Longitudinal evaluation of cerebral morphological changes in Parkinson's disease with and without dementia," *Journal of Neurology*, vol. 252, no. 11, pp. 1345–1352, 2005.

[20] Y. Zhang, I. W. Wu, D. Tosun, E. Foster, N. Schuff, and the Parkinson's Progression Markers Initiative, "Progression of regional microstructural degeneration in Parkinson's disease: a multicenter diffusion tensor imaging study," *PLoS One*, vol. 11, no. 10, article e0165540, 2016.

[21] C. Huang, C. Tang, A. Feigin et al., "Changes in network activity with the progression of Parkinson's disease," *Brain*, vol. 130, no. 7, pp. 1834–1846, 2007.

[22] B. Segura, N. Ibarretxe-Bilbao, R. Sala-Llonch et al., "Progressive changes in a recognition memory network in Parkinson's disease," *Journal of Neurology, Neurosurgery, & Psychiatry*, vol. 84, no. 4, pp. 370–378, 2013.

[23] E. Mak, L. Su, G. B. Williams, and J. T. O'Brien, "Neuroimaging correlates of cognitive impairment and dementia in Parkinson's disease," *Parkinsonism & Related Disorders*, vol. 21, no. 8, pp. 862–870, 2015.

[24] A. Bahar-Fuchs, L. Clare, and B. Woods, "Cognitive training and cognitive rehabilitation for persons with mild to moderate dementia of the Alzheimer's or vascular type: a review," *Alzheimer's Research & Therapy*, vol. 5, no. 4, p. 35, 2013.

[25] T. Wykes and W. D. Spaulding, "Thinking about the future cognitive remediation therapy—what works and could we do better?," *Schizophrenia Bulletin*, vol. 37, Supplement 2, pp. S80–S90, 2011.

[26] J. V. Hindle, A. Petrelli, L. Clare, and E. Kalbe, "Nonpharmacological enhancement of cognitive function in Parkinson's disease: a systematic review," *Movement Disorders*, vol. 28, no. 8, pp. 1034–1049, 2013.

[27] R. Biundo, L. Weis, E. Fiorenzato, and A. Antonini, "Cognitive rehabilitation in Parkinson's disease: is it feasible?," *Archives of Clinical Neuropsychology*, vol. 32, no. 7, pp. 840–860, 2017.

[28] C. C. Walton, S. L. Naismith, A. Lampit, L. Mowszowski, and S. J. G. Lewis, "Cognitive training in Parkinson's disease: a

theoretical perspective," *Neurorehabilitation and Neural Repair*, vol. 31, no. 3, pp. 207–216, 2017.

[29] B. J. Lawrence, N. Gasson, R. S. Bucks, L. Troeung, and A. M. Loftus, "Cognitive training and noninvasive brain stimulation for cognition in Parkinson's disease: a meta-analysis," *Neurorehabilitation and Neural Repair*, vol. 31, no. 7, pp. 597–608, 2017.

[30] I. H. Leung, "Cognitive training in Parkinson disease," *Neurology*, vol. 85, pp. 1–9, 2015.

[31] J. Peña, N. Ibarretxe-Bilbao, I. García-Gorostiaga, M. A. Gomez-Beldarrain, M. Díez-Cirarda, and N. Ojeda, "Improving functional disability and cognition in Parkinson disease: randomized controlled trial," *Neurology*, vol. 83, no. 23, pp. 2167–2174, 2014.

[32] A. Petrelli, S. Kaesberg, M. T. Barbe et al., "Effects of cognitive training in Parkinson's disease: a randomized controlled trial," *Parkinsonism & Related Disorders*, vol. 20, no. 11, pp. 1196–1202, 2014.

[33] A. Cerasa, M. C. Gioia, M. Salsone et al., "Neurofunctional correlates of attention rehabilitation in Parkinson's disease: an explorative study," *Neurological Sciences*, vol. 35, no. 8, pp. 1173–1180, 2014.

[34] J. D. Edwards, R. A. Hauser, M. L. O'Connor, E. G. Valdés, T. A. Zesiewicz, and E. Y. Uc, "Randomized trial of cognitive speed of processing training in Parkinson disease," *Neurology*, vol. 81, no. 15, pp. 1284–1290, 2013.

[35] A. P. París, H. G. Saleta, M. de la Cruz Crespo Maraver et al., "Blind randomized controlled study of the efficacy of cognitive training in Parkinson's disease," *Movement Disorders*, vol. 26, no. 7, pp. 1251–1258, 2011.

[36] M. Cella, A. Preti, C. Edwards, T. Dow, and T. Wykes, "Cognitive remediation for negative symptoms of schizophrenia: a network meta-analysis," *Clinical Psychology Review*, vol. 52, pp. 43–51, 2017.

[37] R. Zimmermann, U. Gschwandtner, N. Benz et al., "Cognitive training in Parkinson disease: cognition-specific vs nonspecific computer training," *Neurology*, vol. 82, no. 14, pp. 1219–1226, 2014.

[38] M. Díez-Cirarda, N. Ojeda, J. Peña et al., "Increased brain connectivity and activation after cognitive rehabilitation in Parkinson's disease: a randomized controlled trial," *Brain Imaging and Behavior*, vol. 11, no. 6, pp. 1640–1651, 2017.

[39] E. Sinforiani, L. Banchieri, C. Zucchella, C. Pacchetti, and G. Sandrini, "Cognitive rehabilitation in Parkinson's disease," *Archives of Gerontology and Geriatrics*, vol. 38, pp. 387–391, 2004.

[40] I. Reuter, S. Mehnert, G. Sammer, M. Oechsner, and M. Engelhardt, "Efficacy of a multimodal cognitive rehabilitation including psychomotor and endurance training in Parkinson's disease," *Journal of Aging Research*, vol. 2012, Article ID 235765, 15 pages, 2012.

[41] M. Díez-Cirarda, N. Ojeda, J. Peña et al., "Long-term effects of cognitive rehabilitation on brain, functional outcome and cognition in Parkinson's disease," *European Journal of Neurology*, vol. 25, no. 1, pp. 5–12, 2018.

[42] A. Petrelli, S. Kaesberg, M. T. Barbe et al., "Cognitive training in Parkinson's disease reduces cognitive decline in the long term," *European Journal of Neurology*, vol. 22, no. 4, pp. 640–647, 2015.

[43] J. V. Hindle, T. J. Watermeyer, J. Roberts et al., "Cognitive rehabilitation for Parkinson's disease dementia: a study protocol for a pilot randomised controlled trial," *Trials*, vol. 17, no. 1, p. 152, 2016.

[44] L. E. I. A'Campo, N. G. A. Spliethoff-Kamminga, M. Macht, R. A. C. Roos, and The EduPark Consortium, "Caregiver education in Parkinson's disease: formative evaluation of a standardized program in seven European countries," *Quality of Life Research*, vol. 19, no. 1, pp. 55–64, 2010.

[45] N. Adamski, M. Adler, K. Opwis, and I. K. Penner, "A pilot study on the benefit of cognitive rehabilitation in Parkinson's disease," *Therapeutic Advances in Neurological Disorders*, vol. 9, no. 3, pp. 153–164, 2016.